BULLETIN

OF

The Geological Society of America

DETROIT PUBLIC LIBRARY
APR 14 1960
TECHNOLOGY
DEPARTMENT

VOLUME 71

NUMBER 4

April 1960

PUBLISHED MONTHLY BY THE SOCIETY

COUNCIL

President

HOLLIS D. HEDBERG, Oakmont, Pennsylvania

Past President

MARLAND P. BILLINGS, Cambridge, Massachusetts

Vice-President

THOMAS B. NOLAN, Washington, D. C.

Secretary

FREDERICK BETZ, JR., 419 West 117 Street, New York 27, N. Y.

Treasurer

J. EDWARD HOFFMEISTER, University of Rochester, Rochester 20, N. Y.

Councilors

(Term expires 1960)

H. H. HESS
Princeton, N. J.

HAROLD N. FISK
Houston, Texas

C. O. SWANSON
Trail, British Columbia, Canada

C. C. ALBRITTON, JR.
Dallas, Texas

(Term expires 1961)

JOHN C. FRYE
Urbana, Ill.

CHARLES F. PARK, JR.
Stanford, Calif.

ROBERT P. SHARP
Pasadena, Calif.

E. F. OSBORN
University Park, Pa.

(Term expires 1962)

NORMAN D. NEWELL
New York, N. Y.

GEORGE P. WOOLLARD
Madison, Wis.

VINCENT C. KELLEY
Albuquerque, N. M.

HAROLD L. JAMES
Menlo Park, Calif.

COMMITTEE ON PUBLICATIONS

LAUREN A. WRIGHT, *Chairman*
WILLIAM C. KRUMBEIN
E. N. GODDARD

Conferees
FREDERICK BETZ, JR., *Editor-in-Chief*
AGNES CREAGH, *Managing Editor*

MARCIA VAN METER, *Senior Editorial Assistant*
BARBARA FLYNN, *Junior Editorial Assistant*

MORGAN GUARANTY TRUST COMPANY OF NEW YORK
Bankers and Custodians

PRICE WATERHOUSE & COMPANY
Auditors

HUGH SATTERLEE
Counsel

Y.

Chief
or

Bulletin
of
The Geological Society of America

VOLUME 71 April 1960 NUMBER 4

CONTENTS

	Pages
Diastrophism and mountain building. By Marland P. Billings	363–398
Age of the granitic rocks of Nova Scotia. By H. W. Fairbairn, P. M. Hurley, W. H. Pinson, Jr., and R. F. Cormier	399–414
Geophysical investigation of Mono Basin, California. By L. C. Pakiser, Frank Press, and M. F. Kane	415–448
Role of hydroxyl orientation in mica alteration. By William A. Bassett	449–456
Agua Blanca fault—a major transverse structure of northern Baja California, Mexico. By Clarence R. Allen, Leon T. Silver, and Francis G. Stehli	457–482
Foothills fault system, western Sierra Nevada, California. By Lorin D. Clark	483–496
Short Notes	
Bathymetry and geology of Sala y Gomez, southeast Pacific. By Robert L. Fisher and Robert M. Norris	497–502
Occurrence of normative sodium metasilicate in Washington's tables. By Felix Chayes	503–504
Occurrence of normative sodium metasilicate in Washington's tables: A reply. By O. F. Tuttle	505–506
Symmictite: A name for nonsorted terrigenous sedimentary rocks that contain a wide range of particle sizes. By R. F. Flint, J. E. Sanders, and John Rodgers	507–510
Leached, clay-enriched zones in post-Sangamon drift in southwestern Ohio and southeastern Indiana: New observations and data. By Ansel M. Gooding and Erling Gamble	511–514
Clay mineralogy of the sediments of the Great Salt Lake, Utah. By Ralph E. Grim, Georges Kulbicki, and Albert V. Carozzi	515–520

Subscription $15.00 per year.
Printing Office: Mt. Royal & Guilford Aves., Baltimore 2, Md.
Communications for publications should be addressed to The Geological Society of America, Dr. Frederick Betz, Jr., Secretary, 419 West 117 Street, New York 27, N. Y.
Please give notice of change of address 4 weeks in advance. Claims for nonreceipt of the Bulletin of a given month must be sent to the Secretary of the Society before the end of the second succeeding month.

Second-class postage paid at Baltimore, Md.
Accepted for mailing at special rate of postage provided for in Section 1103
Act of October 3, 1917, authorized on July 8, 1918.

PAPERS IN PRESS FOR FORTHCOMING ISSUES

WIND DIRECTION IN THE WESTERN UNITED STATES IN THE LATE PALEOZOIC. By N. D. Opdyke and S. K. Runcorn

PALEOMAGNETIC OBSERVATIONS IN THE UNITED STATES: NEW EVIDENCE FOR POLAR WANDERING AND CONTINENTAL DRIFT. By D. W. Collinson and S. K. Runcorn

BIOGEOCHEMICAL PROSPECTING FOR MANGANESE IN NORTHEAST TENNESSEE. By F. D. Bloss and R. L. Steiner

PETROLOGY AND STRUCTURE OF THE COCKEYSVILLE FORMATION NEAR BALTIMORE, MARYLAND. By Philip W. Choquette

MODELS AND METHODS FOR ANALYSES OF THE MODE OF FORMATION OF FOSSIL ASSEMBLAGES. By Ralph Gordon Johnson

CLAY MINERALOGY OF MISSISSIPPI RIVER DELTAIC SEDIMENTS. By M. S. Taggart, Jr., and A. D. Kaiser, Jr.

STRATIGRAPHIC AND GEOTECTONIC RELATIONSHIPS IN NORTHERN VERMONT AND SOUTHERN QUEBEC. By Wallace M. Cady

MEMOIRS IN PRESS

80. STILLWATER IGNEOUS COMPLEX: A QUANTITATIVE MINERALOGICAL STUDY. By Harry H. Hess
A detailed study of an example of extreme fractional crystallization by crystal settling. The author thoroughly investigates the order of crystallization and chemistry of the essential minerals and presents new optical-property curves for plagioclases and pyroxenes.

230 pages, 42 figures, 12 plates, 55 tables. Expected date of issue, April 20.

Price to Fellows and Members of GSA, $3.50. Prepublication price (until April 20) to all others, $4.75; postpublication price, $5.50. Remittance should accompany orders.

81. MORPHOLOGY, CLASSIFICATION, AND LIFE HABITS OF THE PRODUCTOIDEA (BRACHIOPODA). By Helen Muir-Wood and G. Arthur Cooper
Comprehensive revision of the Productoidea. Includes all genera described in the world literature plus new families and genera, and their stratigraphic range and geographic distribution. New information and interpretations of shell structure and other features. The authors propose a new classification for Productoidea. Extensive bibliography and illustrations of almost all genera.

About 500 pages, 8 figures, 135 photographic collotype plates. Expected date of issue, June 30.

Price will be about $10 for Fellows and members of GSA and about $15 for all others. Exact prices will be listed in May Bulletin.

NEW MEMOIRS

(See back cover of this issue for further listings.)

77. RELATION OF ORE DEPOSITION TO DOMING IN THE NORTH AMERICAN CORDILLERA. By Edward Wisser. List price, $4.00. Special price to Fellows and Members of GSA, $2.50

78. MOLLUSCAN FAUNAS OF THE FLAGSTAFF FORMATION OF CENTRAL UTAH. By Auréle La Rocque. List price, $4.50. Special price to Fellows and Members of GSA, $3.00

79. ROCK DEFORMATION. By David Griggs and John Handin, *Editors*. List price, $12.00. Special price to Fellows and Members of GSA, $7.50

BULLETIN OF THE GEOLOGICAL SOCIETY OF AMERICA
VOL. 71, PP. 363-398, 34 FIGS. APRIL 1960

DIASTROPHISM AND MOUNTAIN BUILDING

BY MARLAND P. BILLINGS

(Address as Retiring President of The Geological Society of America)

ABSTRACT

For many years the terms orogeny and mountain building have been used so loosely that they no longer convey definite meanings. Because of this lack of precision, hypotheses of diastrophism are often based on false premises.

Folding and thrusting, often referred to as tectogenesis or orogeny, is best displayed by stratified rocks. Some geologists believe that folds and thrusts are due to vertical movements accompanied by lateral spreading, that the strata are stretched an amount commensurate with the intensity of the folding, and that the opposite sides of the sedimentary packet do not move toward each other. Most geologists, however, agree that during folding and thrusting the strata are shortened and that the two opposite sides of the sedimentary packet move toward each other by an amount commensurate with the intensity of the folding. But it is not clear to what extent the entire crust in the deformed belt is shortened. In one extreme view, the two opposite ends of the deformed belt do not move toward each other, and the folds and thrusts result from gravity sliding. At the other extreme, the entire crust is believed to be shortened to the same extent as the sedimentary strata.

An excellent example of broad vertical movements (epeirogenesis) that has never been sufficiently emphasized is in eastern North America, involving the Appalachians, Coastal Plain, and Continental Shelf. During the Mesozoic and Cenozoic the Fall-Line surface was depressed as much as 20,000 feet beneath the Continental Shelf, whereas it was uplifted at least 8000 feet over the Appalachians. The northeastern two-thirds of the Appalachian-Ouachita belt has been going up since the Jurassic, whereas the southwestern third has been going down. Thus the present Appalachians are unrelated to the late Paleozoic folding. Certain metamorphic minerals—such as kyanite—or certain metamorphic assemblages—such as jadeite and quartz—form at confining pressures found only at depths of tens of miles, implying tremendous erosion wherever such minerals or assemblages are exposed.

Broad vertical movements, accompanied by high-angle faulting, are illustrated by the fault-block mountains of the Basin and Range Province and by such features as the Rhine graben and the Rift Valleys of Africa.

Although the nature of the displacement along the San Andreas fault has been known for more than 50 years, only in recent decades have other large strike-slip faults been recognized. But it is now the fad to assign all kinds of faults and even nonexistent faults to the strike-slip category. In recent years seismologists have emphasized the importance of strike-slip faults. The author suggests that in the Fairview Peak-Dixie Valley, Nevada, earthquakes there is evidence that strike-slip movements are invading an area previously characterized by Basin-Range structure. The geologic record indicates that large strike-slip faults have been distinctly subordinate to folding, broad vertical movements, and broad vertical movements accompanied by high-angle faulting.

Possible displacement of the crust or the entire earth relative to the axis of rotation has been emphasized in recent years. Continental drift, if it occurs, is one such type of movement. Slipping of the entire crust over the mantle is another. Much research has been accomplished in paleomagnetism in recent years, but the data are too scanty and conflicting to permit any definite conclusions.

Among the possible causes of diastrophism are (1) contraction of the earth, (2) convection currents, (3) formation of large pockets of magma, (4) sialic material leaking out of the mantle, (5) conversion of sial to mantle by change of low-pressure minerals to high-pressure minerals, or the reverse, and (6) serpentinization or deserpentinization of the upper part of the mantle.

Mountain building is merely one manifestation of vertical movements of the crust. In the past mountain building has been erroneously considered by many to be primarily the result of folding and thrusting. Certainly many modern ranges are the result of verti-

cal uplift unrelated to folding. Many such uplifts are accompanied by high-angle faulting to produce fault-block mountains. Blocks caught between strike-slip faults may be squeezed upward if the blocks move toward each other. Mountainous uplifts have also resulted from folding and thrusting. Conversely, in some folded belts erosion appears to have kept pace with the rise of the folds so that no mountains developed.

CONTENTS

TEXT

	Page
Introduction	364
Diastrophism	365
Types of diastrophism	365
General discussion	365
Folding and thrusting	366
Broad vertical movements	376
Broad vertical movements accompanied by high-angle faulting	380
Large-scale strike-slip displacements	381
Displacement of the crust or entire earth relative to axis of rotation	387
Hypotheses of diastrophism	389
Mountain building	390
Summary and conclusions	393
References cited	394

ILLUSTRATIONS

Figure	Page
1. Folded and thrust-faulted strata, Appalachian Valley and Ridge Province	367
2. Folded and thrust-faulted strata, Jura Mountains	367
3. Overthrusts of the Glarus district, Switzerland	367
4. Folding by lateral compression	367
5. Possible décollement in the Appalachian Valley and Ridge Province	368
6. Folding by gravity sliding	369
7. Some types of gravitational tectonics	369
8. Relation between shortening, thickness of root, and height of mountains	370
9. Folding in Appalachian Valley and Ridge Province and Appalachian Plateaus	370
10. Wathlingen-Hänigsen salt dome, Germany	371
11. Structure resulting from vertical rise of migmatite in East Greenland	372
12. Chester dome, southeastern Vermont	373
13. Injection folding	373
14. Block folding, Causcasus Mountains, Noukha area	373
15. Block folding, Caucasus Mountains, Mt. Dibrar area	373
16. Folding by vertical uplift and lateral spreading	374
17. Effect of type of folding on thickness and circumference of crust	375
18. Map showing deformation of Fall-Line surface in eastern North America	377
19. Cross section showing deformation of Fall-Line surface in eastern North America	378
20. Buried and emergent Appalachians	379
21. Stability fields of some high-pressure minerals	380
22. Horst of the Ruby-East Humboldt Range, Nevada	381
23. Rhine graben	382
24. Alpine and related faults of New Zealand	383
25. Magnetic anomalies associated with Murray fracture zone, eastern Pacific Ocean	384
26. Fault-plane solutions based on data for *P* waves	385
27. Russian fault-plane solutions based on data for *S* waves	386
28. Diastrophism associated with Fairview Peak-Dixie Valley earthquakes, Nevada	387
29. Nature of net slip on surface faults during Fairview Peak-Dixie Valley earthquakes, Nevada	388
30. Variations of magnetic declination and inclination within historic time at London, Boston, and Baltimore	389
31. Structural trends in California	392
32. Shutter ridges	393
33. Buckling associated with strike-slip faulting	393
34. Thrust fault associated with strike-slip faulting	393

TABLES

Table	Page
1. Tectonic processes, after Von Bubnoff	365
2. Tectonic processes, after Sonder	366
3. Types of diastrophism	366

Introduction

"Diastrophism is a general term for the process or processes of deformation of the earth's crust. Products of diastrophism are continents, plateaus and mountains, ocean beds and valleys, faults and folds" (Gilbert, 1890, p. 3). Contrasting, although related, geological processes are volcanism (including both extrusion and intrusion), erosion, and sedimentation.

For many years the thinking of the geological profession has been impaired by numerous misconceptions concerning diastrophism. The

terms orogeny and mountain building are often used so loosely that they no longer have meaning. Hypotheses of orogeny, mountain building, and diastrophism are often concerned with irrelevant subjects and fail to treat the main problems. It is hoped, therefore, that this paper will clarify the problems of diastrophism and mountain building.

Professors Francis Birch and John Miller kindly read an early draft of this paper and made valuable suggestions for its improvement. Professors George C. Kennedy and Leon Knopoff sent copies of their manuscripts prior to publication. Dr. Erwin Raisz graciously drafted most of the illustrations at a time when he was heavily engaged with other work.

DIASTROPHISM

Types of Diastrophism

General discussion.—For many years, geology, especially in the English-speaking countries, has been limping along with a two-fold classification of diastrophism: epeirogeny and orogeny. It is generally agreed that epeirogeny refers to vertical movements affecting areas the size of continents or parts of continents (Gilbert, 1890, p. 3, 340). But orogeny, literally signifying "mountain genesis", has been used in a variety of ways, primarily because of a misconception of how mountains are formed. Because most mountain ranges are characterized by folds and, in many instances by thrusts, it was assumed that the folding and thrusting produced the mountains. It was also a common practice—in the Appalachians, for example—to restore in imagination the now eroded strata and assume that former mountains towered to superalpine heights.

Most geologists use the term orogeny in much the same sense as Upham (1894, p. 383), who said:

> "Previously the correlative terms orogeny and orogenic had come into use, denoting the process of formation of mountain ranges by folds, faults, upthrusts, and overthrusts, affecting comparatively narrow belts and lifting them in great ridges. . . ."

More recently, Holmes (1945, p. 106) has said:

> "... great mountain-building movements have been particularly active at certain times in the earth's history, during which the rocks of long belts of the crust were intensely compressed. Earth movements of this kind, and also the resulting folded belts are described as orogenic . . . ."

One of the principal purposes of this paper is to demonstrate that many modern mountain ranges are not the result of folding and thrusting.

TABLE 1.—TECTONIC PROCESSES
(After Von Bubnoff)

Tectogenesis	Diktyogenesis	Epeirogenesis
Narrow span	Intermediate span	Great span
Structural change	Structural change	Structure retained
Episodic	Episodic and secular	Secular
Not reversible	Partly reversible	Reversible
Not autonomous	Not autonomous	Autonomous
Surficial	Deep	Deep

Von Bubnoff (1954, p. 49) has classified diastrophic processes into three categories (Table 1). Epeirogenesis is used by Von Bubnoff in much the same sense as in the United States; it refers to slow vertical movements affecting large areas. Tectogenesis refers to folding and thrusting; it affects relatively narrow belts of the earth, is episodic, and nonreversible. In the United States, the word orogeny is often used for what Von Bubnoff calls tectogenesis. Diktyogenesis—literally meaning "net building" or "frame building"—refers to vertical movements affecting areas of lesser size than those affected by epeirogenic movements. Von Bubnoff emphasizes that diktyogenesis is an independent diastrophic process and is not a variety of the other two. According to him, most modern mountain ranges, such as the Appalachians, Colorado Front Range, Vosges, and Black Forest, are the result of diktyogenesis and are not the direct result of tectogenesis. Although there is some merit to Von Bubnoff's terminology, Gilbert (1890, p. 340) intended that the term epeirogenic should apply to what has been called diktyogenesis. He says: "The concavity of the Bonneville Basin, whereby it is constituted an area of internal drainage, is epeirogenic."

TABLE 2.—TECTONIC PROCESSES
(After R. A. Sonder)

Nature of activity	Principal processes	Tectonic result
1. Orogenesis	Lateral compression with formation of a local crustal excess	Buckling, folding, overthrusting
2. Epeirogenesis	Vertical crustal movements, which are associated with crustal bending, but without large internal structural changes in the crust	Transgression, regression, formation of geosynclines and geanticlines; the movements produce bedding in the sediments
3. Regmagenesis	Tangential stress of the crust	Origin of radial shear fractures, opening of crustal fractures with magmatic infiltration; formation and retention of regmatic fracture systems; horizontal displacement along major fractures
4. Taphrogenesis	Radial movements of the crust, along steep fractures	Vertical faults, formation of horsts and graben, step faults, etc.
5. Phorogenesis	Tangential displacement (drift movements) of the solid crust over the asthenosphere	No visible tectonic change in the crust, but changes in geographic latitude and longitude
6. Pyrogenesis	Intrusion (plutonism) and extrusion (volcanism) of magma and magmatic derivatives	Intrusive rocks and dike rocks, volcanoes, plateau eruptions, hydrothermal veins, hot springs

TABLE 3.—TERMINOLOGY FOR VARIOUS TYPES OF DIASTROPHISM

Terminology of this paper	Terms used by others
Folding and thrusting	Tectogenesis, orogeny
Broad vertical movements	Epeirogenesis, diktyogenesis
Broad vertical movements with high-angle faulting	Taphrogenesis
Large-scale strike-slip displacements	Regmagenesis
Slipping of crust over mantle	Phorogenesis

R. A. Sonder (1956, p. 13), as shown in Table 2, has a more elaborate classification of diastrophic processes. Horizontal compression, producing folds and overthrusts, is referred to as orogenesis. Vertical movements affecting large areas, and involving warping but not faulting, are called epeirogenesis. If such movements are accompanied by large high-angle faults this process is called taphrogenesis. The term regmagenesis was introduced by Sonder (Sonder and Vening Meinesz, 1947, p. 939) for large steeply dipping fractures along which displacement, if it occurs, is strike slip. Phorogenesis refers to the sliding of the crust over the mantle, either in its entirety or piecemeal, as in continental drift.

Although there may be some advantage in using a terminology based on Greek roots, employing the terms proposed by Von Bubnoff and Sonder, the author prefers to use the English terminology shown in Table 3.

Folding and thrusting.—In this section of the paper we are concerned with folds, fold systems, thrusts, and overthrusts. This type of diastrophism, called tectogenesis by Von Bubnoff (1954), has been referred to as orogeny by R. A. Sonder (1956) and by many in this country. Examples of folds and related thrusts are known from all over the world. Figure 1 illustrates the structure of the Valley and Ridge Province of the Appalachians (Cooper,

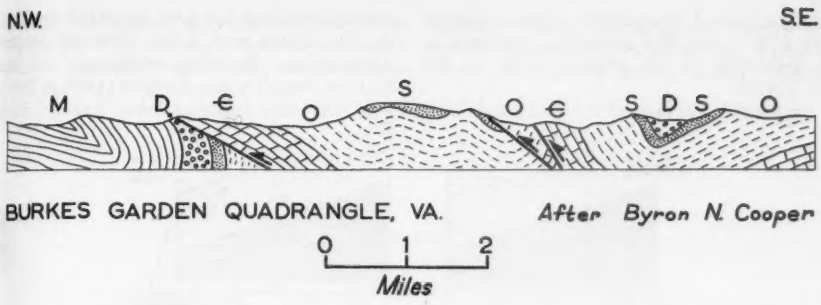

FIGURE 1.—FOLDED AND THRUST-FAULTED STRATA, APPALACHIAN VALLEY AND RIDGE PROVINCE

€ = Cambrian, O = Ordovician, S = Silurian, D = Devonian, M = Mississippian. Symbols used for various systems do not necessarily have any lithologic significance.

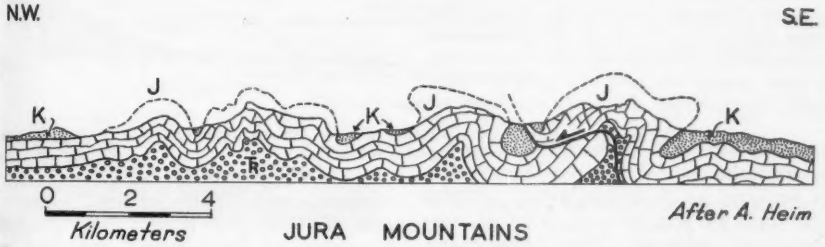

FIGURE 2.—FOLDED AND THRUST-FAULTED STRATA, JURA MOUNTAINS

Tr = Triassic, J = Jurassic, K = Cretaceous. Symbols used for various systems do not necessarily have any lithologic significance.

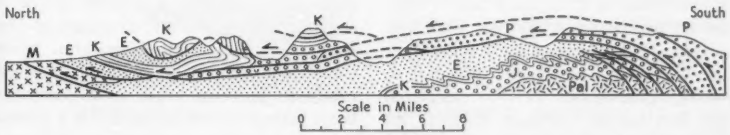

FIGURE 3.—OVERTHRUSTS OF THE GLARUS DISTRICT, SWITZERLAND

Pal = Paleozoic, P = Permian, J = Triassic and Jurassic, K = Cretaceous, E = Eocene, M = Miocene. (After J. Oberholzer). Symbols used for various systems do not necessarily have any lithologic significance.

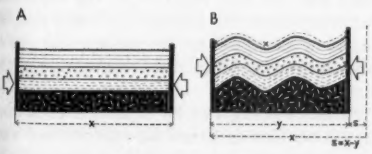

FIGURE 4.—FOLDING BY LATERAL COMPRESSION

A. Before folding. B. After folding. x = width before folding, y = width after folding. s = shortening in miles or kilometers.

1944). Figure 2 represents the structure of the Jura Mountains (Heim, 1919, vol. I, Table XXIII). Figure 3 shows the great overthrusts of the Glarus district of the Alps (Oberholzer, 1933).

It has generally, but not universally, been agreed that such folds involve shortening, at least of the visible rocks near the surface of the earth (Fig. 4). The shortening, s, in miles or kilometers, is the difference between the original width of the packet of sediments (x in Fig. 4) and the width after folding (represented by

y). The ratio of shortening to original width is $s/x = x - y/x$. The shortening, expressed as a percentage of the original width, is 100 $(x - y)/x$.

In the different parts of the Valley and Ridge Province the shortening ranges from zero to 40 per cent; the average is about 30 per cent (Chamberlin, 1910; Cloos, 1940; Philip Fowler, 1948, Term paper, Harvard Univ.). Mansfield (1927, p. 388) gave 21 per cent shortening for southeastern Idaho from folding alone, but obtained 52.3 per cent if the net slip along the Bannock overthrust is 12 miles. Fowler (1948) calculated 25 per cent for the San Francisco folio (Lawson, 1914). An average for the Jura Mountains is 33 per cent (Heim, 1919, vol. I, p. 649–651). Chamberlin (1919) calculated only 8 per cent for the Colorado Rockies, but it is now known that the structure there is more complex than he assumed. The most conservative figure for the Alps, by Heim (1921, vol. II, p. 46–51), assumes 385 km was compressed into 135 km, giving a shortening of 250 km or 65 per cent. A more recent figure by Cadisch (1946) says 630 km was compressed into 150 km, giving a shortening of 480 km or 76 per cent.

To what extent has the entire crust, down to the Mohorovičić discontinuity, been shortened? In recent years a number of geologists have emphasized that folding and thrusting appear to be confined to the upper part of the crust. For half a century the Jura Mountains (Billings, 1954, p. 60) have been considered an example of superficial folding in which the crystalline basement does not participate. A similar hypothesis has been suggested by some for the Valley and Ridge Province of the Appalachians. Referring specifically to the southern Appalachians, Rodgers (1949, p. 1653) says that some geologists "have reasoned from

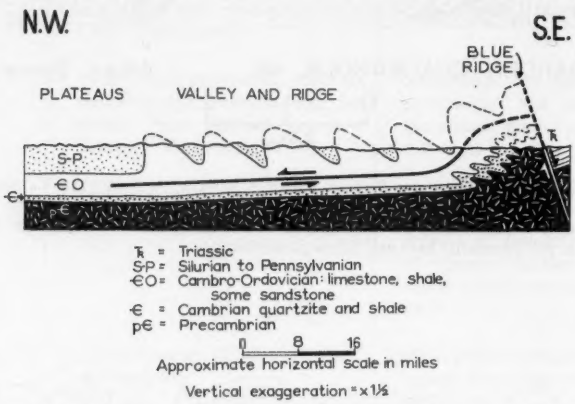

FIGURE 5.—POSSIBLE DÉCOLLEMENT IN THE APPALACHIAN VALLEY AND RIDGE PROVINCE

the great low-angle thrust faults of the area . . . that the Paleozoic rocks . . . were stripped completely off the basement and piled up against the unyielding plateau. . . ."

The Applachians cannot be a simple case of the Paleozoic sediments sliding over an unyielding basement. The Precambrian crystalline basement is intimately involved in the folding of such parts of the Appalachians as the Blue Ridge and the Green Mountains. Moreover, the contact between the Paleozoic and the Precambrian in those areas is an unconformity, not a surface of "shearing off." If a décollement is present in the Appalachians, it must lie in the Cambrian or Ordovician strata (Fig. 5). In the eastern part of the section it could, as shown, come to the surface between the Blue Ridge and the first syncline to the northwest that brings down the Silurian. It is also possible that it never comes to the surface and passes beneath the Cambrian and Precambrian of the Blue Ridge.

Surficial folding can be explained in several ways. One idea is based on experiments with pressure boxes—something pushes one end of a packet of sediments (Billings, 1954, p. 227). A second possible explanation is the now popular hypothesis of gravity sliding (de Sitter, 1956, p. 266–291; Bucher, 1956). As shown in Figure 6, sediments on top of an uplifted area slide down the flanks and crumple (Rich, 1951;

Pierce, 1957). Thus, although the rocks in the sliding block are shortened, the basement is not. Italian geologists believe that masses of rock have traveled many tens of kilometers as the result of a progressive displacement of the zone of uplift (Maxwell, 1953; Billings, 1954, p. 235).

But the concept of gravity sliding cannot be indiscriminately applied everywhere. It has already been pointed out that the Precambrian crystalline basement is intimately involved in the folding of the Appalachians. Similarly, the crystalline basement participates in the great folds of the Colorado Rockies. Even in the Alps, the pre-Triassic crystalline basement is involved in the huge recumbent anticlines of the Pennine nappes. To many this implies horizontal compression involving the basement. Some advocates of gravity sliding, however,

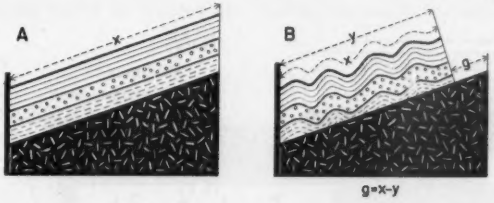

FIGURE 6.—FOLDING BY GRAVITY SLIDING

A. Before sliding. B. After sliding. x = width of strata before folding; y = width of folded belt after sliding; g = gap left at upper end of sliding block.

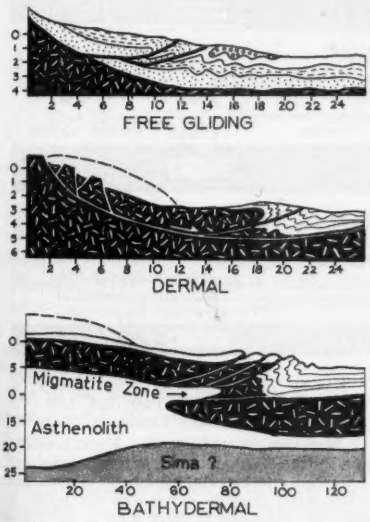

FIGURE 7.—SOME TYPES OF GRAVITATIONAL TECTONICS

Distances in kilometers. Black with white hachures represents basement. After Van Bemmelen

such as Van Bemmelen (1954, p. 96), believe that gravity sliding is not necessarily confined to the superficial cover of sedimentary rocks. According to him the basement participates in dermal gliding, and even the deepest parts of the crust are involved in bathydermal gliding (Fig. 7).

Two major questions have not yet been answered satisfactorily by the advocates of extensive gravity sliding. If the rocks are so weak that they flow downhill like paste, how is it possible to retain rugged mountain topography? Moreover, how great an angle of slope is necessary to permit gravity sliding? Few data are available. In such cases as the Jura Mountains, the slope of the supposed surface of sliding is now inclined toward the south, whereas, to explain the movement, it should incline northward.

We conclude, therefore, that field geology indicates that the crystalline basement often participates in the folding. It is clear that folding is not confined to the sedimentary cover. But it is difficult to accept Van Bemmelen's thesis that the basement complex may be sufficiently weak to be deformed by gravity sliding. In general, gravity sliding is probably confined to the sedimentary cover; wherever the basement is involved in the folding, some mechanism other than gravity sliding must be sought.

If the entire crust in a deformed belt were shortened during folding, a root should have formed—unless deformation were so slow that contemporaneous uplift and erosion prevented its development. The geophysical evidence for a root may be gravitational (Daly, 1940), seismic (Gutenberg, 1943, 1957), or geothermal (Birch, 1950). Three facts should be emphasized, however: a root formed during past de-

formation may now have disappeared; conversely, the root under a modern mountain range may be of recent development and unrelated to the folding; finally, the formation of

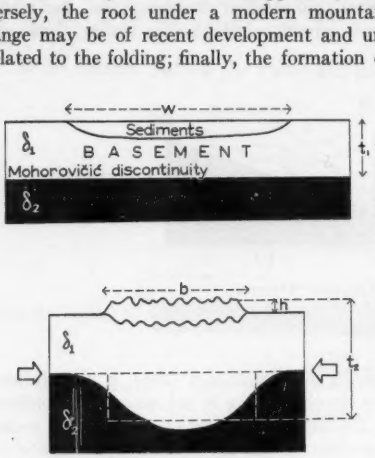

FIGURE 8.—RELATION BETWEEN SHORTENING, THICKNESS OF ROOT, AND HEIGHT OF MOUNTAINS

δ_1 = density of crust (basement and sediments), δ_2 = density of mantle; t_1 = thickness of crust before folding; t_2 = average thickness of crust in folded belt after folding; h = average height of mountains.

a root might be due to some process that produced the root and caused the folding.

If the entire crust is compressed to the same extent as the geosynclinal sediments, as shown in Figure 8, and if deformation is very rapid compared to erosion and uplift,

$$t_2 = \frac{t_1}{1 - p} \qquad (1)$$

where t_1 is the thickness of the crust before folding, t_2 is the thickness of the crust in the deformed belt after folding, and p is the ratio of the shortening to the original width—that is, $x - y/x$ in Figure 4.

If we assume perfect isostasy and that the folded block floats, only a small percentage of the increase in thickness is represented by an increase in altitude:

$$h = \left(\frac{\delta_2 - \delta_1}{\delta_2}\right)(t_2 - t_1) \qquad (2)$$

where h is the increase in altitude, δ_2 is the density of the subcrustal material, and δ_1 is the density of the crust.

Let us now consider the Valley and Ridge Province of the Appalachians, keeping these equations in mind. In western Pennsylvania the restored top of the Pennsylvanian rocks in the Plateaus is a few thousand feet above sea level (Fig. 9 A). But in the Valley and Ridge Province this same horizon, if restored, rises to

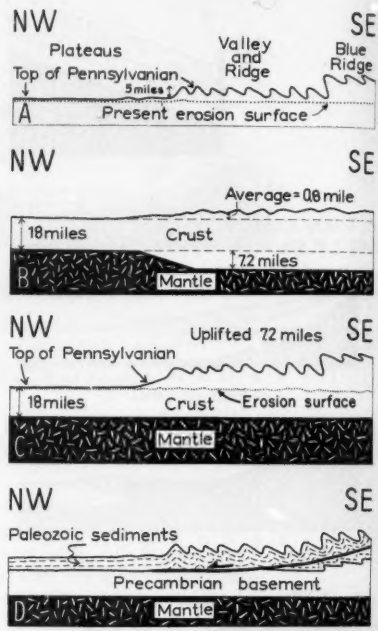

FIGURE 9.—FOLDING IN APPALACHIAN VALLEY AND RIDGE PROVINCE AND APPALACHIAN PLATEAUS

A. Structure at present. B. Hypothetical relations immediately after late Paleozoic folding if a root formed due to compression. C. Hypothetical relations after root is eliminated by uplift and erosion. D. Relations if there were a décollement and no root was produced.

heights of 5 miles above sea level over the anticlines, although it is near sea level in some of the deeper synclines. The average uplift of the top of the Pennsylvanian is 2½ miles. Presumably the relative positions of the strata in the Plateaus and in the Valley and Ridge are inherited from the Appalachian revolution.

Let us assume that the youngest rocks were near sea level at the beginning of the folding, that the crust prior to the folding was 18 miles thick (including 5 miles of Paleozoic sediments), that the average density of the crust was 2.7, that the density of the mantle was 3.0, and that the shortening was 30 per cent. If folding were very rapid, the crust would be thickened to 26 miles, of which 7.2 miles would form a

root, and 0.8 mile would be the average height of the land mass above sea level (Fig. 9 B). Eventually this root would be eliminated by uplift, but in that case the strata on the east margin of the Plateaus would be dragged upward 7.2 miles (Fig. 9 C), and the Valley and Ridge would go up a like amount. Even if folding were so slow that gradual uplift prevented the formation of a root, and erosion prevented the development of mountainous topography, the strata on the east margin of the Plateaus would be gradually dragged upward in a similar way. But the actual profile (Fig. 9 A) suggests that the hypothesis represented by Figures 9 B and 9 C is incorrect.

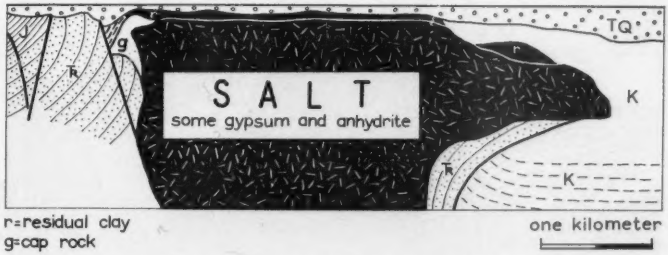

FIGURE 10.—WATHLINGEN-HÄNIGSEN SALT DOME, GERMANY
Tr = Triassic, J = Jurassic, K = Cretaceous, TQ = Tertiary and Quaternary. After Bentz

Let us see what would happen in case of a décollement in the Appalachians (Fig. 9 D). The packet of sediments, originally 5 miles thick, would, after a shortening of 30 per cent, have an average thickness of about 7 miles. If no erosion took place during the folding, the crust would be thickened by 2 miles, the base of the crust would sink 1.8 miles, and the average uplift would be 0.2 mile. This is not consistent with the average uplift shown in Figure 9 A, which is 2½ miles. If erosion kept pace with folding, no extra load would develop on the crust, the base of the crust would not sink, and there would be no net uplift. The structure shown in Figure 9 A would be the result.

The above analysis suggests that the Valley ad Ridge Province is underlain by a décollement, during the formation of which erosion kept pace with the folding and no mountains formed.

To calculate the depth of folding (Billings, 1954, p. 60–61) in the Valley and Ridge Province the following data may be used: present width, 66 miles; original width, 94 miles (assuming shortening of 30 per cent); and average uplift 2½ miles (Fig. 9 A; *see also* Chamberlin, 1910). The calculated depth of folding is 6 miles, essentially the same as the thickness of the Paleozoic section. Thus the results are consistent with a décollement near the base of the sedimentary section. Chamberlin (1910) calculated a much higher value for the average depth of folding, partly because he used too small a figure for the shortening.

Thus several lines of evidence support the idea that in the Valley and Ridge Province the folding was largely confined to the Paleozoic sediments and that the deeper crust was not involved. (*See* also Cloos, 1940, p. 846.) Even if the folding in the Valley and Ridge is surficial and may result from gravity sliding, a similar hypothesis need not apply to the other provinces of the Appalachian Highlands.

Let us now turn briefly to the Alps. Moreover, let us take the most conservative figure for the shortening, 65 per cent (Heim, 1921, vol. II, p. 46–51). If the crust prior to folding were 30 km thick, after folding it would be 85 km thick, and the mountains would stand 5.5 km high. But the crust beneath the Alps is only 40 km thick at present (Daly, 1940). In other words, the added root beneath the Alps is much less than one would expect from the observed shortening. As we shall see below, the reverse is the case in some other ranges.

So far, we have tacitly assumed that folding and thrusting involved shortening of the folded strata, even though gravity sliding from uplifted areas might be the fundamental cause of the deformation. Some geologists question whether any net shortening is involved in folding and thrusting. That is, they believe

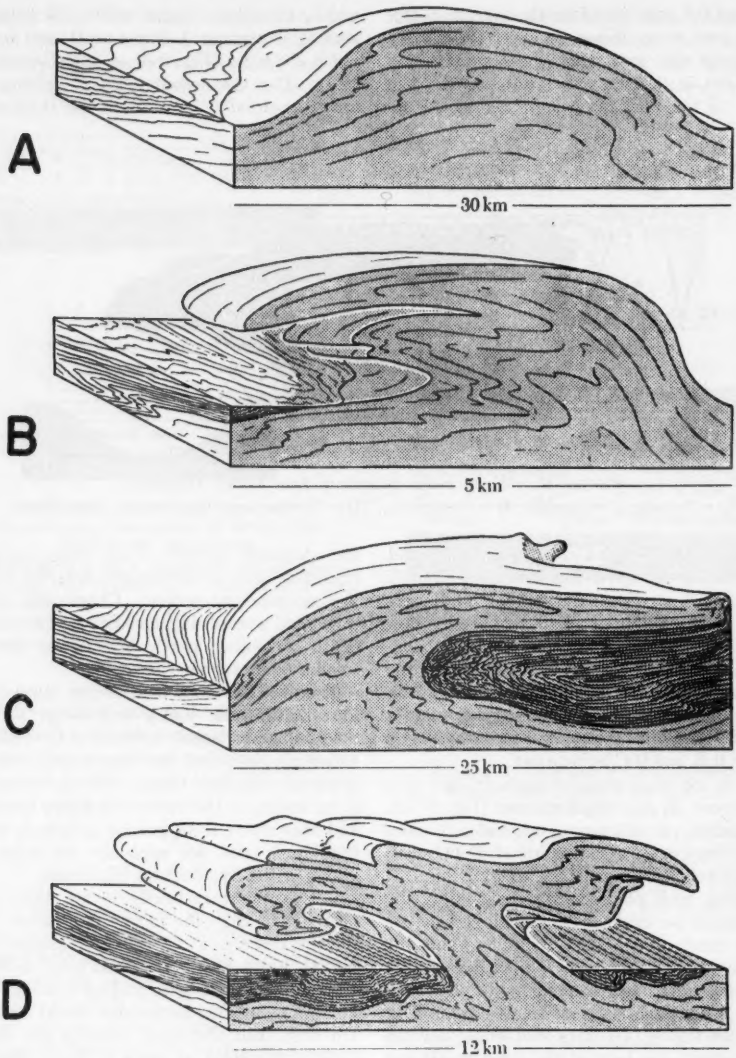

FIGURE 11.—STRUCTURE RESULTING FROM VERTICAL RISE OF MIGMATITE IN EAST GREENLAND

A. Dome. B. Forehead. C. Sheet. D. Mushroom. Schematic, with vertical exaggeration. Lighter gray = migmatite. Darker gray = metamorphic rocks. After J. Haller.

that the opposite ends of the folded packet of sediments have not moved toward each other. Is it possible that much folding is the direct result of vertical movements? Let us pursue this problem further.

There is general agreement that salt domes—at least, in such places as the Gulf Coast of the United States (Halbouty and Hardin, 1959) and northwest Germany (Richter-Bernburg and Schoot, 1959)—rise because of the gravitational instability of a low-density plastic stratum buried by heavier rocks (Nettleton,

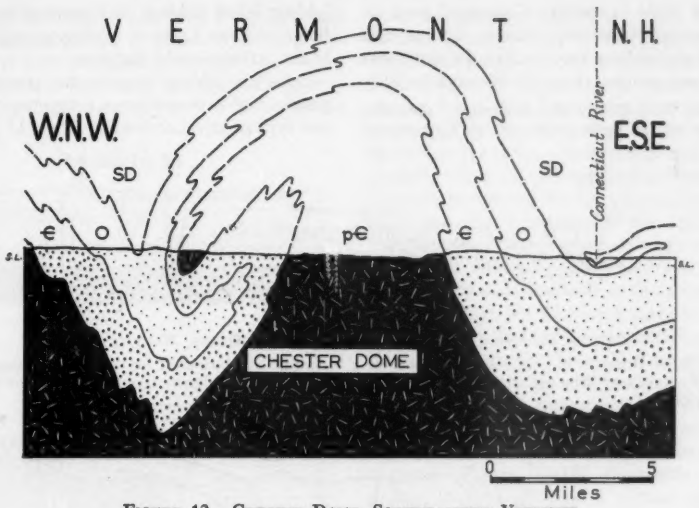

FIGURE 12.—CHESTER DOME, SOUTHEASTERN VERMONT

pC = Precambrian, € = Cambrian, O = Ordovician, SD = Silurian and Devonian. After Thompson and Rosenfeld.

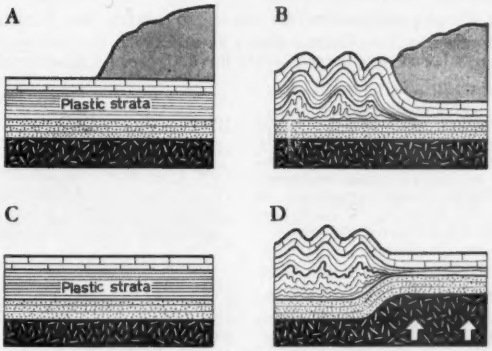

FIGURE 13.—INJECTION FOLDING

A and B, downward pressure because of extra load. C and D, upward pressure because of local uplift of basement. After Beloussov.

1934). In general, sediments must be buried at least 1500 feet if they are to be compacted enough to be heavier than rock salt (Carey, 1954, p. 79). Whether such deformation should be classified as "orogenic" is a problem in semantics. Certainly many geologists would consider this type of deformation as "nonorogenic." This is because they tacitly assume that "orogeny" results from horizontal compression.

Salt-dome tectonics demonstrates that vertical movements may be converted into horizontal displacements. As one example, we may cite the Wathlingen-Hänigsen salt dome, 120 km south of Hamburg, Germany (Bentz, 1949, Tafel II). Oval in plan, it is nearly 4000 m long in a north-northeast direction and nearly 2000 m wide. As shown in Figure 10, there is a pronounced overhang, beneath which an overturned limb of Triassic rocks is thrust over Cretaceous. At depth, the salt rose because it was lighter than the surrounding sediments. Nearer the surface, the salt, being heavier than the surrounding sediments (Carey, 1954, p. 79), spread laterally.

Haller (1956) has suggested that great re-

cumbent folds in eastern Greenland may involve no net shortening; that is, the opposite sides of the sedimentary packet did not move toward one another (Fig. 11). He says (p. 159):

"Under the influence of synorogenic Caledonian granitization, a thick sequence of Precambrian sediments in East Greenland was folded and in the deeper parts of the mountain range was completely transformed. Selective addition of material caused a central area to swell up to form domes and overturned structures. These bodies, granitized in place and of domelike, forehead-like, or mushroom shape, formed the entire active part of the orogen."

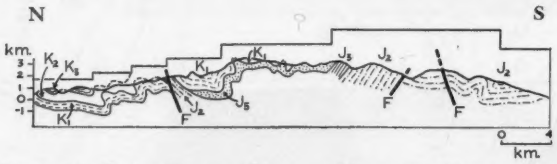

FIGURE 14.—BLOCK FOLDING, CAUCASUS MOUNTAINS, NOUKHA AREA

J_2, J_3, J_5, = Jurassic; K_1, K_2, K_3, = Cretaceous. F = faults. Symbols used for various formations do not necessarily have any lithologic significance. Heavy line above section shows steplike character of structure. After Beloussov.

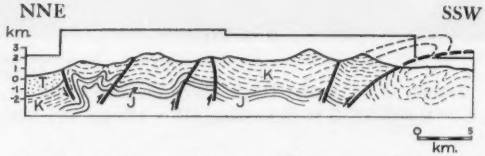

FIGURE 15.—BLOCK FOLDING, CAUCASUS MOUNTAINS, MT. DIBRAR AREA

J = Jurassic, K = Cretaceous, T = Tertiary. Heavy lines are faults. Symbols used for various systems do not necessarily have any lithologic significance. Heavy line above section shows steplike character of structure. After Beloussov.

Even in the Appalachian region it has been suggested that some of the domes and related folds are due to vertical movements analogous to the rise of salt domes. In eastern Vermont, Thompson and Rosenfeld have suggested that the Chester dome (Fig. 12) resulted from the vertical uplift of a plastic core (Billings, Rodgers, and Thompson, 1952). But recent studies by Rosenfeld (personal communication) show that these vertical movements were preceded by recumbent folds indicative of significant horizontal movements.

Carey (1954, p. 67) says: "The universal contortion of Archean gneisses, which is usually regarded as evidence of intense shortening, does not necessarily imply much shortening. . . ."

Beloussov (1959) suggests that much folding, even that of the Appalachian and Alpine types, is the direct result of vertical movements. He recognizes three types of folding: injection folding, block folding, and general crumpling. Some of these types of folding are represented in the accompanying diagrams.

Injection folding requires the presence of a plastic bed between more competent beds. In one type of injection folding (Figs. 13 A and 13 B) a load in one part of an area causes subsidence, thus forcing the incompetent bed to flow plastically to another area. In another type of injection folding (Figs. 13 C and 13 D) the more plastic bed on the crest of a rising anticline is squeezed toward the syncline.

Block folding is illustrated by a cross section (Fig. 14) from the southern slope of the southeast part of the Main Caucasus Ridge (Beloussov, 1959, p. 5). The idea that the structure is the result of vertical movements is based on the fact that the folds rise in a series of steps, as shown in the upper part of the diagram. Strongly overturned folds may be observed at the southwestern end of a similar section, from the same region (Fig. 15). An important part of the theory is that a block rising along steep faults or flexures may spread laterally toward or over the lower block.

What Beloussov calls general crumpling results if there is a large amount of lateral spreading (Fig. 16). The two opposite sides of the folded belt have not moved toward each other. The distance, measured along the beds, however, is much greater than prior to the deformation. The beds have been stretched (Beloussov, 1959, p. 17). If the principle were

to be applied to the Valley and Ridge province of the Appalachians, it would mean that the beds have been stretched 30 per cent.

At least four tests may be applied to Beloussov's hypothesis. One test concerns the extent

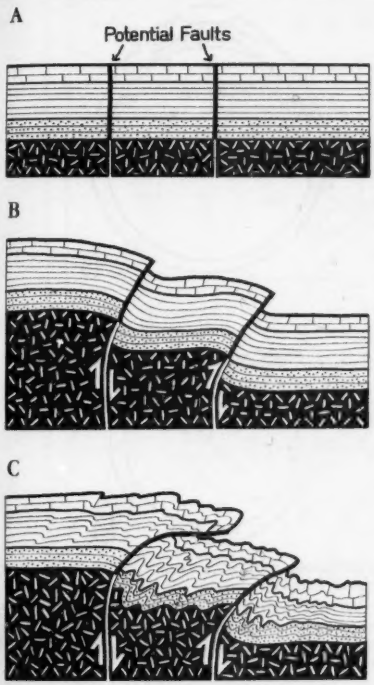

FIGURE 16.—FOLDING BY VERTICAL UPLIFT AND LATERAL SPREADING

A, B, and C are successive stages. The beds in the lowest diagram should be thinner than those in the top diagram, so that the total volume is constant. After Beloussov.

to which lateral spreading can occur. Salt-dome tectonics demonstrates that, although vertical movements may be converted into horizontal thrust (Fig. 10), the amount is limited. In an area such as the Valley and Ridge Province, the pattern shown by the folds is readily explained by shortening and axial divergence (Cloos, 1940) but is very difficult to explain by vertical movements. Thirdly, the hypothesis, as Beloussov clearly recognizes, involves stretching of the beds as much as 30 per cent. But in many places, fossils, cross bedding, ripple marks, and other sedimentary features give no evidence of such stretching. Fourthly, in many tectonic belts, the axial-plane cleavage has a relatively uniform strike and dip; this may be reconciled with a regional compressive force, but it is difficult to understand if the compression were merely incidental to vertical movements.

We are now prepared to summarize the various ideas that have been proposed to explain folding and thrusting. Most geologists agree that the strata are shortened and that the opposite sides of the sedimentary packet are now closer together by an amount commensurate with the intensity of the folding and thrusting. But some geologists, notably Beloussov, do not agree with this. The extent to which the entire crust is involved in the shortening is certainly debatable. The ideas that are in vogue at the present time are summarized diagrammatically in Figure 17. Figure 17 A represents the concept that the folds and thrusts are the direct result of vertical movements; the beds are stretched, but lateral spreading may or may not occur. The radius of the earth remains unchanged. Figure 17 B represents gravity sliding; the beds slide off a central uplift, and the shortening is equal to the gap on top of the uplift. The beds are not stretched, and the radius of the earth remains the same. In Figure 17 C the entire crust in the deformed belt is shortened, and a root is produced. A gap in the crust is equal to the shortening; instead of a gap, thinning might occur. The radius of the earth remains unchanged. Figure 17 D is similar, except that the radius and circumference of the earth become smaller; this is the classical contraction hypothesis.

Agreement is lacking, of course, on the evaluation of these various hypotheses. Most geologists, however, would probably agree that the type of folds found in the Valley and Ridge, Jura, and Alps is the result of shortening even though they may not agree on whether the shortening involves the entire thickness of the crust. Several lines of evidence indicate, however, that horizontal compression involving the basement is the principal factor in folding and thrusting. The long, narrow, and sinuous pattern of folded belts, coupled with the fact that the basement is so often involved, is one piece of evidence. Field observations suggest that slopes high enough to permit extensive gravity sliding were not commonly available. Gravity sliding, important though it may be in some instances, is an incidental process. Likewise, the vertical rise of plastic, magmatic and migmatic material is a supplementary process. When vertical uplift accompanies folding, we should consider the possibility that some or all of the uplift is due to a process other than the rise of anticlines or the formation of a root due to shortening.

Broad vertical movements.—In studying epeirogenic movements, we are immediately confronted by a dilemma. What is our plane of reference when we say that the land has gone up or down? Usually sea level is our datum. We know, however, that the surface of the sea can fluctuate many hundreds of feet, as, for example, during the Pleistocene (Kuenen, 1950, p. 535–540; Flint, 1957, p. 258–271). Transgressing and regressing seas may result either from vertical movements of the land or vertical shifts in sea level. Similarly, the upper Paleozoic cyclothems of the Midwest, indicating cyclical change from marine to nonmarine conditions, are evidence of a shifting strand line (Wanless and Weller, 1932; Wanless, 1950; Moore, 1950). Extensive dissected erosion surfaces, if not climatic, indicate a relative lowering of base level, which may or may not be sea level.

Fortunately, there are some lines of evidence indicating that the crust itself was moving up or down. Compelling evidence is offered by the sedimentary record in geosynclines and the adjacent cratons. Many of these sediments were deposited in shallow water, but they are many times thicker in the geosynclines than on the craton. This is evidence that the basement on which the geosynclinal sediments were deposited was sinking much more rapidly than the basement under the adjacent craton. Deformed Quaternary shore lines, such as those in Scandinavia, can be explained only by deformation of the crust (Flint, 1957, p. 240–257). River terraces that decline upstream likewise can be explained only by warping (Putnam, 1942). Studies of the Mississippi delta show that more than 500 feet of subsidence has taken place during and since late Quaternary (Fisk and McFarlan, 1955). Recently published data based on geodetic studies in the western half of the European part of the Soviet Union show that different parts of a rising or falling block move at different rates (Meshcheryakov, 1959).

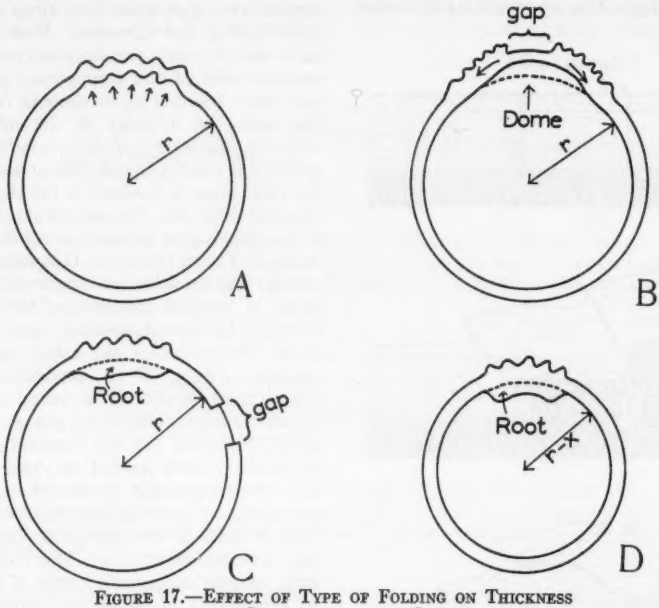

FIGURE 17.—EFFECT OF TYPE OF FOLDING ON THICKNESS AND CIRCUMFERENCE OF CRUST

A. Vertical uplift, with or without lateral spreading. B. Vertical uplift and gravity sliding. C. Horizontal compression, with formation of root, but no change in radius of earth. D. Horizontal compression and formation of root due to contraction of earth. r = radius of earth before deformation; remains unchanged in A, B, and C. x = amount by which radius is reduced; in D the new radius is $r - x$.

As a superb example of epeirogenic movements, we may cite the history of the eastern and southern United States during the late Mesozoic and Cenozoic (Fig. 18). This concerns not only the Appalachian Highlands and their southwesterly continuation as far as the Rio Grande, but also the Coastal Plain and the Atlantic Continental Shelf.

Uplifted and dissected peneplains were recognized in the Appalachians many years ago (Johnson, 1931). The highest surface, developed on crystalline rocks (Fig. 18). Moreover, a well at Cape Hatteras, after penetrating 9878 feet of Cenozoic, Cretaceous, and Jurassic

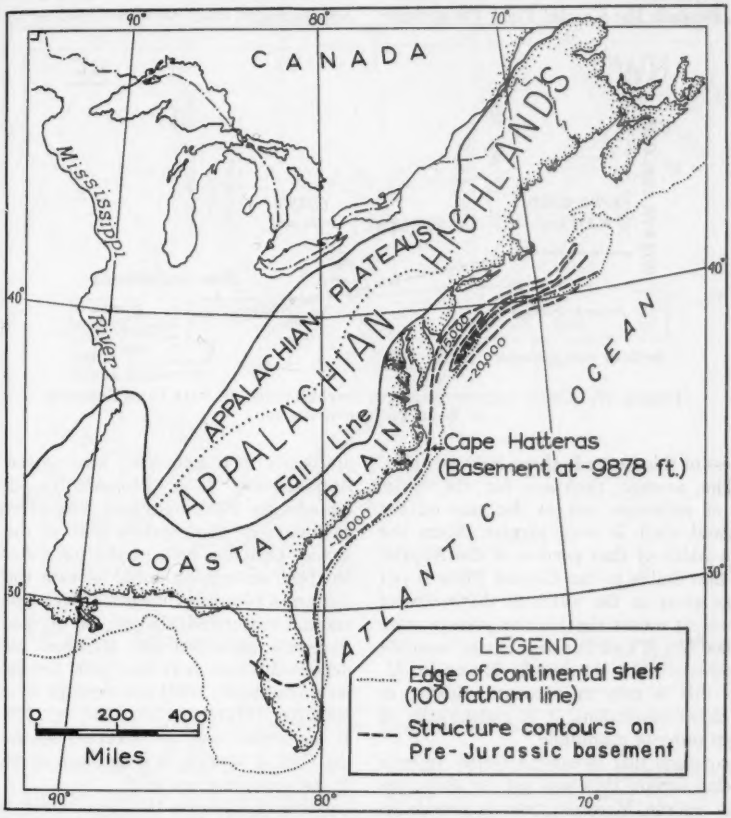

FIGURE 18.—MAP SHOWING DEFORMATION OF FALL-LINE SURFACE IN EASTERN NORTH AMERICA

originally dated as Cretaceous, more recently has been considered to be Tertiary. Such surfaces have been taken as evidence that during the Tertiary the Appalachians have been uplifted 1000 to 2000 feet. It is true that, in recent years, some geomorphologists have cast doubt on the classic interpretation of the geomorphic history of the Appalachians (Hack, 1957, p. 90).

Another line of evidence, however, shows that the Appalachians have been uplifted thousands of feet since the middle of the Mesozoic. The Cretaceous sediments now exposed at the surface on the inner margin of the Coastal Plain were deposited on an erosion surface (?) sediments, encountered the crystalline rocks (Spangler, 1950, p. 105; Swain, 1952). The top of these crystallines is the same surface as that exposed on the inner margin of the Coastal Plain, although it was inundated by transgressing Mesozoic seas earlier than at the Fall Line. Although the Mesozoic erosion surface undoubtedly had some slope, most of the difference in altitude at the present time must be due to differential movements. Seismic evidence 150 miles north of Cape Hatteras shows that this surface is more than 12,000 feet below sea level (Ewing, Worzel, Steenland, and Press, 1950, Pl. 6). Still farther north and northeast (Fig.

18), this surface is more than 20,000 feet below sea level (Cohee, in press).

Most of the sediments of the Atlantic Coastal Plain are clastics derived from the Appalachians. Beneath the Coastal Plain the average thickness of this wedge is about 5000 feet (Fig. 19). The average thickness for the entire wedge of sediments out to the edge of the continental shelf is even greater. Since the average width of that portion of the Appalachians that drains to the Coastal Plain is not quite as great as the width of the wedge of sediments, it means that on the average more than 5000 feet of rock has been eroded from the Appalachians since the middle Mesozoic. Although this is only an estimate, subject to many minor corrections, it is undoubtedly of the right order of magnitude.

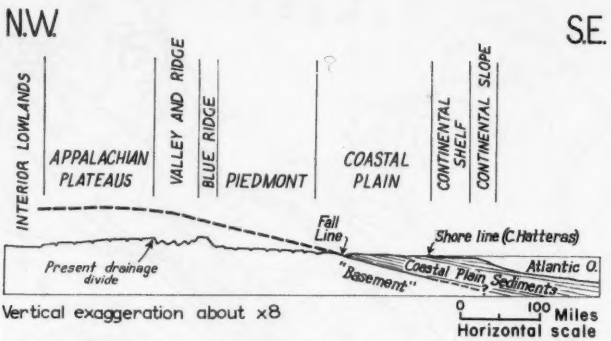

FIGURE 19.—CROSS SECTION SHOWING DEFORMATION OF FALL-LINE SURFACE IN EASTERN NORTH AMERICA

We conclude that in eastern North America an erosion surface that was not far above sea level in middle Mesozoic time is now more than 10,000 feet below sea level under the continental shelf. Over the Appalachians, if it had not been eroded, its average height would be more than 5000 feet above the tops of the present mountains—that is, more than 7000–8000 feet above sea level. This is truly a tremendous amount of crustal deformation in eastern North America during the last 140,000,000 years.

The Appalachian belt has another interesting story to tell. Many have assumed that the Cenozoic uplift of the Appalachians was in some way related to the late Paleozoic folding. Let us see if this is necessarily so.

Although the Appalachians disappear toward the southwest beneath the Coastal Plain sediments in Alabama (Fig. 20), it is generally agreed that the folded belt continues westerly beneath the Coastal Plain sediments and reappears in the Ouachita Mountains, the Marathon Basin, and the Solitario, close to the Rio Grande (King, 1951; Flawn, 1959). The Appalachians, from Newfoundland to Alabama, are nearly 2000 miles long, whereas the buried Appalachians, from Alabama to the Rio Grande, are 1000 miles long. Since the middle Mesozoic the southwestern third of the Appalachian-Ouachita belt, except for a few areas, has been undergoing burial beneath the Mesozoic and Cenozoic sediments. In western Arkansas and western Mississippi, the surface of the basement on which the Mesozoic rocks are deposited is now more than 4000 feet below sea level (Longwell, 1944) and perhaps as much as 8000 feet (Murray *et al.*, 1952, p. 1226–1227). If the surface may be projected southward to the Gulf of Mexico, it is as much as 40,000 or 45,000 feet below sea level.

North of Alabama the Appalachian belt has been rising, whereas to the southwest it has been sinking. In other words, the belt that was folded in the late Paleozoic was not necessarily destined to rise again in the late Cenozoic. The history of the Appalachians during the later half of the Mesozoic and during the Cenozoic was independent of its earlier history.

Gravity data for small portions of the Appalachians have been discussed by Hammer and Heck (1941), Nettleton (1941), and Woollard (1943; 1949). Nettleton (1941, p. 281) thought that the anomalies are most readily explained by "density contrasts rather deep within the earth's crust." Although this may well be true for many of the details, the broad features indicate a root. A map prepared by Lyons (1950, unpublished) shows that between Pennsylvania and Alabama the Bouguer anomalies in milli-

gals are as follows: Coastal Plain +40 to −40, average, 0; Piedmont, +40 to −60, average −10; Blue Ridge and Valley and Ridge, −30 to −90, average −60; and Appalachian Plateaus, 0 to −60, average −30. Woollard (1959, p. 1535) gives an empirical curve for calculating the thickness of the crust from Bouguer anomalies. This curve indicates that the "normal" sea-level crust is 32 km (19 miles) thick, whereas in the western part of the Appalachians the crust would be 35 to 37 km (21 to 23 miles) thick. Andrev's formula, quoted by Woollard (1959, p. 1534), indicates a "normal" sea-level crust 30 km (18 miles) thick, whereas in the western part of the Appalachians it is 33 to 36 km (20 to 22 miles) thick. Thus the extra root under the western Appalachians is 2 to 4 miles thick. In location and magnitude, this root is consistent with the topography. (*Also see* Woollard, 1959, p. 1535.) There is no evidence of a root beneath the Piedmont, although it is part of the deformed belt. This suggests that the present root is unrelated to the late Paleozoic folding. The Mesozoic and Cenozoic history outlined above likewise suggests that the root may be of more recent origin than the Appalachian folding.

Turning to a different aspect of the subject, large vertical uplifts are not confined to areas of

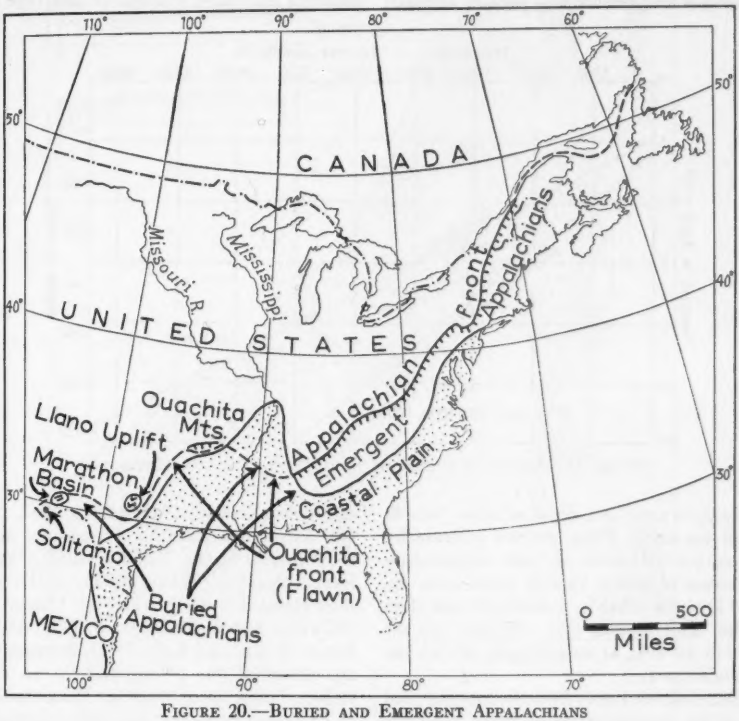

FIGURE 20.—BURIED AND EMERGENT APPALACHIANS

folding. The surface of the Appalachian Plateau, where the rocks are essentially flat, stands several thousand feet above sea level. An even more striking example is the Colorado Plateau, the surface of which is now 5000 to 10,000 feet above sea level. Although this area was gently folded during the Laramide revolution (Kelley, 1955), the shortening is much less than 5 per cent. Even if the entire crust in this area were shortened as much as 5 per cent, the thickness of the crust would be increased by only 2 km. If isostatic conditions prevailed, only about one-tenth of this amount would be expressed by additional elevation. In other words, the youngest strata involved in the folding would have been uplifted only 0.2 km (600 feet); actually they are many thousands of feet above sea level. Moreover, the uplift was much younger than the folding. Compression cannot explain the uplift of these plateaus.

Metamorphic geology and related experi-

mental work offers some interesting data on the magnitude of epeirogenic movements (Fig. 21). According to Clark, Robertson, and Birch (1957), at a temperature of 1,000° C., kyanite forms only if the pressure is at least 17 kilobars, which is equivalent to a depth of more than 40 miles in the crust. These authors indicate by extrapolation that even at room temperature the pressure at which kyanite could form exceeds 5 kilobars—that is, a depth of more than 10 miles. This implies that, wherever we see kyanite in the field, at least 10 miles of rock has been eroded away.

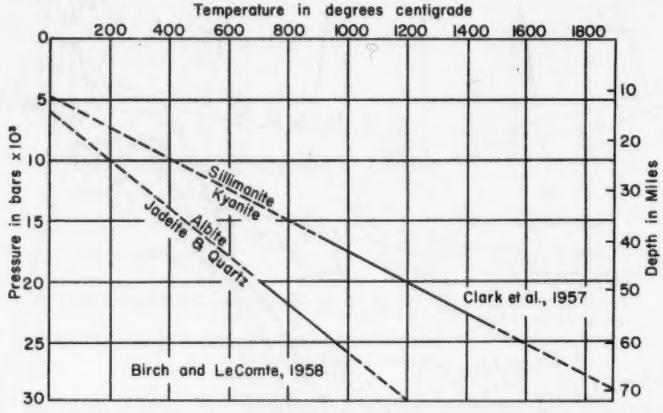

FIGURE 21.—STABILITY FIELDS OF SOME HIGH-PRESSURE MINERALS

Similar evidence comes from the experimental study of the transformation of albite to jadeite and quartz (Robertson, Birch, and MacDonald, 1957; Birch and Lecomte, 1958). At room temperature a pressure of 6 kilobars—equivalent to a depth of 13 miles—would be necessary for jadeite and quartz to exist in equilibrium; at 1000° C a pressure of 26 kilobars—equivalent to a depth of 62 miles—would be necessary. The assemblage jadeite plus quartz has been found in California, Japan, and Celebes (Miyashiro and Banno, 1958). Such deep erosion is possible, of course, only if there is equally great uplift. Most geologists would feel that other lines of evidence do not support the idea of such deep erosion. One possibility is that pressures during metamorphism may at times greatly exceed the load of the overlying rocks.

Broad vertical movements accompanied by high-angle faulting.—Broad vertical movements are often accompanied by high-angle faults. In most areas, these are normal faults that produce graben, horsts, and fault blocks. Where such faults displace the surface of the earth, alternating basins and mountains are produced. This is the source of Sonder's term taphrogenesis.

The Basin and Range Province of North America is a classic example of this type of diastrophism (Nolan, 1943; Hinds, 1952, p. 63–86). As specific examples of areas, we can cite the Oquirrh Range (Gilluly, 1932), Wasatch Range (Eardley, 1933a; 1933b; 1951), Ruby-East Humboldt Range (Fig. 22; Sharp, 1939), Stillwater Range (Muller *et al.*, 1951) and Inyo Range (Knopf and Kirk, 1918). Maxson (1950) has described the deformation of an erosion surface during the uplift of the Panamint Range of California in association with faulting. The modern fault-block structure of the Basin-Range Province began to develop in the later part of the Tertiary.

Fault-block mountains are known in Asia. The Altai Mountains were uplifted chiefly during the Quaternary as a broad arch that trended east–west, accompanied by considerable normal faulting (Belayevskiy *et al.*, 1958, vol. 3, p. 361–362). In northeastern and eastern Russia, a late Miocene peneplain has been differentially uplifted, accompanied by normal faulting and the development of fault-block mountains (Belayevskiy *et al.*, 1958, vol. 3, p. 374–380).

The Rhine graben (Fig. 23) is 280 miles long, 20–25 miles wide, and is broken by numerous smaller faults, all of which are normal (Dorn, 1951, p. 324–337). The formation of the Rhine graben was associated with regional doming. The Black Forest (Hans Cloos, 1951–1952) was uplifted in the late Tertiary and early Quaternary, partly by doming, partly by movement

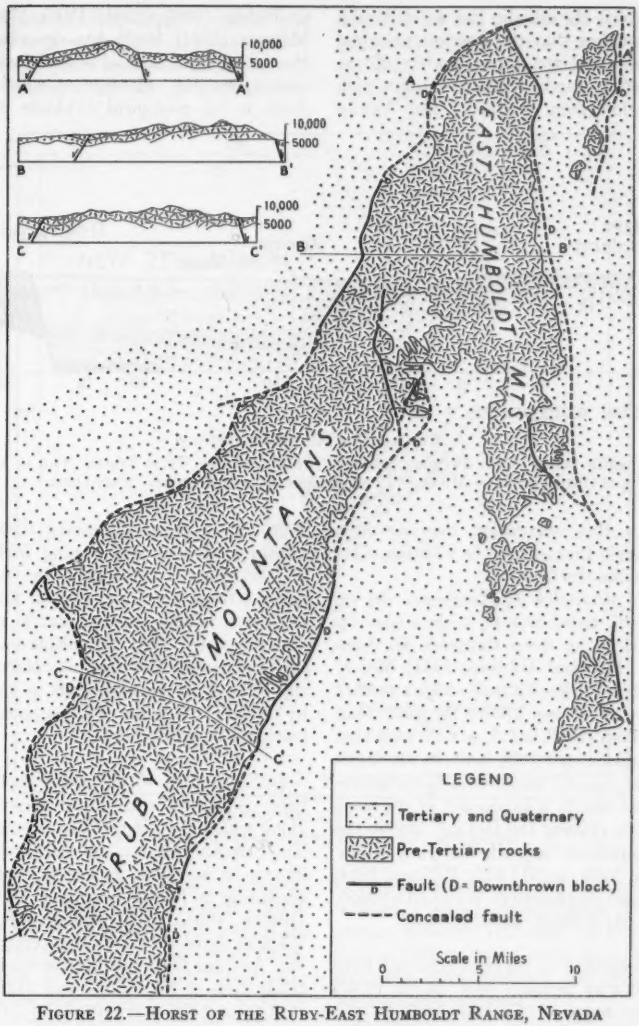

FIGURE 22.—HORST OF THE RUBY-EAST HUMBOLDT RANGE, NEVADA
After R. P. Sharp

along faults (Dorn, 1951, p. 217). Most of the descriptions of the African graben are very generalized (Krenkel, 1922; Gregory, 1921; Hans Cloos, 1939; Hennig, 1938); it is very difficult to obtain any data on the attitude of the fault planes. Shackleton (1955) states that, in that part of the graben just north and south of the equator, the faulting is apparently younger than the "End-Tertiary" erosion surface. Although strong faulting took place at the end of the Pleistocene, the main faulting was earlier. The African Rift Valleys are associated with doming. Currie (1956) has shown experimentally the relation between graben and vertical movements.

Fault blocks, many of them expressed in the topography, are common in New Zealand (Cotton, 1950). However, although some of the boundary faults are normal, others are high-angle thrusts (Cotton, 1950, p. 728–729). The forces that cause high-angle thrusts are not readily explained. A thrust fault that dips 60°

and along which the net slip has no strike-slip component implies that the greatest principal stress axis was inclined approximately 30° to the surface of the earth. Regional stresses with this orientation seem unlikely. But locally of Hobbs (1901; 1904; 1905; 1911). Vening Meinesz (1943; 1947) has described the mechanics of formation of a world-wide fracture system, for the existence of which, however, there is no geological evidence (Umbgrove,

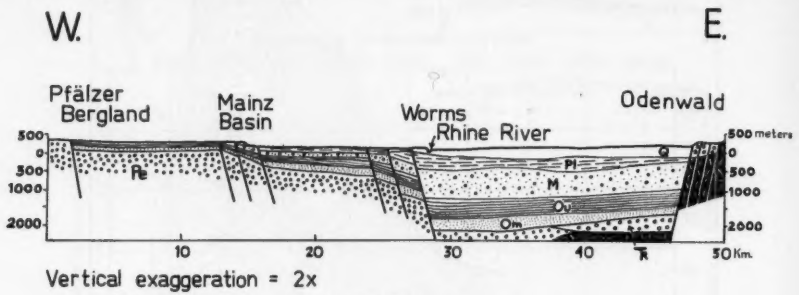

FIGURE 23.—RHINE GRABEN

Black with white dashes = Pre-Permian basement, Pe = Permian, Tr = Triassic, Om = Middle Oligocene, Ou = Upper Oligocene, M = Miocene, Pl = Pliocene, Q = Quaternary. After Dorn.

stresses with this orientation may develop. Some high-angle thrusts may be utilizing older normal or strike-slip faults.

Large-scale strike-slip displacements.—In recent years the possibility of large strike-slip displacements along steep fractures has been emphasized (Hill and Dibblee, 1953; Moody and Hill, 1956). Strike-slip faults with a modest displacement have been known for more than a century. Heim (1919, vol. I, p. 613) says that Escher recognized strike-slip faults in the Santis region of the Alps in the 1840's. Some strike-slip faults are clearly a byproduct of the same forces as those causing the folding. Among the specific examples we may cite the Jura Mountains (Heim, 1919, p. 613-626; Billings, 1954, p. 212-214) and southwestern Wales (Anderson, 1951, p. 60–64; Billings, 1954, p. 214).

A brief digression to consider Sonder's term regmagenesis may be made here. In the 1930's he published maps of Central America, the Atlantic Ocean, and the Aegean Sea showing two or more sets of master fractures, each fracture extending for tens or hundreds of miles. These lineaments were deduced chiefly from the supposed alignment of volcanoes, drainage patterns, and the trend of shore lines. Sonder (1956, p. 118-123) reproduced these maps, along with one of the Mediterranean by Sieberg and one of Africa by Hennig (1938, p. 123). Because of the methods used to deduce such extensive fracture systems, many geologists question their reality. Sonder's methods and conclusions are reminiscent of the earlier work 1946). In a paper discussing these supposed fractures (Sonder and Vening Meinesz, 1947, p. 939), Sonder introduced the term regmagenesis, from the Greek *regma*, meaning cleft or fissure. It also appears that at this time he first suggested that the displacements along such fractures, when they take place, are strike-slip. The term regmagenesis is thus clouded by the fact that many of the supposed regmatic fractures may not exist.

Let us return to our main theme. We are here concerned with large strike-slip faults along which the net slip has been many miles. The San Andreas fault of California is so well known to American geologists that a detailed discussion is hardly necessary here (Hill and Dibblee, 1953). Most geologists familiar with the area agree that the displacement along the San Andreas fault has been colossal. It is certainly tens of miles; Hill and Dibblee believe that the net slip may have been 120 miles since the Cretaceous and 350 miles since the Jurassic. But it is still not clear whether it is a large fracture incidental to the structure of the Coast Range or whether it is a master fracture in the crust of the earth—a geosuture of Hans Cloos (1948)—dominating the deformation of the western part of the North American Cordillera.

The Great Glen fault is one of half a dozen steep northeasterly striking faults in Scotland along which the northwest block has moved relatively southwest (Kennedy, 1946; Billings, 1954, p. 223–225). The net slip along the Great Glen fault is 65 miles.

The northeast-trending Alpine fault of the South Island of New Zealand (Wellman, 1955; 1956) in recent years has been considered to be a right-handed strike-slip fault (Fig. 24).

FIGURE 24.—ALPINE AND RELATED FAULTS OF NEW ZEALAND
Note offset of "marginal syncline" and "schist axis".

Wellman (1955, p. 249) states that the northwest block has moved northeastward relative to the southeast block at least 300 miles since the end of the Jurassic. On the other hand, Kingma (1959, p. 32) says that "large-scale transcurrent movement is therefore unlikely to have taken place along the Alpine fault."

Extensive strike-slip faults in the Caribbean and northern South America have been discussed by Hess and Maxwell (1953, p. 5) and Rod (1956). The map by Hess and Maxwell suggests that Cuba has slid westward 300 km relative to Haiti. Rod states that in Venezuela the net slip along strike-slip faults is tens of kilometers.

Large-scale strike-slip faults thus appear to be a very important type of diastrophism. But it is often difficult to determine the forces involved. Even in California it is not clear whether all the associated structural features—right-handed and left-handed strike-slip faults, folds, and normal faults—can be explained by one set of forces. Moreover, in recent years, many faults elsewhere in the United States have been assigned to the strike-slip category without adequate data. Efforts to explain diversely oriented fractures by a single set of forces, with primary, secondary, and tertiary strike-slip faults (Moody and Hill, 1956), are mechanically unsound.

In recent years some great scarps on the ocean floor have been considered to be controlled by strike-slip faults. Menard (1955) has described four great fracture zones in the eastern Pacific. These zones, which range in length from 1400 to 3300 miles, tend to follow great circles. Each zone, averaging 60 to 100 miles in width, consists of a broad ridge or welt in the midst of which are one or more topographic troughs.

When Menard wrote, there was little direct evidence that the displacement along these fractures was strike slip. More recently Mason (1958) has described a magnetic survey in the

Pacific Ocean west of southern California (Fig. 25). The area covered is about 70,000 square miles and is a flat, abyssal plain nearly 5 km below sea level. The map shows total magnetic intensity in gammas. Alternating highs and lows, between which the difference is about 400 gammas and which are about 25 miles wide, trend north–south. Mason believes that the anomaly belts are offset in a right-handed sense 84 miles along the Murray fracture. But this conclusion may be questioned. For one thing, east of Long. 125° W. no offset of the anomaly belts is apparent. Secondly, although there is obvious interruption of the anomalies along the Murray fracture, some seem to continue on both sides. Thirdly, the anomalies are not fully explained; one suggestion is that the highs are underlain by plates of basalt that are about 2 km thick and trend north–south.

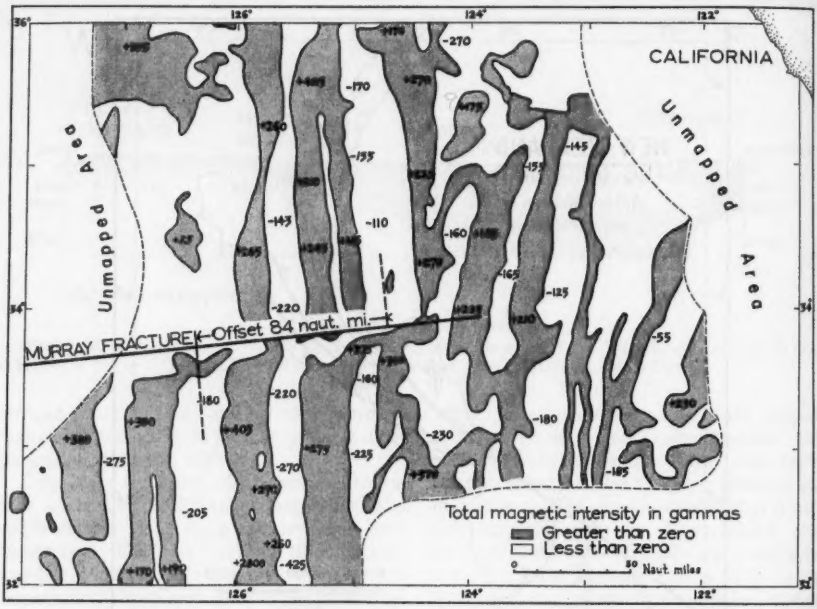

FIGURE 25.—MAGNETIC ANOMALIES ASSOCIATED WITH MURRAY FRACTURE ZONE, EASTERN PACIFIC OCEAN

Plus figures show the greatest positive anomalies; negative figures show the greatest negative anomalies. After Mason.

In recent years many seismologists have concluded that most earthquakes are caused by strike-slip faults (Hodgson, 1957; Scheidegger, 1957b). The original method proposed by Byerly (1926) is based on an analysis of the first motion of the *P* waves at the recording stations; a rapid method of analyzing the data has been developed by Hodgson (1957; 1959). But the method does not give a unique solution, because two possible planes are obtained, either one of which may be the fault. The plane at right angles to the fault and perpendicular to the net slip is called the auxiliary plane. The intersection of these two planes was called the null vector by Hodgson (1957), but McIntyre and Christie (1957) suggested that *B* axis was a more suitable term. Regardless of which of the two planes is the fault, the *B* axis is at right angles to the net slip. If the *B* axis is vertical, the net slip is horizontal, and the fault is a strike-slip fault. If the *B* axis is horizontal, the fault is a dip-slip fault. Since the *B* axis is generally steep, the seismologists conclude that most earthquakes are caused by strike-slip faults.

A more quantitative approach is possible. The present author has prepared Figure 26 from data assembled by Scheidegger (1955) for 100 earthquakes. Two points are shown for each quake. One point shows the dip of the fault plane and the rake (pitch) of the net slip. The second point shows the dip of the auxiliary plane and the rake of a line in this plane at

right angles to the *B* axis. It is impossible, however, tc tell which points represent the faults and which represent the auxiliary planes. The dip of the fault (or auxiliary plane) is plotted on the ordinate, whereas the rake or pitch of the net slip (or comparable line in auxiliary plane) is plotted on the abscissa. Points in the upper left-hand corner represent vertical strike-slip faults; points in the upper right-hand corner represent vertical dip-slip faults. Theoretically, there should be 200 points, two for each quake; actually, there are only 194 points because of the incompleteness of the data. The 157 points that lie in the left half of the diagram represent either faults in which the strike-slip component is larger than the dip-slip component, or auxilliary planes in which the rake of a line at right angles to the *B* axis is less than 45°. The 37 points that lie in the right half of the diagram represent either faults in which the dip-slip component is greater than the strike-slip component or auxilliary planes in which the rake of a line at right angles to the *B* axis is greater than 45°. From these data, rather than to say that most faults are strike-slip faults, it would be more correct to say that, in 81 per cent of the faults studied, the strike-slip component is larger than the dip-slip component.

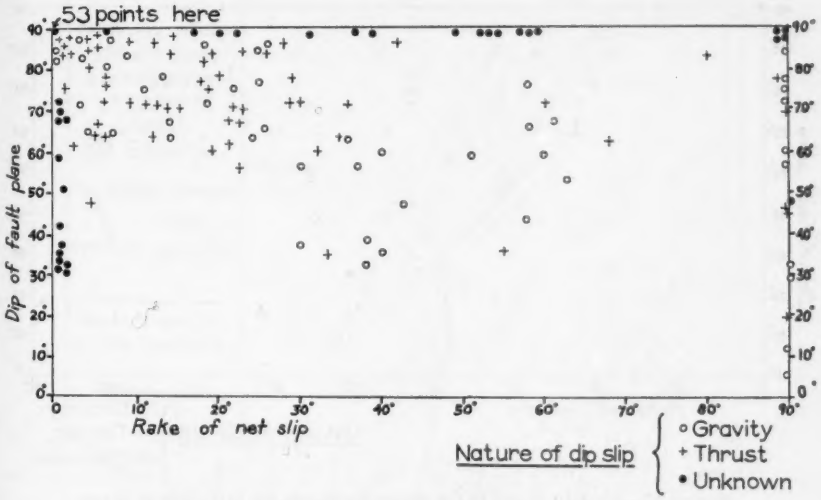

FIGURE 26.—FAULT-PLANE SOLUTIONS BASED ON DATA FOR *P* WAVES

Because of ambiguity in method, half the points represent a fault; the other half represent the so-called auxiliary plane. The ordinate gives the dip of the fault plane or the dip of the auxiliary plane. The abscissa gives the rake of the net slip or the rake of a line in the auxiliary plane at right angles to the null vector (*B* axis). Based on tables prepared by Scheidegger (1955).

More recently Scheidegger has proposed a method to give a unique solution by combining the results of several earthquakes in a single area. "If a series of fault-plane solutions is available for a certain geographic area, it is possible to determine the tectonic displacement by a least squares solution (Scheidegger, 1958b, p. 19)".

Scheidegger (1958a) and others have shown that it is theoretically possible to get a unique solution by utilizing the data from *S* waves. Scheidegger (1957a) has summarized in tabular form the data obtained by Russian seismologists between 1953 and 1957. Results for 84 earthquakes are plotted on Figure 27. The dips of the faults planes range from 10° to 90°. The rake (pitch) of the net slip also shows considerable spread, ranging from "small" to 90°. In 49 cases, the rake exceeds 45°, and in only 35 cases is it less than 45°. Thus, in the majority of these cases the dip-slip component exceeds the strike slip. The results thus differ considerably from those based on analysis of *P* waves.

Actually, there are still some uncertainties in the seismic method. Some authors (Adams, 1958) have reported poor agreement between the results obtained from study of the *S* waves and those obtained from a study of the *P* waves for the same quakes. Moreover, the pattern of

compression and tension around a focus is more complex than has been generally assumed (Knopoff and Gilbert, 1960, p. 133–134).

Study of the Dixie Valley-Fairview Peak, surface faults along which displacement took place during the quakes is about N. 15° E., parallel to the trend of the mountain ranges. The net slip along these faults can be resolved

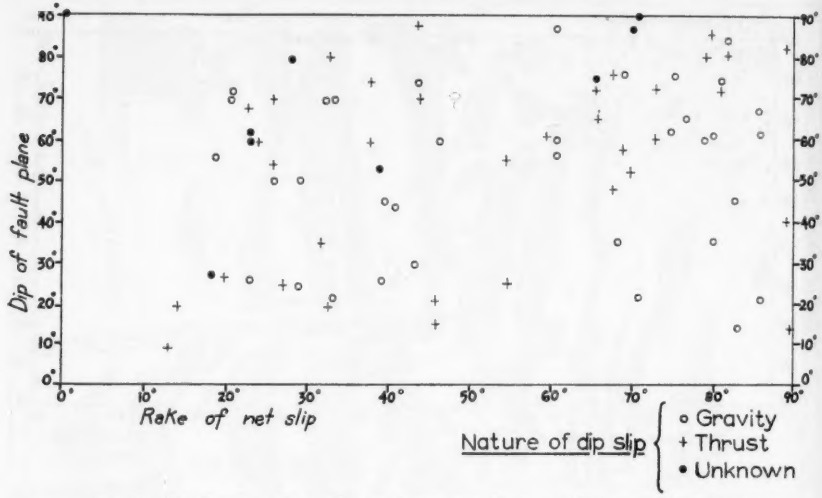

FIGURE 27.—RUSSIAN FAULT-PLANE SOLUTIONS BASED ON DATA FOR *S* WAVES

Each point represents results obtained from one earthquake. The ordinate gives the dip of the fault plane, the abscissa gives the rake of the net slip. Based on table prepared by Scheidegger (1957a).

Nevada, earthquakes of December 16, 1954, offers some significant information (Tocher *et al.*, 1957). The epicenter southeast of Fairview Valley (Fig. 28) represents a quake that occurred at 3:07 a.m., P. S. T., with a depth of focus of about 15 km. The epicenter northwest of Dixie Valley represents a quake that occurred at 3:11 a.m., P. S. T., with a depth of focus of about 40 km. An analysis of the seismic records by the Byerly-Hodgson method indicates that the fault causing the first shock strikes N. 11° W., dips 62° E., and that the net slip is such that the east wall moved downward at a plunge of 24° S. Because of the complexity of the records it was not possible to make a similar analysis for the second shock.

Fortunately a geodetic survey of the area had been conducted in the summer prior to the earthquakes. By rerunning the survey in 1955 it was possible to determine the relative displacements that had taken place during the earthquakes; the displacements are shown by arrows in Figure 28. Most of the stations within 25 miles of the Fairview Peak (southerly) epicenter moved several feet south-southeast or north-northwest. But the average strike of the into a normal dip-slip component and a strike-slip component in which the eastern block moved south. A couple in which the forces are parallel to the arrows shown in Figure 28 would not produce faults of this orientation and type of displacement. It appears, therefore, that the surface faults were controlled by a set of older Basin-Range faults. This in turn suggests that the strike-slip displacements of the San Andreas type are now invading an area that was previously deformed by dip-slip faults. Figure 29 illustrates the movement along the surface faults, where block *B* has moved downward and southward relative to block *A*, and block *C* has moved upward and southward relative to block *B*.

In summary, strike-slip faults are being greatly emphasized at the present time by geologists and seismologists. Some papers even suggest that this is the primary type of diastrophism and that most other kinds of deformation are secondary effects. In many places the supposed geological evidence is based on faulty interpretation. The seismic method needs careful analysis, particularly because the conclusions differ, depending upon whether one

uses *P* waves or *S* waves. A study of the structure of the various continents indicates that large strike-slip faults have not been important in the past. It is possible that strike-slip faults are much more important now in crustal evolution than they were in the past.

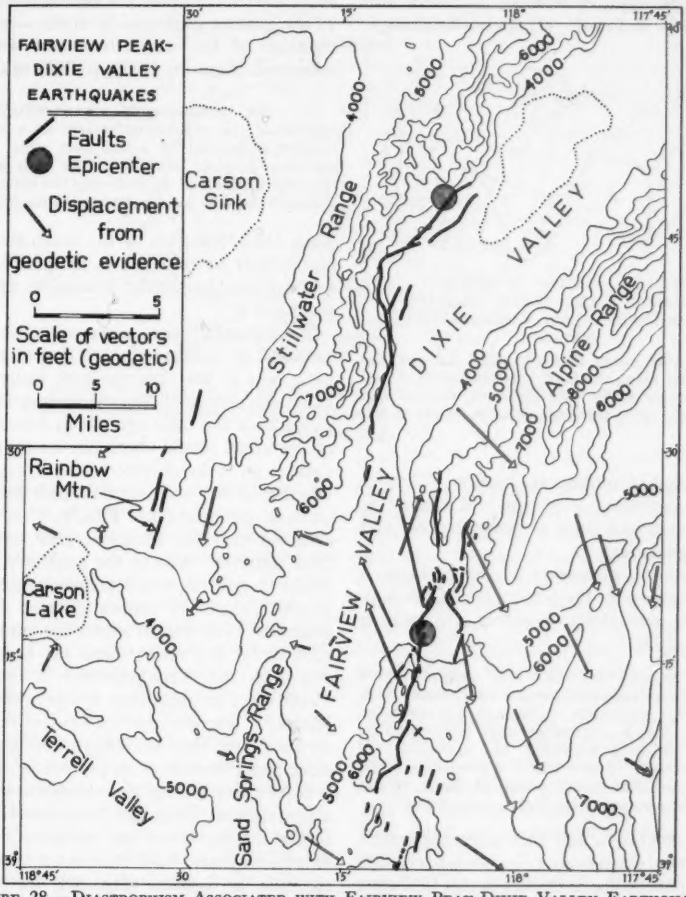

FIGURE 28.—DIASTROPHISM ASSOCIATED WITH FAIRVIEW PEAK-DIXIE VALLEY EARTHQUAKES, NEVADA

Arrows indicate movement of various bench marks during earthquakes; amount is shown by "scale of vectors". More southerly of two shaded circles is epicenter of Fairview Peak earthquake. More northerly shaded circle is epicenter of Dixie Valley earthquake. Based on maps in Tocher *et al.* (1957).

Displacement of the crust or entire earth relative to the axis of rotation.—We are here concerned with three types of displacement: (1) the more or less uniform slipping of the crust over the mantle; (2) continental drift, in which portions of the crust move relative to one another and may even rotate about vertical axes; and (3) displacement of the entire body of the earth relative to the axis of rotation. For the first two types of displacement Sonder (1956, p. 13) used the term phorogenesis, which is defined as "tangential displacements (drift movements) of the solid crust over the asthenosphere".

The concept of continental drift has been debated for many years, but especially since

the first edition of the book by Wegener (1915, 1924) appeared. At least two symposia have been held on the subject, one arranged by Van der Gracht (1928), the other by Carey (1958). The principal types of evidence that were used before 1945 included: (1) paleoclimatology;

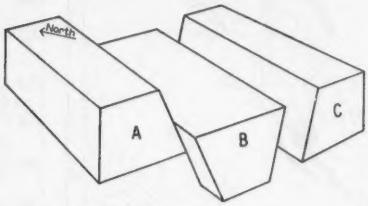

FIGURE 29.—NATURE OF NET SLIP ON SURFACE FAULTS DURING FAIRVIEW PEAK-DIXIE VALLEY EARTHQUAKES, NEVADA

Along those faults that dip east, the net slip was like that along the fault between blocks *A* and *B*. Along those faults that dip west, the net slip was like that along the fault between blocks *B* and *C*.

(2) matching of continental borders; (3) similarity of geological structure and history in areas on opposite sides of ocean basins; and (4) biological data.

An extensive discussion of the problem is beyond the scope of the present paper. We may summarize our views, however, by quoting Longwell (1958):

"These critical comments may suggest that I am an incurable skeptic toward continental drift. I admit to skepticism . . . because (1) evidence known to me is suggestive and circumstantial only—no clinching argument has appeared; (2) quite aside from the problem of a propelling force, the supposed horizontal creep of sialic blocks through sima seems to be highly improbable."

In recent years a new tool, paleomagnetism, has been used extensively to investigate changes in geographic position. Studies in this field were published 20 years ago by McNish and Johnson (McNish and Johnson, 1940; McNish, 1941; 1943). It was not until after World War II, however, that tremendous interests in this subject developed, especially in Great Britain and Japan (Nagata, 1953).

The methods employed in paleomagnetic studies vary in detail but are fundamentally similar (McNish, 1941; Runcorn, 1956). Where the strata are not horizontal, the attitude of the beds is measured, so that the original position prior to folding may be determined. In Arizona, Runcorn (1956) preferred fine-grained red sandstones, siltstones, and shales. One or two cores, 3.5 cm in diameter, were cut, with the axis of the cylinder perpendicular to the bedding. These cores were then sliced into disks about 1 cm thick. The declination, relative to the present geographical north, and the inclination of the magnetic vector were then measured. Runcorn (1956, p. 304) said:

"... the measurements are essentially observations of the angular deflections of a horizontal magnet suspended by a fine fiber when the rock specimen is raised beneath it. The high sensitivity required is obtained by removing the control of the geomagnetic field on the suspended magnet."

Thus the orientation of the magnetic field at any locality at any time in the past may theoretically be determined if suitable material is available.

Theoretically, one observation should be sufficient to indicate the location of the magnetic pole at the time the rock being investigated was deposited. Several observations made on rocks of the same age but in different parts of the world should check one another. Observations on rocks of different ages would show whether or not the magnetic pole had shifted through geologic time. Finally, if it may be assumed that the magnetic pole has always been relatively close to the geographic pole, it would be possible to determine changes in geographic position of various spots on the earth. Runcorn (1956, Fig. 9) shows the results of one such study. In Precambrian time, according to this map, the north pole was in the eastern Pacific; in Cambrian time it was in the central Pacific; it migrated northwestward during the Paleozoic and then northward during the Mesozoic and Cenozoic to its present position.

Before considering the significance of fossil magnetization, it should be pointed out that within historic times the configuration of the earth's magnetic field has varied greatly. For example, at London (Fig. 30), the magnetic declination changed from 11° E. to 24° W. between 1600 and 1800, a change of 35° in 200 years (McNish, 1941, p. 227). Similarly, the magnetic inclination changed from 74° in 1700 to 66° in 1935, a change of 8° in 235 years. At Boston, the inclination changed from 68½° to 74° between 1723 and 1850. If we accept the assumptions generally made in paleomagnetic studies, we would conclude that Boston drifted 300 miles northward in this period.

The following suggestions have been used to explain why the fossil magnetization differs from the present magnetization: (1) slipping of

the entire crust over the mantle; (2) rotation of the entire body of the earth relative to the axis of rotation (Gold, 1955); (3) continental drift, with or without rotation of continents; (4) periodic or at least episodic reversals of the earth's magnetic field; and (5) reversals due to the eruption of successive lava flows.

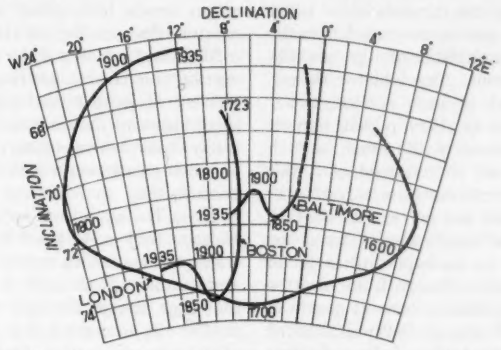

FIGURE 30.—VARIATIONS OF MAGNETIC DECLINATION AND INCLINATION WITHIN HISTORIC TIME AT LONDON, BOSTON, AND BALTIMORE
After McNish

Geologists cannot help viewing with extreme skepticism most of the conclusions reached so far from these paleomagnetic studies. For one thing, the various workers within the field do not agree on their interpretations. Moreover, if slipping of the entire crust is not sufficient to explain their observations, some investigators also invoke drifting and rotating continents (Creer, 1958, p. 100, 101). This, of course, is an unbeatable combination; anything can be explained. Stehli (1957), from a study of Permian climatic zonation, based on the distribution of certain brachiopods and fusilinids, considered that the Permian climatic zones were similar to those existing at present; in other words, his study suggests that little change in the position of the geographic axis of the earth has occurred since then. Doell and Cox (1959) suggest that during Mesozoic and Early Tertiary time the earth's magnetic field was a comparatively rapidly changing dipole, without requiring extensive displacement or rotation of the continents. Munk (1956), on the basis of his mathematical and physical analysis, doubts the probability of polar wandering.

Hypotheses of diastrophism

Hypotheses of diastrophism will be outlined here, but a more critical analysis will be deferred to that part of the paper dealing with mountain building.

Horizontal compression has long been considered a major factor in diastrophism. In fact, the concept of compression was evolved to explain the folds and thrusts that are so well displayed by stratified rocks. Some, among them Sonder (1956), believe that broad warps, with wave lengths of hundreds of miles, may develop when a relatively strong crystalline crust, with few, if any, overlying strata, is compressed. Many believe that a root formed by compression may be later eliminated by slow uplift accompanied by erosion. The horizontal compression may be the result of a contracting crust (Landes, 1952; Lees, 1953; Sonder, 1956; Wilson, 1959) due to cooling of the mantle, formation of denser minerals in the mantle, or eruption of lavas.

In the last few decades many have emphasized subcrustal convection currents (Holmes, 1945).

According to another hypothesis large pockets of liquid form within the crust, and, because of expansion in the change from solid to liquid, vertical uplift ensues (Rich, 1951; Wolfe, 1949; Van Bemmelen, 1954); folding and thrusting are believed to be a consequence of gravity sliding down the flanks of such vertical uplifts.

Hess (1954) has suggested the importance of serpentinization of peridotite below the Mohorovičić discontinuity in causing uplift, primarily in the ocean basins. Similarly, deserpentinization would cause depression.

George C. Kennedy (1959) has suggested

phase changes near the Mohorovičić discontinuity, such as gabbro changing to eclogite. With the addition of heat the minerals in the upper part of the mantle would be converted into the less dense phases characteristic of the crust; uplift would ensue. Conversely, with an excessive loss of heat, the minerals in the lower part of the crust might be converted into the denser phases characteristic of the mantle; depression would ensue. Any folds or thrusts would be incidental to such vertical movements. But, as Kennedy (1959, p. 503) himself points out, the thinness of the crust beneath the oceans is difficult to reconcile with this hypothesis; sufficient pressure to convert gabbro to eclogite would not be reached at such shallow depths. The quartz-coesite transition would probably not be an important factor in the supposed reversible change from crust to mantle. Sufficient pressure to convert quartz to coesite (Boyd and England, 1959) is attained only at depths so great that little or no free silica is present.

Vertical movements due to loading and unloading because of the waxing and waning of continental ice caps are the result of special conditions. Vertical movements due to the erosion or deposition of sediments are undoubtedly important, although some other process must cause the initial uplift or depression. The rise of lighter rocks through overlying heavier strata is important in the rise of salt domes, and the rise of magma may cause some of the deformation in the interior of folded belts.

Mountain Building

So far, we have considered the various diastrophic processes that deform the crust of the earth. But what do these have to do with mountain building? In the past, as has already been pointed out, mountain building has often been equated with folding and horizontal compression.

Others have already recognized the fallacy of this concept. Wegman (1955, p. 285) says "... Orogenic movements created relief (mountain and depressions) ... tectogenetic movements are registered in the multiple structures of rock masses." By "tectogenetic movements" he means folding and faulting. He says further, "The two movements do not necessarily accompany one another...." Dorr (1958) says: "Theoretically, it may be desirable to distinguish between orogeny and mountain building." Here he is using orogeny in the sense of folding and thrusting. King (1959, p. 90) says: "Thus, even though the Cordilleran system began to grow later than the Appalachians, their present form is not caused by folding, thrust faulting.... As in the Appalachians, other events took place later which had a greater effect in shaping the present surface."

Mountain building is the result of an upward vertical movement, whether or not it be the indirect result of horizontal compression. But should upward movements be considered separately from downward movements? Men were long ago greatly impressed by mountain ranges because they were such a formidable barrier to cross. Basins did not impress them so much, because they were filled by sediments or by water, across which travel was much easier. But tectonically a basin is as important as a mountain range. Perhaps the only difference is that the formation of a mountain range or plateau involves work against gravity.

Most modern mountain ranges are not the direct result of folding. Many have been demonstrated to be the result of epeirogenesis—diktyogenesis, if we wish to use Von Bubnoff's term—entirely unrelated to folding. We may cite such ranges as the Appalachians, the Caledonides of Scandinavia, the Vosges, the Black Forest, the Rockies, and the Andes. Plateaus, such as the Appalachian Plateaus and the Colorado Pleateaus, are obviously the product of regional uplift and not folding.

But what causes these vertical movements? Some of the hypotheses listed in a previous section of this paper may now be considered more fully. One popular hypothesis, which, however, has not been too carefully thought out, assumes that such belated uplift is the result of isostatic adjustment because of a root that developed under horizontal compression. But there are several objections to this. One is the time factor. In many ranges, such as the Laurentians, the Torngats, the Scandinavian Ranges, and the Appalachians, the folding was hundreds of millions of years ago. Secondly, between the time of the folding and the most recent uplift, these ranges—this would also apply to the Sierra Nevada—were reduced to surfaces of low relief. Thirdly, as will be pointed out later, the amount of uplift is in many cases excessive compared with the amount of shortening. Finally, the hypothesis fails to explain the uplift of plateaus, such as the Appalachians and Colorado Plateaus.

A second hypothesis is that large-scale

vertical movements are the result of horizontal compression, the crust buckling into great broad warps with a wave length of hundreds of miles. In eastern North America the Fall Line surface may be used as the plane of reference for the late Mesozoic and Tertiary deformation (Fig. 19). Over the present mountains it has been warped up into a great anticline, whereas the lowest parts lie at the continental slope or beyond. The amplitude of this great fold is at least 4 miles. If the crust had been merely compressed into this great fold—with a wave length of several hundred miles—the Mohorovičić discontinuity beneath the Appalachians would be at least 4 miles higher than under the Continental Slope. But gravity data show this is not so. Certainly the base of the crust is deeper beneath the Appalachians than beneath the Atlantic Plain. Horizontal compression does not appear to be the explanation of the broad vertical movements of the crust.

A third hypothesis is that sialic material moves at depth from one area to another. Such a theory applied to eastern North America suggests that since the middle Mesozoic sialic material has been continuously transferred from beneath the sinking Atlantic Plain and has been accumulating beneath the Appalachians. Which was cause and which was effect is a problem. Did erosion and sedimentation, during which the debris moved southeasterly, cause a deep-seated counter flow of sial from southeast to northwest? Or did movement of sial, caused by convection currents, cause depression in the Atlantic Plain and uplift in the Appalachians?

The uplift of the North American Cordillera presents an even more formidable problem. In analyzing this subject the following data are used: (1) width, 1000 miles; (2) average altitude 1.5 miles; (3) average Bouguer anomaly, −150 milligals (Lyons, 1950, unpublished map); (4) thickness of crust prior to Nevadan-Laramide revolution was 18 miles; and (5) until late Jurassic, and in many places until late Cretaceous, the region was close to sea level and receiving sediments. Although such a sweeping analysis may at first appear unjustified, a summation of studies covering smaller areas would undoubtedly lead to similar conclusion. It is also assumed that the gravity data are more reliable than some of the seismic data in this area (Tatel and Tuve, 1955; Woollard, 1959).

Whereas the gravity anomalies indicate that the crust beneath the Cordillera averages 28 miles thick, the average altitude suggests, assuming isostatic conditions, that the crust is 32 miles thick (graph in Woollard, 1959, p. 1535). To produce such a root by horizontal compression, a shortening of 40 per cent would be necessary; that is, the belt that is now 1000 miles wide was originally 1650 miles wide. Available data indicate, however, that the shortening, especially since the end of the Jurassic, was much less. The hypothesis of compression is inadequate to explain the uplift of the North American Cordillera.

The Sierra Nevada offer some pertinent data. Axelrod (1957) has recently given an excellent account of the uplift of the Sierra Nevada in late Tertiary and Quaternary time; in one area, 3500 feet of the uplift took place along faults, whereas an additional 1800 to 3000 feet of uplift was produced by warping. The root beneath the Sierra Nevada raises an interesting problem. The sialic crust here may be 50 km thick, twice as thick as the "normal crust" nearer the Pacific Coast (Tsuboi, 1956; *see also* Press, 1956; Byerly, 1938; Gutenberg, 1943; Oliver, 1956). When and how did this root originate? One hypothesis is that it is a relic of the Nevadan revolution. There are, however, several objections to this. In the first place, the pre-Cretaceous basement beneath the Great Valley is presumably as highly folded as the rocks of the same age in the Sierra Nevada (Fig. 31). Should not as great a root have formed under what is now the Great Valley as beneath the Sierra Nevada? Secondly, why did the Sierra stand relatively low throughout much of Tertiary time? Only one answer seems reasonable—the present root has formed in late Tertiary and Quaternary time, but little crustal shortening has occurred.

Whence has this sial beneath the Sierra and the entire North American Cordillera come? One possibility is that the sial has been transferred from elsewhere, but there seems to be no adequate source. (*See also* Kennedy, 1959, p. 494). A second is that new sial, leaking out from the mantle, has recently accumulated beneath the Sierra. This assumes that the difference between the crust and the mantle is largely chemical. But the amount is prodigious. If sial were added to the crust at the same rate in pre-Tertiary times, the continents would be much larger. Or, in accordance with Kennedy's suggestion, mantle may have been converted into sial.

Pure strike-slip faulting by itself will not normally produce relief. Local relief (Fig. 32)

may result if a high area is brought into juxtaposition to a low area (Cotton, 1956, p. 198), but some other process must have produced the original differences in relief. If strike-slip faulting is accompanied by buckling of the moving block (Fig. 33; Cotton, 1956, p. 190) or thrust faulting (Fig. 34; Cotton, 1957a, p. 940), differences in relief may result.

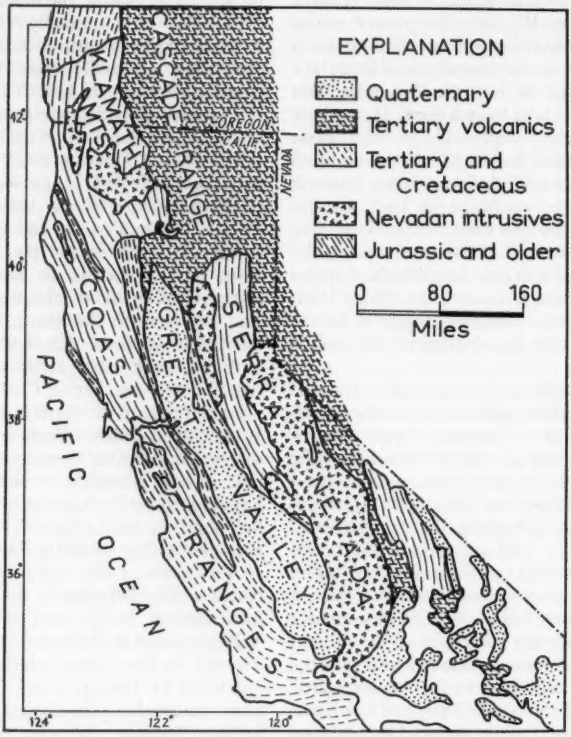

FIGURE 31.—STRUCTURAL TRENDS IN CALIFORNIA

Kingma (1958; 1959) has suggested that a block caught between two strike-slip faults may be squeezed up. If the blocks are free to move laterally the shape of the blocks will not change, even though their positions do. If the blocks move toward one another, however, they are shortened at right angles to the strike of the faults; the resulting expansion may well be vertical.

We may well ask whether folding and thrusting produces mountains. Often evidence is not available. The Valley and Ridge Province has already been discussed. The folding took place some time between early Permian and late Triassic. By late Triassic time strata several miles thick had been removed by erosion from some areas. Where are the products of this erosion? No one seems to know. However, as pointed out previously, it is possible that erosion kept pace with the folding, and that no mountains developed. Nevertheless, there is evidence that mountains formed as a result of the mid-Devonian Acadian revolution in the northeastern United states and adjacent Canada. In New Hampshire, the youngest sedimentary rocks involved in the Acadian folding are upper Lower Devonian (Billings, 1956). Syntectonic igneous rocks appear to be early Mid-Devonian. The folded belt occupied most of New England and presumably extended southwestward beneath what is now the Coastal Plain. Moreover, at this same time the Catskill delta of Pennsylvania and New York began to form (Barrell, 1914). A layer of rock 2 to 4 miles thick must have been

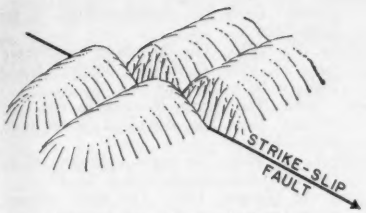

FIGURE 32.—SHUTTER RIDGES
After Cotton

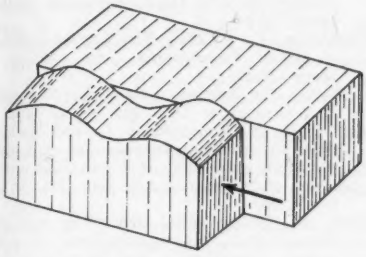

FIGURE 33.—BUCKLING ASSOCIATED WITH STRIKE-SLIP FAULTING
After Cotton

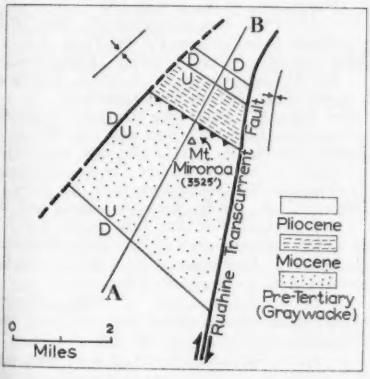

FIGURE 34.—THRUST FAULT ASSOCIATED WITH STRIKE-SLIP FAULTING
Mt. Miroroa area, New Zealand. After Kingma and Cotton.

eroded from the source area southeast of New York and Pennsylvania during the Devonian. In the Wasatch Plateau, Spieker (1946) has shown that the influxes of Cretaceous gravels resulted from folding to the west. In western Wyoming, Dorr (1958) has shown that a belt of thrusting in Paleocene time was the source of clastic sediments in the Hoback Basin. In the Alps, as a result of Oligocene folding and thrusting, the Oligocene-Miocene molasse—sandstone with conglomerate—was deposited. Collet (1927, p. 119) says: "... the Alps traveling forward and the pebbles going forward from the chain as it grows, and then the chain riding over its own debris."

We conclude, therefore, that folding and thrusting may result in the formation of mountains. This uplift may be the direct result of the folding—that is, from the rise of the crests of anticlines. It may also be isostatic uplift because of the formation of a root.

SUMMARY AND CONCLUSIONS

The chief purpose of this paper has been to consider the relative importance of the various types of diastrophism and especially their relation to mountain building.

Folding and thrusting is the most spectacular type of diastrophism insofar as changes in the shape of rock bodies are concerned. Not all geologists agree that the folded strata have been shortened. Most Americans would agree that shortening has taken place but would not agree on the extent to which the basement has been shortened or on the question of whether there has been any reduction in the circumference of the earth. Epeirogenesis is by no means as spectacular as folding, because it does not change the shape of rock bodies. But epeirogenesis produces striking topographic effects. When vertical movements are accompanied by large high-angle faults, important topographic and structural effects result. Although large strike-slip faults are prominent is some areas, and many seismologists believe that most earthquakes originate on faults in which the strike-slip component exceeds the dip-slip component, such faults appear to have been of minor importance in the past.

The problem of mountain building is only part of the entire subject of vertical movements of the crust of the earth. For many decades it has been customary to equate mountain building with folding and thrusting. Originally it was believed that the uplift was the direct result of the folding, similar to the rise of anticlines in pressure-box experiments. Later it was suggested that the uplift might be augmented by the isostatic rise of the root formed during the folding.

Although some mountains apparently result

from folding, many do not. Rather, they are the result of vertical movements that have no obvious genetic connection with earlier periods of folding. In some areas the crust fractures during these vertical movements, producing fault-block mountains and graben. Sialic roots under modern mountain ranges are of recent origin and are unrelated to the earlier folding. Mountain ranges may also form when blocks are squeezed upward between strike-slip faults.

Mountain building should not be equated with one type of diastrophism. A successful theory of diastrophism and mountain building must explain among other things (1) the horizontal compression that is essential to form belts of folded and thrust-faulted strata; (2) extensive vertical movements, with or without high-angle faulting, and unrelated to folding; and (3) extensive strike-slip faults.

References Cited

Adams, W. M., 1958, A study of earthquake mechanism using S wave data: Seismol. Soc. Am. Bull., v. 48, p. 201–219

Anderson, E. M., 1951, The dynamics of faulting and dyke formation, with applications to Britain, 2nd. ed.: London, Oliver and Boyd 206 p.

Axelrod, Daniel I., 1957, Late Tertiary floras and the Sierra Nevada uplift: Geol. Soc. Am. Bull., v. 68, p. 19–46

Barrell, Joseph, 1914, The Upper Devonian delta of the Appalachian geosyncline: Am. Jour. Sci., 4th ser., v. 37, p. 87–109, 225–253.

Belayevskiy, N. A., *et al.*, 1958, Geologic structure of the U.S.S.R.: 3 vols., Moscow, Ministry of geology and Conservation of Mineral Resources, U.S.S.R., 1303 p. (in Russian)

Beloussov, V. V., 1959, Types of folding and their origin: Intern. Geology Rev., v. 1, no. 2, p. 1–21

Bentz, A., 1949, Erdöl und Tektonik in Nordwestdeutschland: Hannover-Celle, Amt für Bodenforschung, 389 p.

Billings, Marland P., 1954, Structural geology, 2d ed: New York, Prentice-Hall 514 p.

—— 1956, Geology of New Hampshire, Part II, Bedrock geology: New Hampshire Planning and Development Comm., 203 p.

Billings, M. P., Rodgers, J., and Thompson, J. B., Jr., 1952, Geology of the Appalachian Highlands of east-central New York, southern Vermont, and southern New Hampshire: Guidebook for Field Trips in New England, Nov. 10–12, 1952, p. 1–71

Birch, F., 1950, Flow of heat in the Front Range, Colorado: Geol. Soc. America Bull., v. 61, p. 567–630

Birch, F., and LeComte, P., 1958, Plane of albite composition to 1,000°C. and 26,000 bars (Abstract): Geol. Soc. Am. Bull., v. 69, p. 1760

Boyd, F. R., and England, J. L., 1959, Quartz ⇄ coesite transition (Abstract): Jour. Geophys. Research, v. 64, p. 1095

Bucher, Walter H., 1956, Role of gravity in orogenesis: Geol. Soc. America Bull., v. 67, p. 1295–1318

Byerly, P., 1926, The Montana earthquake of June 28, 1925, G.M.C.T.: Seismol. Soc. Am. Bull., v. 16, p. 209–265

—— 1938, The Sierra Nevada in the light of isostasy, Geol. Soc. Am. Bull., v. 48, p. 48, p. 2025–2031

Cadisch, J., 1946, On some problems of alpine tectonics: Experientia, v. 2, p. 18–23

Carey, S. Warren, 1954, The rheid concept in geotectonics: Geol. Soc. of Australia Jour., v. 1, p. 67–117

—— *Convener*, 1958, Continental drift, a symposium: Hobart, Univ. Tasmania, Geology Dept, 375 p.

Chamberlin, R. T., 1910, The Appalachian folds of central Pennsylvania: Jour. Geology, v. 18, p. 228–251

—— 1919, The building of the Colorado Rockies: Jour. Geology, v. 27, p. 145–164, 225–235

Clark, S. P., Jr., Robertson, E. C., and Birch, F., 1957, Experimental determination of kyanite-sillimanite equilibrium relations at high temperatures and pressures: Am. Jour. Sci., v. 255, p. 628–640

Cloos, E., 1940, Crustal shortening and axial divergence in the Appalachians of southeastern Pennsylvania and Maryland: Geol. Soc. America Bull., v. 51, p. 845–872

Cloos, Hans, 1939, Hebung, Spaltung, Vulkanismus: Geol. Rundschau, v. 30, p. 406–527

—— 1948, Grundschollen und Erdnähte: Geol. Rundschau, v. 35, p. 133–154

—— 1951–1952, Der Schwarzwald: Mitt. Naturf. Gesell, Schaffhausen, Bd. XXIV, p. 1–6

Cohee, George, *Editor*, (in press), Tectonic map of the United States: U. S. Geol. Survey and Am. Assoc. Petroleum Geologists

Collet, Leon W., 1927, The structure of the Alps: London, Edward Arnold and Co., 289 p.

Cooper, Byron H., 1944, Geology and mineral resources of the Burkes Garden quadrangle, Virginia: Va. Geol. Survey Bull. 60, 299 p.

Cotton, C. A., 1950, Tectonic scarps and fault valleys: Geol. Soc. Am. Bull., v. 61, p. 717–758

—— 1956, Geomechanics of New Zealand mountain building: New Zealand Jour. Sci. Technology section B, v. 38, p. 187–200

—— 1957a, An example of transcurrent-drift tectonics: New Zealand Jour. Sci. and Tech. Section B., vol. 38, p. 939–942

—— 1957b, Geomorphic evidence and major structures associated with transcurrent faults in New Zealand: Revue de Geographie Physique et de Geologie Dynamique, (2), v. 1, Fasc. 1, p. 16–30

Creer, K. M., 1958, Symposium on paleomagnetism and secular variation: Roy. Astron. Soc. Geophys. Jour., v. 1, no. 1, p. 99–105

Currie, John B., 1956, Concurrent deposition and deformation in development of salt-dome graben: Am. Assoc. Petroleum Geologists Bull., v. 40, p. 1–16

Daly, R. A., 1940, Strength and structure of the earth: New York, Prentice Hall, Inc., 434 p.

deSitter, L. U., 1956, Structural geology: New York, McGraw-Hill Book Co., Inc., 552 p.

Doell, B. R., and Cox, A., 1959, Analysis of paleo-

magnetic data (Abstract): Geol. Soc. America Bull., vol. 70, p. 1590

Dorn, Paul, 1951, Geologie von Mitteleuropa: Stuttgart, E. Schweizerbart'sche, 474 p.

Dorr, John A., Jr., 1958, Early Cenzoic vertebrate paleontology, sedimentation and orogeny in central western Wyoming: Geol. Soc. Am. Bull., v. 69, p. 1217–1244

Eardley, A. J., 1933a, Strong relief before block faulting in the vicinity of the Wasatch Mountains, Utah: Jour. Geology, v. 41, p. 243–267

—— 1933b, Structure and physiography of the southern Wasatch Mountains: Mich. Acad. Sci., Arts and Letters, Papers, v. 19, p. 377–400

—— 1951, Structural geology of North America: New York, Harper and Bros., 624 p.

Ewing, M., Worzel, J. L., Steenland, N. C., and Press, F., 1950, Geophysical investigations in the emerged and submerged Atlantic Coastal Plain, Part V: Woods Hole, New York, and Cape May sections: Geol. Soc. America Bull., v. 61, p. 877–892

Fisk, H. N., and McFarlan, E., Jr., 1955, Late Quaternary deltaic deposits of the Mississippi River, p. 279–302 *in* Poldervaart, Arie, *Editor*, Crust of the earth: Geol. Soc. Am. Spec. Paper 62, 762 p.

Flawn, Peter T., 1959, The Ouachita structural belt, p. 20–29 *in* Geology of the Ouachita Mountains, a Symposium: Dallas Geol. Soc. and Ardmore Geol. Soc., 208 p.

Flint, Richard F., 1957, Glacial and Pleistocene geology: New York, John Wiley and Sons, Inc., 553 p.

Gilbert, Grove K., 1890, Lake Bonneville: U. S. Geol. Survey, Mon. 1, 438 p.

Gilluly, James, 1932, Geology and ore deposits of the Stockton and Fairfield quadrangles, Utah: U. S. Geol. Survey Prof. Paper 173, 171 p.

Gold, T., 1955, Instability of the earth's axis of rotation: Nature, vol. 175, p. 526–529

Gregory, J. W., 1921, The rift valleys and geology of East Africa: London, Seeley, Service and Co., Ltd., 479 p.

Gutenberg, B., 1943, Seismological evidence for the roots of mountains: Geol. Soc. America Bull., v. 54, p. 473–498

—— 1957, Discrepancies between thickness of the crust calculated from seismic and from gravity data (Abstract): Am. Geophys. Union Trans., v. 38, p. 392

Hack, John T., 1957, Studies of longitudinal stream profiles in Virginia and Maryland: U. S. Geol. Survey Prof. Paper 294, p. 45–97

Halbouty, Michel T., and Hardin, George C., Jr., 1959, A geological appraisal of present and future exploration techniques on salt domes of the Gulf Region of the United States: 5th World Petroleum Cong., Section I, Paper 5, 13 p.

Haller, John, 1956, Probleme du Tiefentektonik Bauformen in Migmatit-Stockwerk der Ostgrönlandischen Kaledoniden: Geol. Rundschau, Bd. 45, p. 159–167

Hammer, S., and Heck, S. T., 1941, A gravity-profile across the central Appalachians, Buckhannon, West Virginia, to Swift Run Gap, Virginia: Am. Geophys. Union Trans. Pt. II, 22nd Annual Meeting, p. 353–362

Heim, Albert, 1919; 1921, Geologie der Schweiz, vol. 1, 704 p., 1919; vol. II, 1018 p., 1921: Leipzig, Chr. Herm. Tauchnitz

Hennig, E., 1938, Regionale Geologie der Erde, Bd. 1, Abs. V, Afrika: Akademische Verlagsgesellschaft M.B.H., Leipzig, 142 p.

Hess, H. H., 1954, Serpentines, orogeny, and epeirogeny, p. 391–408 *in* Poldervaart, Arie, *Editor*, Crust of the earth: Geol. Soc. America Spec. Paper 62, 762 p.

Hess, H. H., and Maxell, J. C., 1953, Caribbean research project: Geol. Soc. Am. Bull., v. 64, p. 1–6

Hill, Mason L., and Dibblee, T. W., Jr., 1953, San Andreas, Garlock, and Big Pine faults, California: Geol. Soc. Am. Bull., v. 64, p. 443–458

Hinds, Norman E. A., 1952, Evolution of the California landscape: Calif. Div. Mines Bull. 158, 240 p.

Hobbs, W. H., 1901, The river system of Connecticut: Jour. Geology, vol. IX, p. 469–484

—— 1904, Lineaments of the Atlantic border region: Geol. Soc. Am. Bull., v. 15, p. 483–506

—— 1905, The correlation of fracture systems and the evidences for planetary dislocations within the earth's crust: Wis. Acad. Sci., Arts and Letters Trans., vol. XV, p. 15–29

—— 1911, Repeating patterns in the relief and the structure of the land: Geol. Soc. Am. Bull., v. 22, p. 123–176

Hodgson, John H., 1957, Nature of faulting in large earthquakes: Geol. Soc. Am. Bull., v. 68, p. 611–644

Hodgson, J. H., *Editor*, 1959, The mechanics of faulting with special reference to the fault-plane work, a symposium (1957): Pubs. of Dominion Observatory, Ottawa, vol. XX, p. 251–418

Holmes, Arthur, 1945, Principles of physical geology: New York, The Ronald Press Company, 532 p.

Johnson, Douglas, 1931, Stream sculpture of the Atlantic slope: New York, Columbia Univ. Press, 142 p.

Kelley, Vincent C., 1955, Regional tectonics of the Colorado Plateau and relationship to the origin and distribution of uranium: Univ. N. Mex., Pub. Geology, no. 5, 120 p.

Kennedy, George C., 1959, The origin of continents, mountain ranges, and ocean basins: Am. Scientist, v. 47, p. 491–504

Kennedy, W. Q., 1946, The Great fault: Geol. Soc. London Quart. Jour., v. CII, p. 41–76

King, P. B., 1951, The tectonics of middle North America: Princeton, Princeton Univ. Press, 203 p.

—— 1959, The evolution of North America: Princeton, Princeton Univ. Press, 190 p.

Kingma, J. T., 1958, Possible origin of piercement structures, unconformities, and secondary basins in the eastern geosyncline, New Zealand: N. Z. Jour. Geology and Geophysics, v. 1, p. 269–274

—— 1959, The tectonic history of New Zealand: New Zealand Jour. Geology & Geophysics, v. 2, p. 1–55

Knopf, A., and Kirk, E., 1918, A geological reconnaissance of the Inyo Range and the eastern slope of the Sierra Nevada, California: U. S. Geol. Survey Prof. Paper 110, 130 p.

Knopoff, L., and Gilbert, F., 1959, Radiation from

a strike-slip fault: Seismol. Soc. Am. Bull., v. 49, p. 163–178

Knopoff, L., and Gilbert, F., 1960, First motions from seismic sources: Seismol. Soc. Am. Bull., v. 50, p. 117–134

Krenkel, E., 1922, Die Bruchzonen Ostafrikas: Berlin, Gebrüder Borntraeger, 184 p.

Kuenen, Ph. H., 1950, Marine geology: New York, John Wiley and Sons, Inc., 568 p.

Landes, K. K., 1952, Our shrinking globe: Geol. Soc. Am. Bull., v. 63, p. 225–239

Lawson, A. C., 1914, San Francisco folio: U. S. Geol. Survey. Geol. Atlas of the United States

Lees, G. M., 1953, The evolution of a shrinking earth: Geol. Soc. London Quart. Jour., v. 109, p. 217–257

Longwell, C. R., *Editor*, 1944, Tectonic map of the United States: Am. Assoc. Petroleum Geologists

Longwell, C. R., 1958, My estimate of the continental drift concept, p. 1–12, *in* Carey, S. W., *Convener*, Continental drift: Hobart, Univ. Tasmania Geology Dept., 375 p.

Mansfield, G. R., 1927, Geology, geography, and mineral resources of southeastern Idaho: U. S. Geol. Survey Prof. Paper 152, 409 p.

Mason, R. G., 1958, A magnetic survey off the west coast of the United States between latitudes 32° and 36° N., longitudes 121° and 128° W.: Geophys. Jour., v. 1, p. 320–329

Maxson, John H., 1950, Physiographic features of the Panamint Range, California: Geol. Soc. America Bull., v. 61, p. 99–114

Maxwell, J. C., 1953, Geology of the Northern Appenines, by Giovanni Merla; Composite wedges in orogenesis, by Carlo I. Migliorini, Am. Assoc. Petroleum Geologists Bull., v. 37, p. 2196–2202

McIntyre, Donald B., and Christie, John M., 1957, Nature of faulting in large earthquakes: Geol. Soc. Am. Bull., v. 68, p. 645–652

McNish, A. G., 1941, The significance of fossil magnetism: Am. Philos. Soc. Proc., v. 84, p. 225–237

—— 1943, Fossil magnetism: Sci. American, v. 168, p. 166–167

McNish, A. G., and Johnson, E. A., 1940, Determination of the secular variation in declination in New England from magnetic polarization of glacial varves: Intern. Geod. Geophys. Union, Assoc. Terrestrial Magnetism and Electricity, Trans., Washington Meeting, Sept. 4–15, 1939, Bull., no. 11, p. 339–347

Menard, Henry W., 1955, Deformation of the northeastern Pacific basin and the west coast of North America: Geol. Soc. Am. Bull., v. 66, p. 1149–1198

Meshcheryakov, Yu. A., 1959, Contemporary movements in the earth's crust: Intern. Geology Rev., v. 1, no. 8, p. 40–51

Miyashiro, A., and Banno, S., 1958, Nature of glaucophanitic metamorphism: Am. Jour. Sci., v. 256, p. 97–110

Moody, J. D., and Hill, M. J., 1956, Wrench-fault tectonics: Geol. Soc. Am. Bull., v. 67, p. 1207–1246

Moore, R. C., 1950, Late Paleozoic cyclic sedimentation in the central United States: 18th Intern. Geol. Cong. Rept., pt. IV, p. 5–16

Muller, S. W., Ferguson, H. G., and Roberts, R. J., 1951, Geology of the Mount Tobin quadrangle, Nevada: U. S. Geol. Survey, Geol. Quad. Maps of the United States, no. 7

Munk, W. H., 1956, Polar wandering: a marathon of errors: Nature, v. 177, p. 551–554

Murray, Grover, E., *et al.*, 1952, Sedimentary volumes in Gulf Coastal Plain of United States and Mexico: Geol. Soc. America Bull., v. 63, p. 1157–1228

Nagata, T., 1953, Rock magnetism: Tokyo, Maruzen Co., Ltd., 225 p.

Nettleton, L. L., 1934, Fluid mechanics of salt domes: Am. Assoc. Petroleum Geologists Bull., v. 18, p. 1175–1204

—— 1941, Relation of gravity to structure in the northern Appalachian area: Geophysics, v. 6, p. 270–286

Nolan, Thomas B., 1943, The Basin and Range province in Utah, Nevada, and California: U. S. Geol. Survey Prof. Paper 197, p. 141–196

Oberholzer, J., 1933, Geologie der Glarneralpen: Beiträge Geol. Karte der Schweiz, Neue Folge, Lieferung 28

Oliver, Howard W., 1956, Isostatic compensation for the Sierra Nevada, California (Abstract): Geol. Soc. Am. Bull., v. 67, p. 1724

Pierce, W. G., 1957, Heart Mountain and South Fork detachment thrusts: Am. Assoc. Petroleum Geologists, v. 41, p. 591–626

Press, Frank, 1956, Determination of crustal structure from phase velocity of Rayleigh waves. Part I: Southern California: Geol. Soc. Am. Bull., v. 67, p. 1647–1658

Putnam, William C., 1942, Geomorphology of the Ventura region, California: Geol. Soc. Am. Bull., v. 53, p. 691–754

Rich, John L., 1951, Origin of compressional mountains and associated phenomena: Geol. Soc. America Bull., v. 62, p. 1179–1222

Richter-Bernburg, G., and Schott, Wolfgang, 1959, The structural development of northwest German salt domes and their importance for oil accumulation: 5th World Petroleum Cong., Section I, Paper 4, 13 p.

Robertson, E. C., Birch F., and MacDonald, G. J. F., 1957, Experimental determination of jadeite stability relations to 25,000 bars: Am. Jour. Sci., v. 255, p. 115–137

Rod, Emile, 1956, Strike-slip faults of northern Venezuela: Am. Assoc. Petroleum Geologists Bull., v. 40, p. 457–476

Rodgers, John, 1949, Evolution of thought on structure of middle and southern Appalachians: Am. Assoc. Petroleum Geologists Bull., v. 33, p. 1643–1654

Runcorn, S. K., 1956, Paleomagnetic survey in Arizona and Utah: Geol. Soc. Am. Bull., v. 67, p. 301–316

Scheidegger, A. E., 1955, The physics of orogenesis in the light of new seismological evidence: Royal Soc. Canada Trans., v. XLIX, ser. III, p. 65–93

—— 1957a, Table of Russian fault plane solutions: Pubs. Dominion Observatory, v. XIX, p. 99–109

—— 1957b, Distribution of seismic faulting in the world: Geofisica pura e applicata, v. 38, p. 1–9

—— 1958a, On fault plane solutions of earthquakes: Geofisica pura e applicata, vol. 39, p. 13–18

Scheidegger, A. E., 1958b, Tectonophysical significance of fault plane solutions of earthquakes: Geofisica pura e applicata, v. 39, p. 19–25

Shackleton, R. M., 1955, Pleistocene movements in the Gregory Rift Valley: Geol. Rundschau, v. 43, p. 257–263

Sharp, R. P., 1939, Basin-Range structure of the Ruby-East Humboldt Range, northeastern Nevada: Geol. Soc. America Bull., v. 50, p. 881–920

Sonder, R. A., 1956, Mechanik der Erde, Stuttgart, E. Schweizerbart'sche, 291 p. *Reviews by*: H. H. Suter, Am. Assoc. Petroleum Geologists Bull., v. 41, p. 764–773, 1957; A. G. Fischer, Am. Jour. Sci., v. 256, p. 139–142, 1958

Sonder, R. A., and Vening Meinesz, F. A., 1947, Discussion of "Shear patterns of the earth's crust" by F. A. Vening Meinesz: Am. Geophys. Union Trans., v. 28, p. 939–946

Spangler, Walter B., 1950, Subsurface geology of Atlantic Coastal Plain of North Carolina: Am. Assoc. Petroleum Geologists Bull., v. 34, p. 100–132

Spieker, Edmund, 1946, Late Mesozoic and early Cenozoic history of central Utah: U. S. Geol. Survey Prof. Paper 205, p. 117–161

Stehli, Francis G., 1957, Possible Permain climatic zonation and its implications: Am. Jour. Sci., v. 255, p. 607–618

Swain, Frederick M., 1952, Ostracoda from wells in North Carolina: U. S. Geol. Survey Prof. Paper 234, 93 p.

Tatel, H. E., and Tuve, M. A., 1955, Seismic exploration of a continental crust, p. 35–50 *in* Poldervaart, Arie, *Editor*, Crust of the earth: Geol. Soc. America Special Paper 62, 762 p.

Tocher, Donald, *et al.*, 1957, The Dixie Valley-Fairview Peak, Nevada, earthquakes of December 16, 1954: Seismol. Soc. Am. Bull., v. 47, p. 299–396

Tsuboi, Chuji, 1956, Crustal structure in northern and middle California from gravity-pendulum data: Geol. Soc. Am. Bull., v. 67, p. 1641–1646

Umbgrove, J. H. F., 1946, Recent theories of polar displacement: Am. Jour. Sci., v. 244, p. 105–113

Upham, Warren, 1894, Wave-like progress of an epeirogenic uplift: Jour. Geology, v. 2, p. 383–395

Van Bemmelen, Rein W., 1954, Mountain building: The Hague, Martinusnijhoff, 177 p.

Van der Gracht, W. A. J. M. van Waterschoot, *Editor*, 1928, Theory of continental drift: Am. Assoc. Petroleum Geologists, 240 p., Tulsa.

Vening Meinesz, F. A., 1943, Spanningen in de aardkorst tengevolge van poolverschuivingen: Nederl. Akad. v. Wetensch. Afd. Natuurk., Verslag. dl. 52, no. 5, p. 185–196

—— 1947, Shear patterns of the earth's crust: Am. Geophys. Union Trans., v. 28, p. 1–61

Von Bubnoff, Serge, 1954, Grundprobleme der Geologie: Berlin, Akademie-Verlag 234 p.

Wanless, H. R., 1950, Late Paleozoic cycles of sedimentation in the United States: 18th Intern. Geol. Cong. Rept., part IV, p. 17–26

Wanless, H. R., and Weller, J. M., 1932, Correlation and extent of Pennsylvanian cyclothems: Geol. Soc. America Bull., v. 43, p. 1003–1016

Wegener, Alfred, 1915, Die Entstehung der Kontinente und Ozeane: Sammlung Vieweg, Heft 23, Braunschweig (Brunswick, Germany), 94 p.

Wegener, Alfred, 1924, The origin of continents and oceans, translated from 3rd German edition by J. G. A. Skerl: London, Methen and Co., Ltd., 212 p.

Wegman, E., 1955, Vue d'ensemble sur les travaux de la reunion de printemps 1954 a Mayence: Geol. Rundschau, v. 43, p. 273–306

Wellman, H. W., 1955, New Zealand Quaternary tectonics: Geol. Rundschau, v. 43, p. 248–257

—— 1956, Structural outline of New Zealand: New Zealand Dept. Sci. Indus. Research Bull. 121, 36 p.

Wilson, J. Tuzo, 1959, Geophysics and continental growth: Am. Scientist, vol. 47, pp. 1–24.

Wolfe, C. W., 1949, The blister hypothesis and the orogenic cycle: New York Acad. Sci. Trans., ser. 2, v. 2, p. 188–195

Woollard, George P., 1943, Transcontinental gravitational and magnetic profile of North America and its relation to geologic structure: Geol. Soc. America Bull., v. 54, p. 747–790

—— 1949, Gravity anomalies and the nature of the earth's crust: Am. Geophys. Union Trans., v. 30, p. 189–201

—— 1959, Crustal structure from gravity and seismic measurements: Jour. Geophys. Research, v. 64, p. 1521–1544

Dept. of Geology, Harvard Univ., Cambridge 38, Mass.

Manuscript Received by the Secretary of the Society, December 10, 1959

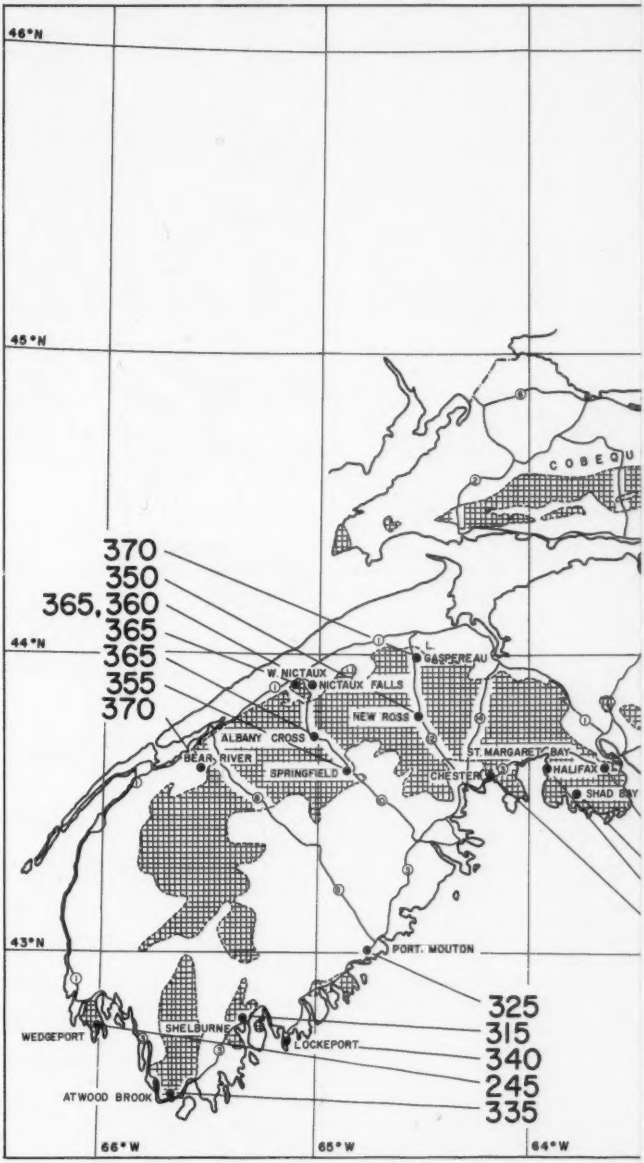

MAP SHOWING DISTRIBUTION AND

Number

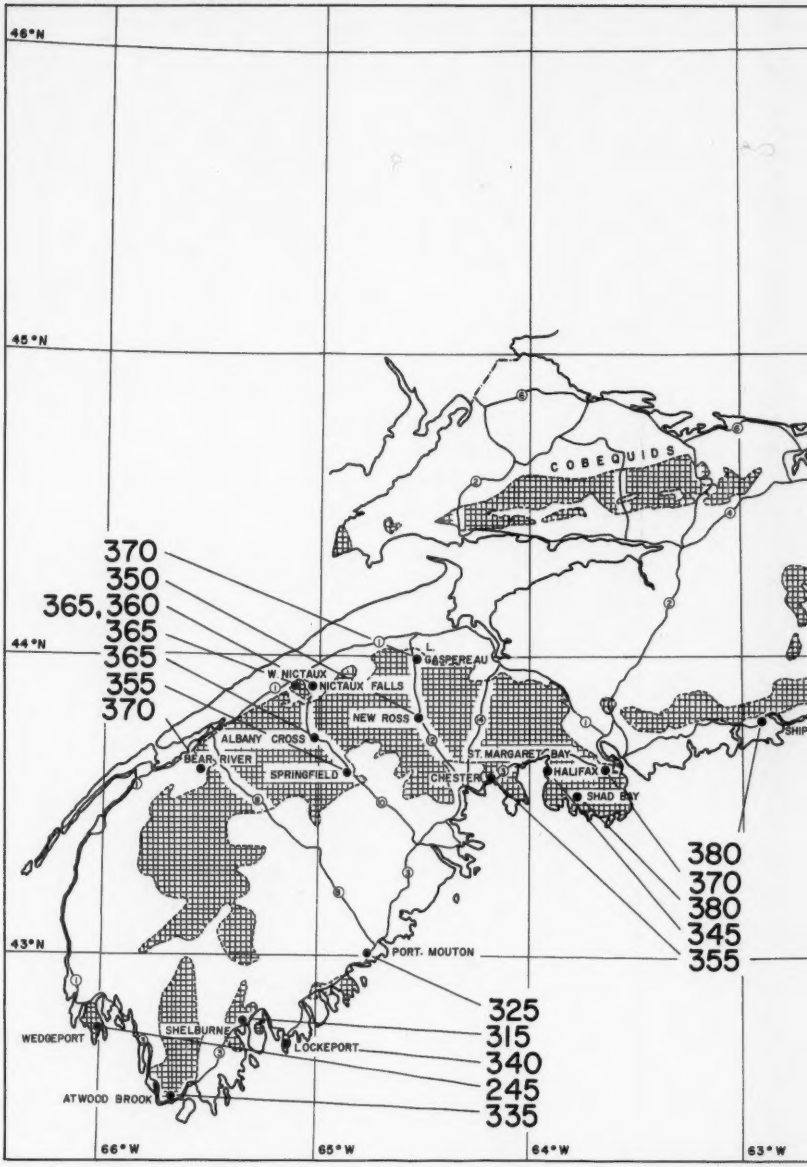

MAP SHOWING DISTRIBUTION AND AGE OF G

Numbers are sample loca

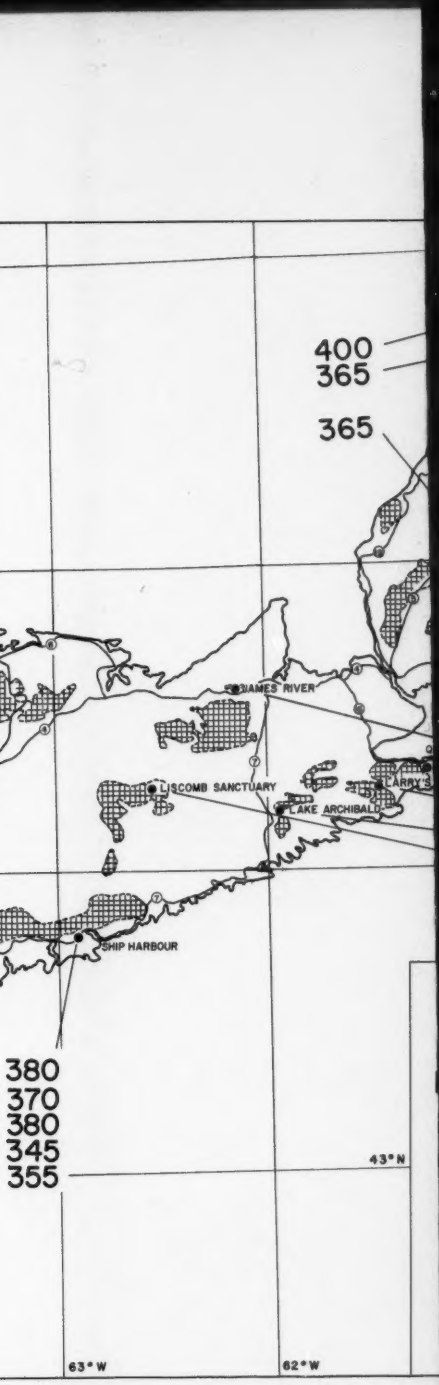

GE OF GRANITIC ROCKS IN

e sample localities.

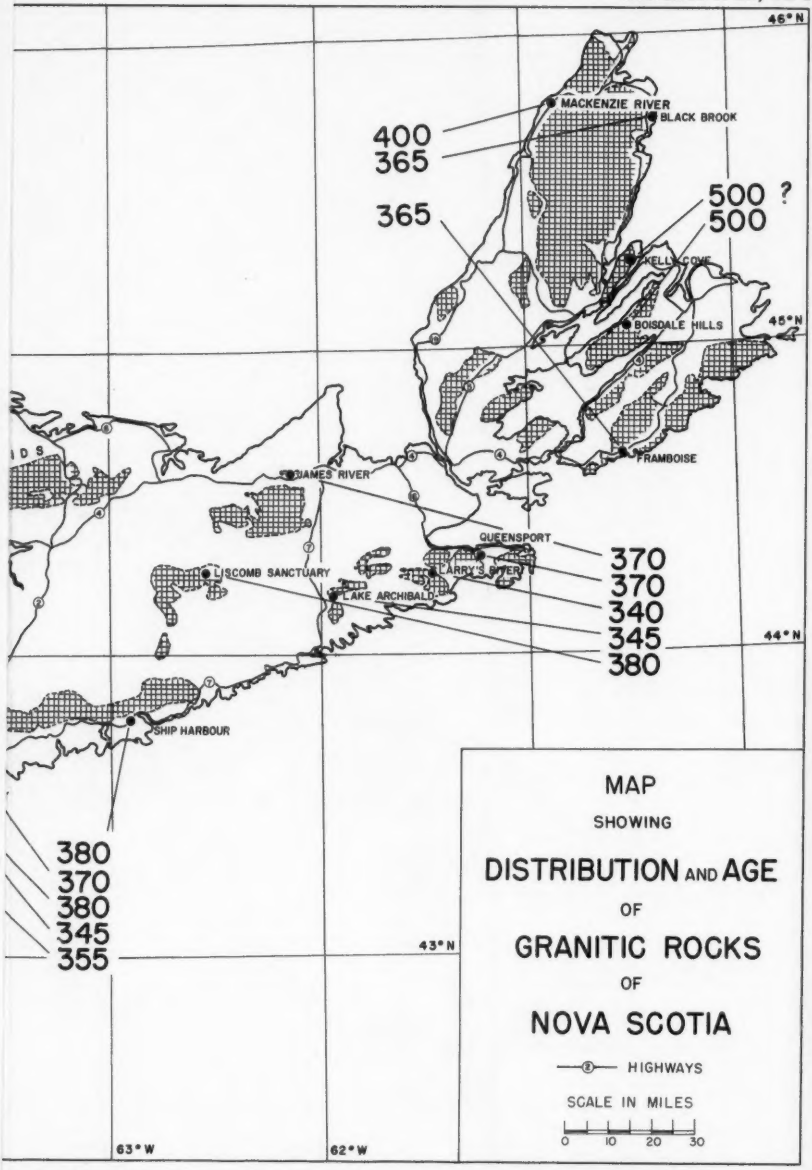

) AGE OF GRANITIC ROCKS IN NOVA SCOTIA

rs are sample localities.

BULLETIN OF THE GEOLOGICAL SOCIETY OF AMERICA
VOL. 71, PP. 399–414, 4 FIGS., 1 PL. APRIL 1960

AGE OF THE GRANITIC ROCKS OF NOVA SCOTIA

BY H. W. FAIRBAIRN, P. M. HURLEY, W. H. PINSON, JR., AND R. F. CORMIER

ABSTRACT

The ages of biotite, muscovite, and potassium feldspar in granitic rocks from 27 localities in Nova Scotia, as determined by A/K and Sr/Rb methods, fall in the range 300 to 400 m.y. At two localities, where nearby intrusive contacts with upper Lower Devonian fossiliferous sedimentary rocks are established, the best estimate of the age of the intrusive rocks is 365 ± 20 m.y. Biotite and potassium feldspar in granite from Boisdale Hills (Cape Breton Island), associated with nearby Middle Cambrian sedimentary rocks, have an estimated age of 500 ± 20 m.y. A single age analysis of biotite in the metamorphosed Meguma series gives 340 m.y. Radiation-damage ratios for zircon at nine localities where the age has been determined show one concordant result and eight which are lower than the A/K and Sr/Rb ages by 16 to 33 per cent.

The evidence of the mineral ages in the granitic rocks investigated thus far in Nova Scotia strongly suggests a protracted period of intrusion in the Devonian, with the upper Lower Devonian older than 365 m.y. Middle Cambrian is tentatively believed to be older than 500 m.y.

Holmes' B time scale, with Cambrian limits of 430 and 510 m.y. and Devonian limits of 255 and 313 m.y., would require an extension of 10–25 per cent to meet the Nova Scotia data.

CONTENTS

TEXT

	Page
Introduction	399
Acknowledgments	400
Methods of analysis	400
Rubidium-strontium analyses	401
Potassium-argon analyses	401
Comparison of Sr/Rb and A/K age data	404
Correlation of radiation-damage ratios with A/K and Sr/Rb ages	405
Stratigraphic aspects of the age data	406
Metamorphic aspects of the age data	410
Conclusions	412
References cited	412
Appendix: Details of sample localities	413

ILLUSTRATIONS

Figure	Page
1. Plot showing sample variation of Rb/Sr and $^{*}Sr^{87}/Sr$	404
2. Age histograms	405
3. Correlation of A/K and Sr/Rb age data	407
4. Radiation-damage ratios and Sr/Rb-A/K age data	411
Plate	**Facing page**
1. Map showing distribution and age of granitic rocks in Nova Scotia and sample localities	399

TABLES

Table	Page
1. Analytical data for Sr/Rb ages of biotite, muscovite, and K feldspar	402
2. Age errors for samples with varying Rb/Sr	404
3. Biotite - muscovite and biotite - feldspar pairs	406
4. Analytical data for A/K ages of biotite and muscovite	408
5. Summary of ages	410
6. Comparison of age estimates (mica and K feldspar) with radiation-damage ratios	410
7. Critical age localities	411

INTRODUCTION

A large part of Nova Scotia is dominated by granitic rocks. From Wedgeport in the southeast to Cape North at the tip of Cape Breton Island, an over-all distance of about 400 miles, the sedimentary and metamorphic horizons of the province are everywhere associated with granite, granodiorite, diorite, and related rock types. Although no detailed petrographic study of the entire area has ever been made, enough is known to indicate great textural and

compositional variation. Despite their heterogeneous character, the rocks are for the most part rich in mica, particularly biotite. This feature has made the present investigation possible.

Our interest in Nova Scotia age problems stems from a combination of a few established sedimentary-intrusive igneous contacts and a much larger number of ill-defined and undated field associations. The results obtained have on the whole been enlightening, although, as is usual, additional problems have been encountered. We are reporting at this time on 27 localities, representative of the entire province with the exception of the Cobequid area on the northern edge (*See* Plate 1).

Acknowledgments

The Atomic Energy Commission, Division of Research, made possible the analytical work through a series of annual grants to P. M. Hurley, supervisor of the laboratory.[1]

The Nova Scotia Research Foundation, through its director, Harold Smith, gave financial assistance for collection of samples. The Geological Society of America, through a grant-in-aid to H. W. Fairbairn (666-55) made possible the correlation of zircon radiation-damage ratios with absolute ages. The active assistance of A. J. Boucot, W. H. Whitehead, and D. J. MacNeil of the Nova Scotia Centre for Geological Sciences is gratefully acknowledged. We acknowledge also the co-operation of W. H. Dennen, C. F. Hickox, Jr., D. G. Kelley, L. H. King, E. R. W. Neale, W. G. Smitheringale, and P. R. Whitney in obtaining field samples for the work. The assistance of L. F. Herzog, Jr., was invaluable during the early stages of the Sr/Rb mass-spectrometric work.

Methods of Analysis

Fresh field samples of approximately 10 to 50 pounds were crushed and screened, and concentrates of biotite, muscovite, and K feldspar were obtained by magnetic and heavy-liquid separation. Most of the final products contained less than 10 per cent impurities. Facilities for both A/K and Sr/Rb methods of age determination were available, and a number of samples were analyzed by both methods. Co-existing minerals, particularly muscovite and biotite, were analyzed wherever possible.

The Sr/Rb analytical data were obtained by mass spectrometric analysis, using a stable-isotope dilution procedure. Details of the method are essentially the same as described from our laboratory by Herzog and Pinson (1955), as developed by Davis and Aldrich (1953), Tilton, Aldrich, and Inghram (1954), Inghram (1955), and Aldrich *et al.* (1956). We have introduced a few modifications, such as a radioactive Sr^{85} tracer to aid in monitoring the separation of the sample Sr.

The A/K analytical data were obtained by mass spectrometric analysis of argon and flame-photometric analysis of potassium. Aldrich and Nier (1948) pioneered in the determination of A^{40} in potassium minerals; application to age problems has since been extensively investigated (Smits and Gentner, 1950; Wetherill, Aldrich, and Davis, 1955; Wasserburg and Hayden, 1955). In our laboratory the general procedure is as follows.

Argon is released from the samples by direct fusion using induction heating, and the spiked gases are purified with hot titanium metal. Air contamination is determined by measurement of A^{36}. In most cases, the air-contamination corrections have been less than 5 per cent. The calibration of the argon system was carried out using spectroscopically pure argon and measured volumes. Independent analyses of the argon content of standard air have yielded an average value of 0.937 per cent total argon, using the spike and apparatus constants employed in the runs on unknowns. This value is close to the value of 0.94 per cent commonly given for the argon content of air, so the calibrations are considered to be sufficiently accurate. In addition, the argon measurements on a standard biotite, B3203, average 3.891×10^{-4} std. cc/g, which is within 1 per cent of a value determined at the Carnegie Institution of Washington (G. W. Wetherill, personal communication).

A Perkin-Elmer, Model 146, flame photometer, augmented by a mass spectrometer for checking, was used for the potassium analyses. Replicate photometer determinations were made, using at least two independent solutions, with lithium as an internal standard, until a satisfactory mean was obtained. This mean agreed satisfactorily with isotope-dilution analysis by mass spectrometer wherever checks were made. All the analyses were monitored against biotite, feldspar, and rock standards.

[1] Reproduction of the work in whole or in part is permitted for any purpose of the U. S. Government.

Rubidium-Strontium Analyses

Table 1 shows the analytical data from 23 localities, arranged in approximate geographic sequence from southwest to northeast across the province. With four exceptions, the Rb/Sr ratio was large enough in all analyses for age computation by isotope dilution only; three feldspars and one muscovite required an additional isotope-ratio analysis to reduce errors to an acceptable level. This is normal procedure for all potassium feldspars because of their relatively low Rb/Sr ratios. The muscovite sample had not been sufficiently concentrated, and its reported Sr content of 90.9 ppm is mostly from plagioclase contamination.

Details of calculation of precision of analysis are reserved for another paper, and only a general statement is included here. The variable most directly related to magnitude of precision error is the Rb/Sr ratio, from which a second important ratio $*Sr^{87}/Sr$ can be computed. Where this second ratio is very small, the error in $*Sr^{87}$ may be very large for isotope-dilution analysis. Figure 1 shows the distribution of all the analyses on a plot relating Rb/Sr and $*Sr^{87}/Sr$. As age varies with $*Sr^{87}/Rb^{87}$ for a given decay constant, all samples of a given age will lie on a straight line. The diagram serves as a check on computation and also to show the relative positions of those samples with lowest Rb/Sr and $*Sr^{87}/Sr$ (inset in Fig. 1). The four lowest are those previously mentioned for which additional isotope-ratio analyses were carried out in order to reduce the error in $*Sr^{87}$. Two others, also in the inset, might likewise have been given isotope-ratio analyses but, as their isotope-dilution ages agreed reasonably well with ages of coexisting minerals, the additional analyses were not made.

Calculation of standard precision error in four selected samples gives the results shown in Table 2. The muscovite-biotite pair (2089) shows widely varying Rb/Sr, with resultant lower error in the biotite age than in the muscovite. The difference in age error, however, is not great, as the error assumed in the weight of spike is constant for both samples. A second biotite-muscovite pair (3134) illustrates the effect of very low Rb/Sr. Biotite shows the normal range of error, whereas $*Sr^{87}/Sr$ in the muscovite is so low that the computed error is more than 20 per cent. The isotope-ratio analysis, which avoids the error-sensitive ratio of $*Sr^{87}$ to spike Sr, reduces the age error to an acceptable degree. As a test of this, the computed uncertainties of 24 and 30 m.y. in B3134 and M3134 overlap.

Precision error has not been computed for all the analyses, but probably none exceeds 10 per cent and the great majority are approximately 5 per cent.

No adequate test of accuracy of Rb and $*Sr^{87}$ analyses in mica and feldspar has yet been made. Work is progressing on a suite of lepidolites in an effort to correct this situation (Aldrich *et al.*, 1956; Herzog and Pinson, in press), and accuracy of at least 5 per cent has already been demonstrated for $*Sr^{87}/Rb^{87}$. These lepidolite samples, although intended as interlaboratory standards, are suspect as to homogeneity, and no reserve stock is available. Interlaboratory work reported over a period of years on other minerals, using different methods of analysis, likewise suggests 5 per cent accuracy as probable (*e.g.*, Herzog and Pinson, 1956; Smales, 1955).

In the present investigation, if cogenesis as well as coexistence of the minerals is assumed, Table 3 gives geological support for this level of accuracy from most of the mineral pairs listed. Most of the data in Table 5 (comparing Sr/Rb and A/K ages) would likewise fall within the 5 per cent limit.

A histogram of the Sr/Rb ages (Fig. 2, center) shows a spread between 320 and 422 m.y. which is far in excess of these 5 per cent precision and accuracy limits. The significance of this is therefore geological, not analytical, and will be considered later.

Potassium-Argon Analyses

Table 4 lists A/K ages from 17 localities, 13 of which are also included in Table 1. Precision error for argon in these analyses is based on replicate runs on the same sample, which indicate an uncertainty of 0.4 per cent. In most cases the standard weight of the sample used was 5 gm, so that for a pure mineral the variability between each sample taken for analysis does not exceed the analytical error. A conservative estimate of the error in argon determination would therefore be about 1 per cent.

Accuracy of argon analysis is based on checks against the known amount in the atmosphere. Three analyses of atmospheric argon made in our laboratory agreed well within 1 per cent.

Precision of potassium analysis in our laboratory, using photometric methods, may

TABLE 1.—ANALYTICAL DATA FOR Sr/Rb AGES OF BIOTITE, MUSCOVITE, AND K FELDSPAR

Sample No. and Locality	Lat. and Long.	Normal Sr (ppm by wt.)	Radiogenic $*Sr^{87}$ (ppm by wt.)	Rb (ppm by wt.)	Rb/Sr	$*Sr^{87}/Sr$	$*Sr^{87}/Rb^{87}$	Age (m.y.)
B2094								
Atwood Brook	43°31′N.	17.5	0.55	425	24	.031	.00457	*325*
Shelburne Co.	65°42′W.							
B2100								
Shelburne	43°47′N.	4.9	2.17	1666	340	.443	.00460	*330*
Shelburne Co.	65°20′W.							
B2092								
Port Mouton	43°46′N.	4.5	1.10	853	190	.244	.00455	*326*
Queen's Co.	65°24′W.							
B3250								
Bear River	44°37′N.	11.3	0.79	541	50	.070	.00516	*370*
Annapolis Co.	65°33′W.							
B3308A								
Nictaux Falls	44°53′N.	11.5	1.02	665	58	.089	.00542	*391*
Annapolis Co.	65°2′W.							
B3308B								
Nictaux Falls	44°53′N.	7.5	1.36	843	112	.181	.00570	*410*
Annapolis Co.	65°2′W.							
B2095								
West Nictaux	44°54′N.	6.9	0.60	431	62	.087	.00498	*358*
Annapolis Co.	65°7′W.			419				
B2099								
Lake Gaspereau	44°59′N.	16.2	0.82	556	34	.051	.00521	*376*
King's Co.	64°33′W.							
B2096								
Albany Cross	44°43′N.	4.0	0.95	688	172	.238	.00488	*355*
Annapolis Co.	65°2′W.							
B2097								
Springfield	44°37′N.	8.3	1.04	748	90	.125	.00491	*355*
Annapolis Co.	64°52′W.							
B2098								
New Ross	44°48′N.	5.8	0.90	652	112	.155	.00487	*350*
Lunenburg Co.	64°32′W.							
B1710								
Chester	44°36′N.	4.5	1.06	756	168	.236	.00495	*357*
Lunenburg Co.	64°12′W.							
B1712								
St. Margaret Bay	44°37′N.	6.8	1.29	891	131	.190	.00512	*368*
Halifax Co.	63°55′W.							
M1712								
St. Margaret Bay	44°37′N.	3.3	1.61	1229	372	.488	.00463	*332*
Halifax Co.	63°55′W.							
B2091								
Shad Bay	44°32′N.	8.6	1.50	987	115	.174	.00537	*385*
Halifax Co.	63°47′W.							
M2091								
Shad Bay	44°32′N.	26.2	1.29	880	34	.049	.00518	*373*
Halifax Co.	63°47′W.							
B2090								
Halifax	44°38′N.	9.2	0.86	586	64	.093	.00517	*372*
Halifax Co.	63°39′W.							

TABLE 1.—*Continued*

Sample No. and Locality	Lat. and Long.	Normal Sr (ppm by wt.)	Radiogenic $*Sr^{87}$ (ppm by wt.)	Rb (ppm by wt.)	Rb/Sr	$*Sr^{87}/Sr$	$*Sr^{87}/Rb^{87}$	Age (m.y.)
B3128								
Ship Harbour	44°48′N.	8.5	1.90	1287	151	.224	.00522	*376*
Halifax Co.	62°55′W.							
M3128								
Ship Harbour	44°48′N.	14.8	0.95	604	41	.064	.00555	*400*
Halifax Co.	62°55′W.							
F3326								
James River	45°35′N.	56.4	0.50†	342	61	.009	.00513	*370*
Antigonish Co.	62°12′W.							
B1708								
Larry's River	45°16′N.	3.3	1.65	1239	375	.500	.00470	*338*
Guysborough Co.	61°28′W.							
M1708								
Larry's River	45°16′N.	8.4	0.92	683	81	.110	.00475	*342*
Guysborough Co.	61°28′W.							
B2089								
Queensport	45°18′N.	3.3	1.93	1323	401	.585	.00515	*370*
Guysborough Co.	61°14′W.							
M2089								
Queensport	45°18′N.	45.2	0.82	563	12	.018	.00515	*370*
Guysborough Co.	61°14′W.							
B3132								
Boisdale Hills	46°4′N.	35.4	0.53	286	8.1	.015	.00654	*470*
Cape Breton Co.	60°30′W.							
F3132								
Boisdale Hills	46°4′N.	43.3	0.51†	263	6.1	.012	.00685	*486*
Cape Breton Co.	60°30′W.							
B3134								
MacKenzie River	46°50′N.	18.6	0.66	449	24	.035	.00519	*375*
Inverness Co.	60°40′W.							
M3134								
MacKenzie River	46°50′N.	90.9	0.50†	302	3.3	.005	.00587	*422*
Inverness Co.	60°40′W.							
F3129								
Kelly Cove	46°17′N.	47.9	0.79	346	7.3	.016	.0080	*576*
Victoria Co.	60°29′W.		0.575†	347	7.3	.012	.0059	*422*

† Isotope-ratio analysis of unspiked sample
Initial letters B, M, F indicate biotite, muscovite, or K feldspar analysis
Decay constant for Rb^{87} is $\lambda_{Rb} = 1.39 \times 10^{-11}$ yr.$^{-1}$
Relative abundance $Rb^{87} = 0.2785$
Initial Sr^{87} relative abundance = 0.0702

confidently be set at 2 per cent. This is based on photometric error arising from replicate runs of the same sample solution and on discrepancies found between two independently prepared solutions.

Accuracy of potassium analysis has excellent control. Checks against four recognized standards (G-1/W-1, NBS 70, "Haplogranite") agreed in all cases to within 0.5 per cent; checks against three biotites (K analyzed gravimetrically, with Rb correction, by the Rock Analysis Laboratory, University of Minnesota) agreed within 1 per cent.

Precision error in A/K ages, based on the

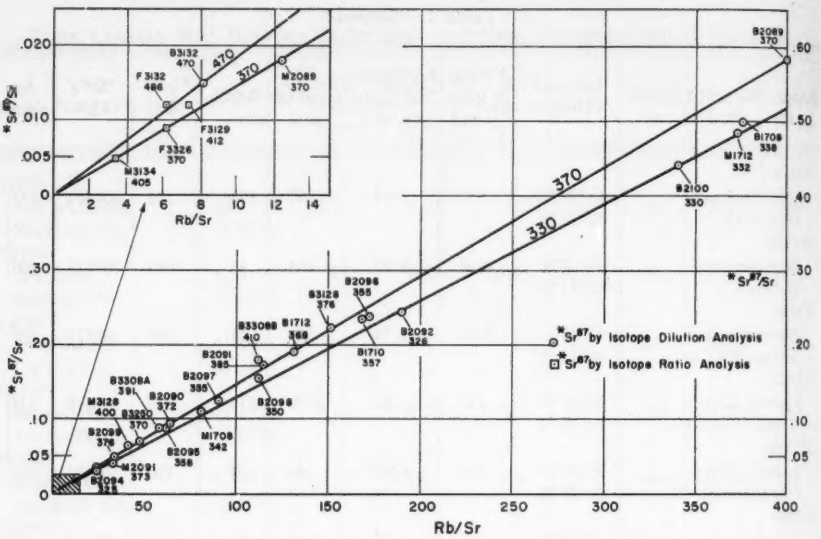

FIGURE 1.—PLOT SHOWING SAMPLE VARIATION OF Rb/Sr AND $*Sr^{87}/Sr$

TABLE 2.—AGE ERRORS† FOR SAMPLES WITH VARYING Rb/Sr

	B2089 Isotope dilution	M2089 Isotope dilution	B3134 Isotope dilution	M3134	
				Isotope dilution	Isotope ratio
Rb/Sr	401	12.5	24.1	3.3	3.3
$*Sr^{87}/Sr$	0.585 ±0.026 ±4.5%	0.181 ±0.0106 ±5.9%	0.035 ±0.002 ±6.2%	0.0039 ±0.0009 ±22%	0.0053 ±0.0004 ±7.3%
Age	370 ±15 m.y. ±4%	370 ±22 m.y. ±5.9%	375 ±24 m.y. ±6.3%	302 ±69 m.y. ±23%	422 ±30 m.y. ±7.4%

† Based on 0.5 per cent error in measured ratios
Based on 0.25 per cent error in normal and spike isotope ratios
Based on 2.0 per cent error in weight of spike used in each analysis

preceding discussion, is estimated not to exceed 3 per cent, and accuracy error is estimated at not more than 2 per cent.

As with the Sr/Rb ages, the A/K determinations show an age spread far in excess of possible experimental errors in precision and accuracy. The bottom histogram of Figure 2 shows the distribution found, with a spread approximately the same as for the Sr/Rb histogram.

COMPARISON OF SR/RB AND A/K AGE DATA

Table 5 recapitulates the data of Tables 1 and 4 and, for each locality, presents a final estimate of the age to the nearest 5 million years. Figure 3 is based on this table, showing by tie lines those samples analyzed by both methods. Excluding the Nictaux Falls data, which will be considered hereafter, the remaining 11 analyses of Figure 3 show that the A/K

and Sr/Rb ages are in essential agreement, with no apparent bias. This result does not agree with ages obtained by Gast, Kulp, and Long (1958) in several Precambrian areas where analytical viewpoint, that the Sr/Rb ages for these Nictaux Falls samples are either superior or inferior to the A/K ages, and a mean of the two has been taken as the final estimate of

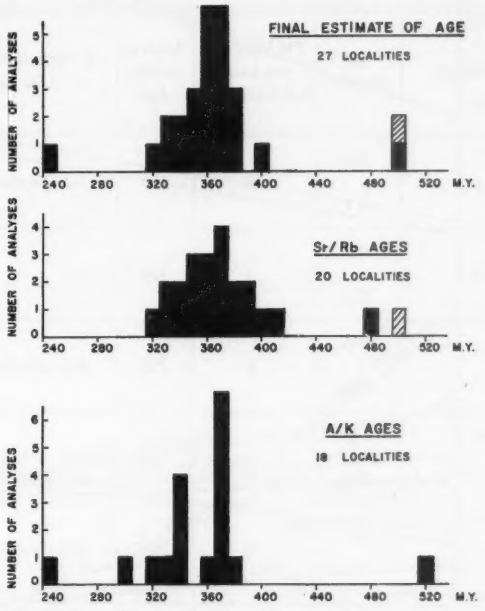

FIGURE 2.—AGE HISTOGRAMS

A/K values are consistently lower than Sr/Rb.

The large discrepancy between the two methods for samples 3308A and 3308B (Table 5) is outside the scope of the small differences considered heretofore. The two localities, about 1 mile apart near Nictaux Falls, are within a few hundred yards of an intrusive contact with fossiliferous upper Lower Devonian and Silurian strata. As the Sr/Rb ages for the A and B samples agree closely (391 and 410 m.y.), it seems unwarranted to assume any uncertainty in the values greater than the expected 5 per cent precision error. Furthermore, Rb/Sr and $*Sr^{87}/Sr$ (Fig. 1) for these localities show normal values which favor low errors.

Close agreement of the A/K ages for the A and B samples (Table 5) (333 and 318 m.y.) is equally striking. Duplicate potassium analyses for each sample showed normal precision error of 2 per cent. An experimental error of about 3 per cent in the A/K ages may reasonably be assumed.

There is thus no reason to believe, from the age in each case. Geological implications of the discrepancy are considered hereafter.

The top histogram in Figure 2 shows the over-all picture of the age data. As with the separate histograms for Sr/Rb and A/K ages, there is an almost continuous age spread between 300 and 400 m.y. which cannot be attributed to analytical error. Although a majority of the determinations center approximately on 365, there are equally satisfactory values both larger and smaller than this. We are therefore faced with real analytical differences which must have a geological cause.

The anomalously low A/K age of 243 m.y. at Wedgeport cannot be evaluated at present. The sample contained considerable chlorite and hornblende which made it unsuitable for Sr/Rb analysis.

CORRELATION OF RADIATION-DAMAGE RATIOS WITH A/K AND Sr/Rb AGES

In a recent study of radiation damage in zircon from granitic rocks (Fairbairn and

Hurley, 1957), ratios were computed from about 40 samples in northern New England and adjacent Canada. In theory such ratios should be equivalent to the time elapsed since crystallization of zircon and thus give the age of the igneous body containing them. In ideal cases this is so (Holland and Gottfried, 1955); in most instances, however, where comparisons have been made, the radiation-damage ratio is smaller than the estimated age and gives only a minimum "age." This is the case for most of the Nova Scotia examples. Table 6 and Figure 4 compare the data for nine localities. With the exception of Atwood Brook, the radiation-damage ratios are lower by 16 to 33 per cent.

No adequate interpretation of these "sub-age" ratios is at hand. As one of the ratios agrees with the mica age, an explanation for the discordant ratios might be that later recrystallization restored in part the damaged zircon structures and so yielded low ratios. The Boisdale Hills discordance is the largest and would lend some support to this. However, the range in age of the younger rocks (310–390 m.y. in Fig. 4) is in phase in almost every example with a correspondingly lower radiation-damage ratio. This would favor a direct correlation in the cooling history of each rock between age and radiation-damage ratio, rather than an independent and later thermal event (recrystallization). Within the limits of present information further speculation is pointless.

TABLE 3.—BIOTITE-MUSCOVITE AND BIOTITE-FELDSPAR PAIRS

Sample No. and Locality	Age (Sr/Rb)	Per cent discrepancy between pairs	Average Sr/Rb Age	Comparison with A/K Age	Sr/Rb and A/K differences in per cent
B1712 St. Margaret Bay M1712	368 332	10	350	340 (biotite)	3
B2091 Shad Bay M2091	385 373	3	379	n.d.	.. ..
B3128 Ship Harbour M3128	376 400	6	388	370 (biotite)	5
B1708 Larry's River M1708	338 342	1	340	362 (biotite) 321 (muscovite)	0.5
B2089 Queensport M2089	370 370	0	370	366 (biotite)	1
B3132 Boisdale Hills F3132	470 486	3	478	518 (biotite)	8
B3134 MacKenzie River M3134	375 422	12	398	n.d.	..

Initial letters—B, biotite; M, muscovite; F, K feldspar

STRATIGRAPHIC ASPECTS OF THE AGE DATA

There is general agreement that all the granitic rocks of Nova Scotia are pre-Carbonif-

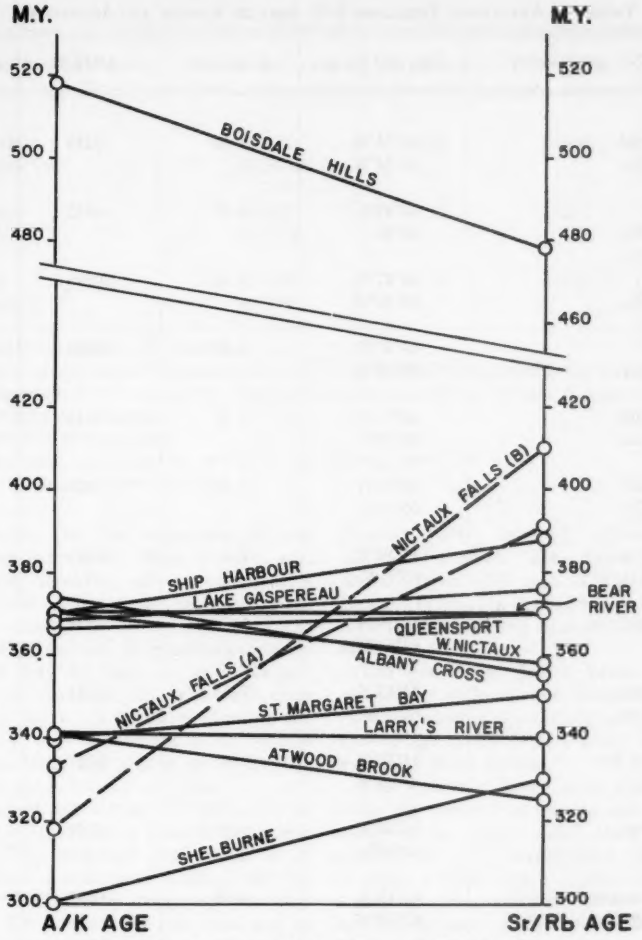

FIGURE 3.—CORRELATION OF A/K AND Sr/Rb AGE DATA

erous. Except in Cape Breton Island, it is likewise agreed that they are restricted to the Paleozoic (Weeks, 1954a, 1954b). These field inferences are confirmed in a general way by the age data presented here. Details of the correlation follow.

Table 7 lists six localities which are particularly important because of their field associations. Two of these, in the neighborhood of Nictaux Falls, have been discussed from the analytical standpoint because of intramethod agreement and intermethod discrepancy. These samples were collected about 1000 feet from metasediments which are baked and transformed to hornfels. Two fossil localities in these rocks are within half a mile of the granite sample localities. The matrix embedding the fossils shows the same metamorphism as the rocks nearest to the granite. Both field and paleontological investigators (A. J. Boucot, C. F. Hickox, Jr., and W. G. Smitheringale) agree without reservation as to the intrusive character of the contact and late Early Devonian age of the fossils.

The remaining samples listed in Table 7 were purposely collected from localities a mile or more distant from known contacts, to exclude possible effects on the age analyses of gain or loss of components. Additional work would be required to establish this point

TABLE 4.—ANALYTICAL DATA FOR A/K AGES OF BIOTITE AND MUSCOVITE

Sample No. and Locality	Lat. and Long.	K per cent	A^{40}/K^{40}	Argon age
B2094				
Atwood Brook	43°31′N.	7.62	.0219	341
Shelburne Co.	65°42′W.			
B3249				
Wedgeport	43°45′N.	6.29	.0152	243
Shelburne Co.	66°W.			
B2100				
Shelburne	43°47′N.	7.34	.0190	300
Shelburne Co.	65°20′W.			
B3250				
Bear River	44°37′N.	6.60	.0240	370
Annapolis Co.	65°33′W.			
B3308A				
Nictaux Falls	44°53′N.	5.97	.0213	333
Annapolis Co.	65°2′W.			
B3308B				
Nictaux Falls	44°53′N.	7.34	.0203	318
Annapolis Co.	65°2′W.			
B2095				
West Nictaux	44°54′N.	7.7	.0228	370
Annapolis Co.	65°7′W.			
B2099				
L. Gaspereau	44°59′N.	6.78	.0238	368
King's Co.	64°33′W.			
B2096				
Albany Cross	44°43′N.	7.15	.0242	374
Annapolis Co.	65°2′W.			
B1712				
St. Margaret Bay	44°37′N.	4.95	.0217	340
Halifax Co.	63°55′W.			
B3128				
Ship Harbour	44°48′N.	6.96	.0239	370
Halifax Co.	62°55′W.			
B3251				
Liscomb Sanctuary	45°15′N.	6.03	.0247	380
Guysborough Co.	62°30′W.			
M3133				
Archibald's Lake	45°12′N.	7.78	.0218	340
Guysborough Co.	61°57′W.			
B1708				
Larry's River	45°16′N.	6.78	.0233	362
Guysborough Co.	61°28′W.			
M1708*				
Larry's River	45°16′N.	8.22	.0205	321
Guysborough Co.	61°28′W.			
B2089				
Queensport	45°19′N.	7.60	.0236	366
Guysborough Co.	61°14′W.			
B1706				
Framboise	45°46′N.	5.68	.0235	364
Richmond Co.	60°33′W.			

TABLE 4.—*Continued*

Sample No. and Locality	Lat. and Long.	K per cent	A^{40}/K^{40}	Argon age
B3132				
Boisdale Hills	46°4′N.	3.69	.0349	518
Cape Breton Co.	60°30′W.			
B3130				
Black Brook	46°47′N.	7.54	.0237	367
Victoria Co.	60°19′W.			
B3252†				
Lockeport	43°43′N.	6.56	.0216	338
Shelburne Co.	65°9′W.			

Initial letters—B, biotite; M, muscovite

* The argon measurement of muscovite from Larry's River (M1708) is probably low because of an early faulty technique which did not apply to other argon measurements reported here. A repeat analysis is not possible, owing to lack of sample.

† Mica schist in Meguma series

Decay constants: $\lambda_e = 0.585 \times 10^{-10}$ yr.$^{-1}$; $\lambda = 5.30 \times 10^{-10}$ yr.$^{-1}$

Relative abundance of $K^{40} = 0.0119$

beyond doubt, but the agreement in age between the Bear River, West Nictaux, and James River localities, all at considerable distance from contacts, is nevertheless in striking contrast with the results from the Nictaux Falls localities. It is probably purely coincidental that the mean of the Sr/Rb and A/K ages for Nictaux Falls is in such close accord with the other localities showing the 360–370 m.y. age. We record it so because there is no analytical reason to prefer the high Sr/Rb age to the low A/K age.

The range of age values (300–400 m.y.) is, as noted, far in excess of possible analytical error (Fig. 2). Although both methods of analysis show culminations around 360–370 m.y., a not insignificant fraction of the total extends to 400 m.y. on the one hand and to 300 m.y. on the other. Localities close to upper Lower Devonian and Silurian strata (Table 7) show concordant ages of 365 m.y.; the mean of the discrepant values for the two Nictaux Falls localities, if significant, is in essential agreement with this. Present evidence therefore points to the age of the upper Lower Devonian strata in Nova Scotia as > 365 m.y. This value forces an appreciable extension, perhaps as much as 25 per cent, of Holmes' B time scale, where the limits of the Devonian are 255 and 313 m.y. (Holmes, 1947).

In agreement with Holmes for the Devonian, however, are (1) glauconite from the Lower Devonian Carlisle Centre formation, Cobleskill, New York (321 m.y. Sr/Rb), reported by Cormier (1957), and (2) sylvite from the Middle Devonian Elk Point formation, Saskatchewan (285 m.y. A/K), reported by Lipson (1956). The correlation of these results with the Nova Scotia data remains a problem for future study.

The granite at James River (Table 7), associated with Lower Ordovician rocks, raises no additional problems, as it is the same general age as the granite found elsewhere in mainland Nova Scotia.

The granite collected from Boisdale Hills, from the evidence of biotite and K feldspar analyses, is clearly older than any other granites we have investigated. The locality[2] is about 1 mile from a contact with Middle Cambrian strata which is regarded as intrusive by Hutchinson (1952). Goranson (1938), however, regarded the granite in this general region as Precambrian. In view of our conclusion that late Early Devonian is older than 365 m. y., it seems more reasonable to place Middle Cambrian > than 500 m.y., following the field conclusions of Hutchinson and Weeks, than to compress all the Cambrian, Ordovician, Silurian, and part of the Devonian into a time interval of about 150 m.y., as would be necessary if the Boisdale Hills granite were interpreted as late Precambrian. On the evidence of one locality, therefore, an early Paleozoic age is preferable. As there is no

[2] Sample collected by D. G. Kelley of the Canadian Geological Survey

TABLE 5.—SUMMARY OF AGES

Sample	A/K m.y.	Sr Rb m.y.	Final estimate (to nearest 5 m.y.)	% Difference between A/K and Sr/Rb ages
2094	341	325	335	+5
3249	243	n d	245	..
2100	300	330	315	−10
2092	n d.	326	325	..
3250	370	370	370	0
3308A	333	391	360	−16
3308B	318	410	365	−25
2095	370	358	365	+3
2099	368	376	370	−2
2096	374	355	365	+5
2097	n.d.	355	355	..
2098	n.d.	350	350	..
1710	n.d.	357	355	..
1712	340	350*	345	−3
2091	n.d.	379*	380	..
2090	n.d.	372	370	..
3128	370	388*	380	−5
3251	380	n.d.	380	..
3326	n.d.	370	370	..
3133	344	n.d.	345	..
1708	341*	340*	340	0
2089	366	370*	370	−1
1706	364	n.d.	365	..
3132	518	478*	500	+8
3134	n.d.	398*	400	..
3130	367	n.d.	365	..
3129	n.d.	(422)	(420)	..
3252	338	n.d.	340	..

* Average of mineral pairs (*See* Table 2)

major stratigraphic discontinuity between Middle Cambrian and Early Ordovician (Hutchinson, 1952), the granite may be as young as Early Ordovician. If so, Late Cambrian is older than 500 m.y., compared with Holmes' estimate of 430 m.y.

It is of interest here to note that Weeks (1954b), in a discussion of the unfossiliferous Middle River group (which rests unconformably on Middle Cambrian) believes the granite to be at least Late Ordovician and possibly Early Devonian. This would be evidence of a pre-Devonian orogeny (Taconic?) which in

TABLE 6.—COMPARISON OF AGE ESTIMATES (MICA AND K FELDSPAR) WITH RADIATION-DAMAGE RATIOS (ZIRCON)

Sample no. and locality	Estimate of absolute age	Radiation-damage ratio	Per cent difference
2094 Atwood Brook	335	335	0
2092 Port Mouton	325	270	−17
2099 Lake Gaspereau	370	320	−14
2096 Albany Cross	365	280	−23
2097 Springfield	355	270	−24
2098 New Ross	350	290	−17
2090 Halifax	370	310	−16
3132 Boisdale Hills	500	333	−33
3129 Kelly Cove	(422) (576)	370	−26

turn might account for the pre-Devonian age of the Boisdale Hills granite.

At a nearby locality (Kelly Cove) an inferior analysis of K feldspar (*See* Table 1) gives an age number which is greater than the 300 to 400 m.y. range and which may be comparable with Boisdale Hills. We quote it here mainly to emphasize that further age investigations in Cape Breton Island are urgently needed.

METAMORPHIC ASPECTS OF THE AGE DATA

No serious attempt was made in the present study to investigate metamorphic rocks, although metamorphism, as might be expected, is widespread. The Meguma series, for example, forms a metamorphic belt extending the entire length of the mainland area. Biotite from a schist at Lockeport (B3252) gives an A/K age of 340 m.y., which is in reasonable agreement with the time of intrusion of granites in the immediate neighborhood (315–335 m.y.). As these are at the low end of the age spectrum (Fig. 2), the parallel age of the biotite in the schist supports the geological reality of a long-continued period of intrusive activity which both antedated and outlasted the

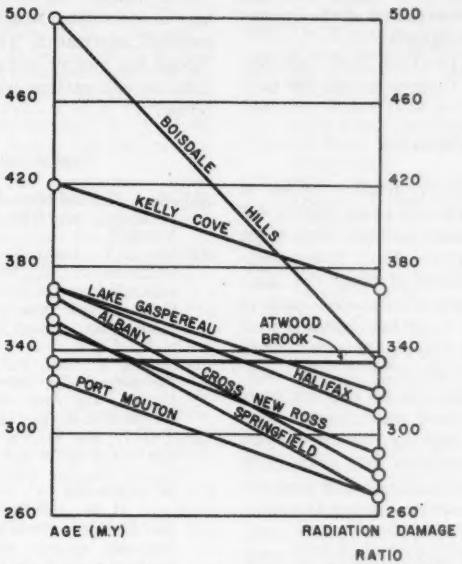

FIGURE 4.—RADIATION-DAMAGE RATIOS AND Sr/Rb-A/K AGE DATA

TABLE 7.—CRITICAL AGE LOCALITIES

Sample no. and locality	Stratigraphic relationship	Sr/Rb age	A/K age	Final estimate
B3250 Bear River	Granite about 1 mi. east intrudes fossiliferous upper Lower Devonian*	370	370	370
B3308A Nictaux Falls	Granite a few hundred yards fron intrusive contact with Silurian	391	333	360
B3308B Nictaux Falls	Same as B3308A, about 1 mi. north, and a few hundred yards from contact with upper Lower Devonian	410	318	365
B2095 West Nictaux	Sample locality is about 2 mi. NW of Silurian slates. Upper Lower Devonian is contiguous with Silurian	358	370	365
F3326 James River	Granites of this area intrude strata generally regarded as Lower Ordovician	370	n.d.	370
B3132 F3132 Boisdale Hills	Granite about 1 mi. away intrudes Middle Cambrian (Hutchinson, 1952). Goranson (1938) regarded these granites as Precambrian	470 486	518	500

* Previous descriptions indicate Lower Devonian in general. According to A. J. Boucot (Personal communication) more properly upper Lower Devonian.

intrusive episode at 365 m.y. when Devonian and earlier sediments were metamorphosed.

Fifteen miles northeast of the tip of Cape Breton Island, in Cabot Strait, the small island of St. Paul displays gneisses and schists of the same structural trend as comparable rocks in Newfoundland and Nova Scotia. Biotite from a schist on the island collected by

W. G. Phinney since completion of the present study gives the following data:

Sample B3280: K per cent, 6.45; A^{40}/K^{40}, 0.023; air correction, 1 per cent; age, 360 m.y.

Conclusions

Most of the extensive granitic bodies of Nova Scotia fall in the age range 300 to 400 m.y. (Boisdale Hills and possibly other Cape Breton granites excepted). There is a perceptible grouping of granites of about the same age, particularly in the southwestern part of the province and in a broad belt east and west of Nictaux Falls. The youngest intruded strata (late Early Devonian) are older than 365 m.y. Although limits cannot yet be set, the time, 300–400 m.y., when these granitic rocks were emplaced, may well constitute all the Devonian. Weeks (1954a) discusses field evidence in Cape Breton and Newfoundland which supports this concept. He believes that Lower Devonian granites underwent erosion contemporaneously with emplacement of Late Devonian plutons. The granite age data for Nova Scotia thus far provide strong support for this conclusion.

Although no comparable age statistics are available for the 500 m.y. granite locality in Boisdale Hills, its association with older (Middle Cambrian) sediments is undoubtedly significant. Nearby granites in Cape Breton Island (Pl. 1) do not bridge the age gap between 400 and 500 m.y., and it is therefore believed on present evidence that Boisdale Hills includes some granite at least which is associated with a pre-Devonian orogeny, possibly Taconic.

On the analytical side there is abundant evidence from this investigation that coexisting biotite, muscovite, and K feldspar resulting from igneous crystallization give accordant results by the Sr/Rb method and that comparable agreement for biotite and muscovite can be obtained with the A/K method. No consistent bias between the two methods has been found.

Future work, in addition to filling in regional gaps in the Cobequids and in Cape Breton, might include lead ages on zircon as well as Sr/Rb and A/K studies of mica and K feldspar. Recent work by Tilton *et al.* (1958) in Appalachian gneisses has shown consistently older ages for zircon and feldspar compared with much younger and somewhat variable ages for coexisting biotite. In Nova Scotia K feldspar from James River accords with mica ages in nearby localities, and at Boisdale Hills the ages of coexisting biotite and feldspar are in essential agreement. These relationships, although too meager to be conclusive, suggest a different age pattern which future work may reveal.

References Cited

Aldrich, L. T., and Nier, A. O., 1948, Argon 40 in potassium minerals: Phys. Rev., v. 74, p. 876–877

Aldrich, L. T., Davis, G. L., Tilton, G. R., and Wetherill, G. W., 1956, Radioactive ages of minerals from the Brown Derby mine and the Quartz Creek granite near Gunnison, Colorado: Jour. Geophysical Research, v. 61, p. 215–232

Cormier, R. F., 1957, Rubidium-strontium ages of the mineral glauconite: U. S. Atomic Energy Comm., 4th Ann. Progress Rept. Contract AT(30–1)-1381, p. 2–23

Davis, G. L., and Aldrich, L. T., 1953, Determination of the age of lepidolites by the method of isotope dilution: Geol. Soc. America Bull., v. 64, p. 379–380

Fairbairn, H. W., and Hurley, P. M., 1957, Radiation damage in zircon and its relation to ages of Paleozoic igneous rocks in northern New England and adjacent Canada: Am. Geophys. Union Trans., v. 38, p. 99–107

Gast P. W., Kulp, J. L., and Long, L. E., 1958, Absolute age of early Precambrian rocks in the Bighorn basin of Wyoming and Montana, and southeastern Manitoba: Am. Geophys. Union Trans., v. 39, p. 322–334

Goranson, E. A., 1938, Sydney Sheet (marginal notes): Geol. Survey Canada Map 360A, (work done jointly with W. A. Bell)

Herzog, L. F., and Pinson, W. H., 1955, The Sr and Rb contents of the granite G-1 and the diabase W-1: Geochim. et Cosmochim. Acta, v. 8, p. 295–298

——in press, Rb-Sr analyses and age determinations of certain lepidolites, including an international comparison suite: Am. Jour. Sci.

Holland, H. D., and Gottrfied, D,. 1955, The effect of nuclear radiation on the structure of zircon: Acta Crystall., v. 8, p. 291–300

Holmes, A., 1947, The construction of a geological time scale: Geol. Soc. Glasgow Trans., v. 21, p. 117–130

Hutchinson, R. D., 1952, The stratigraphy and trilobite faunas of the Cambrian sedimentary rocks of Cape Breton Island, Nova Scotia: Geol. Survey Canada Mem. 263

Inghram, M. G., 1955, Stable isotope dilution analysis: Stanford, Cal., Annual Reviews Inc., Annual Reviews of Nuclear Science, v. 4

Lipson, J., 1956, Potassium-argon dating of sediments: Geochim. et Cosmochim. Acta, v. 10, p. 149–158

Smales, A. A., 1955, Some trace-element determinations in G1 and W1 by neutron activation: Geochim. et Cosmochim. Acta, v. 8, p. 300

Smits, F., and Gentner, W., 1950, Argonbestimmungen an Kalium-mineralien 1. Bestimmungen an tertiaren Kalisalzen: Geochim. et Cosmochim. Acta, v. 1, p. 22–27

Tilton, G. R., Aldrich, L. T., and Inghram, M. G., 1954, Mass spectrometric determination of thorium: Anal. Chemistry, v. 26, p. 894–898

Tilton, G. R., Wetherill, G. W., Davis, G. R., and Hopson, C. A., 1958, Ages of minerals from the Baltimore gneisses, near Baltimore, Md.: Geol. Soc. America Bull., v. 69, p. 1469–1474

Wasserburg, G. J., and Hayden, R. J., 1955, $Argon^{40}$-$potassium^{40}$ dating: Geochim. et Cosmochim. Acta, v. 7, p. 51–60

Weeks, L. J., 1954a, The Appalachian region, p. 123–206 *in* Stockwell, C. H., *Editor*, Geology and economic minerals of canada: Geol. Survey Canada, Econ. Geol. Ser No. 1

——1954b, Southeast Cape Breton Island, Nova Scotia: Geol. Survey Canada Mem. 277, 112 p.

Wetherill, G. W., Aldrich, L. T., and Davis, G. L., 1955, A^{40}/K^{40} ratios of feldspars and micas from the same rock: Geochim. et Cosmochim. Acta, v. 8, p. 171–172

Department of Geology and Geophysics, Massachusetts Institute of Technology, Cambridge, Massachusetts (Fairbairn, Hurley, and Pinson); Department of Geology, St. Francis Xavier University, Antigonish, Nova Scotia (Cormier)

Manuscript Received by the Secretary of the Society, December 16, 1958

Massachusetts Institute of Technology Age Studies, No. 3

Appendix: Details of Sample Localities

2094—On Route 3, 1 mile east of Atwood Brook Shelburne County

3249—On road to Comeau Hill, about 2 miles west of Wedgeport, Shelburne County

2100—On Route 3, near Shelburne, Shelburne County. Collected by L. H. King

2092—On Route 3, 3.8 miles east of Port Mouton, Queen's County

3250—About 3 miles east of Bear River, Annapolis County, on road, connecting with Route 8

3308A—About 1 mile south of Nictaux South, between railway and river, Annapolis County. Collected by C. F. Hickox, Jr.

3308B—On Route 10, at Nictaux South, Annapolis County. Collected by C. F. Hickox, Jr.

2095—From quarry near West Nictaux, Annapolis County, on secondary road just south of Route 1

2099—On Route 12 at Lake Gaspereau, King's County, 8 miles south of Kentville

2096—On Route 10, half a mile east of Albany Cross, Annapolis County

2097—On Route 10, 1 mile south of Springfield, Annapolis County

2098—On Route 12, at school 3.5 miles north of New Ross, Lunenberg County

1710—On Route 3, 5 miles east of Chester, Lunenberg County

1712—East side of St. Margaret Bay, Halifax County, 7 miles from Route 3 on way to Peggy's Cove

2091—Shad Bay, southwest of Halifax, Halifax County

2090—On Route 3, western outskirts of Halifax, Halifax County

3128—On Route 7, just west of Ship Harbour, Halifax County

3251—North side of Liscomb Game Sanctuary, Guysborough County, on road connecting New Glasgow and Sheet Harbour

3326—On James river, Antigonish County, about 1 mile northwest of railway and 7 miles west of Antigonish. Collected by D. J. MacNeil

3133—From Archibald's Lake, Guysborough County, northeast of Sherbrooke. Collected by P. R. Whitney

1708—On road between Guysborough and Larry's River, Guysborough County, 9.5 miles from road intersection near Guysborough

2089—From quarry, half a mile south of Route 16, at Queensport, Guysborough County

1706—On road between Framboise and Grand River, Richmond County, 12 miles south of Framboise

3132—About 3 miles from Boisdale, on road to Steel Crossing, Cape Breton County. Collected by D. G. Kelley

3134—From MacKenzie River, at Cabot Trail near bridge, Inverness county. Collected by E. R. W. Neale

3130—On Cabot Trail, 1.7 miles south of Black Brook, Victoria County

3129—On road south of Kelly Cove and New Campbellton, Victoria County

3252—Along shore, just southwest of Lockeport, Shelburne County

All samples are granitic in character except the biotite schist from Lockeport (3252). Latitudes and longitudes are given in the tables.

BULLETIN OF THE GEOLOGICAL SOCIETY OF AMERICA
VOL. 71, PP. 415-448, 17 FIGS., 1 PL. APRIL 1960

GEOPHYSICAL INVESTIGATION OF MONO BASIN, CALIFORNIA

BY L. C. PAKISER, FRANK PRESS, AND M. F. KANE

ABSTRACT

Gravity and seismic studies in Mono Basin, Mono County, California, completed during the summer of 1957 revealed a large, roughly triangular block that had subsided about 18,000 ± 5000 feet and received an accumulation of about 300 ± 100 cubic miles of light clastic sediments and volcanic material of Cenozoic age. The seemingly near-vertical faults that bound this great block are displaced toward the center of the basin from the surrounding mountain masses, but in general they are parallel to well-defined Basin and Range trends.

The gravity minimum anomaly associated with the Mono Basin structure has a residual gravity relief of about 50 mgals, and the lowest gravity readings (on Paoha Island) yield a complete Bouguer gravity value of about −260 mgals with respect to the International Ellipsoid. The computed depth of subsidence is based on a density of 2.3 gms/cm³ for the basin fill and 2.7 gms/cm³ for the basement rocks. Seismic-refraction profiles at several places in the basin demonstrate that the Cenozoic deposits are thick where the gravity is low and relatively thin where the gravity is higher. Along common seismic and gravity profiles steep seismic dips coincide with steep gravity gradients. Numerous seismic reflections are present within the basin fill. Anomalies on four aeromagnetic profiles are related in part to volcanic material within the Cenozoic section.

It is concluded that Mono Basin may be a volcano-tectonic depression caused by subsidence along faults, following extrusion of magma from a magma chamber at depth. Volcanic rocks of Pliocene(?) and Pleistocene ages are exceptionally abundant in this area.

CONTENTS

TEXT

	Page
Introduction	416
Acknowledgments	416
Geology of Mono Basin	417
General geologic setting	417
Rocks of the area	418
Cenozoic structures	419
Volcanism and faulting	420
Geophysical survey	420
General statement	420
Gravity field methods and computations	421
Seismic field methods and reduction of data	421
Aeromagnetic profiles	422
Physical properties	422
General statement	422
Density	422
Seismic velocity	423
Magnetic properties	424
Analysis of data	424
Analysis of gravity data	424
Gravity-contour map	424
Gravity profiles	428
Analysis of seismic profiles	428
Analysis of aeromagnetic profiles	432
Geologic interpretation	440
Structure of Mono Basin	440
Nature of Cenozoic deposits in Mono Basin	441
Balance sheet of rock volumes	444
Origin of Mono Basin	445
Age of Mono Basin	446
References cited	447

ILLUSTRATIONS

Figure		Page
1.	Regional geologic setting of Mono Basin	417
2.	Interpretation of gravity anomaly along profile *A-A′*	426
3.	Interpretation of gravity anomaly along profile *B-B′*	427
4.	Comparison of gravity and seismic data along gravity profile *C-C′* and seismic profile 1	429
5.	Analysis of seismic profile 1	430
6.	Analysis of seismic profile 2	431
7.	Analysis of seismic profile 3	431
8.	Analysis of seismic profile 4	432
9.	Analysis of seismic profile 5	433
10.	Analysis of seismic profile 6	434
11.	Sample seismograms	435
12.	Analysis of aeromagnetic profile 37-57	436
13.	Analysis of aeromagnetic profile 18-33	437
14.	Analysis of aeromagnetic profile 81-94	438
15.	Analysis of aeromagnetic profile 67-75	439
16.	Generalized geologic cross section of Mono Basin along profile *A-A″* based on geophysical evidence	442
17.	Interpretation of gravity anomaly along profile *D-D′* in Long Valley	443

Plate — Facing page

1. Combined gravity and geologic map of Mono Basin, California, showing locations of seismic and aeromagnetic profiles..... 415

TABLES

Table — Page

1. Velocities and thicknesses of layers..... 423
2. Velocities and time intercepts..... 434

Introduction

In the Great Basin region of the American West the unconformable surface between the clastic and volcanic deposits of Cenozoic age and the buried pre-Tertiary rocks is a geologic boundary of major importance; the pre-Tertiary rocks, wherever they project above the broad alluviated valleys that conceal them, form the main masses of the present ranges of the Great Basin. East of the Sierra Nevada, the unconformity separates rocks that were deformed during the Nevadan orogeny of late Mesozoic time and the Basin and Range block faulting of late Tertiary and Pleistocene time. A knowledge of the buried attitude of this unconformity is, therefore, important to the understanding of Basin and Range diastrophism.

Fortunately, this important geologic boundary is marked by sharply contrasting densities and seismic velocities. Most of the older pre-Tertiary rocks are significantly denser than the Cenozoic deposits, and their seismic velocity is also greater. Therefore, combined gravity and seismic studies can be used to determine with considerable reliability the attitude of this boundary. In addition, magnetic studies can indicate much information about the distribution of volcanic rocks of Cenozoic age that lie buried beneath the surface.

Mono Basin, Mono County, California (Fig. 1), lies at the base of the eastern escarpment of the Sierra Nevada at the 38th parallel, and it is one of a series of depressions that separate the Sierra from the Great Basin region to the east. Mono Basin was also the locus of intense local late Cenozoic volcanism which may be genetically related to diastrophism. The Mono Basin area has, therefore, attracted the interest of geologists since Russell's (1889) classic report on the Quaternary history of Mono Valley.

An opportunity to make a reconnaissance geophysical study of Mono Basin came during the summer of 1957 in conjunction with seismic recording of a series of large blasts detonated in Mono Lake by the U. S. Navy. The U. S. Navy Ordnance Test Station (China Lake, California), the California Institute of Technology, and the U. S. Geological Survey made seismic recordings of these blasts. The gravity, seismic, and magnetic data presented and interpreted herein were obtained through a joint field program of the U. S. Geological Survey and the California Institute of Technology. These data were obtained for the purpose of studying the geologic structure of Mono Basin.

Acknowledgments

We wish to acknowledge the contributions to this study of John H. Healy of the California Institute of Technology, R. E. Warrick, Donald Murrey, and Gerry Turner of the U. S. Geological Survey, and Roger Sumner and Alan Carlin of the California Institute of Technology and temporary summer employees of the U. S. Geological Survey, all of whom assisted in the field work. We also wish to express our appreciation to Howard Oliver of the U. S. Geological Survey, who provided some of the gravity data, and to W. J. Dempsey of the U. S. Geological Survey, who made available some aeromagnetic data. The advice of Isidore Zietz of the U. S. Geological Survey in interpretation of the aeromagnetic data is gratefully acknowledged. The co-operation of personnel of the U. S. Navy Ordnance Test Station (China Lake, California), especially in providing boat transportation to Paoha Island for gravity readings there, is also gratefully acknowledged. We are indebted to George C. Kennedy of the Institute of Geophysics at the University of California (Los Angeles) and Konrad B. Krauskopf of Stanford University for much stimulating and fruitful correspondence and discussion on the origin of Mono Basin. Finally we wish to thank John Verhoogen and Howel Williams, both of the University of California (Berkeley), for critically reviewing an early draft of the manuscript. We have benefited richly from the ideas of these earth scientists, but we alone are responsible for the conclusions recorded herein.

Geology of Mono Basin

General Geologic Setting

Mono Basin (Pl. 1) is a large depression of irregular shape which is occupied by Mono Lake. The lake is highly saline and now has an area of about 85 square miles. In Pleistocene time it may have covered as much as 300 square miles, essentially the area of the present basin (Russell, 1889; Putnam, 1949; 1950). The maximum depth of the water is 170 feet. The basin is bounded on the west by the Sierra Nevada, which rises from an altitude of 6403 feet at Mono Lake to 13,050 feet at the summit of Mt. Dana on the crest of the Sierra, a distance of only 7 miles. On the north and east, Mono Basin is confined by basalt-capped mountains of irregular trend that stand more than 2000 feet above the lake level. Granite Mountain projects upward at the edge of the basalt flow about 6 miles southeast of Mono Lake, and other hills of granitic rocks may be seen south and west of Granite Mountain. An east-trending ridge, capped with volcanic rocks, limits Mono Basin on the south. Bald Mountain rises to an altitude of 9045 feet near the center of this ridge, and, to the east, Glass Mountain stands at an altitude of 11,127 feet, high above Mono Lake about 20 miles to the northwest. Farther east, the lofty White Mountains stand higher above Mono Basin than the Sierra Nevada in this latitude.

Mono Craters, a line of peaks built of obsidian and pumice, lie immediately south

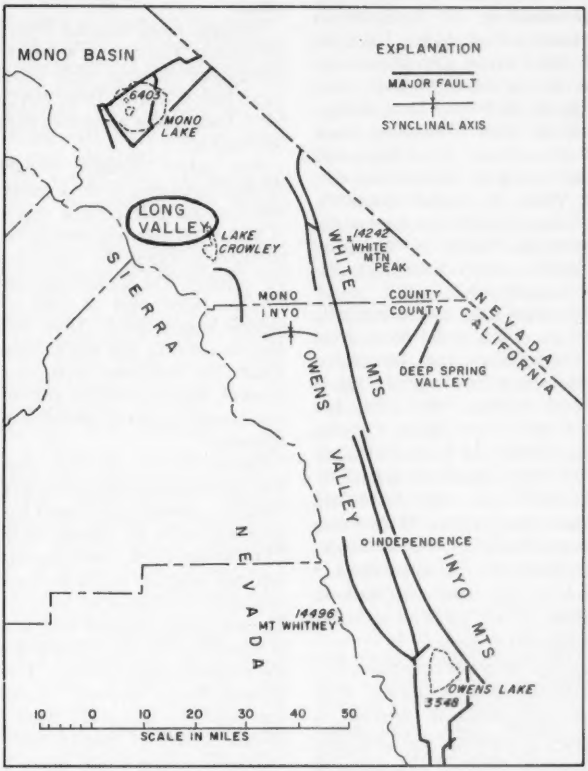

Figure 1.—Regional Geologic Setting of Mono Basin

of Mono Lake, above which they rise to a maximum altitude of 9164 feet. Mono Craters, except for their southern extension, are within the confines of Mono Basin.

The physiographic expression of Mono Basin is strikingly different from that of nearby Owens Valley, which trends with almost perfect linearity about S. 15° E. from its northern limit southeast of Mono Lake for more than 100 miles along the White-Inyo mountain chain to its southern limit near Owens Lake (Fig. 1). However, Long Valley, immediately south of Mono Basin, has much in common with Mono Basin. Mono Basin and Long Valley are roughly equidimensional, whereas Owens Valley is greatly elongated. Mono Basin and Long Valley are marked by an intense and complex history of volcanism. Both of these basins occupy prominent embayments in the Sierra Nevada front.

Russell (1889) made the first systematic study of the geology of the Mono Basin area; Putnam (1949) designated the Pleistocene predecessor of Mono Lake as Lake Russell in his honor. Putnam (1938; 1949; 1950) has restudied Mono Craters, and Mayo, Conant, and Chelikowsky (1936) have studied their southern extension. Two important papers by Putnam (1949; 1950) on the Quaternary history and glacial geology of the Mono Basin area have appeared in recent years. Gilbert (1938; 1941) has studied the volcanic rocks and geologic structure in the area southeast of Mono Lake. Gilbert (1941) gives an excellent summary of the regional geology.

No detailed geologic map has been published of the Mono Basin area, but the authors hope that this paper will stimulate interest in quadrangle mapping at a scale of 1:62,500 and, in particular, a careful study of the chemical composition and petrography of the volcanic rocks of the region. Ron Kistler, a graduate student at the University of California (Berkeley), has been mapping the area southwest of Mono Lake (Howel Williams, written communication). Plate 1 has been mainly adapted from Gilbert (1941), although some information along the southern part has been obtained from the mapping of Rinehart and Ross (1957 and written communication) in the Long Valley area to the south. The areal geology north of the 38th parallel and west of longitude 119°06′ is based on a brief reconnaissance by the senior author.

Rocks of the Area

The Sierra Nevada and the higher Basin Ranges (*e.g.*, Granite Mountain, Black Mountain, and the Benton Range) are made up of pre-Tertiary rocks, mainly granitic rocks of Cretaceous (?) age and some older metamorphic rocks.

Volcanic rocks ranging from early Pliocene (?) to late Pleistocene are distributed widely throughout the area. Only brief summaries of these from Gilbert (1938; 1941) will be given here. These rocks have been highly generalized on Plate 1.

The oldest Tertiary volcanic rock is a rhyolite consisting of three massive members of vitric-crystal tuff with a combined thickness of about 100 feet, exposed on the east flank of the Benton Range (Pl. 1). An andesite overlies the rhyolite. The andesite is separated from the rhyolite below and in some places from the olivine basalt flows above by erosional unconformities. It has a maximum thickness of about 200 feet and is composed mainly of massive beds of breccia containing blocks of hornblende-pyroxene andesite up to 3 feet in diameter.

Olivine basalt is the most widespread Tertiary volcanic rock of the area. Most of the Cenozoic andesite and basalt shown on Plate 1 is of this unit. It consists of individual flows 25 to 50 feet thick, which are scoriaceous at the top and vesicular at the base and may reach a combined thickness of several hundred feet. The basalt was erupted over an erosion surface of low relief before fault displacements formed the present ranges (Gilbert, 1941). East of the Benton Range, bedded rhyolite tuffs overlie the basalt; to the south these tuffs lie on an eroded surface of granite. Gilbert (1941) has identified several basalt necks south and west of Granite Mountain.

A hornblende andesite is exposed on the summit and west side of Bald Mountain (Pl. 1). According to Gilbert (1941) it may be intrusive into the olivine basalt and it is overlain by the Bishop tuff of Gilbert (1938). Gilbert (1941) believes that emplacement of this andesite antedated Basin and Range faulting.

Younger rhyolite is exposed on the slopes of Glass Mountain and nearby peaks (Pl. 1). Both glassy and lithoidal types are present, and there may be beds of tuff between the flows. According to Gilbert (1941) the vents from which the rhyolite was extruded prob-

ably lay along the summit and south flank of Glass Mountain, which may have been built by a series of large, domelike protrusions of rhyolite from which short, thick flows occasionally erupted. The rhyolite is several thousand feet thick and has been displaced by faulting so that the southern part now lies beneath the alluvium of Long Valley. Gilbert (1941, p. 795) has noted "... the faulting succeeded the rhyolite eruptions for the southern slope of the range is a scarp along which not only the rhyolite, but the underlying granitic and basaltic rocks east and west of Glass Mountain have been displaced."

Bedded rhyolite tuff of about the same age slopes north from the base of Glass Mountain toward Adobe Valley (Pl. 1). Downslope this tuff grades into stream-transported and stream-deposited unconsolidated tuff and gravel. Gilbert (1941, p. 799) notes: "As the fault movements began to elevate the present ranges, the unconsolidated tuffs, readily stripped from the higher parts of the rising ranges, were deposited down-slope on top of the original beds as 'Pleistocene alluvium'".

Gilbert adds (p. 799), "Following the initiation of normal faulting, volcanic eruptions continued through the Pleistocene period until recent time." The oldest volcanic material erupted of Pleistocene age was the Bishop tuff of Gilbert (1938), which is widely distributed south and east of Mono Lake; it reaches a maximum thickness of several hundred feet. Gilbert (1938) considers the Bishop tuff to be a welded tuff of the *nuée ardente* type. Later flows of basalt and andesite crop out here and there in Mono Basin (Putnam, 1949) and include those on Paoha Island described by Russell (1889). Late in the Pleistocene, explosive eruptions scattered pumice from Mono Craters over much of Mono Basin; an impressive range of volcanic peaks was built from rhyolite obsidian and pumice ejected from the vents. Putnam (1949) has shown that the latest pumice covers late recessional moraines of the latest, or Tioga (Blackwelder, 1931), glaciation. The absence of old shore lines on the slopes of the northern Mono Craters (Putnam, 1949) testifies to the recentness of these eruptions.

Gilbert (1941) has correlated the volcanic rocks of the Mono Basin area with those in the Hawthorne quadrangle of Nevada and in the Sweetwater Range. He concluded that the older volcanic rocks range from early to early-middle Pliocene; the rhyolite of Glass Mountain is younger than the Tertiary basalt flows, and Gilbert (1941) regards it as middle Pliocene. The Bishop tuff is younger than the Sherwin (?) glacial stage of Blackwelder (1931), for it overlies a till identified as Sherwin (Rinehart and Ross, 1957) in places. Rinehart and Ross (1957) accept the ages Gilbert assigned to the volcanic rocks of the region, except for the rhyolite exposed in the center of Long Valley, which Gilbert, following Chelikowsky (1940), regarded as late Pleistocene; Rinehart and Ross correlate it with the rhyolite of Glass Mountain.

Putnam (1949) has described the lake beds of Mono Basin. Silt, with very little clay, makes up about 60 per cent of these lake beds; sand and gravel make up 40 per cent. Freshwater limestones are exposed in places in Mono Basin. The exposed lake beds are Pleistocene, but older lake beds may lie buried at depth in Mono Basin.

Well-developed moraines of the Tahoe and Tioga glacial stages of Blackwelder (1931) are exposed on the slopes of the Sierra in Mono Basin. Putnam (1950) has described these in detail; he found evidence for all four stages in Mono Basin. The till given the name *Aeolian Buttes* by Putnam (1950) and correlated by him with the McGee stage may actually be the Sherwin stage of Blackwelder (1931), however.

Putnam (1949) has also made a detailed study of the old shore lines of Mono Basin and correlated them with the glacial stages. Lake Russell shore lines were found at about 650 feet (Tioga) and, less certainly, at about 700 feet (Tahoe) above the present lake level. Putnam (1949) concluded that, at the highest water level, Lake Russell overflowed into Adobe Valley during the Tahoe glacial stage and, through a series of gorges and canyons, into Owens Valley. Russell (1889) earlier stated his belief that Pleistocene Mono Lake overflowed northeastward and filled Aurora Valley in nearby Nevada.

Pleistocene and Recent alluvium covers many of the valleys of the Mono Basin area.

Cenozoic Structures

Gilbert (1941) mapped the faults of the area southeast of Mono Lake (Pl. 1) and found that, where they could be observed, they are normal faults with dips of 60° to 75°. The most common fault directions are between northeast

and northwest; the faults are nearly straight and intersect to form a mosaic (Gilbert, 1941). Gilbert found little evidence for a strike-slip component of fault movement. The faulting that defined the present ranges did not begin before middle or late Pliocene time, and it has continued to the present. As Gilbert (1941) has shown, volcanic rocks of these ages were erupted over a surface of low relief and displaced later by faulting. Most of the Basin and Range faulting was completed before the Bishop tuff of Gilbert (1938) was erupted, for the fault scarps in the Bishop tuff indicate relatively small displacements.

Putnam (1949) concluded that movement on many of the faults has been recurrent. Older moraines are offset more than recent ones. Putnam found that moraines of the Sherwin stage might be offset about 100 feet and those in nearby areas of the Tahoe stage about 20 feet. Moraines of the Tioga stage may not be displaced at all. Putnam (1949, p. 1294) concluded that "Much of the displacement along the Sierran front occurred before the Sherwin glacial stage"; this is in agreement with Gilbert's (1938) conclusion cited previously. Putnam also expressed doubt that there is a single, large-scale fault along the Sierra Nevada; he found evidence of faults of different directions and evidence that fault movement may be distributed through a zone of closely spaced faults. Dips of the exposed faults, according to Putnam (1949), range from vertical to 70°.

Russell (1889) had noted that the Mono Lake basin must be downfaulted and tilted downward to the west because the lake washes the base of the Sierra. Russell (1889) concluded that Mono Craters lie along fractures that are part of the Sierra Nevada displacement, a conclusion essentially confirmed by Mayo, Conant, and Chelikowsky (1936) and Putnam (1949).

Volcanism and Faulting

Russell (1889, p. 391) first noted a possible relationship between volcanism and faulting in Mono Basin. He wrote: "The relations of Lake Mono to the Sierra Nevada fault and to the volcanoes of the region are such that a movement of the fault might admit the waters of the lake to the heated rocks beneath the surface and thus bring on an eruption. . . ." However, as Howel Williams (Written communication) has pointed out, no products of phreatic eruptions have been noted, so this mechanism must be discounted. Williams (1941, p. 323), in discussing the volcano-tectonic depressions of the Pilomasin Basin of Sumatra, noted briefly that possibly ". . . the basin containing Mono Lake is of similar origin, being related to the repeated eruptions of pumice from the Mono Craters immediately to the south."

Long Valley is similar in many respects to Mono Basin; Gilbert (1938, p. 1860) wrote that perhaps the ". . . recent faulting in Long Valley is the result of the extrusion of so much magma from beneath that area. . . ." Chelikowsky (1940, p. 435) remarked: "It is believed that the early expulsion of the great volume of basic lavas, together with the material of the welded tuffs, which are disposed on three sides of the basin, led to the collapse of what is now Mammoth embayment".

Some volcano-tectonic mechanism is indicated for Mono Basin, and this problem will be briefly explored after presentation and interpretation of the geophysical data.

Geophysical Survey

General Statement

Previous gravity studies in the Sierra Nevada by H. W. Oliver (Written communication) and by two of the present authors (Pakiser and Kane) in the area surrounding Long Valley showed a steep gravity gradient associated with the faulting along the Sierra Nevada front in Mono Basin. These gravity data suggested that Mono Basin subsided relative to the Sierra to the west and the Basin Ranges to the east and received a thick accumulation of light clastic and volcanic deposits of Cenozoic age. A large gravity minimum anomaly, with a residual gravity relief of about 75 mgals, was found by a detailed study of Long Valley, and it was postulated that a similar anomaly might be found by a gravity survey in Mono Basin.

At the suggestion of Press, the combined gravity and seismic study of Mono Basin was done in June and July of 1957 as a co-operative effort of the Seismological Laboratory of the California Institute of Technology and the U. S. Geological Survey. The California Institute of Technology obtained most of the seismic data, and the U. S. Geological Survey obtained the gravity data. The U. S. Geological Survey obtained the aeromagnetic data during the summer of 1956 as a reconnaissance extension of more detailed work done at the same time in Long Valley and northern Owens Valley.

Gravity Field Methods and Computations

About 100 gravity stations were established in the Mono Basin area. Most of the readings were made in July 1957, but a few stations previously established by H. W. Oliver and by Pakiser and Kane have been incorporated in Plate 1. The stations along seismic profile 1 and at Cowtrack Mountain were established during short field trips after the main field program was completed to provide additional control in critical areas. A Worden gravity meter, with a scale value of about 0.5 mgal per dial division, was used for the readings. All gravity measurements were made with respect to a base station on U. S. Highway 395 just west of Mono Craters, which in turn had been earlier tied, through a network of base stations in Owens Valley, to the U. S. Coast and Geodetic Survey pendulum station at Independence, California (Duerksen, 1949, p. 180). The principal facts for this base station, an auxiliary base established at the Mono Lake Post Office, and the gravity measurements and corrections for all stations are on file at the U. S. Geological Survey, Denver, Colorado.

Gravity measurements were made in single loops from a base station, and base readings were repeated at intervals of 4 or 5 hours (except for a longer interval for the traverse on Paoha Island) to determine the combined instrument drift and tidal variation. Each series of station measurements between base readings included a measurement at a station that had been read previously, either during the July 1957 field work or the earlier work in the Long Valley area. No repeated station reading differed from the earlier reading by more than 0.3 mgal.

Two-thirds of the stations were set at bench marks of the U. S. Geological Survey, the U. S. Coast and Geodetic Survey, and the U. S. Army Corps of Engineers. Most of the remainder were set along the Mono Lake shore line, for which an altitude of 6403 feet had just been established by a topographic party of the U. S. Geological Survey. Station-elevation differences from the level of the lake were estimated, but none are considered to be in error by more than 5 feet. Elevations of a few gravity stations were established by plane-table and alidade surveying and by altimetric methods. Some of these may be in error by as much as 10 feet. Station positions as located on topographic maps conceivably may be in error by as much as 500 feet of horizontal distance.

The errors in gravity caused by inaccuracies in gravity readings and station positions are considered to be less than 0.5 mgal for practically all the stations; the error almost certainly does not exceed 1 mgal for any gravity station. When the magnitude of the anomalies and uncertainties in terrain corrections and density assumptions are considered, errors of 1 mgal or less are negligible.

The gravity measurements have been reduced for drift, elevation, and latitude using standard methods (Nettleton, 1940, p. 51–56). An elevation factor of 0.060 mgal/foot, corresponding closely to a rock density of 2.67 gms/cm^3, was used to make the elevation corrections. This is the average density of the pre-Tertiary rocks of the area in which the greatest range in elevation is found. Terrain corrections were made using the Bullard modification of the Hayford-Bowie system (Swick, 1942, p. 67–68). The terrain corrections were extended through zone "O" of this system, or about 100 miles from each station. Gravity values were reduced to the complete Bouguer anomaly with respect to the International Ellipsoid; 1000 mgals has been added to the gravity values as they appear on Plate 1 so that all gravity contours are positive.

Combined errors of 2 or 3 mgals may have been introduced in the elevation and terrain corrections, but relative errors from these sources for adjacent stations should not exceed 1 mgal. The negative effect on gravity measured on land of the water in Mono Lake is negligible.

Seismic Field Methods and Reduction of Data

Seismic field operations were organized to permit a rapid reconnaissance of the unconformity surface between the Cenozoic deposits and the pre-Tertiary crystalline basement in part of Mono Basin. Major velocity discontinuities in the Cenozoic section were also investigated. A method of line-refraction surveying was used in which partly reversed profiles are obtained by shooting in one direction (Dix, 1952, p. 263).

Unfortunately it was impossible with the recording and communications facilities and time available to obtain seismic data in the area covered by Mono Lake. Extremely difficult conditions for vehicle operations along and near the shore of Mono Lake made it impracticable to obtain detailed seismic data there. However, a combination of seismic and gravity data in the area around the lake

permits extrapolation with some confidence into the central part of the basin where the gravity field is approximately known.

It is worthwhile to repeat the assumptions underlying the method of interpretation (Ewing, Woollard, and Vine, 1949, p. 262–267) because the accuracy of the results is limited by the extent to which these assumptions approximate actual conditions: (1) each layer is bounded at top and bottom by planes and transmits seismic waves with constant velocity; (2) at an interface between two layers, the path of a wave is determined by Snell's law; (3) the apparent velocity of a wave is $V/\sin \alpha$ for travel along the upper surface of a layer, where V is the velocity in the layer above and α the angle of incidence on the surface; (4) travel time is unchanged if shot point and recording position are interchanged.

The first assumption is most likely to be violated. If the surfaces are not planes the solution yields apparent plane surfaces and mean velocities which approximate actual conditions with accuracy usually sufficient for reconnaissance purposes. When data are insufficient for a reversed profile, either zero dip or a true velocity typical of the layer is assumed. In profile 5 (fig. 9), evidence was found for a change in dip of the basement surface. To obtain an approximate adjustment of the data, a fictitious station (Ewing *et al.*, 1950, p. 880) was inserted to obtain two profiles; the velocities and dips of layers in each case were taken as constant.

Aeromagnetic Profiles

Four aeromagnetic traverses were flown at a constant barometric altitude of 14,000 feet above sea level along the lines shown in Plate 1. The magnetic profiles were plotted on an arbitrary magnetic datum and corrected for a latitude variation of 10 gammas per mile, increasing to the north.

Physical Properties

General Statement

The pre-Tertiary rocks have, in general, significantly greater density and seismic velocity than the Cenozoic deposits. Therefore, the combined erosional and structural boundary that separates the Cenozoic deposits from the pre-Tertiary rocks can be rather reliably defined by a combination of gravity and seismic measurements. In addition, there are seismic-velocity interfaces of possible geologic significance within the Cenozoic deposits, and some of these can be defined by seismic-refraction or seismic-reflection recordings. Of the Cenozoic volcanic rocks, the basalts are significantly higher in magnetic susceptibility so their distribution can be studied by measurements of the magnetic field.

Density

Densities of the pre-Tertiary plutonic and metamorphic rocks in the Mono Basin area are known with considerable accuracy. Although no measurements of density were made within Mono Basin proper, the senior author collected a number of samples in the nearby Long Valley area, and William Huff of the U. S. Geological Survey made measurements of density.

Measured densities of dry samples of the plutonic rocks range from a minimum of 2.42 to a maximum of 2.69 gms/cm^3; the average density of these samples is 2.60 gms/cm^3. Measured densities of dry samples of metamorphic rocks range from 2.63 to 2.94 gms/cm^3, and the average density is 2.78 gms/cm^3. A representative density of 2.7 gms/cm^3 is assigned to water-saturated pre-Tertiary rocks for purposes of interpretation, but it is recognized that the average density contrast of about 0.2 gm/cm^3 between the plutonic and metamorphic rocks may have some influence on the measured gravity field. However, it is known from gravity work in Long Valley, where alternating bands of granitic and metamorphic rocks project into the steep gravity gradient on the south side of the valley, that gravity anomalies caused by density contrasts within the pre-Tertiary rocks are much smaller than the great gravity anomalies caused by thick accumulations of Cenozoic deposits. The effect is to superimpose on anomalies of several tens of mgals much smaller anomalies of a few mgals.

It is exceedingly difficult to determine a reliable average density for the Cenozoic deposits because of their extreme heterogeneity: densities of samples collected at the surface can be misleading. Samples of Cenozoic rocks collected in the Long Valley area (excluding basalts) range in density from a minimum of 1.36 for the Bishop tuff of Gilbert (1938) to a maximum of 2.37 gms/cm^3 for coarse lake beds. Gilbert (1938) found that the Bishop tuff ranges uniformly in density from 1.3 gms/cm^3 at the surface to 2.32 gms/cm^3 at a

vertical distance of about 400 feet below the top of the tuff.

The deposits of Cenozoic age that fill Mono Basin include alluvial deposits, lake beds, glacial till, and a wide assortment of volcanic deposits, and these deposits range in density from less than 1 gm/cm³ for pumice to at least 2.73 gms/cm³ for basalt.

An average density of 2.3 gms/cm³ is assigned to the Cenozoic deposits for purposes of interpretation. This average density yields depths that are consistent with those determined from seismic-refraction results in Mono Basin and Owens Valley and agrees closely with the average density determined by a combination of gravity and seismic methods by the Shell Oil Company in Railroad Valley, Nevada (R. J. Bean, written communication). However, the fill of Railroad Valley is somewhat different from that of Mono Basin. D. R. Mabey of the U. S. Geological Survey (Written communication) has determined a similar average density after extensive sampling of the deposits of Cenozoic age in the Mojave Desert and Death Valley regions of California.

In the interpretation of the gravity data, therefore, an average density contrast between the Cenozoic deposits and the pre-Tertiary rocks of −0.4 gm/cm³ was assumed. It is acknowledged that the density contrast may be as much as −0.7 and as little as −0.3 gm/cm³ and that density may increase with depth as a result of compaction and more complete induration, so depths may range from about 60 per cent to 130 per cent of those computed from the gravity data. With comparison of depths from seismic and gravity data the range in density contrast is narrowed to about −0.5 to −0.3 gm/cm³, corresponding to a range in depth of about 80 per cent to 130 per cent. In spite of the wide range of possible depths, the configuration of the Mono Basin structure as determined from the gravity data is changed little when the density assumptions are changed.

TABLE 1.—VELOCITIES AND THICKNESSES OF LAYER

Profile	V_1	V_2	V_3	V_B	H_{1E}	H_{1W}	H_{2E}	H_{2W}	H_{3E}	H_{3W}	H_{tE}	H_{tW}
1E	1760	..	8600*	..	..	..	..	..	..	..	..	..
1W±	(1760)	..	7800	16,700	135	335	..	..	3840	2170	3975	2505
2	(1100)	..	8200*	15,000*	..	85	..	..	..	1615	..	1700
3	1100	..	10,800*	16,400*	110	..	..	..	715	..	825	..
4	1850	5600*	10,500*	17,750*	125	..	760	..	1430	..	2315	..
5′-5W	1100	6200*	8800	(17,000)	45	45	2190	1095	2355	1740	4590	2880
5E-5′	(1100)	(6200)*	8800	(17,000)	45	45	2410	2190	3075	2050	5530	4285
6	1600	..	10,400	16,400	145	325	..	..	3255	1750	3400	2075

V is true velocity in ft./sec.; *H* is layer thickness in feet; subscripts 1, 2, 3, and *B* refer to weathered layer, lower-velocity Cenozoic layer, higher-velocity Cenozoic layer, and crystalline basement respectively; *E* and *W* subscripts signify East or West end of profile; *t* subscript indicates total thickness; ( ) indicates assumed velocity; * indicates unreversed profile; ±West end of profile taken at SP5 for thickness calculation

Seismic Velocity

Seismic-refraction surveys reveal the variation of compressional wave velocity with depth. It is difficult to obtain uniquely, without auxiliary information, the material distribution with depth because of the wide range of velocities reported for specific materials and the frequent overlapping of velocity ranges for different materials.

Table 1 summarizes the velocities and depths of layers at each profile. The boundary between the Cenozoic section and the pre-Tertiary granitic and metamorphic rocks marks a profound velocity discontinuity, one which can be followed with some reliability from shallow depths near outcrops of pre-Tertiary rocks to great depths in the basin. Basement velocities range from 15,000 to 17,750 fps, values which are proper for the rocks which make up the pre-Tertiary terrain.

The identification of rocks in the Cenozoic section with observed velocities poses a greater difficulty. From the known geology of the region, it is probable that the basin deposits are primarily stream-transported sediments of

granitic and volcanic origin interbedded with volcanic material. Three major velocity types were found. The unconsolidated, unsaturated surface sediments have velocities typical for this material, 1100 to 1850 fps. The layer with velocity 5500 to 6200 fps is not everywhere present and may represent water-saturated, unconsolidated or semiconsolidated clastic and pyroclastic deposits. The velocity range 7800 to 10,800 fps may correlate with more consolidated and older versions of this material, or, in the higher part of this range, with flow rocks.

Magnetic Properties

W. Huff has measured the magnetic properties of a number of samples of pre-Tertiary plutonic rocks and Cenozoic volcanic rocks from the Long Valley area. Of these samples only plutonic rocks of dioritic composition and basalts are significantly high in magnetic susceptibility.

Plutonic rocks of dioritic composition have a measured magnetic susceptibility of about 0.003 cgs unit. The more silicic plutonic rocks average about 0.0004 cgs unit in susceptibility. The basalts range in susceptibility from 0.001 to 0.0037 cgs unit and have an average magnetic susceptibility of about 0.002 cgs unit. The volcanic rocks ranging from intermediate composition to rhyolite (including the Bishop tuff) have an average magnetic susceptibility of about 0.0002 cgs unit, and none differs significantly from this average. Some oriented samples of basalt collected from the surface exhibit magnetic moment vectors that differ significantly from the present direction of the earth's magnetic field.

Analysis of Data

Analysis of Gravity Data

In this study, the analysis of the gravity data was made in the following order:

A qualitative study was made of the gravity-contour map (Pl. 1) to reach general conclusions on the nature of the subsurface configuration of the pre-Tertiary rocks. The gravity field shown by the gravity-contour map is assumed to be a true representation of the gravity field on the surface of the ground, corrected for elevation, latitude, and terrain effects. This assumption is believed to be correct over most of the area, but where significant local elevation differences occur in materials whose density differs from that assumed for the elevation corrections, the relative gravity may be slightly different from that shown on the map.

Selected gravity profiles were analyzed by measuring the solid angle subtended from a position on the surface of the ground by each of a sequence of horizontal slabs of low-density Cenozoic material that could then be assembled to represent the configuration of the Cenozoic and pre-Tertiary interface in Mono Basin. The gravity anomaly at any location was calculated by multiplying the total solid angle subtended by all the slabs at that location by a constant factor that depends on the assumed density contrast and the thickness of each slab. A slab thickness of 4000 feet was used, and the density contrast between the Cenozoic deposits and the pre-Tertiary rocks was assumed to be -0.4 gm/cm^3. A solid-angle chart designed by A. H. Lachenbruch of the U. S. Geological Survey for geothermal studies was used to make the measurements of solid angle.

Gravity-Contour Map

Inspection of Plate 1 shows that the gravity field tends to be high over exposures of pre-Tertiary rocks and relatively low over areas where Cenozoic deposits are found at the surface. This correspondence of high gravity over rocks of high density and low gravity over deposits of low density suggests the configuration of the surface of the pre-Tertiary rocks. The amplitude of negative departure of the gravity field from the higher values over exposures of pre-Tertiary rocks is related to the thickness of the Cenozoic deposits, but the form of the gravity contours does not in general correspond to the actual configuration of the Cenozoic and pre-Tertiary boundary. (See, *e.g.*, Fig. 2 and 3.)

Bott (1953) has noted that negative gravity anomalies are common over intrusive masses of silicic rock, and this explanation of the gravity minima of the Mono Basin area must be considered. Bott attributes such negative anomalies to the density contrast between granite and more dense metamorphic or sedimentary country rock. Residual anomalies as large as -40 mgals were noted by Bott, but most were much smaller: 8 mgals per mile was the maximum gradient noted (Bott and Masson-Smith, 1953), but most were about 3 mgals per mile. This explanation for the large gravity low of Mono Basin and the smaller gravity minima is considered to be unlikely for the following reasons:

(1) Granitic rocks predominate in the pre-

Tertiary outcrops in and around Mono Basin, so there can be no large mass of granite enclosed in more dense metamorphic or sedimentary rocks.

(2) Gravity minima in the Mono Basin area are found only in areas where deposits of Cenozoic age crop out.

(3) The residual gravity relief of the largest negative anomaly in the Mono Basin area (50 mgals) is larger than any noted by Bott, and the largest gradient (15 mgals per mile) is about twice as large as the largest gradient noted by Bott.

(4) Where confirmatory seismic data are available, they invariably establish the existence of thick deposits of low seismic velocity in areas of low gravity.

Nevertheless, a small fraction of the largest anomaly may be the expression of density contrasts within the pre-Tertiary rocks.*

The maximum gravity relief in the Mono Basin area is about 50 mgals between the high in the northern end of the Benton Range and the low at Paoha Island. The gravity field tends to be nearly constant over exposures of pre-Tertiary rocks, so no regional gradient can be defined. Gravity anomalies were analyzed on the assumption that the regional gradient is zero. The lack of a pronounced regional gradient seems to indicate that Mono Basin is at or near the thickest part of the earth's sialic crust, for the regional gravity is known from data in nearby areas (Oliver, 1956; Pakiser and Kane, 1956) to increase eastward and westward from a low axis trending toward Mono Basin. This observation may be significant in terms of the isostatic compensation of the Sierra Nevada and other high mountain masses of the region (Press, 1956; Oliver, 1956; Thompson and Sandberg, 1958).

The dominant feature of the gravity map is the large gravity low roughly covering the area of Mono Lake; the lowest gravity values were found along the shore of Paoha Island. Because the water-covered area of the lake was inaccessible for gravity observations, the form of this anomaly was not fully defined. The steep gravity gradients on the northwest and southwest sides of the anomaly are rather well controlled by gravity observations, but to the south and east the form of the anomaly is not completely known. Possibly lower values of gravity would be found east of Paoha Island in Mono Lake if measurements could be made there.

The measured amplitude of the large gravity low is about 50 mgals. From a simple computation, using the formula for the gravity attraction of an infinite horizontal sheet and an assumed density contrast of -0.4 gm/cm^3, it may be concluded that the minimum thickness of the Cenozoic deposits under Mono Lake is 10,000 feet. From the steepness of the gravity gradients on the northwest and southwest sides of this anomaly, and from the straightness of the contours, it can be concluded that the Cenozoic and pre-Tertiary interface is either vertical or dips steeply toward the center of Mono Lake along these linear zones of closely spaced gravity contours. The steepest gradients do not lie along the Sierra Nevada front on the southwest and the escarpment of the basalt-capped mountains on the northwest; they are toward the center of the basin. Although the form of the anomaly on the south and east is not well defined, it may be concluded that the deepest part of Mono Basin is approximately a depression of triangular shape in plan, filled with more than 10,000 ± 3000 feet of low-density deposits of Cenozoic age, around which the Cenozoic and pre-Tertiary interface dips steeply on all sides.

The northernmost part of Mono Craters lies on the southern apex of this triangle. A subdued gravity low is inferred to trend south from this apex along Mono Craters, but no gravity observations were made near the axis of this low; therefore, it is poorly defined. Putnam (1949) has prepared a geologic cross section of a tunnel that crosses Mono Craters. This cross section shows a marked thickening of the Bishop tuff and other light Cenozoic deposits above dense pre-Tertiary metamorphic rocks under Mono Craters. The gravity low probably results from this thickening of lighter deposits.

The broad area of relatively low gravity northeast of Mono Lake probably represents a shallower northeastward extension of the deepest part of Mono Basin. In this area computation of the thickness of an infinite sheet with a gravity anomaly equal to the amplitude of the measured gravity low indicates

* Izumi Yokoyama (Gravity survey on Kuttyaro Caldera Lake: Jour. Physics of the Earth, v. 6, p. 75-79, 1958) found a gravity low of amplitude −46 mgals on Lake Kuttyaro, Hokkaido, Japan. Lake Kuttyaro lies in the western half of a large circular caldera. The gravity anomaly found by Yokoyama is very similar in form and size to the largest negative anomaly in the Mono Basin area. Yokoyama interpreted the Lake Kuttyaro anomaly as the gravity expression of a layer of coarse pumice that thickens to about 4 km toward the center of caldera.

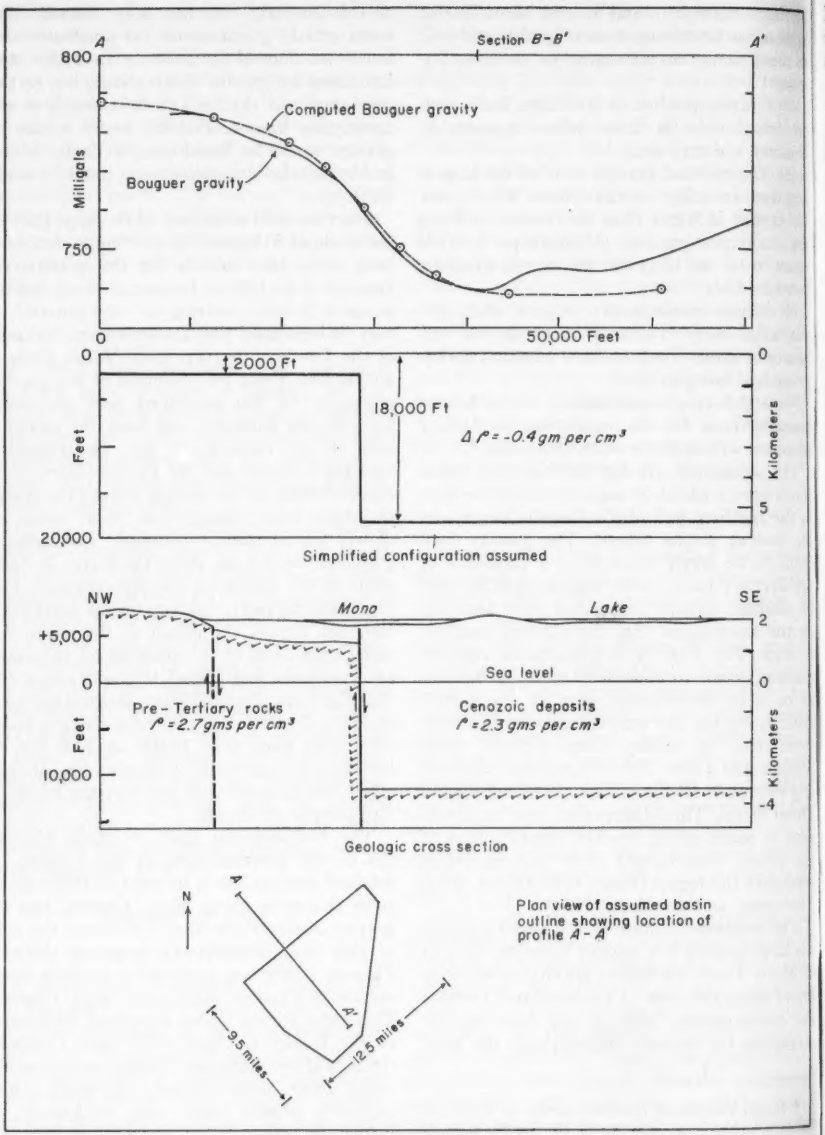

FIGURE 2.—INTERPRETATION OF GRAVITY ANOMALY ALONG PROFILE *A-A'*

that the pre-Tertiary rocks lie buried under several thousand feet of Cenozoic deposits. The seismic-refraction results confirm this qualitative conclusion.

Other valley areas that have received stream-transported sediments during Cenozoic time are marked by gravity minimum anomalies (*e.g.*, Adobe Valley and the valley between

Black Mountain and the Benton Range, Pl. 1). Only a few gravity observations were made in Adobe Valley, but a gravity minimum anomaly with an amplitude of about 10 mgals was revealed there. Therefore, the deposits of Cenozoic age in Adobe Valley must be at least 2000 feet thick and may be about twice that thick. South of Bald Mountain the gravity field drops off sharply toward Long Valley. Earlier measurements (Pakiser and Kane, 1956) showed that the amplitude of the gravity minimum anomaly in Long Valley is about 75 mgals; this indicates that a structural basin in Long Valley very similar to Mono Basin is present.

Two roughly circular high-gravity anomalies lie along the contact of the pumice ejecta and the Bishop tuff south and east of Mono Craters. These anomalies may express dense volcanic necks that were sources for the basalt flows of this area. The aeromagnetic profiles seemingly confirm this interpretation.

In the detailed interpretation that follows only the Mono Basin anomaly and its extension to the northeast will be considered.

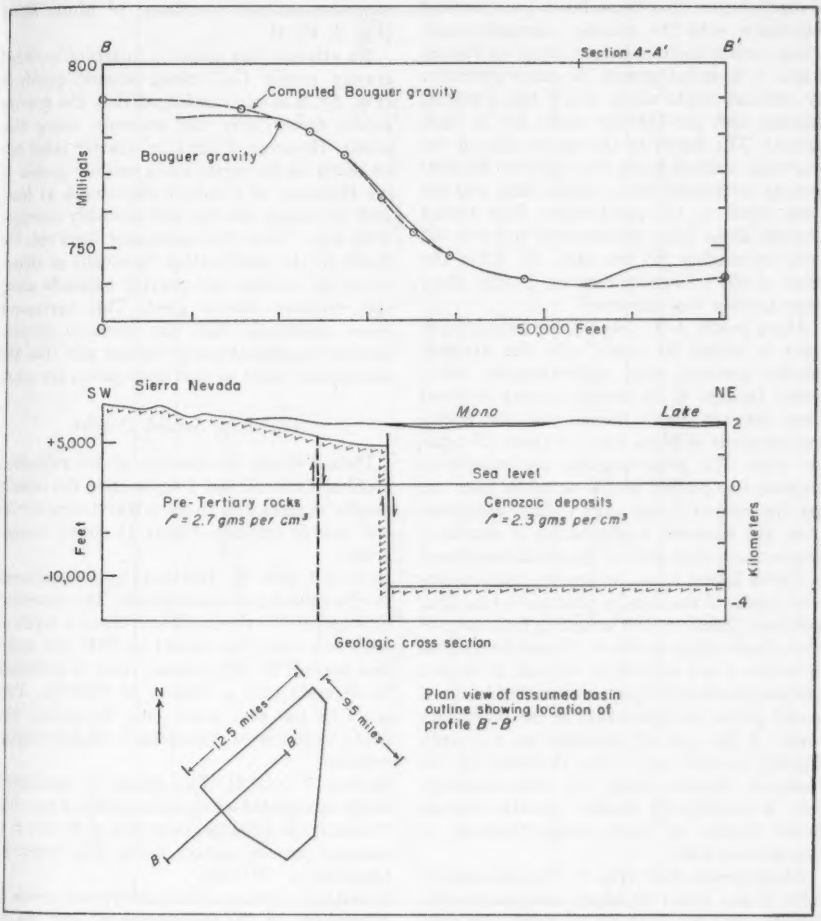

FIGURE 3.—INTERPRETATION OF GRAVITY ANOMALY ALONG PROFILE *B-B'*

Gravity Profiles

Two gravity profiles were analyzed in detail (Figs. 2 and 3). It was assumed, for purposes of computation, that Mono Basin is a structural depression with the roughly triangular horizontal outline and dimensions shown on Figures 2 and 3, bounded around its entire perimeter by vertical faults along which the Cenozoic deposits and pre-Tertiary rocks are in fault contact. The depth to the upper edge of the bounding vertical faults was taken to be 2000 feet, as determined from seismic data, and the total depth to the pre-Tertiary floor buried beneath Mono Lake was assumed to be 18,000 feet, or roughly 5.5 km (Fig. 2). Thus the effect of the entire structure on gravity along these profiles was examined.

Along profile *A-A'* (Fig. 2) the total gravity relief is about 50 mgals, and the steepest gravity gradient, only approximately determined because of the lack of gravity observations between Paoha Island and the northwestern shore of Mono Lake, is about 15 mgals per mile. The point-for-point correspondence between the gravity profile as taken from the gravity-contour map and that computed from the assumed configuration is excellent, except along that part of the profile southeast of Paoha Island where no gravity observations were made. If the density contrast is near that assumed, therefore, the bounding fault zone of Mono Basin along profile *A-A'* must be vertical or within a few degrees of vertical. A density contrast significantly greater than that assumed would permit interpretation of the subsurface cause of the gravity anomaly as a steeply dipping normal fault. The thickness of the Cenozoic deposits would be correspondingly less. A significantly smaller density contrast would require an even greater thickness of Cenozoic deposits.

Along profile *B-B'* (Fig. 3) the total gravity relief is also about 50 mgals, and the steepest gravity gradient is about 13 mgals per mile. Exactly the same configuration as that assumed for profile *A-A'* yields equally excellent agreement between the gravity profile as taken from the gravity-contour map and the computed gravity profile. The steep gradient is better defined by gravity stations along profile *B-B'* than along profile *A-A'*. The fault zone is thus seen to be probably vertical on both the northwest and southwest boundaries of Mono Basin. The basin has probably subsided an equal vertical distance along both of these bounding fault zones. The bounding fault zone of Mono Basin is more than a mile northeast of the frontal fault of the Sierra Nevada (Fig. 3; Pl. 1). The bounding fault zone is about 3 miles southeast of the escarpment of the basalt-capped mountains northwest of Mono Basin (Fig. 2; Pl. 1).

No attempt was made to interpret in detail gravity profile *C-C'* along seismic profile 1 (Fig. 4); it is not considered that the gravity values define fully the anomaly along this profile. However, if the total gravity relief can be taken as 10 mgals along seismic profile 1, the thickness of Cenozoic deposits is at least 2000 feet along this line and probably averages 3000 feet. Thus the agreement between the depth to the pre-Tertiary basement as determined by seismic and gravity methods along this common line is good. This agreement gives confidence that the assumed density contrast is approximately correct and that the conclusions based on that assumption are valid.

Analysis of Seismic Profiles

Plate 1 shows the location of the refraction profiles. Tables 1 and 2 summarize the seismic results. Figures 5 to 10 show travel-time curves and seismic sections. Figure 11 shows seismograms.

PROFILE 1 (FIG. 5): The shots to the northwest in effect yield a reversed profile. The basement dips upward to the northwest from a depth of 3800 feet under the spread to 2500 feet under shot point 5 W. The surface layer is underlain by deposits with a velocity of 7800 fps. Two shots to the east serve only to obtain the depth to this layer, indicating a slightly higher velocity.

PROFILE 2 (FIG. 6): This profile is unreversed and is interpreted on the assumption of zero dip. A velocity of 1100 fps, observed at Profile 3, is assumed for the surface layer. The depth to basement is 1700 feet.

PROFILE 3 (FIG. 7): This unreversed profile is interpreted on the assumption of zero dip to reveal basement at a depth of 800 feet. The small decrease in depth from Profile 2 is consistent with the gravity difference between these stations.

PROFILE 4 (FIG. 8): This profile is unreversed and interpreted by assuming zero dip. Below the weathered layer the Cenozoic section shows two layers with velocities of 5600 fps and 10,500 fps. The pre-Tertiary basement is 2300 feet deep.

PROFILE 5 (FIG. 9): The marked irregularity in the gravity-anomaly gradient together with

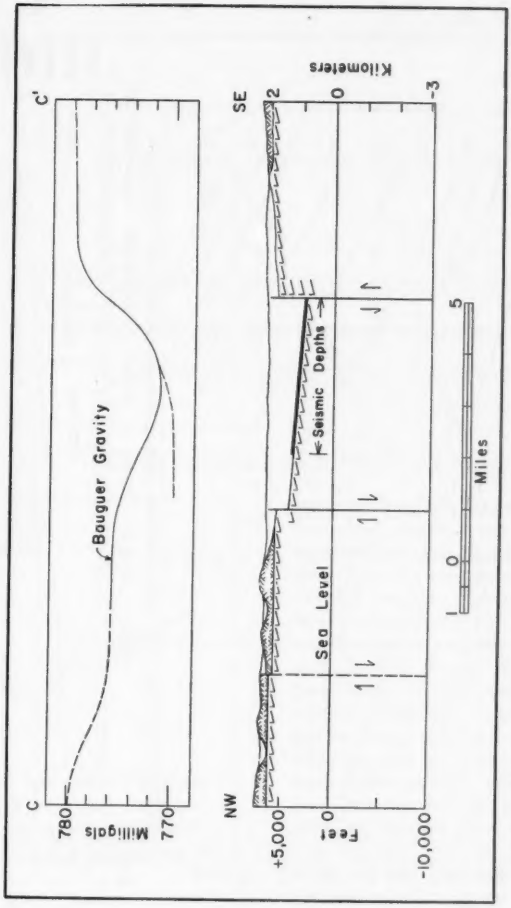

FIGURE 4.—COMPARISON OF GRAVITY AND SEISMIC DATA ALONG GRAVITY PROFILE *C-C'* AND SEISMIC PROFILE 1

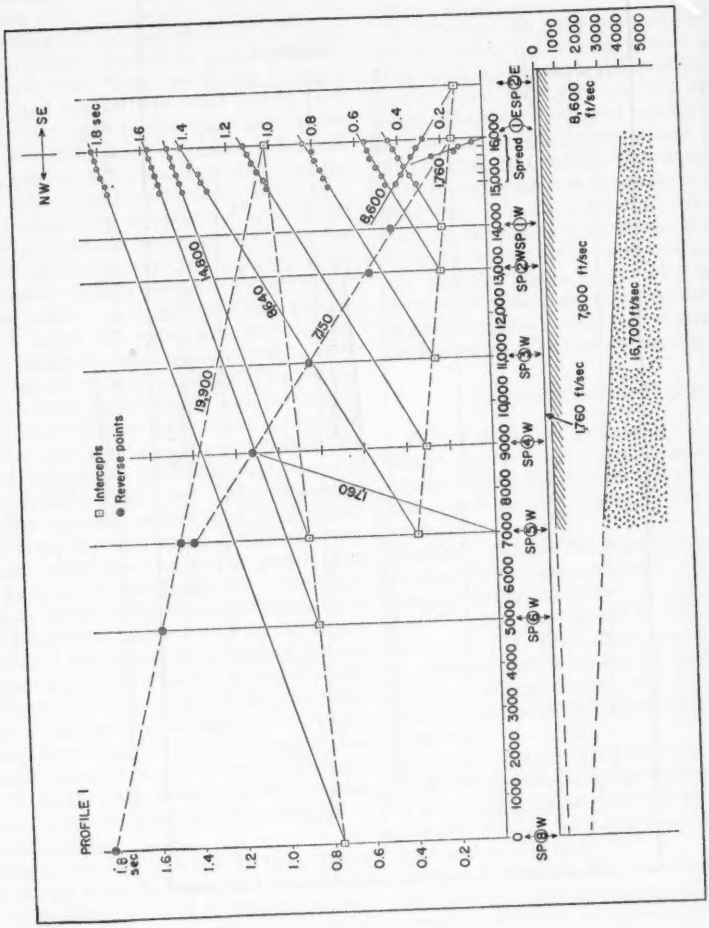

FIGURE 5.—ANALYSIS OF SEISMIC PROFILE 1

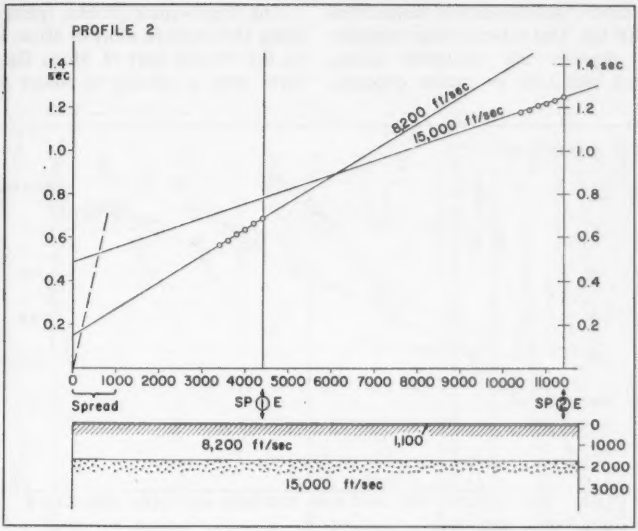

FIGURE 6.—ANALYSIS OF SEISMIC PROFILE 2

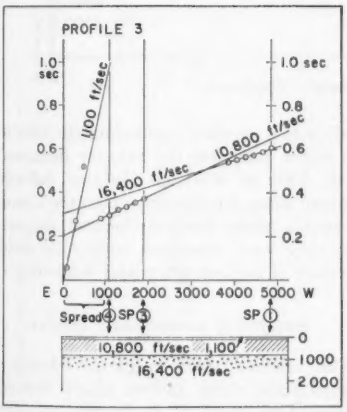

FIGURE 7.—ANALYSIS OF SEISMIC PROFILE 3

the high apparent basement velocity indicates a change in basement dip along the profile. An approximate adjustment was made by inserting a fictitious station (5′) and considering the two subsidiary profiles 5′-5 W. and 5′-5 E., in each of which there are no changes in dip and velocity.

The weathered-layer velocity of 1100 fps observed from shot 5 was used for both profiles. Since reverse data for the underlying layer were not obtained, zero dip was assumed. The next layer was reversed for 5′-5 W., the two apparent velocities yielding a true velocity of 8800 fps. It was necessary to assume this velocity and zero dip in order to extend this layer into profile 5′-5 E. Two apparent velocities were determined for the basement: 42,500 fps in profile 5′-5 W. and 14,500 fps from reverse points in profile 5′-5 E. Assuming the reasonable value of 17,000 fps for true basement velocity and requiring matched intercepts at 5′, we have sufficient data for a solution. In this approximate determination, the basement deepens from 2900 feet at 5 W. to 4400 feet at 5′ and 5500 feet at shot point 4. Quite possibly the high apparent velocity indicates a fault, in which case even greater basement dip is present than indicated in Figure 9.

PROFILE 6 (FIG. 10): In this partly reversed profile a 10,400 fps layer is beneath the weathered layer. The basement is at a depth of 3400 feet under the geophone spread and rises to 2100 feet at the west end of the profile.

No quantitative interpretations were made of Profiles 7 and 8 (Pl. 1) because available communications between the shot point and recording locations failed as a result of the great distances involved, so the intercept times for the larger depths are unknown.

Profiles 1, 2, 3, and 6 reveal that the velocity in materials immediately under the surficial

FIGURE 5.—ANALYSIS OF SEISMIC PROFILE 1

low-velocity layer characteristically ranges from 7800 to 10,800 fps. This velocity range suggests that these deposits are indurated rocks; well-indurated lake beds or stream deposits,

The long seismic profiles (profiles 7 and 8) along the southern shore of Mono Lake (Pl. 1), in the deepest part of Mono Basin, reveal a layer with a velocity of about 5500 fps ex-

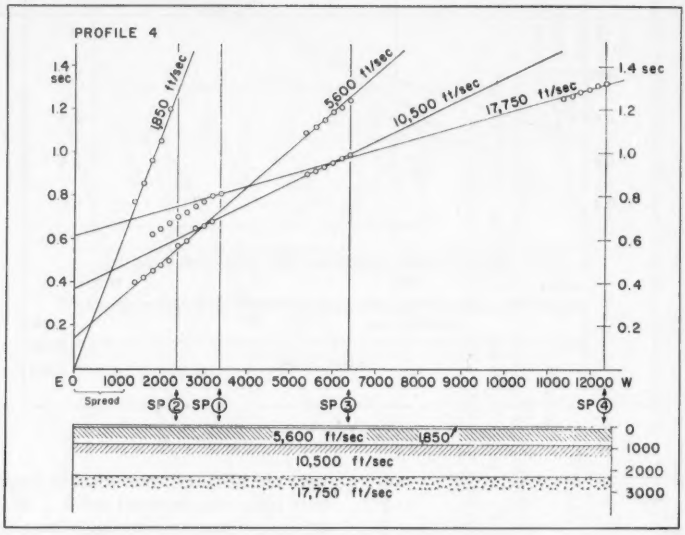

FIGURE 8.—ANALYSIS OF SEISMIC PROFILE 4

welded tuff, or even fresh-water limestone or flow rocks are likely representatives of this velocity range. These seismic profiles, along which relatively high-velocity rocks of Cenozoic age lie immediately below the surface, are all some distance outside the bounding fault system of the deepest part of the structural basin.

Profile 4, which extends southwestward immediately outside the southwestern bounding fault of Mono Basin, reveals a layer with a velocity of 5600 fps that is nearly 1000 feet thick, and this layer overlies a layer with a velocity of 10,500 fps. The near-surface layer probably represents relatively unconsolidated, water-saturated, clastic and pyroclastic deposits of Pleistocene(?) and Recent ages. The higher-velocity layer is similar in velocity to the material that lies at shallow depths below profiles 3 and 6, and it may represent the same layer. Seismic profile 5, in the deepest part of the northeastern extension of Mono Basin, also reveals two layers within the deposits of Cenozoic age. The maximum thickness of the layer of lower velocity (6200 fps) is nearly 2500 feet.

tending to a depth of approximately 1600 feet, and below 1600 feet the velocity increases to about 7000 or 8000 fps. Seismic reflections recorded along this line show that the Cenozoic deposits in Mono Basin are layered, suggesting that they were deposited largely by orderly processes of sedimentation and volcanism.

Analysis of Aeromagnetic Profiles

The relative total magnetic intensity is defined only along rather widely separated profiles (Figs. 12–15; Pl. 1), flown at an altitude several thousand feet above the surface of the ground. Because the profiles are so widely spaced and because they were not flown at right angles to geologic trends, depth analyses of the magnetic anomalies may be in error by 25 per cent or more. The interpretive method used in the report is patterned after the methods described in Vacquier *et al.* (1951). The method involves measurement of the horizontal extent of the steepest gradient and is based on the principle that for a body of given shape and intensity of magnetization the steeper the magnetic gradients the smaller the depth of

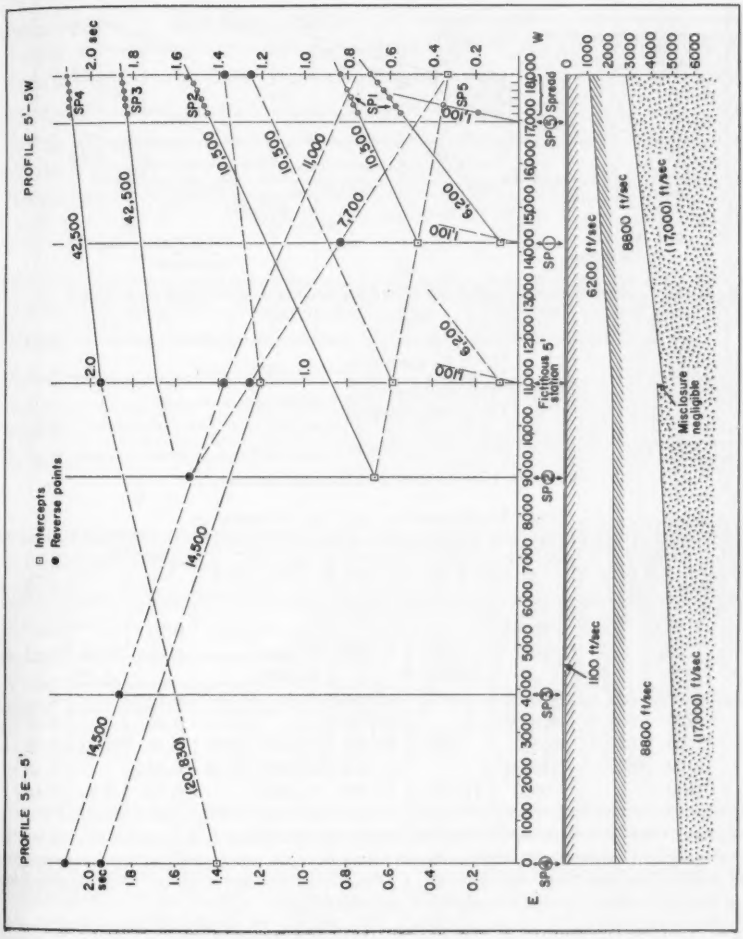

FIGURE 9.—ANALYSIS OF SEISMIC PROFILE 5

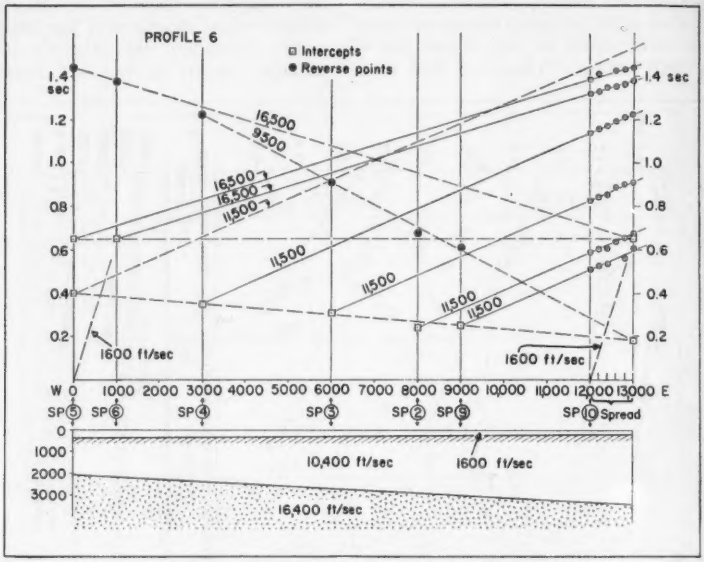

FIGURE 10.—ANALYSIS OF SEISMIC PROFILE 6

TABLE 2.—VELOCITIES AND TIME INTERCEPTS

Profile	V_1	V_{2E}	V_{3E}	V_{3W}	V_{BE}	V_{BW}	T_{2E}	T_{3E}	T_{3W}	T_{BE}	T_{BW}
1E	1760	..	8600*	..	..	..	..	0.17	..	..	..
1W	(1760)	..	7150	8640	19,900	14,800	..	0.15	0.37	1.02	0.87
2	(1100)	..	..	8200*	..	15,000*	..	..	0.15	..	..
3	1100	..	10,800*	..	16,400*	..	..	0.2	..	0.3	..
4	1850	5600*	10,500*	..	17,750*	..	0.13	0.37	..	0.61	..
5′–5W	1100	6200*	10,500	7700	42,500	(11,000)	0.08	0.58	0.33	1.20	0.75
5E–5′	(1100)	(6200)*	(8800)*	..	(20,800)	14,500	0.08	0.63±	..	1.40	1.20
6	1600	..	9500	11,500	16,500	16,500	..	0.18	0.4	0.66	0.66

V is apparent velocity in ft./sec.; *T* is intercept in seconds; subscripts 1, 2, 3, and *B* refer to weathered layer, lower-velocity Cenozoic layer, higher-velocity Cenozoic layer, and crystalline basement respectively; *E* and *W* signify East and West end of profile; ( ) indicates assumed velocity; * indicates unreversed profile; ± average between intercept at station 5′ and shotpoint 2

burial. Some subjectivity is involved in measurement of the horizontal extent of the steepest gradient, but experience has shown (Isidore Zietz, oral communication) that different interpreters will make measurements that differ very little. In the present study three interpreters have made independent measurements of the horizontal extents of the steepest gradients that are within 10 per cent of each other.

Steenland (*in* Vacquier *et al.*, 1951, p. 11–15) has shown that for rectangular prismatic models with cross-sectional dimensions large compared to the depth of burial, the horizontal extents of steepest gradients are approximately equal to the depth; experience has shown that along profiles flown over a terrain covered by a thin magnetic sheet, such as a lava flow, the measured horizontal extents of steepest gradients yield computed depths somewhat shallower than true depths.

In the discussion of the individual profiles

that follows, no conclusions will be drawn about the magnetic body that causes a particular anomaly other than to determine the depth to its upper surface unless there is independent gravity or geologic support for a more detailed interpretation or unless the anomaly shows unusual characteristics. In general, it will be seen that the depth below the flight altitude defines the surface of basalt flows.

PROFILE 37–57 (FIG. 12): The numbers identifying the profile are the terminal identification points (Pl. 1). Eight measurements of the horizontal extents of steepest gradients were made (D_1, D_1', D_2, D_3, D_3', D_4, D_4', and D_5). These have been plotted below the flight line, and they define approximately the surface of the ground. When two measurements were made on the same anomaly, they were averaged and plotted below the flight line.

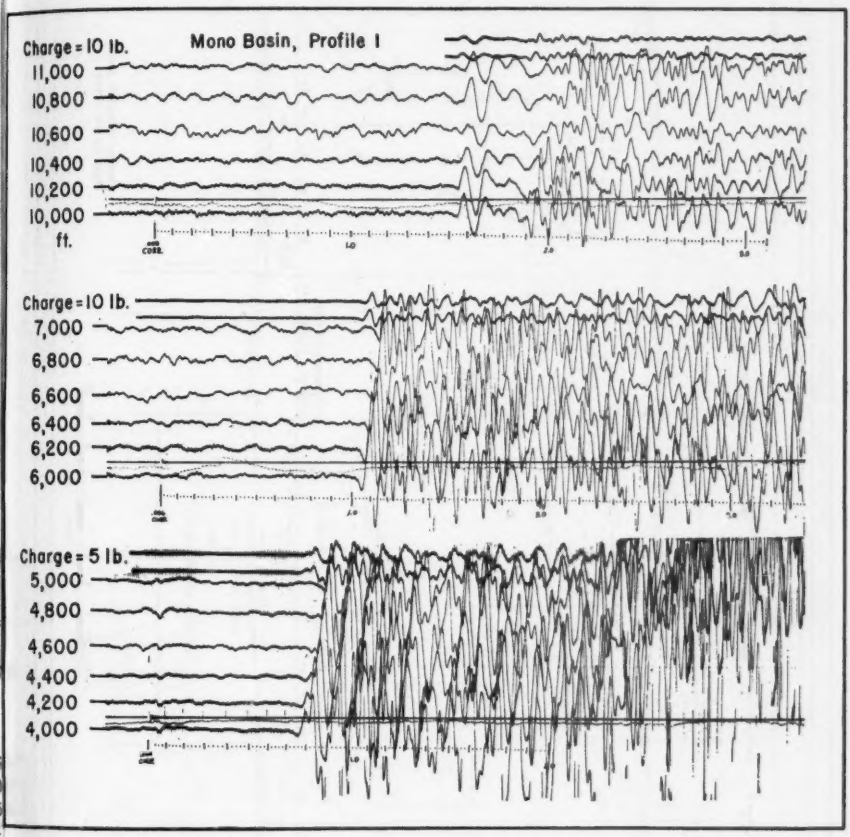

FIGURE 11.—SAMPLE SEISMOGRAMS

Anomaly A coincides in position with a small, roughly circular gravity high (Pl. 1); the anomaly could be caused by a volcanic neck that may have been the source of the basalt flows in the area.

Anomaly B has the same position as a poorly defined gravity high near the center of Mono Basin (Pl. 1). A similar gravity high, much better defined, was found in Long Valley (Pakiser and Kane, 1956) and coincides with a magnetic high there. Anomaly B may be caused by a pile of intrusive and flow rocks that were emplaced during the deposition of the basin

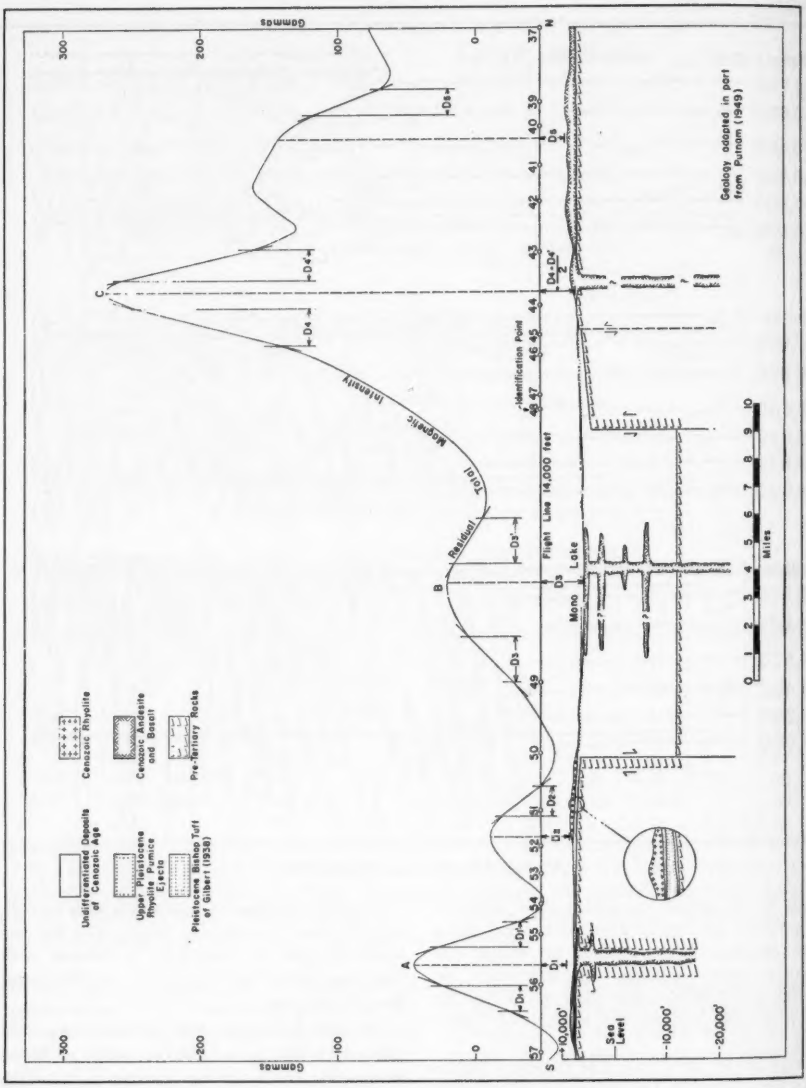

FIGURE 12.—ANALYSIS OF AEROMAGNETIC PROFILE 37-57

FIGURE 12.—ANALYSIS OF AEROMAGNETIC PROFILE 37-57

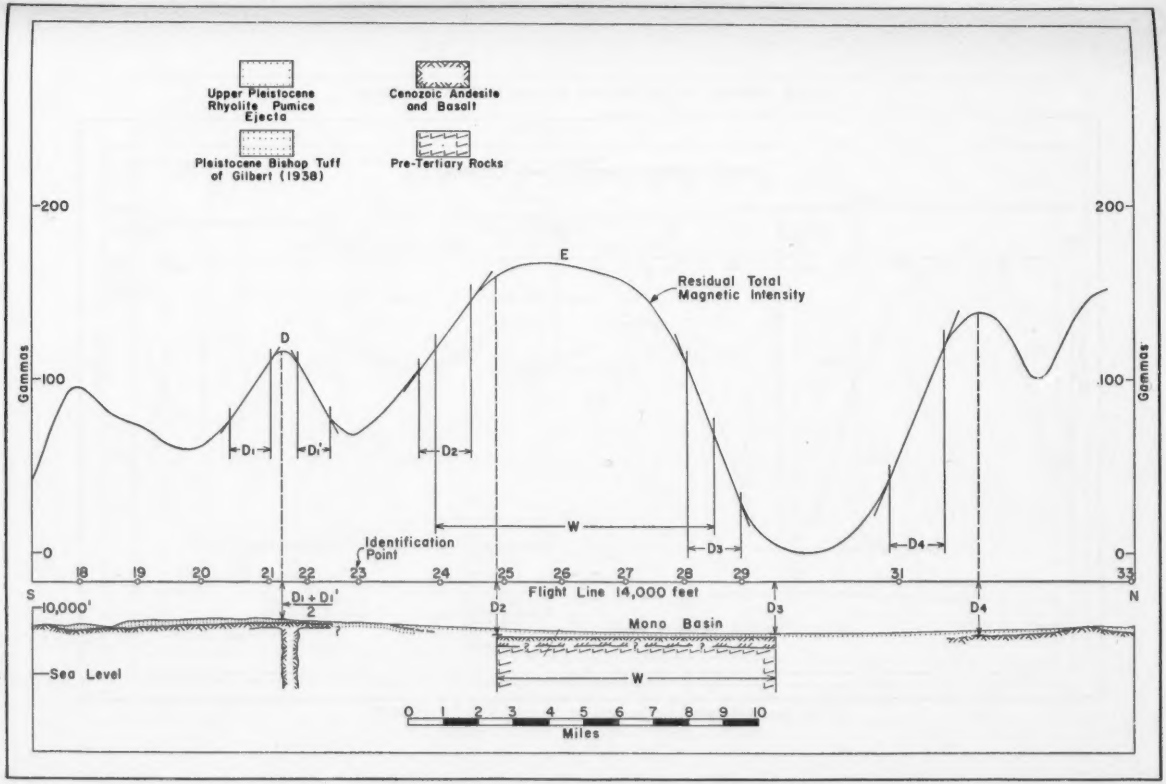

FIGURE 13.—ANALYSIS OF AEROMAGNETIC PROFILE 18-33

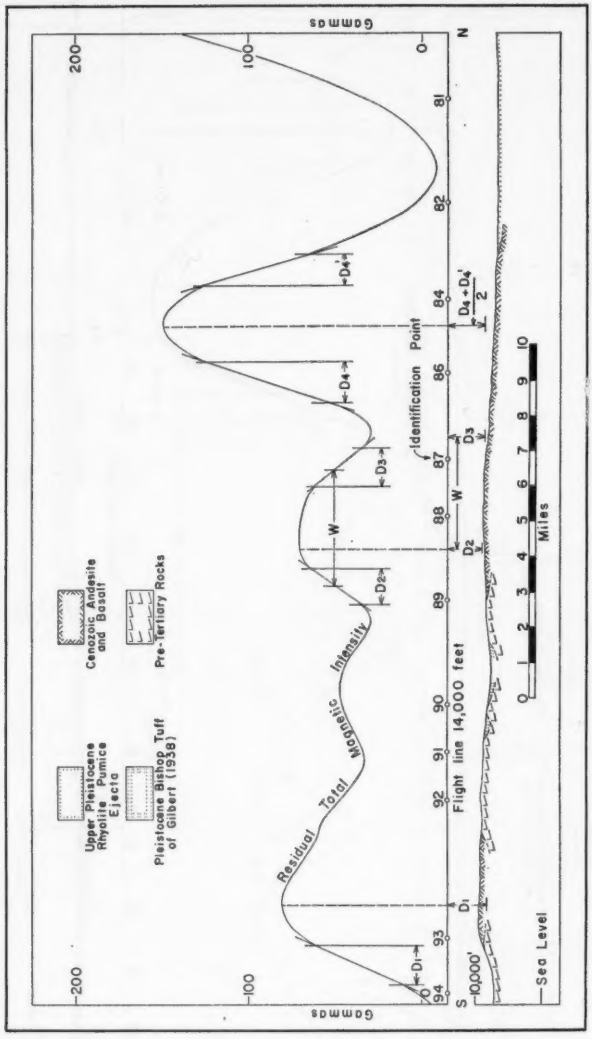

FIGURE 14.—ANALYSIS OF AEROMAGNETIC PROFILE 81-94

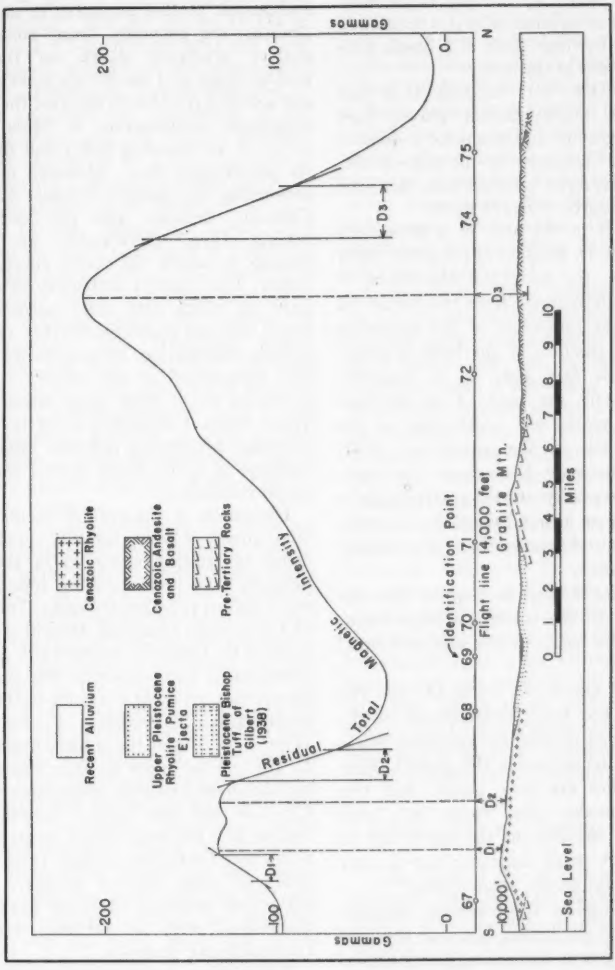

FIGURE 15.—ANALYSIS OF AEROMAGNETIC PROFILE 67-75

fill. This is suggested by the lavas on Paoha Island.

Anomaly C has a very large amplitude and coincides in position with the edge of a basalt flow. It may be caused by the edge of the flow, but on the basis of its large relief it is concluded that it may be the expression of a basalt dike that was the source of the flow.

PROFILE 18–33 (FIG. 13): Anomaly D is just east of a small, roughly circular gravity high (Pl. 1), so the gravity and magnetic anomalies are assumed to be caused by the same dense, magnetic feature, *e.g.* a volcanic neck that may have been the source of basalt flows.

Anomaly E is in the area of a prominent gravity high (Pl. 1). Because of the great width of the anomaly, the horizontal dimensions of the body were determined from the horizontal separation of the midpoints of the maximum gradients. The position of the body is determined from the fact that, at a magnetic inclination of 60°, the peak of an anomaly approximately marks the south edge of the body (*See* models in Vacquier *et al.*, 1951, p. 114–127). Anomaly E supports the interpretation of the poorly defined gravity high in the same area as being caused by a fault-bounded structural block that is probably capped by basalt.

The depth D_4 is used to suggest that the basalt exposed to the north continues southward under the near-surface unconsolidated deposits.

PROFILES 81–94 AND 67–75 (FIGS. 14, 15): The depths determined from measurement of the horizontal extents of steepest gradients define approximately the surface of the ground. Most of the anomalies are over basalt, but two prominent anomalies that merge into each other are over rhyolite on the south end of profile 67–75. A small magnetic low is over Granite Mountain on the same profile.

Rough estimates of the magnetic susceptibility of the magnetic bodies, based on assumed horizontal dimensions and anomaly amplitudes (Vacquier *et al.*, 1951, p. 18), suggest that the magnetic susceptibility of the materials of these bodies ranges from 0.001 to 0.003 cgs unit. This is higher than the susceptibility of any rhyolite sample from Long Valley for which the susceptibility was measured. The rock of most of the magnetic masses is probably basalt or mafic andesite.

GEOLOGIC INTERPRETATION

Structure of Mono Basin

Using the detailed analyses of the gravity and seismic profiles presented in the preceding sections, the generally linear zones of steep gravity gradients shown on the gravity-contour map, and the known areal geology, we are now in a position to describe the subsurface structural configuration of Mono Basin in terms of its bounding faults and the depth of its pre-Tertiary floor. Although uncertainties concerning the density contrast between the Cenozoic deposits and pre-Tertiary rocks remain, these uncertainties are not large enough to affect the major conclusions that follow. The inherent ambiguity of the gravity data, on which data these major conclusions are based, has been considerably narrowed by seismic information, measurements of density, and comparison of the density relationships in Mono Basin with those elsewhere in the Great Basin. Considerations of the volume of Cenozoic deposits of different origin that are confined in Mono Basin further support these major conclusions.

Discussion of the gravity profiles indicated that zones of steep gravity gradient mark zones of faulting along which the Cenozoic deposits have been displaced relatively downward against pre-Tertiary rocks. The amplitude of the gravity minimum anomalies over areas covered by Cenozoic deposits is a guide to the thickness of these deposits. The magnitude of the steepest gradient is a guide to the dip of the bounding faults. Profiles *A-A'*, *B-B'*, and *C-C'* (Figs. 2, 3, 4) and the seismic profiles (Figs. 5 to 10) can be taken as lines along which information on the depth and configuration of the Cenozoic and pre-Tertiary interface is controlled. It is relatively simple to extrapolate the subsurface configuration from these lines along zones of steep gravity gradient. Thus the subsurface structure of Mono Basin has been determined with an accuracy sufficient for reconnaissance purposes.

The combined geophysical and geologic map of Mono Basin (Pl. 1) reveals that a large, roughly rectangular block of pre-Tertiary rocks, bounded by near-vertical or steeply dipping normal faults, subsided and received a thick accumulation of light sediments and volcanic deposits of Cenozoic age. The Mono Basin structure as a whole conforms in general to the physiographic outline of the basin, but

the bounding faults are in general removed basinward from the physiographic escarpments. The southwestern half of the structural basin has subsided about 18,000 ± 5000 feet (5.5 ± 1.5 km) to form a deep triangular block whose pre-Tertiary floor lies nearly 12,000 ± 5000 feet (3.5 ± 1.5 km) below mean sea level. The northeastern half of the structural basin has subsided a maximum of about 6000 feet, or only about one-third the subsidence of the southwestern half, and the depth decreases progressively northeast of Mono Lake to a minimum near the California-Nevada border.

The simple outline of the structural basin is interrupted by the triangular salient that projects into the basin northwest of Cowtrack Mountain, and the nature of the structure in that area is not clearly understood because of the lack of detailed geophysical information there. Presumably this triangular salient represents an area that remained relatively stable while Mono Basin subsided to the east and west of it. The high gravity field in this area may represent, however, at least in part, an accumulation of dense volcanic rocks. This is suggested by the aeromagnetic profile (Fig. 13) and the areal geology.

The Cenozoic deposits that fill the basin are in fault contact with the confining pre-Tertiary rocks essentially throughout the entire vertical extent of these deposits. Therefore, the Cenozoic deposits must have been displaced by faulting against the pre-Tertiary rocks after the Cenozoic deposits were laid down. Because it is considered to be extremely unlikely that the entire section of Cenozoic deposits (18,000 ± 5000 feet) accumulated before faulting, it is concluded that deposition of the Cenozoic section and fault displacement were essentially simultaneous. Fault movement may have been continuous or repeatedly rejuvenated while streams were carrying clastic debris eroded from the surrounding mountains into Mono Basin and volcanoes were ejecting immense volumes of pyroclastic material, and probably some lavas, over the Mono Basin area. These newly deposited beds must have subsided into Mono Basin along faults soon after they were laid down.

As has been noted, Mono Craters lie in part along the southwestern bounding fault of Mono Basin and, from the southernmost apex of the Mono Basin structure they continue southward in a nearly straight line into the western part of Long Valley (Putnam, 1938; Mayo, Conant, and Chelikowsky, 1936), presumably along a south-trending fault. Thus the extrusion of the rhyolitic obsidian and pyroclastic ejecta from Mono Craters was probably governed by a zone of weakness created by the intersection of three faults, two of which are a part of the major system of faults that bounds Mono Basin. The exposure of basalt on the Mono Lake shore line northwest of Paoha Island is terminated by the fault that bounds the structural basin on the northwest. Indeed, Mono Basin is everywhere surrounded by rocks of volcanic origin except on the extreme west where the Sierra Nevada rises high above Mono Lake. Thus an intimate association between Mono Basin and Cenozoic volcanism is suggested.

As can be seen from profile *A-A″* (Fig. 16), the vertical extent of the Mono Basin structure is a very large fraction (about one-third) of its width, and in plan the deepest triangle of the structural basin is essentially equidimensional. Mono Basin is approximately twice as deep as the deepest basins of known depth in the remainder of the Basin and Range province, with the single exception of Long Valley, immediately to the south, which is strikingly similar to Mono Basin and is presumed to be of similar origin. The vertical dimensions of the bounding faults of Long Valley from the gravity results there (Pakiser and Kane, 1956) are almost identical to those of Mono Basin (Fig. 17). Most basins in the Great Basin region are elongated in plan. Owens Valley, Death Valley, and Panamint Valley are typical. The fact that Mono Basin subsided along faults that do not form a common boundary with the surrounding mountain masses is also significantly different from the usual relationship.

Nature of Cenozoic Deposits in Mono Basin

Some idea of the nature of the deposits of Cenozoic age that fill Mono Basin can be gained from a study of the exposed, upper surface of these deposits. Because this surface is not a plane surface, but ranges in altitude from a bout 6400 feet at the shore of Mono Lak to 8000 feet or more in the mountain slopes, at least some information in three dimensions is revealed by geologic mapping. The surface geologic evidence has already been discussed and has been described in more detail by Russell (1889), Gilbert (1941), and Putnam (1949; 1950). Geologic mapping indicates that

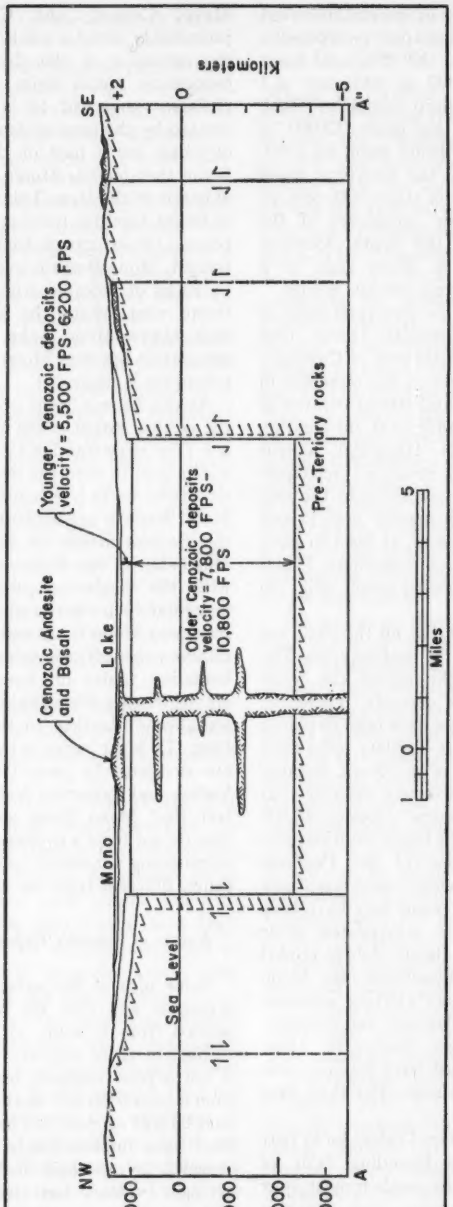

FIGURE 16.—GENERALIZED GEOLOGIC CROSS SECTION OF MONO BASIN ALONG PROFILE *A-A"* BASED ON GEOPHYSICAL EVIDENCE

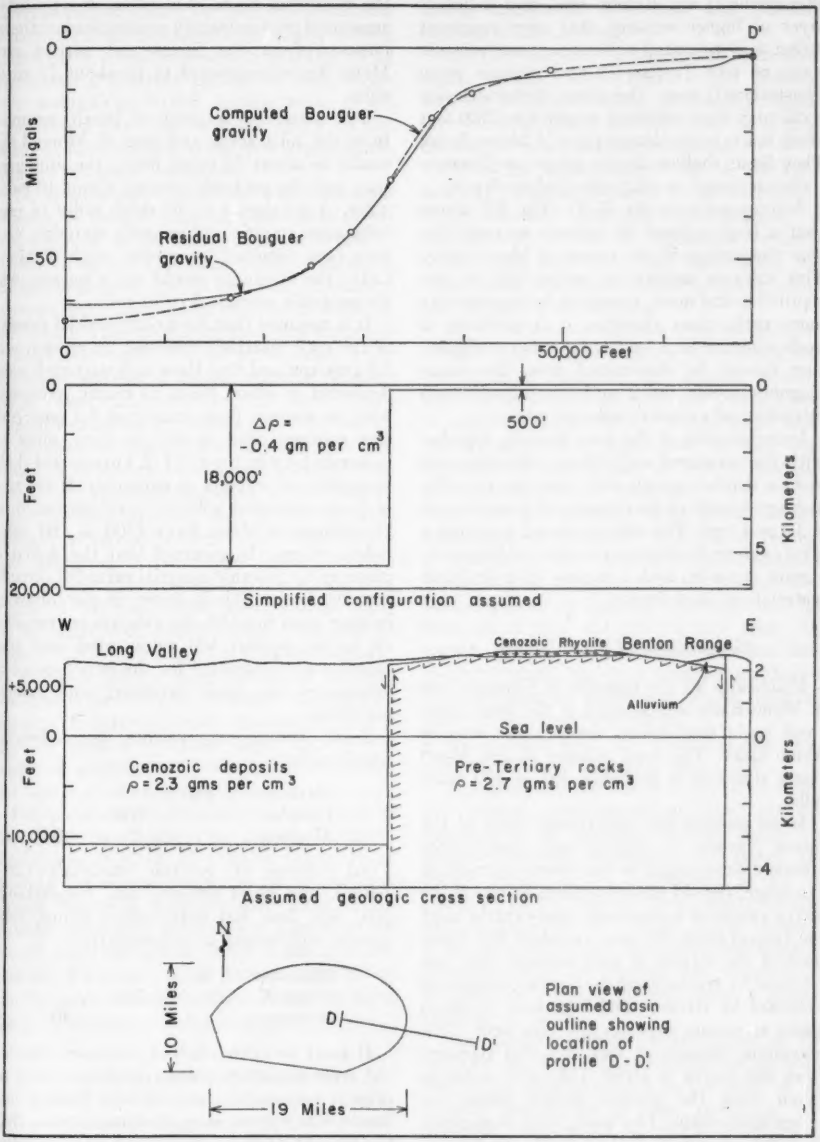

FIGURE 17.—INTERPRETATION OF GRAVITY ANOMALY ALONG PROFILE *D-D'* IN LONG VALLEY

Mono Basin probably contains predominantly stream-transported sediments and material of volcanic origin and of low average density.

In general, the deposits of Cenozoic age are divided into two units on the basis of seismic velocity: a shallow layer of relatively low velocity that may represent essentially unconsolidated clastic and pyroclastic deposits of

Pleistocene(?) and Recent ages, and a deeper layer of higher velocity that may represent rather well-indurated sedimentary and volcanic rocks of late Tertiary(?) and perhaps early Pleistocene(?) ages. The older, higher-velocity rocks may have subsided as much as 2500 feet along faults in the deeper parts of Mono Basin. They lie at shallow depths where pre-Tertiary rocks are found at relatively shallow depths.

Aeromagnetic profile 37–57 (Fig. 12) shows that a large volume of volcanic material lies near the surface at the center of Mono Basin. This volcanic material is rather high in susceptibility and must, therefore, be considerably more mafic than rhyolite; it is probably a mafic andesite or a basalt. Its exact configuration cannot be determined from the single magnetic profile, but it probably includes both intrusive and extrusive volcanic rocks.

Interpretation of the gravity data, together with the measured and inferred densities and seismic depths, reveals only that the probable average density of the deposits of Cenozoic age is 2.3 gms/cm³. This density would represent a good average density for a mixture of lake beds, stream deposits, and a variety of pyroclastic material and lava flows.

Balance Sheet of Rock Volumes

Practically all the deposits of Cenozoic age in Mono Basin are confined in the deep structural basin that covers roughly the area of Mono Lake. The total volume of the Mono Basin structure is probably 300 ± 100 cubic miles.

If we assume that the frontal fault of the Sierra Nevada is vertical and that, before stream erosion began to tear down the rocks of the range, the old erosion surface on top of the Sierra extended horizontally eastward to meet the frontal fault, we may calculate the upper limit of the volume of rock material that was removed by erosion from the Sierra, transported eastward by streams, and laid down in Mono Basin as stream deposits and lake beds. This maximum amount of rock material removed from the Sierra is about 135 cubic miles as taken from the present surface shown on topographic maps. The lower limit of material removed, assuming that virtually no erosion has taken place since the uplift of the Sierra, is zero.

The Sierra Nevada is not bounded by a single, vertical fault (Putnam, 1949), and it seems reasonable to assume that warping may have accounted for some of the deformation in the mountain block. Therefore, the probable amount of predominantly granitic rock material removed from the Sierra and carried into Mono Basin is assumed to be about 75 cubic miles.

The maximum amount of basalt removed from the hills north and east of Mono Lake would be about 25 cubic miles, the minimum zero, and the probable amount about 10 cubic miles. A maximum of 10 cubic miles of miscellaneous granitic and volcanic materials may have been removed by erosion south of Mono Lake; the minimum would again be zero and the probable amount 5 cubic miles.

It is assumed that the average initial density of the rock materials removed by erosion was 2.7 gms/cm³ and that these rock materials were deposited in Mono Basin as clastic sediments with an average final density of 2.3 gms/cm³. The volumes cited heretofore, then, must be increased by a factor of 2.7/2.3 to convert them to equivalent volumes as sediments. If the sum of these converted volumes is subtracted from the volume of Mono Basin (300 ± 100 cubic miles), it may be assumed that the deficit is made up by volcanic material extruded directly into the basin. This is shown in the following balance sheet in which the volumes are rounded off to the nearest 100 cubic miles and trial balances are calculated for the entire range of volume of the basin structure and eroded materials.

Total volume equivalents as sediments (cubic miles):

Maximum	200	..	..
Probable	..	100	..
Minimum	..	..	0

Total volume of volcanic materials (first, second, and third columns are, respectively, 200, 300, and 400 cubic miles minus total volume equivalents as sediments):

Minimum	0	..	..
Probable	..	200	..
Maximum	..	..	400

It must be acknowledged, however, that an old erosion surface about which we have no present information, and streams flowing into Mono Basin from more distant sources than the present drainage basin, may have supplied clastic debris while Mono Basin was subsiding. Although this is unlikely, it cannot be ruled out altogether. On the other hand, stream outlets in the past could have transported finer clastic debris and materials in solution out of the Mono Basin area. Putnam (1949) believes that

this did happen during the period of maximum extent of Pleistocene Lake Russell, and Russell (1889) made a similar assumption, although he postulated a different channel of exit. These two possibilities would oppose each other; they would have but a minor effect on the balance sheet compared to the larger uncertainties discussed hereafter.

The balance sheet shows that if the maximum amount of eroded material (200 cubic miles) was supplied to the Mono Basin structure of minimum volume (200 cubic miles), a balanced erosion-deposition budget could be maintained without requiring volcanic material to make up the deficit. The probability that this happened is considered small. On the other hand, if the minimum amount of eroded material (0 cubic miles) was transported to the Mono Basin structure of maximum volume (400 cubic miles), all the material deposited in the basin structure would have had to be volcanic in origin. The probability that this happened is even smaller than the first extreme. But if the probable amount of eroded material (100 cubic miles) was deposited in the Mono Basin structure with the probable volume of 300 cubic miles, a deficit of 200 cubic miles remains to be made up by material of volcanic origin. The range of possibilities is very large, but it seems necessary to conclude that a large volume of volcanic material is buried in Mono Basin. This may be verified in part by direct observation of the exposed surface of Mono Basin and by the magnetic evidence of volcanic material near the center of the basin structure.

For purposes of discussion we may assume that about two-thirds of the material in Mono Basin may be of direct volcanic origin. However, of the material supplied by erosion and stream transport, probably only about three-fourths came from pre-Tertiary sources in the Sierra and one-fourth came from volcanic sources. Therefore, about three-fourths of all the Cenozoic deposits in Mono Basin may be of direct or secondary volcanic origin.

Origin of Mono Basin

We now possess a large inventory of facts and inferences on which a theory for the origin of Mono Basin can be constructed. These may be summarized as follows:

(1) Mono Basin is a large structural depression, bounded by vertical or near-vertical faults, that has subsided and received an accumulation of about 18,000 ± 5,000 feet of stream-transported sediments and volcanic deposits of Cenozoic age.

(2) The deepest, southwestern triangular block, which contains most of the Cenozoic deposits of Mono Basin, is roughly equidimensional in plan, and its depth is a large fraction of its horizontal dimensions.

(3) Of the approximately 300 ± 100 cubic miles of Cenozoic deposits in Mono Basin, a large fraction (perhaps three-fourths) is probably of direct or secondary volcanic origin, but some (perhaps one-fourth) was transported into Mono Basin by streams from pre-Tertiary rock sources.

(4) The Cenozoic deposits in Mono Basin are divided into 2 major units: a layer about 2000 feet thick of relatively low seismic velocity, and a layer extending to the pre-Tertiary floor of relatively high velocity. These major units are layered and are presumed to have been deposited at least in part by orderly processes of sedimentation and volcanism.

(5) The subsidence of Mono Basin has been continuous or repeatedly rejuvenated through an interval of late Tertiary(?) and Pleistocene times so that deposits near the surface have been displaced by faulting relatively much less than those near the pre-Tertiary floor. The recent deposits at the surface have not been displaced at all, and as a consequence there is no physiographic expression of the bounding faults of the structural basin.

(6) Volcanic rocks are intimately associated with the Mono Basin structure.

The unusually high ratio of depth to width, the roughly equidimensional plan, and the prominence of volcanic activity make the usually assumed mechanism of Basin and Range block faulting inadequate as an explanation for the origin of Mono Basin. Another mechanism must be sought. It is therefore postulated that Mono Basin subsided along its bounding faults as support was removed by extrusion of volcanic material from a magma chamber at depth.

The physicochemical relationships of the volcanic activity in Mono Basin are too complex to be explained fully on the basis of our present knowledge of the petrology and chemical composition of the volcanic rocks. However, we may attempt to explain the origin of Mono Basin in terms of kinematic concepts (*i.e.*, movement of magma and of a block of solid rock) without making any assumptions on the ultimate nature of the energy involved.

To do this we assume that the volcanic rocks of andesitic and more silicic composition were

withdrawn from a magma chamber within the earth's sialic crust. The basalts (except perhaps for minor products of magmatic differentiation) are excluded on the assumption that they were withdrawn from a deeper source in the lower part of the crust or the upper part of the mantle. The andesites and rhyolites considered are assumed to be less dense as volcanic rocks after eruption than were their original materials in the magma chamber before eruption. The mass of these materials before and after eruption must have remained constant, so they were expanded to occupy a larger volume after eruption, and they are assumed to have been spread over an area larger than that of the magma chamber from which they came. If this is so, a net deficiency of mass will result in and above the magma chamber, and this must be expressed by a gravity minimum anomaly on the pre-eruption surface.

The problem then becomes one of finding the volcanic rocks corresponding to the mass deficiency of the source area and of attempting to describe the relationships between volcanic activity and subsidence of Mono Basin.

If the basin deposits of volcanic origin occupy a volume of, say, 200 cubic miles and if the volume of the basin structure is, say, 300 cubic miles and if all the subsidence was caused by withdrawal of magma from a magma chamber at depth, by a simple computation it can be shown that about 100 to 150 cubic miles of volcanic deposits must be found outside the basin structure. These numbers indicate the general magnitude of the volumes required.

There are few such deposits in the area immediately surrounding Mono Basin. About that much volcanic material can be found, however, by looking far enough: the older rhyolite and andesite on the east flank of the Benton Range, the andesite of Bald Mountain, the large volume of rhyolite of Glass Mountain and its surroundings, the Bishop tuff of Gilbert (1938), and the pumice and obsidian erupted from Mono Craters. But Long Valley is a structure of the same type as Mono Basin, and most of these rocks are more intimately associated with Long Valley than with Mono Basin. This difficulty can be solved hypothetically by assuming that a magma chamber extended under both Mono Basin and Long Valley. Then both of these structures could have subsided in response to eruption of volcanic material from either of the structures. If this hypothesis is used the large volume of rhyolite piled above the general level near the center of Long Valley can be used to account for part of the volcanic rocks needed.

However, the volume of the Long Valley structure is about the same as that of the Mono Basin structure, so the amount of surplus volcanic material that must be found should be doubled. The total volume of the andesites and rhyolites (including pumice and tuff) not confined in the basin structures is probably about enough, and intrusive rocks about which we have no knowledge may be buried in the area. There is no available way at present of finding out precisely the volume of the volcanic material, and a wide range of uncertainty has been acknowledged about the balance sheet of rock volumes that would make any such precision of doubtful significance. The explanation given remains a plausibility argument in the absence of more precise information than is available now.

To complete the argument, it may be assumed that magma was propelled upward from the magma chamber by an internal pressure that exceeded the least principal stress plus the (essentially negligible) tensile strength of the surrounding rocks.[1] The most likely internal pressure is the partial pressure of dissolved water, and the physicochemical mechanism may have been similar to that proposed by Kennedy (1955). The paths traveled by the magma may have extended some distance beyond the basin structures, perhaps by migration along a surrounding system of fissures, to the places from which the volcanic rocks were erupted.

We conclude, as did Williams (1941), that Mono Basin may be regarded as a volcano-tectonic depression which subsided along faults that may have been blocked out by the same tectonic forces that produced Basin and Range faulting in the area. The vertical movement, however, was caused mainly by the force of gravity pulling the block down as support was removed below.

Age of Mono Basin

No objective data are available on which to date the earliest subsidence of Mono Basin.

[1] Pakiser (1960) has suggested that southward movement of the Sierra Nevada block with respect to the Great Basin acted as a mechanism for reducing the principal stress parallel to the Sierra Nevada. This would tend to stretch or pull apart large offsets of the Sierra Nevada front, such as that containing Mono Basin and Long Valley, and bring on eruption.

Subsidence probably began with the earliest Pliocene(?) volcanic activity (Gilbert, 1941) and ended with the latest explosions from Mono Craters. Because it is known that the Basin Ranges of the Mono Basin area were not blocked out by faults before late Pliocene or early Pleistocene time (Gilbert, 1941), it would seem that the subsidence of Mono Basin began before elevation of these ranges. The Sierra Nevada probably existed as a range of at least moderate altitude, however, before subsidence of Mono Basin began. Perhaps the subsidence of Mono Basin was initiated synchronously with an early Pliocene(?) uplift of the Sierra Nevada (Matthes, 1930).

References Cited

Blackwelder, Eliot, 1931, Pleistocene glaciation in the Sierra Nevada and Basin ranges: Geol. Soc. America Bull., v. 42, p. 865–922

Bott, M. H. P., 1953, Negative gravity anomalies over acid "intrusions" and their relation to the structure of the earth's crust: Geol. Mag., v. 90, p. 257–267

Bott, M. H. P., and Masson-Smith, D., 1953, Gravity measurements over the northern Pennines: Geol. Mag., v. 90, p. 127–131

Chelikowsky, J. R., 1940, Tectonics of the rhyolite in the Mammoth embayment, California: Jour. Geology, v. 48, p. 421–435

Dix, C. H., 1952, Seismic prospecting for oil: N. Y., Harper and Bros., 414 p.

Duerkson, J. A., 1949, Pendulum gravity data in the United States: U. S. Coast and Geod. Survey Spec. Pub. 244, 218 p.

Ewing, M., Woollard, G. P., and Vine, A. C., 1949, Geophysical investigations in the emerged and submerged Atlantic Coastal Plain, Part III, Barnegat Bay, New Jersey, section: Geol. Soc. America Bull., v. 60, p. 257–296

Ewing, M., Worzel, J. L., Steenland, N. L., and Press, F., 1950, Geophysical investigations in the emerged and submerged Atlantic Coastal Plain, Part II, Woods Hole, New York, and Cape May sections: Geol. Soc. America Bull., v. 61, p. 877–892

Gilbert, Charles M., 1938, Welded tuff in eastern California: Geol. Soc. America Bull., v. 49, p. 1829–1862

—— 1941, Late Tertiary geology southeast of Mono Lake, California: Geol. Soc. America Bull., v. 52, p. 781–816

Kennedy, George C., 1955, Some aspects of the role of water in rock melts, p. 489–503 *in* Poldervaart, Arie, Editor, Crust of the earth: Geol. Soc. America Special Paper 62, 762 p.

Matthes, Francois E., 1930, Geologic history of the Yosemite Valley: U. S. Geol. Survey Prof. Paper 160, 137 p.

Mayo, E. B., Conant, L. C., and Chelikowsky, J. R., 1936, Southern extension of the Mono Craters, California: Am. Jour. Sci., v. 32, p. 81–97

Nettleton, L. L., 1940, Geophysical prospecting for oil: N. Y., McGraw-Hill Book Co., 444 p.

Oliver, Howard W., 1956, Isostatic compensation for the Sierra Nevada, California (Abstract): Geol. Soc. America Bull., v. 67, p. 1724

Pakiser, L. C., 1960, Transcurrent faulting and volcanism in Owens Valley, California: Geol. Soc. America Bull., v. 71, p. 153–160

Pakiser, L. C., and Kane, M. F., 1956, Gravity study of the structural geology of Owens and Long Valley, California (Abstract): Geol. Soc. America Bull., v. 67, p. 1724

Press, Frank, 1956, Determination of crustal structure from phase velocity of Rayleigh waves, Part 1, Southern California: Geol. Soc. America Bull., v. 67, p. 1647–1658

Putnam, W. C., 1938, The Mono Craters, California: Geog. Rev., v. 28, p. 68–82

—— 1949, Quaternary geology of the June Lake District, California: Geol. Soc. America Bull., v. 60, p. 1281–1302

—— 1950, Moraine and shoreline relationships at Mono Lake, California: Geol. Soc. America Bull., v. 61, p. 115–122

Rinehart, C. Dean, and Ross, Donald C., 1957, Geology of the Casa Diablo Mountain quadrangle, California: U. S. Geol. Survey Geologic Quadrangle Map 99

Russell, Israel C., 1889, Quaternary history of Mono Valley, California: U. S. Geol. Survey, 8th Annual Rept., p. 261–394

Swick, Clarence H., 1942, Pendulum gravity measurements and isostatic reductions: U. S. Coast and Geod. Survey Spec. Pub. 232, 82 p.

Thompson, George A., and Sandberg, Clarence H., 1958, Structural significance of gravity surveys in the Virginia City-Mount Rose area, Nevada and California: Geol. Soc. America Bull., v. 69, p. 1269–1282

Vacquier, V., Steenland, Clarence, Henderson, Roland G., and Zietz, Isidore, 1951, Interpretation of aeromagnetic maps: Geol. Soc. America Mem. 47, 151 p.

Williams, Howel, 1941, Calderas and their origin: Univ. of Calif. Pubs. in Geol. Sci., v. 25, p. 239–346

U. S. Geological Survey, Denver, Colorado; California Institute of Technology, Pasadena, California; U. S. Geological Survey, Washington, D. C.

Manuscript Received by the Secretary of the Society, January 6, 1959

Publication Authorized by the Director, U. S. Geological Survey

California Institute of Technology Contribution No. 904

BULLETIN OF THE GEOLOGICAL SOCIETY OF AMERICA
VOL. 71, PP. 449–456, 5 FIGS., 1 PL. APRIL 1960

ROLE OF HYDROXYL ORIENTATION IN MICA ALTERATION

By William A. Bassett

Abstract

Phlogopite and biotite are generally more susceptible to alteration by ion exchange than muscovite. The key mechanism responsible for this difference is considered to be hydroxyl orientation.

Single-crystal study with the infrared spectrophotometer established the orientation and bonding of the hydroxyl ions. The dipole moments of the hydroxyl ions in phlogopite, a trioctahedral mica, are perpendicular to the cleavage, whereas those in muscovite, a dioctahedral mica, are obliquely oriented.

The hydroxyl ions in phlogopite absorb a higher frequency (3700 Cm^{-1}) infrared than those in muscovite (3600 Cm^{-1}). Biotite and iron-rich phlogopite generally show absorption at two frequencies, which indicates both trioctahedral and dioctahedral configurations. The inclined hydroxyl ions in dioctahedral mica place the potassium ions in a more negative environment than the perpendicular hydroxyl ions in trioctahedral mica. The more negative environment binds the potassium ions more securely in the lattice.

CONTENTS

TEXT

	Page
Introduction	449
Acknowledgments	450
Mica alteration and potassium fixation	450
Infrared investigation	451
Potassium fixation and hydroxyl orientation	453
Biotite and synthetic phlogopite	453
Conclusions	455
References cited	455

ILLUSTRATIONS

Figure	Page
1. X-ray diffractometer patterns of three specimens from the Wind River Mountains, Wyoming	450
2. Diagrammatic illustration of the interaction of an infrared beam with hydroxyl ions in two orientations	451
3. Infrared absorption spectra of phlogopite from Bedford, Ontario	452
4. Infrared absorption spectra of muscovite from Branchville, Connecticut	452
5. Infrared absorption spectra of biotite from Madoc, Ontario	453

Plate	Facing page
1. Atomic models of phlogopite and muscovite with the silica and alumina tetrahedra removed	450

TABLES

Table	Page
1. Hydroxyl absorptions for 15 mica specimens	454

Introduction

Laboratory and field observations indicate that trioctahedral micas alter more readily than dioctahedral micas. They characteristically alter to vermiculite and chlorite by the loss of potassium ions and the acquisition of hydrated magnesium, aluminum, and iron ions in the intersilicate or exchange position.

Fifteen specimens of mica from the Columbia University mineralogical collection were immersed in molar magnesium chloride at 100°C. for 24 hours. These specimens were then examined by X-ray diffraction for the presence of vermiculite. Of the four muscovite specimens none showed any indication of alteration. All five phlogopite specimens and all five biotite specimens showed partial alteration to vermiculite. The X-ray patterns for these showed both the 10Å reflection for mica and the 14Å reflection characteristic of vermiculite. These ion-exchange procedures were patterned after similar experiments conducted by Barshad (1948).

In the field many rocks contain both altered biotite and unaltered muscovite, in many cases

only inches apart. At the northwest end of the Wind River Mountains in Wyoming many pegmatite dikes cut the gneiss in the crystalline core of the range. Both muscovite and biotite

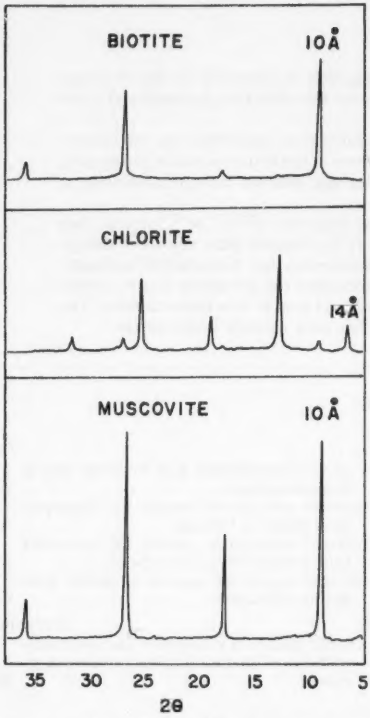

FIGURE 1.—X-RAY DIFFRACTOMETER PATTERNS OF THREE SPECIMENS FROM THE WIND RIVER MOUNTAINS, WYOMING

Biotite from an unsheared pegmatite dike. Chlorite altered from biotite in a sheared pegmatite dike. Unaltered muscovite from the same sheared pegmatite dike.

in most of these pegmatite dikes are unaltered and give diffraction patterns showing 10Å mica reflections. Some pegmatites in the region have been highly sheared by nearby Laramide faults. The biotite in these sheared pegmatites has been altered to chlorite, whereas the muscovite is still fresh (Fig. 1). The shearing apparently permitted access for solutions, whether supergene or hypogene, to come into contact with the micas and effect an alteration of the biotite to chlorite.

The mechanism involved in the alteration of mica to vermiculite or chlorite is essentially ion exchange. The potassium ions in the intersilicate position are replaced by hydrated (H_2O in vermiculite, OH^- in chlorite) magnesium, iron, or aluminum ions. These hydrated ions are larger than the potassium ions and therefore produce a structure that has a larger basal spacing.

ACKNOWLEDGMENTS

The laboratory work reported in this paper was conducted in the mineralogical laboratory at Columbia University under the supervision and encouragement of Prof. Paul F. Kerr. The work was financed in part by means of a grant from The Geological Society of America. The author owes a debt of gratitude to Mr. Theron Wasson of the Pure Oil Company. His knowledge of the Wind River Mountains was invaluable. The author is also very grateful for the assistance and advice given generously by the other members of the mineralogical laboratory at Columbia University.

MICA ALTERATION AND POTASSIUM FIXATION

In micas susceptibility to alteration is a function of potassium fixation. In a mica that resists alteration the potassium ions are more tightly bound than they are in a mica that readily alters. One factor generally accepted as having an important influence on the binding of the potassium ions is the amount of negative charge originating in the silicate layers because of substitution in the tetrahedral and octahedral positions. If this charge is low, then there are fewer potassium ions than there are positions in the intersilicate layer. This gives rise to a greater mobility of potassium ions and hence a

PLATE 1.—ATOMIC MODELS OF PHLOGOPITE AND MUSCOVITE WITH THE SILICA AND ALUMINA TETRAHEDRA REMOVED

FIGURE 1.—Phlogopite model illustrating the orientation of hydroxyl ions perpendicular to the octahedral layer

FIGURE 2.—Muscovite model illustrating the orientation of hydroxyl ions inclined to the octahedral layer

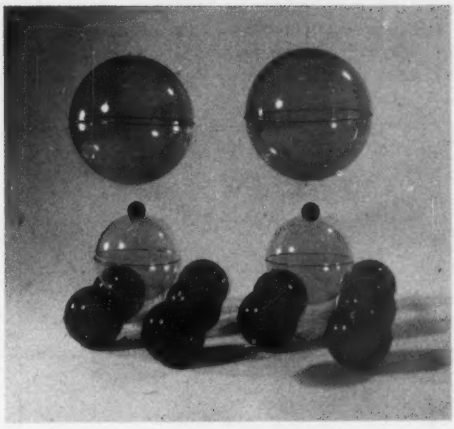

Potassium +1

Hydrogen +1

Oxygen —2

Magnesium +2

FIGURE 1

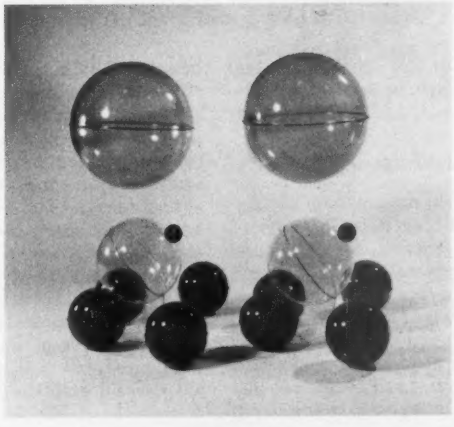

Potassium +1

Hydrogen +1

Ogygen —2

Aluminum +3

FIGURE 2

ATOMIC MODELS OF PHLOGOPITE AND MUSCOVITE WITH THE SILICA AND ALUMINA TETRAHEDRA REMOVED

greater susceptibility to alteration. This mechanism is probably responsible for the variable susceptibility observed in the phlogopites and biotites, but it does not account for the fact that muscovites resist alteration altogether.

repelled away from them. Since the distribution of charge over the three magnesium ions is uniform, the hydroxyl dipoles should be perpendicular to the octahedral layer. The octahedral layer parallels the cleavage; therefore, the hydroxyl ions in phlogopite should be oriented with their dipoles perpendicular to the cleavage.

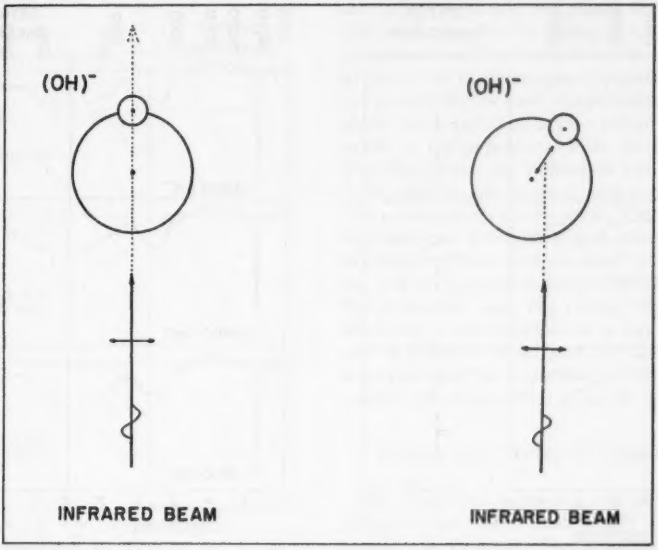

FIGURE 2.—DIAGRAMMATIC ILLUSTRATION OF THE INTERACTION OF AN INFRARED BEAM WITH HYDROXYL IONS IN TWO ORIENTATIONS

This problem resolves itself into the question of the basic structural differences between the dioctahedral and trioctahedral micas and what effect these differences have on potassium fixation. The writer suggests that the orientation of the hydroxyl ions in the mica structure is the key mechanism. In order to examine the hydroxyl ions and their relationship to the octahedral layer and the potassium ions, it is advantageous to strip away the silica and alumina tetrahedra. Figure 1 of Plate 1 illustrates the octahedral layer, the hydroxyl ions, and the potassium ions of phlogopite after the silica and alumina tetrahedra have been removed. Figure 2 of Plate 1 shows the same for muscovite.

In the phlogopite structure each hydroxyl ion rests on three magnesium ions and under one potassium ion. Each of the magnesium ions is relatively small and has a plus two charge. Thus the negative or oxygen end of the hydroxyl ion should be attracted toward them, and the positive or hydrogen end should be

INFRARED INVESTIGATION

If the configuration proposed for phlogopite is correct, then its validity can be tested by means of the infrared spectrophotometer. Figure 2 shows the way in which infrared radiation interacts with a hydroxyl ion. When the dipole is oriented parallel to the direction of propagation of the infrared beam, no absorption takes place. If the hydroxyl ion is oriented so that the dipole has a component lying across the direction of propagation or parallel to the direction of vibration of the infrared, then absorption takes place when the frequency of vibration corresponds to the resonance frequency of the hydrogen-oxygen bond. Thus, if the orientation of the hydroxyl dipoles in phlogopite is perpendicular to the cleavage as suggested, there should be no absorption of the

infrared by hydroxyl ions if the phlogopite is oriented with its cleavage perpendicular to the infrared beam.

The first spectrophotometer chart in Figure 3 shows this to be the case. When the phlogopite flake is inclined with reference to the beam, absorption by the hydroxyl ions appears at 3700 Cm^{-1} and becomes more intense as the inclination increases. Thus the infrared spectrophotometer confirms the proposed orientation for the hydroxyl ions in the phlogopite.

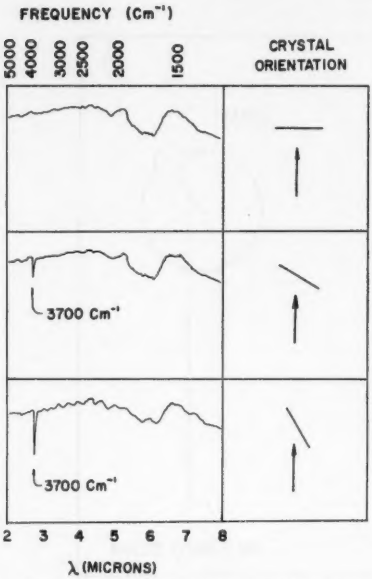

FIGURE 3.—INFRARED ABSORPTION SPECTRA OF PHLOGOPITE FROM BEDFORD, ONTARIO

A flake 0.02 mm thick was run in the three orientations indicated at the right.

Serratosa and Bradley (1958) arrived at the same conclusions using an experimental procedure very similar to the author's and obtaining similar data.

The muscovite structure is pictured in Figure 2 of Plate 1. In muscovite the octahedral layer consists of aluminum ions. Since the aluminum ions are trivalent, they occupy only two-thirds of the available octahedral positions. This results in holes in the octahedral layer. Each hydroxyl ion sits on two cations and a hole. The hydroxyl ions should not be perpendicular to the octahedral layer in this situation as in the phlogopite. They should be oriented with the oxygen end extending toward the aluminum ions and the hydrogen end extending away from the aluminum ions.

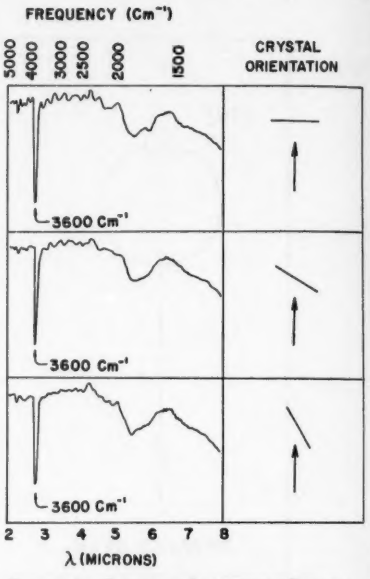

FIGURE 4.—INFRARED ABSORPTION SPECTRA OF MUSCOVITE FROM BRANCHVILLE, CONNECTICUT

A flake 0.02 mm thick was run in the three orientations indicated at the right.

If this is the true configuration, then a beam of infrared passing through a flake of muscovite perpendicular to its cleavage should reveal absorption by the hydroxyl ions. The frequency of the absorption should be lower, since the aluminum ions carry a greater charge than the magnesium ions. This greater charge has the effect of pulling the oxygen closer to the aluminum and pushing the hydrogen farther away, thereby lengthening the hydrogen-oxygen bond and lowering the response frequency.

The spectrophotometer charts given in Figure 4 indicate strong absorption by the hydroxyl ions in spite of the orientation of the muscovite flake in the infrared beam. The frequency of absorption by these hydroxyl ions is lower as predicted. One might ask why there is not some orientation of the muscovite flake which permits no absorption by the hydroxyl ions. The muscovite specimens examined by

Tsuboi (1950), by Serratosa and Bradley (1958), and by the author have all been 2M polytypes. In the 2M structure the dipoles within one layer may be parallel to each other

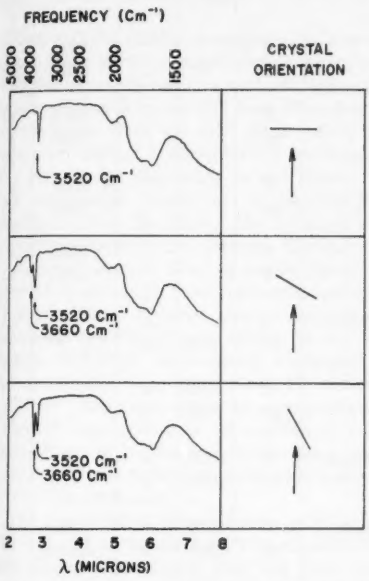

FIGURE 5.—INFRARED ABSORPTION SPECTRA OF BIOTITE FROM MADOC, ONTARIO

A flake 0.07 mm thick was run in the three orientations indicated at the right.

and probably are, but the dipoles in adjacent layers cannot be parallel. Laue symmetry demands that if orientations in a given layer are parallel, orientations in alternating layers must be disposed alternately symmetrically about the (010) plane. The only polytype that might be expected to have all its hydroxyl dipoles parallel is 1M. This has not yet been tested because of the difficulty of obtaining megascopic specimens of a 1M dioctahedral mica.

Tsuboi (1950) detected variations in absorption with changes in the orientation of a flake of muscovite. He concluded that the hydroxyl ions in the muscovite are oriented obliquely to the cleavage and calculated the angles at which they are oriented. The variations that he observed are small, however, compared to the variations observed in phlogopite and biotite.

POTASSIUM FIXATION AND HYDROXYL ORIENTATION

The effect of the hydroxyl orientation on the binding of the potassium ions is illustrated in Plate 1. In the phlogopite structure the orientation of the hydroxyl ion places the hydrogen end or the proton in juxtaposition with the potassium ion. The inclined orientation of the hydroxyl ion in the muscovite structure places the proton farther from the potassium ion and places the negative or oxygen end of the dipole closer to the potassium. Thus the phlogopite structure places the potassium ion in a relatively positive environment with a proton just above and a proton just below. The potassium in muscovite, however, is in a more negative environment because the inclined orientation of the hydroxyl ion places the proton farther from the potassium and the oxygen closer. This difference in the environment of the potassium ions is believed to account for the fact that most trioctahedral micas alter by ion exchange, whereas the dioctahedral micas do not.

BIOTITE AND SYNTHETIC PHLOGOPITE

The biotite specimens and two of the darker phlogopite specimens show a pair of hydroxyl absorptions (Fig. 5). The absorption at the higher frequency is sensitive to the orientation of the specimens, and the lower frequency absorption is not. The higher frequency absorption is attributed to trioctahedral configuration as in magnesian phlogopite. The lower frequency absorption is attributed to dioctahedral configuration as in muscovite. The octahedral layer of biotite and the darker, iron-bearing phlogopite is occupied by magnesium, ferrous, and ferric ions. Many specimens of biotite from pegmatites contain appreciable amounts of ferric iron and are more properly designated lepidomelane. The excess charge resulting from the presence of the ferric ions is balanced by holes in the octahedral layer, just as holes in the octahedral layer of muscovite balance the plus three charge of the aluminum. In biotite, therefore, holes occur throughout the octahedral layer. Some hydroxyl ions must sit on two cations and a hole as in muscovite, and others must sit on three cations as in magnesian phlogopite, thus producing the two frequencies.

In Table 1 the absorption frequencies show a shift downward as the biotite becomes progressively darker or more iron rich. This may

TABLE 1.—HYDROXYL ABSORPTIONS FOR 15 MICA SPECIMENS

Specimen	Color	Sample orientation	Frequency Cm^{-1}	Absorption	Frequency Cm^{-1}	Absorption
Muscovite						
Branchville, Connecticut	Colorless	0°	..	..	3600	s
		60°	..	..	3600	s
Muscovite						
Ural Mountains, Russia	Colorless	0°	..	..	3600	s
		60°	..	..	3600	s
Muscovite						
Pennsbury, Pennsylvania	Colorless	0°	..	..	3600	s
		60°	..	..	3600	s
Muscovite						
Chester County, Pennsylvania	Colorless	0°	..	..	3600	s
		60°	..	..	3600	s
Phlogopite						
Bedford, Ontario	Very light brown	0°	..	..	..	..
		60°	3700	m	..	..
Phlogopite						
Lewis County, New York	Colorless	0°	3700	w	..	..
		60°	3700	m	..	..
Phlogopite						
Gouveneur, New York	Very light brown	0°	3700	w	..	..
		60°	3700	m	..	..
Phlogopite						
Norwich, New York	Medium brown	0°	3700	w	3600	w
		60°	3700	m	masked	
Phlogopite						
St. Lawrence County, New York	Medium brown	0°	3700	w	3600	w
		60°	3700	m	masked	
Biotite						
Keene Valley, New York	Medium brown	0°	..	..	3600	vw
		60°	3700	m	masked	
Biotite						
Orange County, New York	Dark brown	0°	3680	w	3600	m
		60°	3680	m	3600	m
Biotite						
Munroe, New York	Medium green	0°	3690	w	masked	
		60°	3680	m	masked	
Biotite						
Arendal, Norway	Dark green	0°	3680	vw	3540	w
		60°	3680	m	3540	w
Biotite						
Madoc, Ontario	Very dark brown	0°	3660	vw	3520	m
		60°	3660	m	3520	m
Synthetic phlogopite (fluorine replaces hydroxyl)	Colorless	0°	..	..	..	..
		60°	..	..	..	..

result from a strong bonding of hydroxyl ions to iron ions, although the details of this have not yet been worked out.

Synthetic phlogopite in which fluorine ions replace hydroxyl ions shows no absorption in this region. Serratosa and Bradley (1958) made

this same observation. The synthetic phlogopite undergoes no alteration to vermiculite when subjected to the magnesium chloride treatment.

Conclusions

Hydroxyl orientation is suggested as a factor influencing a mica's susceptibility to alteration. If all the hydroxyl ions in a mica are inclined to its cleavage as in muscovite, then alteration by ion exchange does not take place unless the potassium content is exceptionally low because of a low charge originating in the tetrahedral and octahedral layers as in dioctahedral montmorillonite. If some of the hydroxyl ions are perpendicular to the cleavage, this seems to be sufficient in most cases to permit the initiation of ion exchange. Once potassium ions held by perpendicular hydroxyl ions are removed the remaining potassium ions submit to ion exchange. In biotite, for instance, where part of the potassium ions are bound by inclined hydroxyl ions and part by perpendicular hydroxyl ions alteration takes place in most cases. Even in biotite and phlogopite a very high content of potassium may inhibit alteration by ion exchange.

The treatment of this subject is qualitative. The infrared spectrophotometer is capable of a high degree of accuracy and has been used extensively by organic chemists for quantitative investigations. Therefore, useful studies of the micas by quantitative treatment should be possible. The infrared data used in conjunction with chemical, spectrographic, and X-ray structure analyses should serve as a powerful method for studying substitution and ion configurations in micas and other sheet silicates. For instance, it should be possible to obtain accurate values for the ratio of ferrous to ferric iron. This is difficult to achieve by present methods of analysis. Such data might yield valuable information about the conditions obtaining when the mica formed.

References Cited

Barshad, I., 1948, Vermiculite and its relation to biotite as revealed by base exchange reactions, X-ray analysis, differential thermal curves and water content: Am. Mineralogist, v. 33, p. 655–678

Serratosa, J. M., and Bradley, W. F., 1958, Determination of the orientation of OH bond axes in layer silicates by infrared absorption: Jour. Phys. Chemistry, v. 62, p. 1164–1167

Tsuboi, Masamichi, 1950, On the positions of the hydrogen atoms in the crystal structure of muscovite as revealed by the infra-red absorption study: Chem. Soc. Japan Bull., v. 23, p. 83–88

Dept. of Geology, Columbia University, New York 27, N. Y.

Manuscript Received by the Secretary of the Society, March 16, 1959

BULLETIN OF THE GEOLOGICAL SOCIETY OF AMERICA
VOL. 71, PP. 457–482, 10 FIGS., 4 PLS. APRIL 1960

AGUA BLANCA FAULT—A MAJOR TRANSVERSE STRUCTURE OF NORTHERN BAJA CALIFORNIA, MEXICO

BY CLARENCE R. ALLEN, LEON T. SILVER, AND FRANCIS G. STEHLI

ABSTRACT

Agua Blanca fault is a major right-handed strike-slip fault at least 80 miles in length that cuts transversely across the peninsula of Baja California about 70 miles south of the international border. Its trend is anomalous in being more nearly parallel to the Transverse Ranges of southern California than to the San Andres fault system that elsewhere dominates the tectonic grain of the peninsula. Geographic features delineating the fault trace are, from east to west: Paso San Matías, Valle de La Trinidad, Cañon de Dolores, Valle de Agua Blanca, Valle de Santo Tomás, Bahía Soledad (south branch of fault), Punta Banda (north branch). Farther west, both branches of the fault control submarine topography, and possibly the fault system is continuous with the northwest-trending San Clemente fault off the southern California coast.

Physiographic expression of the Agua Blanca fault is remarkably similar to that of the San Andreas. Typical features are Recent scarps, offset streams, shutterridges, fault sags and saddles, side-hill ridges, and fault-controlled valleys. Most of these features are particularly well exhibited in Valle de Agua Blanca, which is designated as the type locality.

Rocks cut by the fault are mainly Cretaceous plutonic rocks of the southern California batholith and Lower Cretaceous (Albian) metavolcanic rocks. Along the Pacific Coast, the fault cuts Upper Cretaceous (Maestrichtian) post-batholithic sedimentary rocks that are otherwise surprisingly little deformed as compared to rocks of similar age in most of California.

Agua Blanca fault shows a history of right-lateral displacement throughout its length: Recent stream offsets occur from Valle de La Trinidad nearly to the Pacific Ocean; distinctive Quaternary(?) fan gravels in Valle de Agua Blanca are offset laterally 3 miles from their most likely source area across the fault; in the same area, a fault slice of distinctive antiperthitic granodiorite is best explained by 7 miles of lateral displacement, and a nearby slice of quartz diorite may indicate displacement as great as 14 miles. In general, evidence of both Recent activity and amount of total displacement appear to increase westward. The fault coincides in gross aspect with a broad east-west zone of seismic activity in a region elsewhere characterized by relative quiescence, but no large historical earthquakes can be positively correlated with this fault.

Despite its orientation athwart the regional tectonic grain, Agua Blanca fault does not appear to represent a deep-seated structural feature analogous to those of the Transverse Ranges. Instead, it is probably one of several paths by which the San Andreas fault tends to break around the "knot" caused by the great bend of the San Andreas in southern California.

CONTENTS

TEXT

	Page
Introduction	458
Regional geology	460
General features	460
Pre-batholithic rocks	460
Batholithic rocks	460
Post-batholithic rocks	461
Structure	461
Punta Banda-Santo Tomás sector	463
General features	463
Northern branch	463
Southern branch	465
Agua Blanca sector	465
Valle de Santo Tomás	465
Valle de Agua Blanca	467
Fault displacement in Valle de Agua Blanca	467
General approach	467
Pre-batholithic rocks	469
Las Cuevas granodiorite	469
Agua Blanca granodiorite	470
Other plutonic rocks	470
Lateral displacement of alluvial fans	471
Possible bedrock displacements	472

Page
Cañon de Dolores sector 472
Valle de La Trinidad sector 474
Offshore sector 476
Summary of evidence relating to displacement 478
Seismicity 479
Regional tectonic relationships 480
References cited 481

ILLUSTRATIONS

Figure Page
1. Simplified fault map of southern California and northern Baja California 459
2. Index map 459
3. Sketch map of Punta Banda-Santo Tomás sector 462
4. Sketch map of drainage patterns along fault 464
5. Sketch map of Agua Blanca sector 466
6. Geologic map of Agua Blanca fault at type locality 468
7. Sketch map of Cañon de Dolores sector 473
8. Sketch map of Valle de La Trinidad sector 475
9. Map of submarine topography off Southern California and Northern Baja California 477
10. Map of earthquake epicenters in northern Baja California 479

Plate Following page
1. Physiographic features of faulting 470
2. Aerial views of fault toward its western end 470
3. Oblique aerial view of Rancho Agua Blanca 470
4. Aerial views of fault toward its eastern end 470

TABLE

Table Page
1. Percentages of rock types in boulders of alluvial fans 472

Introduction

Continuing widespread interest in the San Andreas fault has stimulated this study of a major structural break that assuredly must be related to the San Andreas system. Previous studies have provided much detailed information on the fault pattern of southern California (Fig. 1); the same tectonic environment extends into adjacent Mexico but has received little study there. The discovery in Baja California of a major structural break—the Agua Blanca fault—demonstrates the importance of extending structural studies southward. Added impetus was given this study by the anomalous trend of the Agua Blanca fault, which, although related to the San Andreas system, is markedly transverse to the structural grain of Baja California. The same anomalous trend characterizes the nearby Transverse Ranges of southern California, and its tectonic significance there has been the subject of much speculation.

The existence of a throughgoing fault extending across northern Baja California was first suggested by geologic reconnaissance in connection with our studies of the Cretaceous rocks of Baja California (Silver, Stehli, and Allen, 1956; Silver, Stehli, and Allen, in press). Several investigators had pointed out that Paso San Matías and Valle de La Trinidad (Fig. 2) represent the first major topographic break in the Peninsular Ranges south of San Gorgonio Pass, about 200 miles to the north. The anomalous east-west trend of Valle de La Trinidad and the colinear Cañon de Dolores (Fig. 2) indicate some sort of structural control transverse to the regional tectonic grain. The only previous suggestion of faulting along any part of this line, however, seems to have been made by Böse and Wittich (1913, p. 326, 459; repeated by Beal, 1948, p. 102), who attributed to faulting the hot springs, linear topography, and submarine escarpment along the north side of Punta Banda (Fig. 3). Beal (1948, p. 102) also postulated that many of the summit valleys, including Valle de La Trinidad, possibly owed their origin to faulting. Aerial reconnaissance in 1956 by the authors and John Shelton confirmed the existence of a throughgoing break from Paso Matías to Punta Banda and first called attention to stream offsets and other features typical of the San Andreas and associated active strike-slip faults of California. In subsequent field work the authors have gone to nearly every part of the fault and have traversed most of its length on foot.

This study was supported by generous grants from the Penrose Bequest of The Geological Society of America (Grant 733-56) and from the California Institute of Technology. Aerial-reconnaissance examinations were made with the help of John Shelton, Gifford Ewing, and Paul MacCready. C. F. Richter and Pierre St. Amand assisted in compiling the seismic data. We appreciate the co-operation of the Institute of Geology of the University of Mexico, Ing. G. P. Salas, Director. Those who have helped us in the field include A. E. J. Engel, W. B. Kamb,

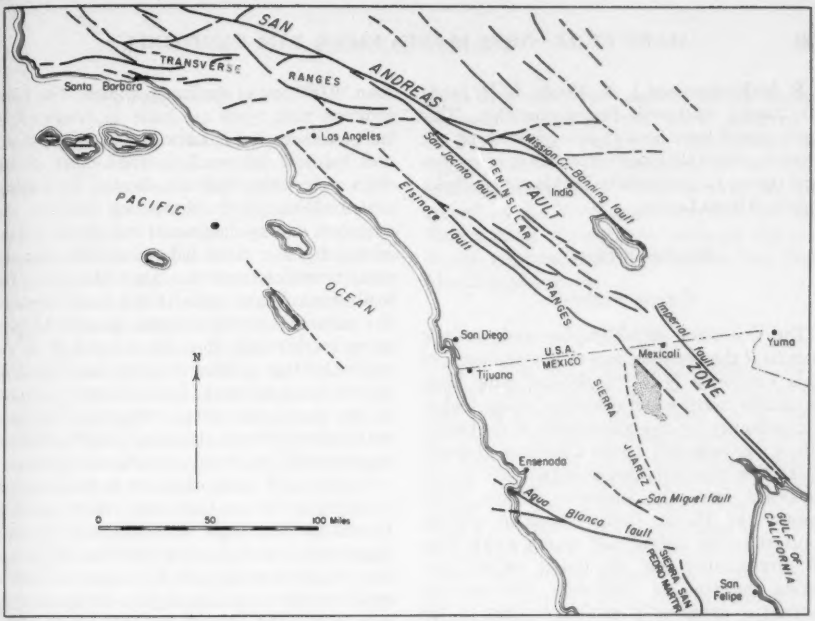

FIGURE 1.—SIMPLIFIED FAULT MAP OF SOUTHERN CALIFORNIA AND NORTHERN BAJA CALIFORNIA
Shows relation of Agua Blanca fault (bottom) to San Andreas and associated fault systms. Most faults shown are "active".

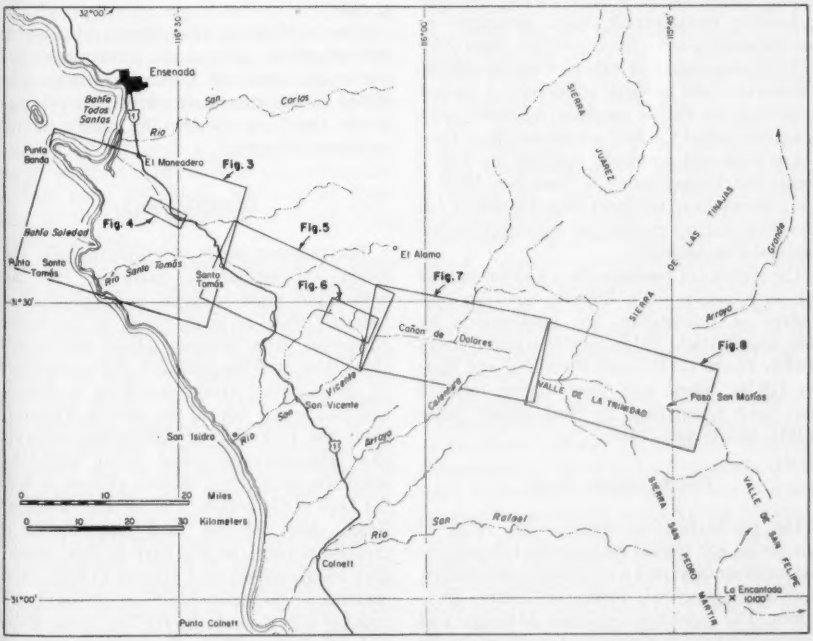

FIGURE 2.—INDEX MAP
Insets show areas covered by more detailed sketch maps along Agua Blanca fault zone.

C. R. McKinney, and J. A. Noble. R. H. Jahns has kindly criticized the manuscript. This study would have been impossible without the generous hospitality and assistance of numerous local residents, particularly Sr. Manuel Collado, and Sr. Arturo Lerma.

Regional Geology

General Features

The dominant physiographic and geologic feature of the northern part of the peninsula of Baja California is its "backbone"—the high, essentially north-south mountain range underlain primarily by crystalline rocks of the batholith of southern and Lower California (Larsen, 1948). The relatively gentle slopes that extend westward from the summits of this range toward the Pacific Ocean stand in marked contrast to the rugged east slopes, which drop off precipitously into the desert valleys bordering the Gulf of California. The over-all pattern is remarkably similar to that of the Sierra Nevada of California, as was first pointed out by Lindgren (1888).

The foothills between the high ranges and the Pacific Coast are underlain mainly by pre-batholithic metamorphic rocks, although numerous small plutons have intruded these older rocks throughout their extent. Post-batholithic sedimentary and volcanic rocks form a narrow strip along the Pacific coast and a broader strip along the Gulf of California coast and have been left as erosional remnants capping the higher Peninsular Ranges north of Paso San Matías. Thus the rocks of northern Baja California fall into three distinct groups: pre-batholith, batholith, and post-batholith.

The geology of northern Baja California is as yet surprisingly little known, but the best sources of information are publications by Böse and Wittich (1913), Santillán and Barrera (1930), Flores (1931), and Woodford and Harriss (1938). These and other sources recently have been summarized by Beal (1948), Jahns (1954), and Wisser (1954).

Pre-Batholithic Rocks

The pre-batholithic metamorphic rocks of this region are typical eugeosyclinal deposits—metasedimentary rocks of volcanic derivation, flows and pyroclastic rocks, and sparse limestones. The repetitious volcanic lithology and unknown structure preclude accurate estimates of thickness at this time, but certainly more than 10,000 feet of section is exposed. The most common rock types are basic to intermediate tuffs and breccias, basaltic and andesitic flows, and volcanic graywackes. That most of the units were water laid is indicated by sorting, cross-bedding, and channeling within the sequence, and by the presence of marine fossils. Metamorphism varies from negligible near the coast to intense near the larger plutons of the main sierra. Sparse rudistid limestones crop out in a persistent zone that forms the one through-going marker unit thus far recognized in the pre-batholithic section. The regional strike of the metamorphic rocks is northwest, and most of the rocks are steeply dipping. The pre-batholithic section is described in greater detail elsewhere (Silver, Stehli, and Allen, in press).

Fossils have been collected from numerous localities in the pre-batholithic rocks south of Ensenada. We concur with Allison (1955) that these rocks are of Early or Middle Albian age (late Early Cretaceous). No older rocks have been identified in this region, although they may well exist. North of the international border, Triassic fossils have been reported from pre-batholithic rocks of the northern Santa Ana Mountains (cited in Larsen, 1948, p. 18).

West of Valle de Agua Blanca, rocks of the pre-batholithic section are predominant both north and south of the Agua Blanca fault, except in the immediate vicinity of the coast, where they are overlain by post-batholithic sedimentary rocks.

Batholithic Rocks

The plutonic rocks of northern Baja California are similar to parts of the same batholithic mass mapped and described by Larsen (1948) in areas north of the border. Numerous large plutons adjoin one another along the axis of the peninsula but are separated by metamorphic screens increasing in thickness and coalescence toward the west until along the coast the rocks are predominantly metamorphic. The eastward extent of the batholith is unknown, although it extends at least as far as the Gulf of California. The most detailed published study of the field relations of the crystalline rocks in any part of this region is that by Woodford and Harriss (1938), which pertains to the batholithic and pre-batholithic rocks of a part of the Sierra San Pedro Mártir and adjacent foothills 30 miles south of the Agua Blanca fault (Fig. 2).

Post-Batholithic Rocks

The only known post-batholithic rocks exposed in the area of Figure 2 are: (1) Upper Cretaceous and younger marine sedimentary rocks that crop out in a narrow strip along the Pacific coast; (2) Upper Cenozoic volcanic and associated nonmarine sedimentary rocks that form erosional remnants capping the Sierra Juárez and the coastal hills north of Ensenada; and (3) Quaternary alluvium and fan gravels.

The Upper Cretaceous rocks of this region are here assigned to the Rosario formation of Beal (1948, p. 40) because of their similar lithology, implied sedimentary environment, and fossils, as well as their near continuity with beds at the type area 100 miles to the south. Sedimentary features indicate that the shore line of the Late Cretaceous sea was very nearly the same as that of today; indeed, many present embayments between headlands of resistant Albian volcanic rocks were also embayments in Late Cretaceous time, as was pointed out by Allison (1955, p. 403). The Rosario formation comprises a variety of clastic types ranging from extremely coarse conglomerate to shale; siltstone is predominant. These rocks have been left little deformed except where they are cut by both the northern and southern branches of the Agua Blanca fault (Fig. 3). The Rosario in the area of Figure 2 have been assigned a Maestrichtian age by Durham and Kirk (1950) and by Oakes (M. S. Thesis, Univ. Calif., Berkeley, 1954), and a Campanian age by Bandy (1952). On the basis of numerous independent fossil collections, we consider these rocks to be Late Campanian or Early Maestrichtian in age.

The southern part of the Sierra Juárez, north of the Agua Blanca fault, is capped by dissected relatively flat-lying volcanic flows and associated nonmarine sedimentary rocks. These rocks have been described locally by Shor and Roberts (1958, p. 111) and are similar to the more fully studied rocks north of the border near Jacumba (Brooks and Roberts, 1954). In both areas the flows are truncated by the precipitous eastern escarpment of the range and clearly must have been extruded under conditions of lower relief than exist today. The age of these rocks is unknown, but they are similar in lithology and degree of deformation to the very widespread flows of the Comondú formation of the middle part of the peninsula that have been dated as middle(?) or late Miocene (Wilson and Rocha, 1955). On the other hand, Quarternary volcanic rocks are known from areas both north and south of the border, and sporadic volcanism may have occurred in northern Baja California throughout late Cenozoic time. It is interesting to note that erosional remnants of volcanic rocks are wide spread on the Sierra Juárez north of the Agua Blanca fault, whereas such rocks are unknown on the adjacent part of the Sierra San Pedro Mártir to the south.

Structure

Even with our limited knowledge of northwestern Baja California it seems safe to say that this terrane is less broken up by major faults than are the adjoining northern Peninsular Ranges or the Transverse Ranges of California. The almost undeformed state of Upper Cretaceous beds along much of the northern Baja California coast is surprising to anyone familiar with the intense deformation of both these and younger deposits only 150 miles to the north. The San Diego area evidently shares this relative stability with Baja California, as has recently been argued by Carter (1957). These conclusions are further supported by the recorded seismic history of the region. The major faults in northern Baja California west of the San Andreas zone appear to be (1) those controlling the Sierra Juárez and Sierra San Pedro Mártir, (2) the San Miguel fault, and (3) the Agua Blanca fault (Fig. 1).

The north-northwest trend of the Sierra Juárez and Sierra San Pedro Mártir is determined predominantly by faulting on the east, although this trend lies at a distinct angle to that of the San Andreas fault zone (Fig. 1). The linear and continuous east face of the Sierra Juárez was first recognized as a fault scarp by Lindgren (1888). Recent scarps are not abundant at its base, but numerous stepped-down blocks of volcanic rocks testify to fault control along at least the southern end of the escarpment.

The eastern escarpment of the Sierra San Pedro Mártir is even more impressive than that of the Sierra Juárez; the 8000-foot drop from the summit of Cerro de La Encantada (10,100 feet) to the valley floor takes place in a horizontal distance of only about 5 miles. Numerous Recent scarps delimit the southern part of the range and probably occur at the foot of the northern part as well. Beal (1948, Pl. 1) postulated that the fault zones bordering the Sierra San Pedro Mártir and the Sierra Juárez may be one and the same. If so, vertical displacement in the intervening area has been neither

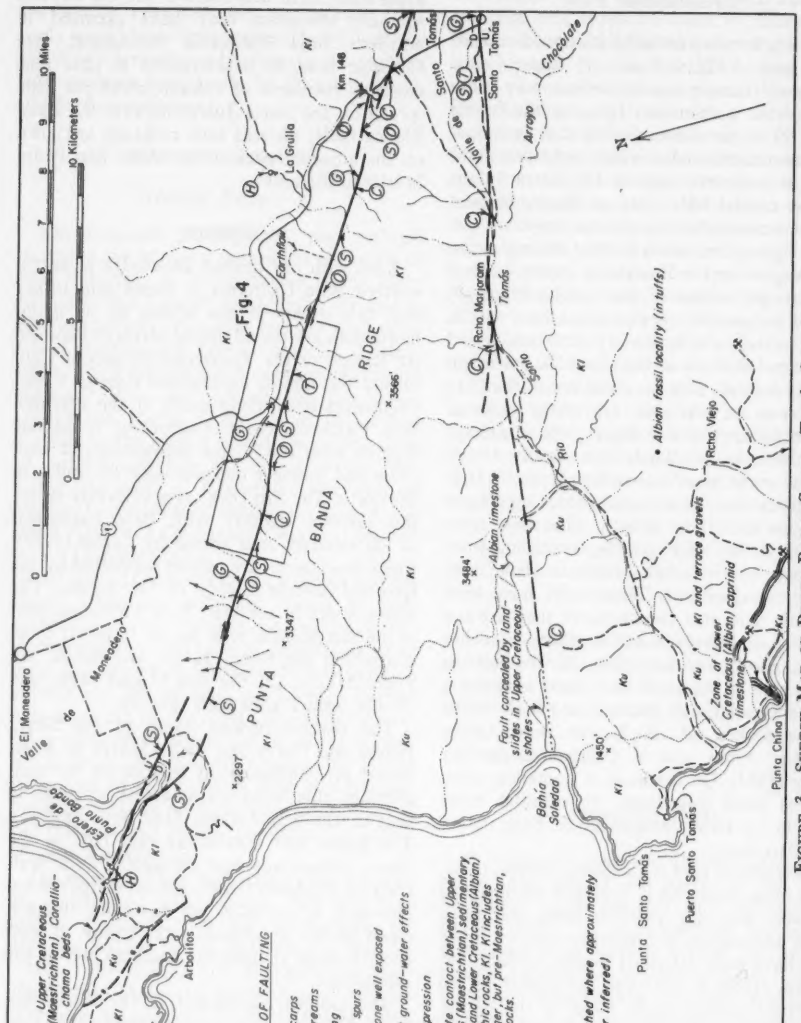

FIGURE 3.—SKETCH MAP OF PUNTA BANDA-SANTOS TOMÁS SECTOR
Inset shows location of Figure 4.

as great nor as recent as in areas farther north and south, and certainly the two ranges have not behaved as a single block. The gross structure of both sierras is that of westward-tilted fault blocks, but the structure of the Sierra San Pedro Mártir is complicated by a fault zone on the west (Woodford and Harriss, 1938, p. 1325–1327), so that the summit area is a westward-tilted horst.

The San Miguel fault was named and first described by Shor and Roberts (1958) on the basis of a field study following the earthquakes of February 1956. Ground displacement associated with these earthquakes occurred along about 12 miles of the fault trace (the solid-line segment on Fig. 1) and was uniformly right-lateral and relatively up on the northeast. Shor and Roberts (1958, p. 106) point out that the San Miguel fault zone certainly extends northwest beyond the segment broken in 1956 and probably controls the Valle de San Rafael, which Lindgren (1888) earlier attributed to faulting; possibly the fault zone continues still farther northwest. Southeast from the 1956 break, evidence for throughgoing faulting is less convincing, and certainly the volcanic rocks that cap the range in this area have not been greatly displaced. In general, the thickness of the crushed zone along the San Miguel fault, the topographic expression of the fault, and the contrast of rock types on the two sides of the fault are not nearly so impressive and suggestive of major displacement as are similar features along the Agua Blanca fault.

FIGURE 3.—SKETCH MAP OF PUNTA BANDA-SANTOS TOMÁS SECTOR
Inset shows location of Figure 4.

PUNTA BANDA-SANTO TOMÁS SECTOR

General Features

The western end of the Agua Blanca fault is split into two diverging traces (Fig. 3), here referred to as the northern and southern branches. It is not clear which of these, if either, should be considered the "parent" fault; impressive crushed zones are associated with both, and both appear to control submarine topography off the coast. Recent displacements, on the other hand, have occurred primarily along the northern branch, so that its trace is more obvious in the field. The various types of field evidence indicative of faulting in the Punta Banda-Santos Tomás sector are shown in Figure 3. Throughout this paper, only those features deserving of special mention are discussed in the text, inasmuch as most of our field observations are summarized in the sketch maps.

Northern Branch

The northern branch of the Agua Blanca fault delimits the north escarpment of Punta Banda Ridge (Pl. 1); indeed it is responsible for the gross coastal outline of Punta Banda itself, as was suggested by Böse and Wittich (1913, p. 325–326). The fault zone can be followed continuously through most of this sector but is marked only by isolated Recent scarps in the alluviated area near Estero de Punta Banda (Fig. 3). The continuity of the fault into the ocean is indicated by hot springs at the very edge of the bay, where clouds of steam rising from the beach are particularly spectacular at low tide during periods of cold weather.

Physiographic evidence for Recent right-lateral displacement is perhaps more abundant along this segment of the fault than anywhere else. Stream courses show consistent right-lateral offsets amounting to as much as 900 feet, although most of the sharp offsets are 200 to 300 feet (Fig. 4; Pl. 1, fig. 1). Those shown in Figure 4 are particularly convincing because the offsets are in the "uphill" direction; that is, stream capture by erosion in the fault zone would tend to cause apparent offsets in the opposite direction, inasmuch as this is the direction of regional gradient toward the ocean. Lateral offsets of deeply dissected canyons in this area have formed particularly good examples of shutterridges (Pl. 1, fig. 1), similar to those in New Zealand (Cotton, 1957) and along the San Andreas fault in California (Buwalda, 1937). A history of Recent strike-slip displacement is also supported by numerous reversals in the direction toward which Recent scarps face. Scarps near Km 136[1] (Fig. 4) consistently face north, whereas those 4 miles farther west (Pl. 1, fig. 2) face south. Side-hill ridges and fault sags, characteristic features of the San Andreas fault (G. K. Gilbert *in* Lawson *et al.*, 1908, p. 33), are particularly well developed along the Agua Blanca fault on the north slopes of Punta Banda Ridge.

The Upper Cretaceous *Coralliochama* beds of Punta Banda (Fig. 3) have dips as great as 55°, and this tilting is an exception to the pattern of generally undeformed post-batholithic

[1] Km 136 and other similar designations indicate marker signs along Mexico Highway 1, measuring distances south from the international border.

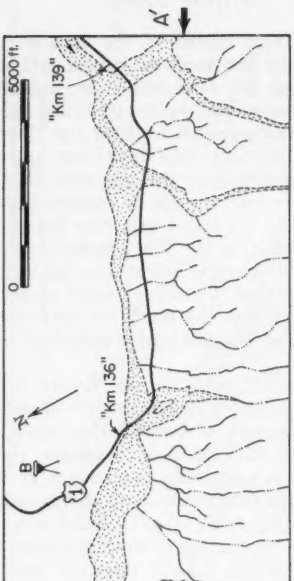

FIGURE 4.—SKETCH MAP OF DRAINAGE PATTERNS ALONG FAULT

Location is 7 miles southeast of El Maneadero (Fig. 3). The most recent movements have been along line A-A', which is also marked by fault scarps and a wide crushed zone. Photograph of Figure 1 of Plate 1, was taken from point "B".

rocks in northern Baja California. This deformation must be related to the nearby Agua Blanca fault, and the beds may lie within a fault sliver. Their contact with igneous rocks along the backbone of Punta Banda is thought to be a fault because of its linearity and the fact that bedding dips into the contact, but possibly this boundary is a depositional feature similar to others along the rugged Late Cretaceous shore line. The *Coralliochama* beds are pervasively fractured, and westward along the sea cliff they are faulted against red beds of unknown age (Walton, 1955, p. 957). Seven miles east along the Agua Blanca fault, in the area shown in Figure 2 of Plate 1, steeply dipping sandstones and conglomerates lie unconformably beneath fan gravels on the south side of the fault; these rocks also are of unknown age, but assuredly they have been faulted into their present position.

Numerous marine terraces on Punta Banda were first pointed out by Lindgren (1888, p. 170). These terraces are not obviously deformed near the fault, although the major break presumably passes north of Punta Banda, and correlative terraces have not been identified across the valley to the northeast. At least 13 distinct terraces are exposed on Punta Banda; rough barometric measurements indicate that the nick points at the heads of these terraces on the southeast slope of peak 1264 (Fig. 3) are at respective elevations of about 50, 130, 190, 310, 410, 440, 530, 690, 750, 860, 930, 1030, and 1140 feet above present sea level. Even the uppermost terrace is characterized by well-rounded pebbles of rock types foreign to the immediate area. The authors have not recognized terraces this high along the coast south of Punta Banda. The lowermost terraces of this region have yielded an abundant late Pleistocene fauna (Emerson, 1956), but little is known of the age of the older terraces; perhaps some of the highest are pre-Pleistocene.

A thick zone of pulverized rock is associated with the northern branch of the Agua Blanca fault throughout this sector, and perhaps the best exposures are in road cuts near the highway pass (a fault saddle) at Km 148. The crushed zone here is nearly a quarter of a mile wide and comprises slices of various types of altered andesitic pre-batholithic rocks. Recent activity on the fault is indicated by a linear closed depression on the crest of the ridge 1500 feet west of Km 148.

Southern Branch

In contrast to the northern branch of the Agua Blanca fault, the southern branch shows no evidence of Recent displacement for at least 10 miles inland from its intersection with the coast line at Bahía Soledad (Fig. 3). In this sector the fault has, in a general way, controlled the course of the Rio Santo Tomás, but the principal evidences of faulting are (1) a marked zone of pulverized rock, and (2) the juxtaposition of contrasting rock types. Exposures of the fault within 2 miles of the coast are lacking because of massive landsliding in the Upper Cretaceous shales.

The crushed zone along this branch of the fault is particularly well exposed in the streamcliffs half a mile west of Rancho Marjoram (Fig. 3). Several poorer exposures exist farther west, as on the trail to Bahía Soledad. Upper Cretaceous beds of the Rosario formation are offset in this coastal area, so that a left-lateral separation of 4½ miles appears on Figure 3. It is not necessary, however, that this separation be caused by strike-slip fault movement; the Late Cretaceous shore line was highly irregular, and the 3000-foot elevation of Upper Cretaceous(?) basal conglomerates on the ridge north of the fault suggests a considerable vertical component of displacement. Even if these ridge-capping conglomerates are not Upper Cretaceous, vertical displacement along the fault is indicated, inasmuch as no other post-batholithic sedimentary rocks are known at such elevations in this area.

Another clue to fault displacement in this area is the possible offset of the rudistid limestone beds of the pre-batholithic section. These distinctive rocks apparently occur in only one limited zone in the stratigraphic column, and steeply dipping beds of this unit form continuous outcrops for more than 80 miles southeast from Punta China (Fig. 3) (Silver, Stehli and Allen, in press). Although local structural complications certainly exist at Punta China, these beds would intersect the fault about 5 miles out to sea if projected northwestward with the regional trend. A thick fossiliferous limestone of similar Albian age and generally similar trend crops out north of the fault on the south flank of peak 3484 (Fig. 3) and is truncated by the fault so as to suggest a right-lateral displacement of about 11 miles. This argument, however, is only suggestive at best; we have not demonstrated conclusively that the two limestone units are correlative or that the limestones on the south are truncated by the fault. Nevertheless, these lines of evidence, when considered with the offshore submarine topography and the known relations elsewhere along the fault, suggest to us a strong component of right-handed strike-slip on this branch of the fault.

Farther east along the south branch of the fault, evidence for Recent displacements becomes abundant. Numerous scarplets and conspicuous triangular facets are present along the south wall of Valle de Santo Tomás west of the village. These Recent features do not appear to demand strike-slip movement, although the peculiar reversed course at the mouth of Arroyo Chocolate is consistent with right-lateral displacement.

Agua Blanca Sector

Valle de Santo Tomás

Valle de Santo Tomás (Fig. 5; Pl. 2, fig. 1) is a fault-controlled valley whose relief is due both to erosion in the fault zone and to actual fault displacements along the valley's margins. This is the area of juncture of the north and south branches of the fault, and undoubtedly more breaks underlie the alluviated valley floor than are shown in Figure 5. Southwest of Rancho Dolores, for example, several outlying hills are composed of thoroughly brecciated rhyolite, and this cataclasis must be related to faulting that is not directly reflected in Recent displacements.

Along the north side of the valley, the northern branch of the fault is not everywhere obvious because: (1) the fault trace is parallel to the strike of the stratification of the pre-batholithic volcanic rocks; (2) the fault has not been recently active over this entire segment; and (3) massive landslides probably have concealed parts of the fault trace. Near the mouth of Cañon Verde, for example, the rocks on the two sides of the fault are similar, and there is no marked crushed zone. Possibly these anomalous relations are caused by massive bedding-plane landslides that have occurred intermittently with faulting; the stratification here strikes parallel to the fault and dips steeply south toward the valley floor. Continuation of the fault through this area, nevertheless, is indicated by marked lines of vegetation—reflecting ground-water control by Recent dis-

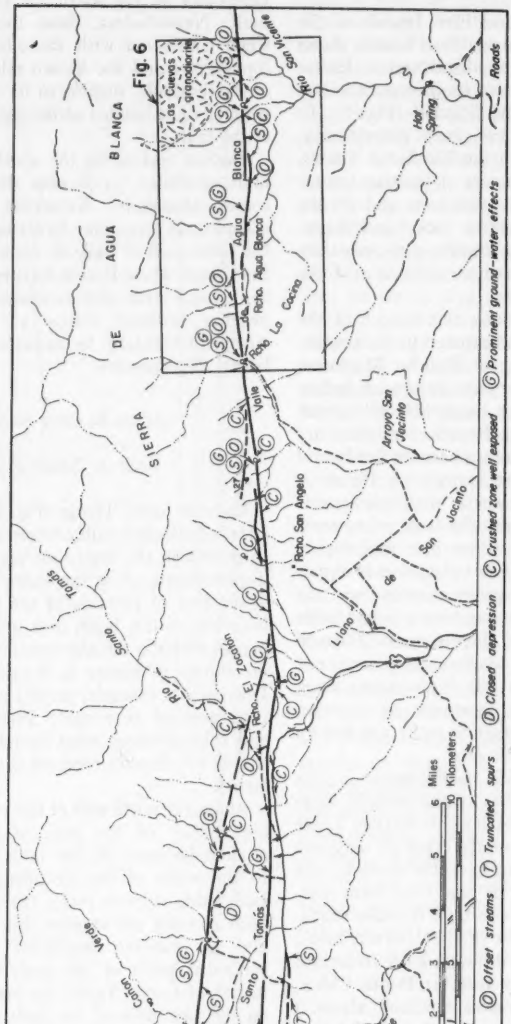

FIGURE 5.—SKETCH MAP OF AGUA BLANCA SECTOR
Inset shows location of Figure 6.

placements—across the mouths of Cañon Verde and adjacent canyons. Ground-water effects are particularly well developed along this branch of the fault several miles farther east (Pl. 2, fig. 1C), and Recent scarps and a large closed depression in the intervening area testify to continuity of the fault. At the eastern end of the valley, an unbroken terrace covers the extended trace of the fault, indicating that Recent activity has been confined to limited segments; however, continuity of the major break across this area is demonstrated by a wide crushed zone exposed in the stream banks north of Rancho El Zacatón.

The southern branch of the fault is delineated by a continuous Recent scarp in the valley floor that extends 2 miles east from the village of Santo Tomás (Pl. 2, fig. 1B). Several large springs occur along the fault near the village and were responsible for establishment of the Dominican mission here in 1794 (Meigs, 1935, p. 91). Farther east along this same break, the principal evidence of Recent movement is a marked vegetative line—almost invisible on the ground—that reflects differences in ground-water levels on the two sides of the fault (Pl. 2, fig. 1A). The crushed zone of the southern branch of the fault in this area is particularly well exposed along the highway grade between Km 163 and Km 164, where the fault zone contains wedges of pulverized rhyolite porphyry, basalt porphyry, and andesitic tuffs and breccias. Landsliding has further complicated the relationships on this steep slope.

Valle de Agua Blanca

Valle de Agua Blanca has been designated as the type locality of the Agua Blanca fault (Allen, Silver, and Stehli, 1956), because the fault is limited there to one clearly defined zone and shows exceptionally well most of the geologic features typical to this fault (Pl. 2, fig. 2).

Valle de Agua Blanca is a classic rift feature, exhibiting in every way except scale the rift characteristics of the San Andreas fault so clearly described 50 years ago by G. K. Gilbert (*in* Lawson *et al.*, 1908, p. 25–30): the fault zone consists of numerous parallel and interfingering breaks, some more recently active than others; the valley is at least in part a structural trough, not solely the product of stream erosion; the trough is remarkably straight; stream drainages are anomalous and generally trend across the valley rather than along it; springs and swampy areas are abundant and commonly are associated with Recent scarplets; side-hill ridges are locally well developed; as followed along their traces, Recent scarps reverse the directions in which they face; and small ridges and valleys are common parallel to and within the rift. Most of the rock types in this region have similar resistance to erosion, however, so that individual fault slices do not attain the same degree of differential relief that is common along many parts of the San Andreas fault. Most of these features are shown in Plate 3 and Figure 6.

Right-lateral stream offsets are characteristic of nearly all the individual breaks of this area. Particularly conspicuous among these are the following: (1) the arroyo walls at Rancho La Cocina (Figs. 5, 6) are clearly offset about 150 feet along the line of Recent scarps, as are many drainages in the next 2 miles to the west; (2) a small arroyo half a mile east of Rancho Agua Blanca (Pl. 3A) is sharply offset about 175 feet in line with a break that forms a very fresh-appearing scarp to the west and a conspicuous side-hill sag to the east; (3) Cañon de Las Cuevas is offset about 600 feet where crossed by the most recent break (Fig. 6), and an abandoned channel just south of the fault here suggests that the next canyon to the east once exhibited a still larger offset.

Ground-water effects are particularly marked where the many normally dry washes cross the fault zone nearly at right angles. Perhaps the most conspicuous of these effects is the ground-water damming at Rancho Agua Blanca (Pl. 3).

The zone of crushed rock is poorly exposed within the Valle de Agua Blanca because here the valley floor is mantled with alluvium. But west of the valley, particularly north of Rancho San Angelo (Fig. 6), white crushed granitic rocks in the fault zone are in marked contrast to the adjacent dark unbroken metavolcanic rocks and are visible from points many miles away. East of Valle de Agua Blanca, the fault zone is deeply dissected by streams tributary to the Río San Vicente (Fig. 6), so that in Arroyo Cieneguitas, for example, a 1000-foot thickness of pulverized quartz diorite is well exposed in the canyon walls.

Fault Displacement in Valle de Agua Blanca

General approach.—Evidence for about 3 miles of right-handed strike-slip in Valle de Agua Blanca is demonstrated by distinctive fan gravels south of the fault that are laterally offset from their source area across the fault to the north. The crystalline bedrock evidently

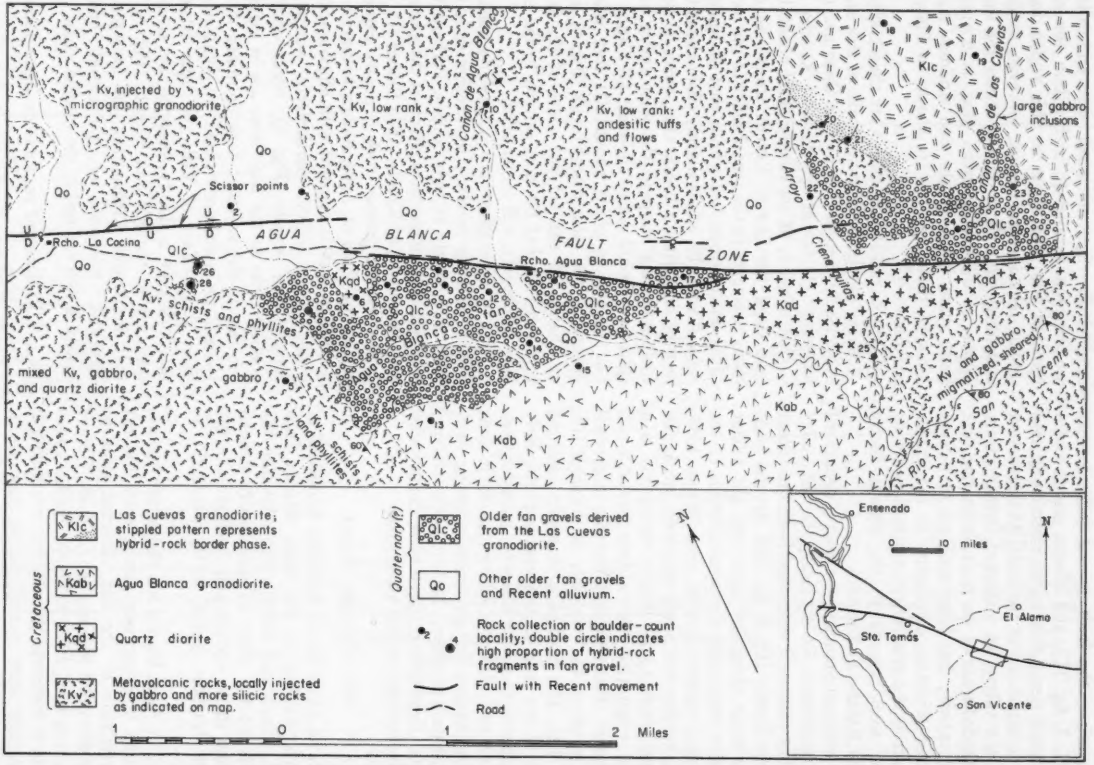

FIGURE 6.—GEOLOGIC MAP OF AGUA BLANCA FAULT AT TYPE LOCALITY
This map shows geologic evidence for 3 miles of Quaternary(?) right-lateral displacement described in text.

has been displaced even more—possibly as much as 14 miles. These conclusions necessarily depend upon a knowledge of the crystalline rocks of this area; therefore the major rock types will be discussed before specific evidence for lateral displacement is presented.

Pre-batholithic rocks.—The oldest rocks both north and south of the fault in Valle de Agua Blanca are metavolcanic tuffs, breccias, flows, and tuffaceous sedimentary rocks, but these rocks display a marked contrast in degree of metamorphism on opposite sides of the fault. On the north the rocks generally retain all their original pyroclastic and epiclastic textures; the only common metamorphic effect is the incipient appearance of very fine-grained (0.02 mm) red-brown mica among the finer-grained minerals. On the south, however, original textures are almost entirely replaced by phyllitic and schistose textures. In rocks exposed near the junction of Cañon de Las Cuevas and Río San Vincente (Fig. 6; Pl. 2, fig. 2), the rank of metamorphism attained corresponds to the amphibolite facies, and highly sheared migmatitic schist and gneiss are well exposed in the walls of both these canyons.

The structural trends in these older rocks are generally similar on both sides of the fault except where locally modified near younger plutons. The bedding and foliation, where observed, strike N. 00–30°W., with dips near vertical.

Las Cuevas granodiorite.—The type area of the Las Cuevas granodiorite is here designated as Cañon de Las Cuevas (Fig. 6), where outcrops are particularly widespread. Outside the area of Figure 6 the outline of the pluton is not known exactly, but observations of float indicate that it cannot extend into drainages farther west and cannot extend east for distances of more than 2½ miles. Thus the pluton is relatively limited in areal extent, and the rock type is distinct from those observed else where in the area of this study.

The predominant rock type of the Las Cuevas pluton is a fine-grained equigranular biotite-hornblende granodiorite. Its approximate composition is: quartz, 30 per cent; antiperthitic oligoclase and albite (Ab_{85-95}), 50–55 per cent; microcline-microperthite, 10–15 per cent; blue-green hornblende, 3–5 per cent; green-brown biotite, 2–6 per cent. Accessory minerals include iron ores, zircon, sphene, apatite, and allanite; alteration minerals include sericite, chlorite, clay(?), clinozoisite, and carbonate. A distinctive textural feature results from the abundant anhedral quartz grains—consistently about 1 mm in diameter—distributed with almost mosaic regularity throughout the rock. On the unusually smooth exfoliation surfaces of weathered boulders, individual quartz grains have regular fractures that give the weathered surface a distinctive glossiness in reflected light.

The Las Cuevas granodiorite shows a history of both protoclastic and cataclastic modification. The quartz displays extreme undulatory extinction; feldspar grains commonly are bent or broken and are healed by minute veinlets of quartz, microcline, and biotite. Original hornblende crystals typically now are parts of somewhat sheared aggregates of biotite and hornblende. Although most of these effects apparently were protoclastic and accompanied by recrystallization, the quartz grains also have been broken by younger shearing that has developed sutured contacts and trains of quartz "mortar". These cataclastic textures are widespread but become more prevalent close to the fault zone.

The most distinctive microscopic characteristic of this rock is the extreme development of antiperthite. Microcline that is itself commonly a braided microperthite has pervasively attacked and replaced the plagioclase both internally and externally. This phenomenon appears to have been in part contemporaneous with the protoclastic history.

Only one important variant to the typical granodiorite has been observed in this pluton. Along the southwest contact (Localities 20 and 21, Fig. 6) is a distinctive border facies concontaining dark-green xenolithic inclusions amounting to as much as 60 per cent by volume. These inclusions range from half an inch to 6 inches in diameter and give the weathered surface of the rock the appearance of plum pudding; we have assigned to such material the field name of hybrid rock. Scattered inclusions are present throughout the Las Cuevas pluton, but only in this area is the distinctive hybrid rock texture evident.

The dark inclusions in the hybrid rock are typically composed of 30–45 per cent green hornblende, 40–60 per cent sodic laboradorite or andesine, and 1–5 per cent quartz and minor accessory minerals. The fragments appear to be somewhat recrystallized clasts of the older andesitic metavolcanic rocks. A general similarity of the granodioritic matrix of the hybrid rock to the granodiorite of the main Las Cuevas mass is apparent, although the hornblende content is higher in the matrix,

FIGURE 6.—GEOLOGIC MAP OF AGUA BLANCA FAULT AT TYPE LOCALITY
This map shows geologic evidence for 3 miles of Quaternary(?) right-lateral displacement described in text.

the quartz texture is slightly micrographic in some places, and the plagioclase is distinctly more calcic and somewhat less antiperthitic.

Agua Blanca granodiorite.—A second pluton of this region consists of the Agua Blanca granodiorite, named from the excellent exposures half a mile south of Rancho Agua Blanca (Fig. 6; Pl. 3). This rock, too, is a biotite-hornblende granodiorite; its approximate composition is: quartz, 25–30 per cent; plagioclase, 45–55 per cent; microcline, 5–10 per cent; hornblende, 5–8 per cent; biotite, 4–6 per cent; accessory minerals (ores, sphene, zircon, apatite) and alteration minerals (chlorite, sericite, epidote), 2–3 per cent. The rock has a slightly foliated texture, with considerable variation in the grain size (0.2–8 mm) and abundance of dark minerals. Protoclastic modification of the normal granodioritic texture is evident in thin section.

Although grossly similar in composition to the Las Cuevas granodiorite, the Agua Blanca granodiorite can be clearly distinguished as follows:

(1) The seriate grain-size distribution, somewhat variable mean grain size, and subhedral grain shape of the Agua Blanca granodiorite contrast with the equigranular, equidimensional, anhedral texture of the Las Cuevas granodiorite.

(2) Boulders of the Las Cuevas granodiorite weather with distinctive smooth, glossy surfaces of exfoliation that are lacking on weathered boulders derived from the Agua Blanca mass.

(3) The Agua Blanca plagioclase is subhedral to euhedral and strongly zoned; single crystals range in composition from calcic laboradorite to oligoclase; and the average composition is sodic andesine or calcic oligoclase. The plagioclase of the Las Cuevas granodiorite is anhedral sodic oligoclase or albite, unzoned or only slightly zoned, and distinctly antiperthitic.

(4) No inclusion-rich border facies similar to the Las Cuevas hybrid rock has been observed in the Agua Blanca pluton.

Other plutonic rocks—Quartz diorite crops out south of and within the fault zone throughout much of Valle de Agua Blanca (Fig. 6). This rock is typically medium- to coarse-grained, hypidiomorphic, and inequigranular, with a composition of: quartz, 20–25 per cent; andesine, 50–60 per cent; microcline, 0–5 per cent; biotite, 5–12 per cent; and hornblende, 5–10 per cent. In most places the quartz diorite is so thoroughly shattered that it could not have contributed boulders to the alluvial fans. Two exceptions are at locality 6 (Fig. 6; Pl. 3) and on the slopes south of Rancho La Cocina (Fig. 6). Boulders from these areas are readily distinguishable from boulders of Las Cuevas granodiorite by their coarser texture, tabular subhedral or euhedral andesine, absence of antiperthitic feldspars, and the presence of large (3–5 mm) crystals of hornblende and biotite.

A small mass of micrographic hornblende granodiorite crops out about 1 mile northeast of Rancho La Cocina (locality 1, Fig. 6 and Pl. 3). Although compositionally similar to the Las Cuevas granodiorite, it is texturally distinct. The rock is a fine-grained aggregate of tabular subhedral plagioclase and quartz. No textures resembling this have been observed in clasts in the older fan gravels or in any of the other plutonic rocks of the area.

Gabbroic rocks with diverse textures and compositions occur in at least four localities

---

PLATE 1.—PHYSIOGRAPHIC FEATURES OF FAULTING

FIGURE 1.—Right-lateral stream offsets along Agua Blanca fault at base of Punta Banda Ridge near Km 136. Photograph is taken from point B on Figure 4, which is a sketch map of stream drainages in this area. Note vegetative line along fault.

FIGURE 2.—Aerial view of disturbed topography on north side of Punta Banda Ridge, 4½ miles south of El Maneadero (Fig. 3). Rocks on near (north) side of fault are fan gravels and steeply dipping Tertiary(?) sedimentary rocks; rocks on far side are Cretaceous metamorphic and plutonic rocks.

PLATE 2.—AERIAL VIEWS OF FAULT TOWARD ITS WESTERN END

FIGURE 1.—Valle de Santo Tomás, looking west. Traces of both branches of the fault are delineated. Note vegetative lines caused by Recent displacements at A, B, and C. Figures 3 and 5 are maps that include most of the area of this photograph.

FIGURE 2.—Aerial view west into Valle de Agua Blanca, which is a rift valley in the fault zone. The named localities may also be identified on the geologic sketch map of this area, Figure 6.

FIGURE 1

FIGURE 2

PHYSIOGRAPHIC FEATURES OF FAULTING

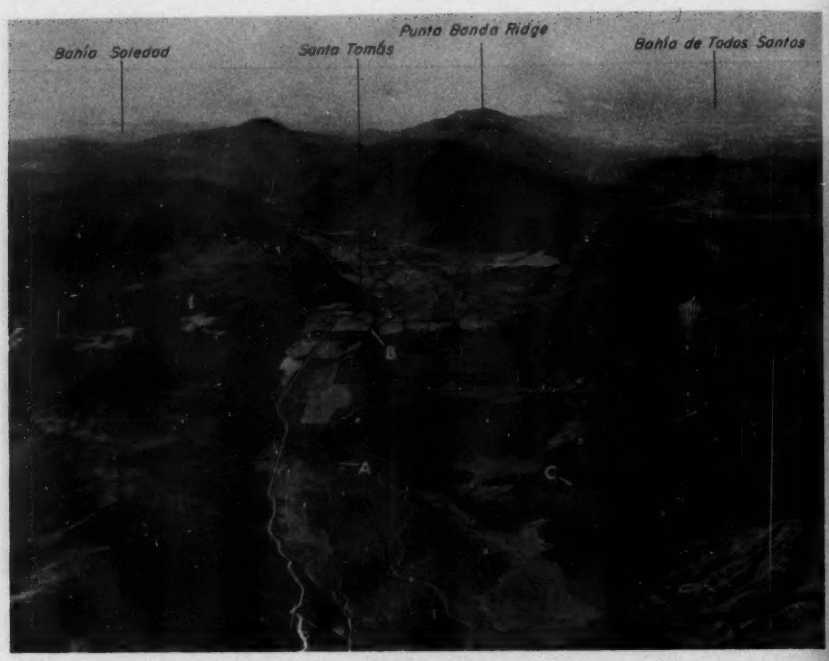

FIGURE 1

FIGURE 2

AERIAL VIEWS OF FAULT TOWARD ITS WESTERN END

OBLIQUE AERIAL VIEW OF RANCHO AGUA BLANCA

FIGURE 1

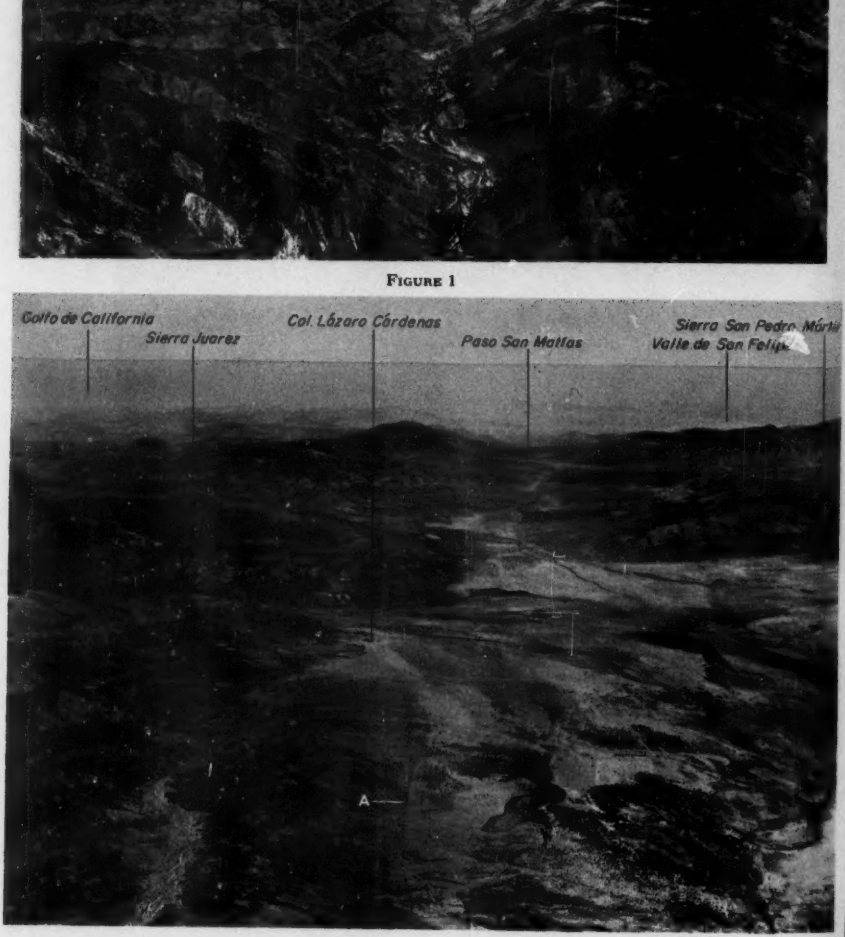

FIGURE 2

AERIAL VIEWS OF FAULT TOWARD ITS EASTERN END

on both sides of Valle de Agua Blanca. They are typically hornblende gabbros and diorites commonly in part uralitized. In contrast to the general textural diversity, the textural equivalent of the medium-grained equigranular hornblende gabbro found among the older fan gravels has been seen in only two areas of bedrock exposure. The more prominent of these is in the upper Cañon de Las Cuevas, where many large inclusions of similar gabbro appear in the Las Cuevas granodiorite. The other locality is in a ravine northwest of Rancho Agua Blanca (near locality 3, Fig. 6 and Pl. 3), but this rock is considerably brecciated and may be part of a slice within the fault zone.

Lateral displacement of alluvial fans.—An uplifted and slightly dissected alluvial fan that we have called the Agua Blanca fan lies mainly southwest of Rancho Agua Blanca (Fig. 6; Pl. 3). Since its development, this fan has been laterally displaced about 3 miles relative to its source area by right-handed strike slip on the Agua Blanca fault, as is indicated by the following features:

(1) Although the morphology of Valle de Agua Blanca gives the impression of a graben cutting across a series of formerly continuous southward-sloping alluvial fans (Pl. 2, fig. 2) the compositions of these fans on the two sides of the apparent graben makes this interpretation untenable (Table 1). The uplifted fans at localities 2 and 11 (Fig. 6; Pl. 3) are entirely different in composition from the nearly adjacent Agua Blanca fan across the fault zone to the south. The rock types characteristic of the Agua Blanca fan could have been derived only from the area underlain by Las Cuevas granodiorite. Not only are the Las Cuevas granodiorite and hybrid rock distinctive rock types, but the proportions of these and other types are reasonable for the relative abundances in the outcrop areas. Some of the boulders on the Agua Blanca fan are of gabbro that was injected by Las Cuevas granodiorite; similar relations are observed in the upper Cañon de Las Cuevas.

(2) The Agua Blanca fan contains abundant clasts of Las Cuevas hybrid rock only at its west end (localities 4, 26, 28), which is consistent with the bedrock position of the hybrid rock at the western contact of the Las Cuevas pluton. This relation provides the best evidence of the amount of fault displacement of the fan, which is about 3 miles.

(3) The possibility that the Agua Blanca fan could have been derived solely by westward stream flow from the Las Cuevas area without lateral fault displacement—is ruled out for three reasons: (a) The sharp compositional contrast between the nearly adjacent fans north and south of the fault would be almost impossible to explain this way. (b) If the fans once sloped west, clasts of quartz diorite and Agua Blanca granodiorite should have augmented the Las Cuevas boulders on the fan. This has not happened, and instead the Agua Blanca fan probably has always sloped south and been dominated by the steep mountains north of the fault. (c) The observed distribution of hybrid-rock fragments would be most unlikely with this interpretation.

We do not contend that the Agua Blanca fan is necessarily the offset portion of the incised fan that now lies north of the fault at the mouth of Cañon de Las Cuevas (Fig. 6; Pl. 2, fig. 2), although this latter fan certainly is truncated by the fault and probably is correlative. Our principal argument is that the Agua Blanca fan must have been formed when it was 3 miles farther east relative to the north block. The slight degree of dissection of the surface of the Agua Blanca fan suggests that this deposit is

---

PLATE 3.—OBLIQUE AERIAL VIEW OF RANCHO AGUA BLANCA

Numbered sites are rock-collection or boulder-count localities, as indicated on Figure 6. Recent fault displacements have dammed ground water, causing vegetative line across canyon near ranch. Note prominent right-lateral stream offset (about 175 feet) at A. North-facing Recent scarp between A and ranch reverses direction of throw as traced toward bottom of photograph.

PLATE 4.—AERIAL VIEWS OF FAULT TOWARD ITS EASTERN END

FIGURE 1.—Cañon de Dolores, looking east from above Valle de Agua Blanca. The canyon is eroded in crushed rocks of the Agua Blanca fault zone for almost 15 miles. Figure 7 is a sketch map of this area.

FIGURE 2.—Valle de La Trinidad, looking east from above its western end. Agua Blanca fault enters the valley in center foreground (note vegetative line, "A") and is responsible for the existence of this anomalous east-west breach in the mountainous backbone of the peninsula. Figure 8 is a sketch map of this area.

of Quaternary age, and the 3-mile separation is therefore thought to represent a Quaternary displacement.

Possible bedrock displacements.—The differences in bedrock types across the Agua Blanca fault in this area suggest that the total lateral displacement must be greater than the 3 miles indicated by the displaced alluvial fans. We have not yet been successful in matching any crystalline rock masses across the fault in this region, other than the widespread metavolcanic series. In particular, the offset portion of the distinctive Las Cuevas pluton has not yet been identified south of the fault; we have seen no corresponding rock mass in this area or for at least 12 miles to the west. Within the fault zone, however, slices of distinctive rock types suggest right-lateral displacements of 7–14 miles.

Slices of intensely sheared and altered white granitoid rock crop out within the fault zone almost continuously from half a mile west of Rancho La Cocina to north of Rancho San Angelo an interval of more than 3 miles (Fig. 5). Although in most places this rock can be identified only as crushed quartz-bearing "granitic" rock, the slices cannot have been derived from the rock masses immediately north or south of the fault zone in this area, inasmuch as these adjacent rocks are either metavolcanic or gabbroic types. Within the fault zone only one specimen was found sufficiently well preserved to justify petrographic comparison; this was obtained from a slice about 2 miles west of Rancho La Cocina (Fig. 5, locality 27). The rock is remarkably similar to the Las Cuevas granodiorite: it is a fine-grained equigranular granodiorite showing antiperthitic replacement of sodic plagioclase by potassic feldspar. Even though the degree of replacement is less than that observed in the Las Cuevas pluton, the correlation is felt to be sound and strongly suggests a right-lateral displacement of at least 7 miles. But whether or not this particular correlation is valid, no other intrusive mass occurs in a position to suggest a lesser displacement in either a right lateral or left-lateral sense. It is unlikely that predominantly vertical movements could have introduced a slice of plutonic rock between walls of older metavolcanic rocks, but this possibility cannot be ruled out.

TABLE 1.—PERCENTAGES OF ROCK TYPES IN BOULDERS OF ALLUVIAL FANS

Locality numbers are keyed to Figure 6 and Plate 3. Most figures represent counts of 200 boulders, each more than 6 inches in diameter.

	North of fault					South of fault								
Locality number	2	11	22	23	24	28	26	4	7	8	9	12	16	17
Las Cuevas granodiorite	..	..	98	99	100	67	93	84	76	89	94	97	96	75
Las Cuevas hybrid rock	..	..	2	..	...	12	4	7	..	2	..	..	..	..
Gabbro	9	3	..	1	...	1	..	1	..	2	2	..	2	5
Other plutonic rocks	20	34	..	..	...	..	..	..	..	..	..	..	..	..
Metavolcanic rocks	71	63	..	..	...	20	3	8	24	7	4	3	2	20

A fault slice of crushed quartz diorite crops out 1 mile northeast of Rancho San Angelo and may indicate an even larger lateral displacement. The nearest known quartz diorite bedrock is south of Rancho La Cocina, but this cannot be a possible source if the thesis of right-lateral movement is accepted. The nearest known quartz diorite on the north side of the fault is in Cañon de Dolores near its junction with Cañon de San Lorenzo (Fig. 7), which represents a 14-mile separation. In the absence of better petrographic comparisons and more adequate regional mapping, however, this figure is only suggestive.

CAÑON DE DOLORES SECTOR

For more than 15 miles, the straight gorge of Cañon de Dolores (Fig. 7; Pl. 4, fig. 1) is controlled by the Agua Blanca fault. Indeed, the canyon is so straight, in contrast to the dendritic patterns otherwise typical of this region, that the lineament shows up well on photographs taken from rockets over White Sands, New Mexico. Cañon de Dolores is a fault-line feature; the canyon is caused primarily by erosion in the crushed rock of the fault zone rather than by actual fault displacements. Evidence for the continuity of the

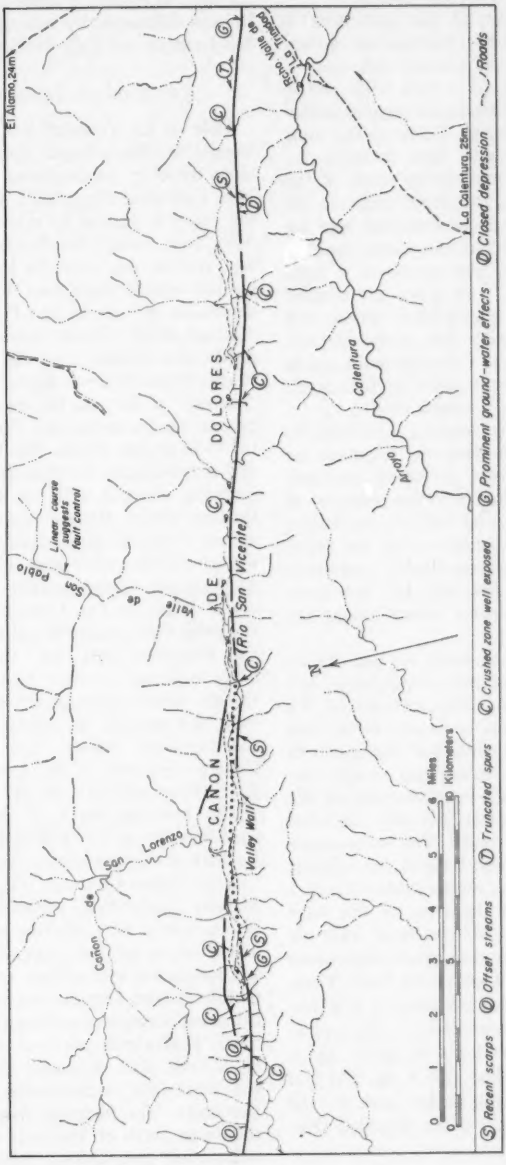

FIGURE 7.—SKETCH MAP OF CAÑON DE DOLORES SECTOR

crushed zone can be observed in the canyon walls over most of the canyon's length.

A good cross section of the fault zone is exposed just west of the westernmost springs shown in Figure 7. The crushed zone here is more than a quarter of a mile wide and is characterized by predominantly gneissic granodiorite and quartz diorite. North of this zone metavolcanic rocks have been intruded by granodiorite and gabbro. Rocks south of the fault in this area and for several miles to the west are more highly metamorphosed than are those across the fault to the north, perhaps because they lie near the border of a large pluton. The principal rock types are sheared migmatized gabbro, amphibolitic gneiss and schist, and quartz diorite. East of the junction of Cañon de Dolores and Cañon de San Lorenzo (Fig. 7), the predominant rock type both north and south of the fault is quartz diorite.

Proof of Recent displacement is difficult to find within Cañon de Dolores, inasmuch as stream-cut embankments are easily confused with fault scarps. Between the mouths of Cañon de San Lorenzo and Valle de San Pablo, however, several escarpments along the south side of the valley floor cross alluvial cones with changes in elevation that rule out the possibility of the escarpments being stream-cut features.

Above the mouth of Valle de San Pablo, Cañon de Dolores narrows considerably and affords good exposures of the crushed zone. Six miles east of this junction is one of the few wedges of sedimentary rock that are caught in the fault zone in this region; here steeply dipping tuffaceous volcanic conglomerates on the north are faulted against intensely fractured quartz diorite on the south. The sedimentary rocks are similar to those beneath the volcanic capping of the southern Sierra Juárez. About 1 mile farther east, on the crest of the ridge separating Cañon de Dolores from Valle de La Trinidad, three elongate closed depressions are aligned along the trace of the fault. These constitute the best proof of recency of displacement on the Agua Blanca fault in this region, and substantiating evidence is given by a distinctive vegetative line (Pl. 4, fig. 2A) and eroded fault scarps still farther east on the northwest slopes of Valle de La Trinidad (Fig. 7).

Limited reconnaissance north of the main fault zone in the Cañon de Dolores and adjacent sectors indicates that a number of linear east-trending valleys may be controlled by faults subsidiary to the Agua Blanca. Figure 7 shows one such alignment 3 miles north of Cañon de Dolores delineated by tributaries of Cañon de San Lorenzo and Valle de San Pablo.

Valle de la Trinidad Sector

Valle de La Trinidad is a broad alluviated trough, 20 miles in length, that cuts athwart the north-trending mountainous "backbone" of Baja California (Fig. 8; Pl. 4, fig. 2). Most of the valley is drained by a stream system that flows west toward the Pacific Ocean, but the east end of the valley is being captured by streams which drain east toward the closed depression of Valle de San Felipe (Fig. 2). The drainage divide between these two systems is so gentle and obscure that the name Paso San Matías generally is not applied to the indistinct "summit" of the pass, but instead to the rugged canyon 5 miles farther east that leads down into the Valle de San Felipe. The Valle de La Trinidad is remarkably straight and is bordered by generally straight walls on the north. These features reflect tectonic control rather than normal erosional development, and it is noteworthy that the above physiographic description would apply almost equally well to the next major break in the Peninsular Ranges—San Gorgonio Pass, some 200 miles to the north. In San Gorgonio Pass, too, the north-trending range is abruptly broken by a deep transverse trough, stream drainage are markedly anomalous, the summit is indistinct, and tectonic control—here related to the Transverse Ranges—appears to be dominant (Russell, 1932; Allen, 1957, p. 318, 347).

The best exposures of the Agua Blanca fault in Valle de La Trinidad are found along the base of the lava-capped mesa 3 miles east of Colonio Lázaro Cárdenas (Fig. 8; Pl. 4, fig. 2). Massive landsliding evidently has occurred intermittently with faulting along this escarpment, but, in general, Upper Cenozoic volcanic and associated sedimentary rocks north of the fault have been brought into juxtaposition with deformed nonmarine sedimentary rocks on the south. Half a mile north of corral No. 1 (Fig. 8), a fault slice of quartz diorite—foreign to the immediate vicinity—lies between these two units. The andesitic flow rocks that cap the mesa north of the fault are underlain by well-sorted, cross-bedded, eolian(?) sandstones, whereas the fluviatile and lacustrine rocks south of the fault comprise poorly sorted muddy sandstones and conglomerates with clasts of pegmatite, gabbro, and volcanic rocks including types

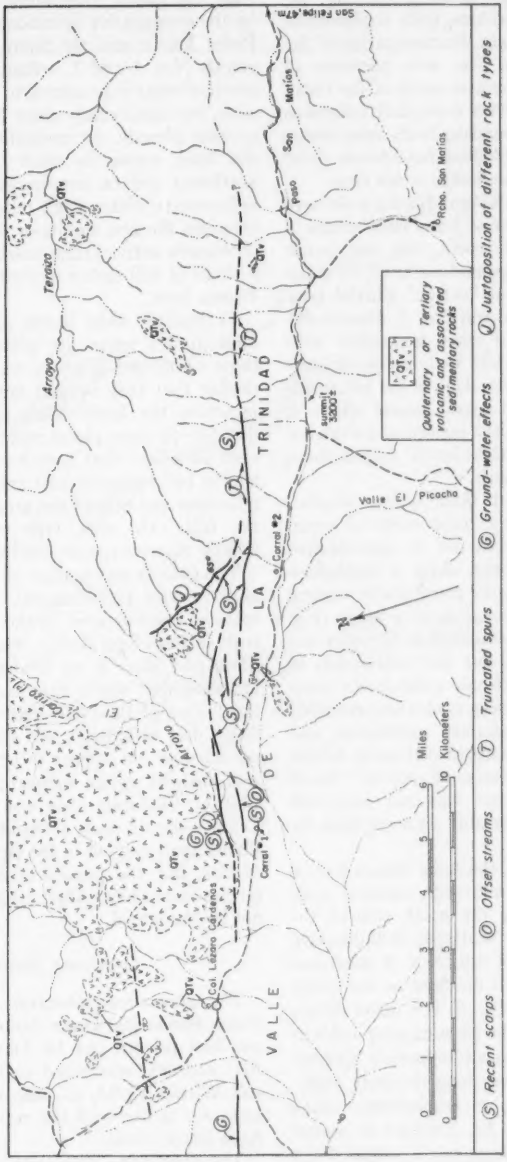

FIGURE 8.—SKETCH MAP OF VALLE DE LA TRINIDAD SECTOR

different from those across the fault to the north. Thus, although some landsliding undoubtedly has occurred here, fault displacement is necessary to complete the explanation of the geologic relationships. One mile northeast of corral No. 1, conglomerates south of the break are in fault contact with water-laid tuffaceous rocks that contain abundant fresh-water fossils but the relationship of these fossiliferous rocks to the mesa-capping andesites is not clear.

Displacements on the Agua Blanca fault have been sufficiently recent to leave fault scarps in these older, dissected rocks, but not recent enough for scarps or ground-water effects to be visible on the adjacent "active" alluvial fans. Half a mile east of corral No. 1, Recent displacements within the tilted nonmarine sedimentary rocks have left well-developed side-hill sags along the south flank of the hill, in addition to several right-lateral stream offsets of 50 to 100 feet. This is the easternmost evidence that we have seen of right-lateral displacement on the Agua Blanca fault.

Numerous dissected fault scarps displace nonmarine sedimentary rocks north of corral No. 2, and these rocks are in turn faulted against crystalline rocks along a northwest-trending fault that shows considerable vertical displacement of the mesa-capping lavas (Fig. 8). These lavas are here underlain by water-laid tuffs and sandstones, but the relationship of these pre- and intravolcanic rocks to the other nearby sedimentary rocks is obscure; certainly some of the little-deformed sandstones and conglomerates, such as many of those in Arroyo El Carrizo and along the south side of Valle de La Trinidad, represent dissected valley-fill material that is considerably younger than the mesa-capping lavas.

East of corral No. 2, the Agua Blanca fault is manifested solely by the very straight, steep mountain front along the north side of the valley, together with scattered well-dissected scarplets at the base of this front. A small outcrop of volcanic rock on the floor of the valley near its eastern end (Fig. 8) is a dense olivine basalt unlike most of the mesa-capping volcanic rocks; possibly this basalt represents Quaternary outpouring of lava along the fault itself.

Evidence pertaining to displacement along the fault in Valle de La Trinidad is sparse: right-lateral stream offsets east of corral No. 1 indicate 50 to 100 feet of Recent strike-slip movement, and the general absence of volcanic rocks capping the mountains south of the fault, when compared to the abundant flows to the north, suggests that the south side has been relatively raised. This notion also is supported by the comparative elevations of the Sierra San Pedro Mártir and the Sierra Juárez. Between corrals Nos. 1 and 2, volcanic rocks crop out south of what is presumed to be the main fault zone, but significantly these flows rest directly, or near directly, on crystalline rocks, whereas the flows across the fault to the north and northwest rest on considerable thicknesses of sedimentary rocks. High relief evidently characterized the area during or prior to the period of volcanic activity, and possibly this relief was a result of still earlier movements on the Agua Blanca fault.

Crystalline rocks north and south of the fault in this sector are generally similar, and those north and south of corral No. 2 are so similar that they suggest only small displacement on the fault. These rocks are quartz diorites—in some places markedly foliated and even schistose—that have been pervasively intruded by pegmatite and aplite dikes. Several miles east and west of this area, on both sides of the fault, the rock type becomes predominantly massive quartz diorite.

The eastern termination of the Agua Blanca fault remains problematical. There is no conspicuous crushed zone on the projection of the fault in Paso San Matías, where exposures are good, and there is no obvious landsliding or thrusting that might have concealed the fault trace. East of Paso San Matías, the alluviated desert floor of Valle de San Felipe as seen from the air does not appear to be broken, but the next bedrock range eastward—almost to the Gulf of California—has not been examined. Tentatively we must conclude that the Agua Blanca fault dies out in the vicinity of Paso San Matías, but the possibility of its continuing farther east or being offset by another fault cannot be discounted.

Offshore Sector

The anomalous submarine topography off Punta Banda and Punta Santo Tomás (Fig. 9) was first pointed out by Davidson (1897, p. 101) and first attributed to faulting by Böse and Wittich (1913, p. 326, 459). These two areas are in line with the two branches of the Agua Blanca fault.

The submarine projection of Punta Santo Tomás extends several miles out to sea, so that depths of only 65 fathoms are recorded as much as 13 miles off the point. The projection drops off steeply on the north, in approximate align-

FIGURE 9.—MAP OF SUBMARINE TOPOGRAPHY OFF SOUTHERN CALIFORNIA AND NORTHERN BAJA CALIFORNIA

ment with the southern branch of the fault, and the topography is consistent with right-lateral displacement.

A series of steep, sharp submarine ridges extends northwest from Punta Banda and very nearly meets a similar group of ridges that extends southeast from Islas Todos Santos (Fig. 9), but a narrow 215-fathom-deep trench cuts across this alignment and prevents continuity of the ridges between the two localities (Walton, 1955, p. 953–957). Certainly the over-all topography must be related to the offshore projection of the north branch of the Agua Blanca fault, and possibly the individual ridges represent fault slices. Although there is no indication on published charts that the deep channel between Punta Banda and the islands has been offset by the fault, the existence of Punta Banda itself supports the idea of right-lateral displacement.

Northwest of Islas Todos Santos, the submarine contours give no clear indication of the prolongation of the Agua Blanca fault zone, but the density of soundings in this area is considerably less than one per square mile. It is interesting to speculate that the fault zone may indeed extend across this area and be continuous with the fault zone represented by the San Clemente basin and escarpment (Fig. 9). Shepard and Emery (1941, p. 21–25), in a detailed study of this northern area, have argued that the San Clemente escarpment and "rift valley" are truly fault features. Furthermore, the reversals in direction of slope of the scarp, and the 25-mile separation of San Clemente Island and Fortymile Bank (Fig. 9) were suggested as evidence of right-lateral displacement. First motions of a number of earthquakes in this area support the idea of this type of displacement (Gutenberg, 1941, Fig. 4), and several earthquakes that have occurred between Fortymile Bank and Punta Banda tend to support the hypothesis of a throughgoing fault zone.

Another possibility is that the Agua Blanca fault turns so as to be continuous with the Coronado escarpment (Fig. 9), which is also thought to be fault-controlled (Emery *et al.*, 1952, p. 544). This would, however, necessitate an abrupt change in trend of the fault zone.

Summary of Evidence Relating to Displacement

(1) Fault scarps and related physiographic features indicate Recent movements along most, but not every part, of the Agua Blanca fault from near Paso San Matías to the Pacific Ocean. In general, features of Recent movement are more abundant and fresher in appearance toward the west.

(2) Stream offsets leave no doubt of Recent right-lateral displacements from east of Colonia Lázaro Cárdenas (Fig. 8) to Punta Banda Ridge south of El Maneadero (Fig. 3). The most recent appearing offsets average 150 to 200 feet. West from Valle de Agua Blanca, abandoned stream channels indicate offsets of as much as 900 feet and suggest still larger displacements.

(3) Quaternary(?) fan gravels laterally offset from their source area across the fault indicate about 3 miles of Quaternary(?) right-handed strike-slip in Valle de Agua Blanca. This is the greatest displacement that has been definitely demonstrated along the Agua Blanca fault.

(4) Even prior to the 3-mile Quaternary(?) displacement in Valle de Agua Blanca, individual plutonic rock units would not have "matched" across the fault. This suggests that the total lateral displacement since Cretaceous time is greater than 3 miles, although vertical movements may have contributed to the discontinuities. In Valle de Agua Blanca, 7 miles of post-Cretaceous right-lateral displacement is very strongly suggested by a fault slice of distinctive antiperthitic granodiorite whose probable bedrock source is known. The possibility of 14 miles of right-lateral displacement is indicated by a nearby fault slice of quartz diorite whose correlation with a bedrock source is less certain, but nevertheless suggestive.

(5) The 3000-foot elevation of basal Upper Cretaceous(?) beds north of the southern branch of the fault near Bahía Soledad suggests considerable vertical component of movement along the fault in this area.

(6) Cappings of Upper Cenozoic volcanic rocks are abundant on the Sierra Juárez but are unknown farther south on the adjacent part of the Sierra San Pedro Mártir. This, together with the relative elevations of these ranges, suggests that the Agua Blanca fault, which separates the two ranges, has had vertical displacement with the south side relatively raised.

(7) The rudistid limestone zone in the Lower Cretaceous section is possibly offset about 11 miles in a right-lateral sense near the mouth of the Río Santo Tomás, but the evidence is suggestive at best.

(8) The topography of Punta Banda and Punta Santo Tomás—with their submarine extensions—is best explained by right-lateral displacements amounting to several miles.

(9) Shepard and Emery (1941, p. 24) suggested 25 miles of right-lateral displacement on the San Clemente fault on the basis of the separation of San Clemente Island and Fortymile Bank. The San Clemente fault must be tectonically related to the Agua Blanca fault; possibly they are part of the same zone.

(10) The Agua Blanca fault juxtaposes "basement" rocks that are grossly similar on the two sides of the fault. These are dominantly pre-batholithic eugeosynclinal rocks that have been intruded by various types of Cretaceous plutons. This relationship does not rule out the possibility of relatively large displacements, however, inasmuch as these rocks are of regional extent; they crop out in a north-south direction for at least 400 miles and are of unknown east-west extent.

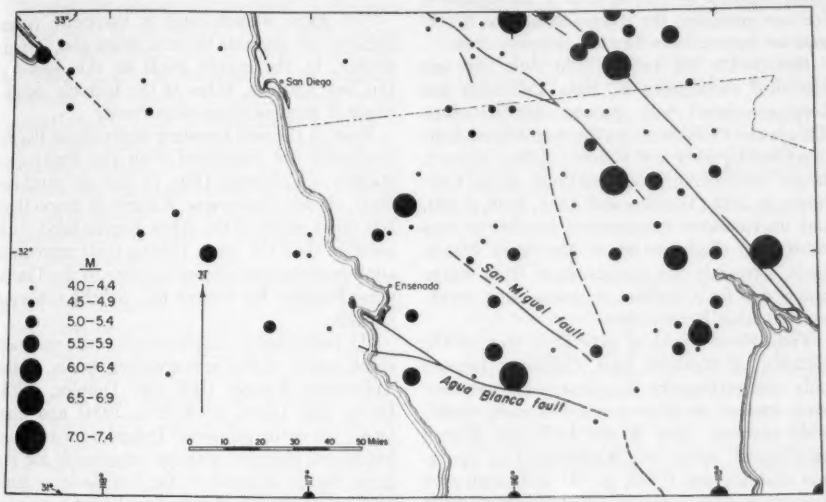

FIGURE 10.—MAP OF EARTHQUAKE EPICENTERS IN NORTHERN BAJA CALIFORNIA, JANUARY 1, 1934 TO DECEMBER 31, 1955

Locations may be in error by 10 miles or more. Where more than one shock occurred at a given epicenter, strain release has been summed to give an effective magnitude. P. St. Amand and C. F. Richter assisted in compiling these data.

SEISMICITY

Seismicity provides a further line of evidence bearing on the tectonic framework of northern Baja California. Epicenters of earthquakes of Magnitude 4.0 or greater that occurred from 1934 through 1955 are plotted on Figure 10. Epicentral determinations for shocks south of the international border are hindered by the fact that all the seismograph stations of the southern California network lie in the same general azimuth. Thus most of the epicenters plotted in Figure 10 have been assigned a "D" rating by the Seismological Laboratory in Pasadena; this means that their locations may be in error by 10 miles or more, so that Figure 10 could give a very misleading impression if this possible error were not kept in mind.

Conclusions drawn from Figure 10 are (in part repeated from Allen, St. Amand, and Richter, 1958):

(1) By far the greatest seismic activity in northern Baja California during this period has been along the San Andreas fault zone near the head of the Gulf of California.

(2) The region surrounding San Diego has shown low seismicity during the period, and the geologic structure of this region supports the idea of a relatively unbroken, stable block. A zone of marked seismic activity, however, limits this block on the south at approximately the latitude of the Agua Blanca and San Miguel faults. Many epicenters shown within 20 miles of these faults in Figure 10 may actually represent earthquakes on them, although a few are definitely farther north. The important point is that the Agua Blanca fault coincides in gross aspect with an east-west zone of seismic activity in a region otherwise marked by relative quiescence.

(3) The relatively stable area surrounding San Diego is terminated on the west by a zone of seismic activity trending through San Clemente Island toward Punta Banda. This lends support to the idea of a throughgoing fracture zone, but the epicenters are too sparse and too inaccurately located to prove this.

Outside the San Andreas fault zone, only one historical earthquake in Baja California has been associated with ground displacements. This is the 1956 shock on the San Miguel fault described by Shor and Roberts (1958). A much larger earthquake shook northern Baja California in 1892 (Townley and Allen, 1939, p. 87), but its epicenter is unknown; possibly it was caused by displacement on the Agua Blanca fault. Certainly the abundance of fresh scarps along this fault testifies to many such occurrences within Recent time.

Fault-plane solutions give little clue to the tectonics of northern Baja California because only one earthquake in recent years has been large enough to allow a solution using worldwide stations. This is the 1956 San Miguel earthquake, which was investigated by Hodgson and Stevens (1958, p. 311–312) and gave two possible solutions: (a) left-lateral fault striking N. 19° E., dipping 85° S.E.; (b) right-lateral fault striking N. 72° W., dipping 72° N.E. The (b) solution corresponds well to the field observations of Shor and Roberts (1958) and to the line of aftershock epicenters.

A series of moderate-sized earthquakes that occurred in 1954–1955 at the latitude of the Agua Blanca fault showed an east-west spread and independently suggested to Richter (1956, p. 162) the possibility of a transverse structure at this latitude. First motions of these earthquakes at the Pasadena stations are compatible with right-lateral displacement on a fault of Agua Blanca trend, but also will permit faults of more northerly orientation, including the San Andreas trend.

In the offshore area between Punta Banda and San Clemente Island, nearly all the earthquakes investigated by Gutenberg (1941, Fig. 4) had first motions compatible with right-lateral movement on northwest-trending faults. This is also true for most of the larger earthquakes that have occurred in this area since the time of Gutenberg's study, although the one conspicuous exception is the largest historical earthquake of the region—the 1951 shock of Magnitude 5.9 at the southeast corner of San Clemente Island (Fig. 10). Compressions were recorded at all stations of the Pasadena network, which demands a large component of dip-slip movement.

Regional Tectonic Relationships

The Agua Blanca fault is markedly transverse to the regional tectonic grain and, in particular, to the master fault of this region—the San Andreas. What is the tectonic significance of such an anomalous trend?

Most of the east-trending faults of the Pacific southwest are associated with the Transverse Ranges of California (Fig. 1), but the southern limit of the Transverse Ranges is more than 100 miles north of the Agua Blanca fault. Is it possible that the Agua Blanca fault represents another structural element similar to the Transverse Ranges? We believe not, for the following reasons:

(1) Left-lateral displacement is common along many of the east-trending faults of the Transverse Ranges (Hill and Dibblee, 1953; Bailey and Jahns, 1954; Hill, 1954) and may typify the entire province.[2] Indeed, such regional left-lateral shearing may be responsible for the great change in trend of the San Andreas fault where it crosses the Transverse Range province. On the Agua Blanca fault, however, all evidence points to a history of *right*-lateral movement.

(2) If the Agua Blanca fault were once parallel to the tectonic grain and has since been "bent" by regional left-lateral distortion—in a manner similar to the possible bending of the San Andreas fault in the Transverse Ranges—then the structure of the adjacent pre-batholithic rocks should show evidence of this distortion. But these rocks strike approximately N. 30° W. not only in the vicinity of the Agua Blanca fault, but for more than 100 miles both north and south as well. Thus a large change in relative orientation of this fault, at least since Early Cretaceous time, seems very unlikely.

(3) The Transverse Ranges appear to be the continental extension of a great submarine fault system—the Murray fracture zone of Menard

[2] Right-lateral displacement has been suggested for the San Gabriel fault (Crowell, 1952) and the Banning fault (Allen, 1957, p. 341), but both of these faults may be more closely allied to the San Andreas system than to the Transverse Ranges system. Also anomalous is the magnetic evidence for right-lateral movement on a part of the Murray fracture zone (Menard and Vacquier, 1958; Mason, 1958), which is the offshore prolongation of the Transverse Ranges. The magnetic evidence, however, even if correctly interpreted, gives no clue as to the age of this displacement, which could be very old.

(1955, p. 1164–1167). Nothing in the known offshore topography west of the Agua Blanca fault suggests a similar fracture zone at ths latitude.

It might be argued that the trend of the Agua Blanca fault is not parallel to the over-all San Andreas trend because it has been "deflected" by older structural features in the bedrock. However, the regional structural trend of the pre-batholithic rocks is remarkably parallel to the San Andreas trend and is *truncated* by the Agua Blanca fault. Similarly, the fault appears to cut across the major trend of the batholith itself, although this trend is harder to identify because of the unknown pre-faulting distribution of the batholithic rocks.

By using the type of fracture analysis elucidated by Anderson (1951, p. 7–21), no one orientation of principal stress axes can explain both the many fault orientations and the displacement patterns of faults in northern Baja California: San Andreas, Sierra Juárez–Sierra San Pedro Mártir alignment, San Miguel, and Agua Blanca (Fig. 1). Indeed, it would be most surprising if such an analysis, which is based on the premise of infinitesimal strain, were to apply *now* to a widespread system of faults that has had a history of finite displacement—perhaps even hundreds of miles on the master fault (Hill and Dibblee, 1953). It is more likely that the stress distribution would differ from block to block, controlled only in a most general way by the regional right-lateral "drift" across the San Andreas zone.

Large-scale right-lateral movement on the San Andreas fault must be meeting considerable opposition from the "great bend" where the fault crosses the Transverse Ranges, and the recent tectonic history of this area has necessarily been one of great complexity (Allen, 1957). Possibly the Agua Blanca and San Miguel faults represent the tendency to break *around* this "knot" on its south side, in the re-establishment of a straighter course between the San Andreas fault zone in the Gulf of California and the San Andreas fault zone in central California.

References Cited

Allen, C. R., 1957, San Andreas fault zone in San Gorgonio Pass, southern California: Geol. Soc. America Bull., v. 68, p. 315–350

Allen, C. R., Silver, L. T., and Stehli, F. G., 1956, Agua Blanca fault—a major transverse structure of northern Baja California, Mexico (Abstract): Geol. Soc. America Bull., v. 67, p. 1664

Allen, C. R., St. Amand, P., and Richter, C. F., 1958, Geologic structure and seismicity in southern California and adjacent areas (Abstract): Geol. Soc. America Bull., v. 69, p. 1672

Allison, E. C., 1955, Middle Cretaceous Gastropoda from Punta China, Baja California, Mexico: Jour. Paleontology, v. 29, p. 400–432

Anderson, E. M., 1951, The dynamics of faulting and dyke formation with applications to Britain, 2d ed.: London, Oliver and Boyd, 206 p.

Bailey, T. L., and Jahns, R. H., 1954, Geology of the Transverse Range province, southern California, p. 83–106 (Chapter 2) *in* Jahns, R. H., *Editor*, Geology of southern California: Calif. Div. Mines Bull. 170, 878 p.

Bandy, O. L., 1952, Foraminiferal evidence as to the age of the Pacific coast *Coralliochama* beds (Abstract): Geol. Soc. America Bull., v. 63, p. 1320–1321

Beal, C. H., 1948, Reconnaissance of the geology and oil possibilities of Baja California, Mexico: Geol. Soc. America Mem. 31, 138 p.

Böse, E., and Wittich, E., 1913, Informe relativo a la exploración de la región norte de la costa occidental de la Baja California: Inst. Geol. de México, Parergones, v. 4, p. 307–529

Brooks, B., and Roberts, E., 1954, Geology of the Jacuma area, San Diego and Imperial Counties, map sheet 23 *in* Jahns, R. H., *Editor*, Geology of southern California: Calif. Div. Mines Bull. 170, 878 p.

Buwalda, J. P. 1937, Shutterridges, characteristic physiographic features of active faults (Abstract): Geol. Soc. America Proc. 1936, p. 307

Carter, G. F., 1957, Pleistocene man at San Diego: Baltimore, Johns Hopkins Press, 400 p.

Cotton, C. A., 1957, Geomorphic evidence and major structures associated with transcurrent faults in New Zealand: Rev. geog. physique et geol. dynamique, v. 1, p. 16–30

Crowell, J. C., 1952, Probable large lateral displacement on San Gabriel fault, southern California: Am. Assoc. Petroleum Geologists Bull., v. 36, p. 2026–2035

Davidson, G., 1897, The submerged valleys of the coast of California, U. S. A., and of Lower California, Mexico: Calif. Acad. Sci. Proc., 3d ser., v. 1, p. 73–103

Durham, J. W., and Kirk, M. V., 1950, Age of the *Coralliochama* beds of the Pacific coast (Abstract): Geol. Soc. America Bull., v. 61, p. 1537

Emerson, W. K., 1956, Pleistocene invertebrates from Punta China, Baja California, Mexico: Am. Mus. Nat. History Bull., v. 111, p. 313–342

Emery, K. O., Butcher, W. S., Gould, H. R., and Shepard, F. P., 1952, Submarine geology off San Diego, California: Jour. Geology, v. 60, p. 511–548

Flores, T., 1931, Carta geológica de la Baja California: Cartas Geol. y Min. de la Rep. Mexicana, no. 1, 22 p.

Gutenberg, B., 1941, Mechanism of faulting in southern California indicated by seismograms: Seismol. Soc. America Bull., v. 31, p. 263–302

Hill, M. L., 1954, Tectonics of faulting in southern California indicated by seismograms: Seismol. Soc. America Bull., v. 31, p. 263–302

Hill, M. L., 1954, Tectonics of faulting in southern California, p. 5–13 (Chapter 4) *in* Jahns, R. H., *Editor*, Geology of southern California: Calif. Div. Mines Bull., 170, 878 p.

Hill, M. L., and Dibblee, T. W., Jr., 1953, San Andreas, Garlock, and Big Pine faults, California: Geol. Soc. America Bull., v. 64, p. 443–458

Hodgson, J. H., and Stevens, A., 1958, Direction of faulting in some of the larger earthquakes of 1955–56: Pub. Dominion Observatory, Ottawa, v. 19, no. 8

Jahns, R. H., 1954, Geology of the Peninsular Range province, southern California and Baja California, p. 29–52 (Chapter 2) *in* Jahna, R. H., *Editor*, Geology of southern California: Calif. Div. Mines Bull. 170, 878 p.

Larsen, E. S., Jr., 1948, Batholith and associated rocks of Corona, Elsinore, and San Luis Rey quadrangles, southern California: Geol. Soc. America Mem. 29, 182 p.

Larsen, E. S., Jr., Gottfried, D., Jaffe, H. W., and Waring, C. L., 1958, Lead-alpha ages of the Mesozoic batholiths of western North America: U. S. Geol. Survey Bull. 1070-B, p. 35–62

Lawson, A. C., *et al.*, 1908, The California earthquake of April 18, 1906: Carnegie Inst. Washington Pub. 87, v. 1, 451 p.

Lindgren, W., 1888, Notes on the geology of Baja California, Mexico: Calif. Acad. Sci. Proc., 2d ser., v. 1, p. 173–196

Mason, R. G., 1958, A magnetic survey off the west coast of the United States between Latitudes 32° and 36° N, Longitudes 121° and 128° W: Geophys. Jour., v. 1, p. 320–329

Meigs, P., 3d, 1935, The Dominican mission frontier of Lower California: Calif. Univ. Pub. Geog., v. 7, 192 p.

Menard, H. W., 1955, Deformation of the northeastern Pacific basin and the west coast of North America: Geol. Soc. America Bull., v. 66, p. 1149–1198

Menard, H. W., and Vacquier, W., 1958, Magnetic survey of part of the deep sea floor off the coast of California: Research Reviews (U. S. Office of Naval Research), June 1958, p. 1–5

Richter, C. F., 1956, Notes on Baja California earthquake of Feb. 9, 1956: Seismol. Soc. America Bull., b. 46, p. 161–162

Russell, R. J., 1932, Land forms of San Gorgonio Pass, Southern California: Calif. Univ. Pub. Geog., v. 6, p. 23–121

Santillán M., and Barrera, T., 1930, Las posibilidades petrolíferas en la costa occidental de la Baja California, entre los paralelos 30° y 32° de latitud norte: Anales del Instituto Geológia (Mexico), v. 5, p. 1–37

Shepard, F. P., and Emery, K. O., 1941, Submarine topography off the California coast; canyons and tectonic interpretation: Geol. Soc. America Spec. Paper 31, 171 p.

Shor, G. G., Jr., and Roberts, E., 1958, San Miguel, Baja California Norte, earthquakes of February, 1956: a field report: Seismol. Soc. America Bull., v. 48, p. 101–116

Silver, L. T., Stehli, F. G., and Allen, C. R., 1956, Lower Cretaceous pre-batholithic rocks of northern Baja California, Mexico (Abstract): Resumenes de los Trabajados Presentados, p. 30

—— in press, Lower Cretaceous pre-batholithic rocks of northern Baja California, Mexico: XX Congreso Geológico International

Townley, S. D., and Allen, M. W., 1939, Descriptive catalog of earthquakes of the Pacific coast of the United States, 1769 to 1928: Seismol. Soc. America Bull., v. 29, p. 1–297

Walton, W. R., 1955, Ecology of living benthonic Foraminifera, Todos Santos Bay, Baja California: Jour. Paleontology, v. 29, 952–1018

Wilson, I. F., and Rocha, V. S., 1955, Geology and mineral deposits of the Boleo copper district, Baja California, Mexico: U. S. Geol. Survey Prof. Paper 273, 134 p.

Wisser, E., 1954, Geology and ore deposits of Baja California, Mexico: Econ. Geology, v. 49, p. 44–76

Woodford, A. O., and Harriss, T. F., 1938, Geological reconnaissance across Sierra San Pedro Mártir, Baja California: Geol. Soc. America Bull., v. 49, p. 1297–1336

Div. Geological Sciences, Calif. Inst. Technology, Pasadena, Calif.; Div. Geological Sciences, Calif. Inst. Technology, Pasadena, Calif.; Pan American Oil Co., Tulsa, Okla.

Manuscript Received by the Secretary of the Society, June 5, 1959

Contribution No. 921, Division of the Geological Sciences, California Institute of Technology

BULLETIN OF THE GEOLOGICAL SOCIETY OF AMERICA
VOL. 71, PP. 483-496, 1 FIG., 4 PLS. APRIL 1960

FOOTHILLS FAULT SYSTEM, WESTERN SIERRA NEVADA, CALIFORNIA

BY LORIN D. CLARK

ABSTRACT

A large fault system, here named the Foothills fault system, is the dominant structural feature of the western Sierra Nevada. The steeply dipping to vertical component faults trend northwestward through an area about 200 miles long and 30 miles wide north of 37°30′ north latitude. The faulted Paleozoic and Mesozoic rocks are overlapped by unfaulted younger rocks, and the total extent of the fault system is not known. It is probably not limited to the western Sierra Nevada. Faults are marked by belts as much as 4 miles wide of cataclastically deformed and recrystallized rocks and by truncated folds. Along one fault, Upper Jurassic rocks are juxtaposed against Paleozoic rocks for at least 100 miles. The direction of fault movement has not been determined. Net displacement on some of the component faults exceeds 3000 feet and may be measurable in miles. Major faults cut beds of Late Jurassic age and are in turn cut by plutonic rocks of probable Late Jurassic and Middle Cretaceous age. Faults that controlled deposition of quartz veins and gold ore bodies of the Mother Lode belt are apparently younger and structurally less important features superimposed on one of the fault zones of the large system.

CONTENTS

TEXT

	Page
Introduction	483
General geology	486
Foothills fault system	486
General statement	486
Relationship of serpentine to fault zones	488
Relationship of fault zones to plutonic rocks	488
Internal structures of fault zones	489
Gross structure	489
Planar structures	489
Fragmental structures	490
Lineation	491
Direction, sense, and amount of movement	491
Mother Lode fissure system	493
Age of faulting	494
References cited	495

ILLUSTRATIONS

Figure	Page
1. Index map of northern California showing location of Foothills fault system and its areal relationship to large faults in the Coast Ranges and Klamath Mountains	484

Plate	Facing page
1. Outline geologic map of the western Sierra Nevada, California, showing faults of the Foothills fault system	483
2. Structures of rocks outside of and within fault zones	490
3. Photomicrographs of sheared rocks	491
4. Geologic cross sections, western Sierra Nevada, California	496

INTRODUCTION

This paper provides a brief preliminary description of a large fault system that profoundly affects the distribution of metamorphic rocks in the western Sierra Nevada. One of the component fault zones has been recognized previously in part. The large fault system, here referred to as the Foothills fault system, is exposed in an area 200 miles long and 30 miles wide extending north-northwestward from about latitude 37°30′ north to latitude 40° north (Fig. 1). The region includes the linear Mother Lode belt, extending from Mariposa to a point north of Placerville (Pl. 1), and other gold-mine areas farther north. The Foothills copper belt lies west of most of the gold deposits. Available evidence of the direction of movement on faults of the Foothills system is inconclusive. More information will become available as field work progresses.

Segments of some components of the Foothills fault system have been mentioned briefly in the literature, and a structure identified as the Mother Lode mineralized fault, corresponding

in part with the Melones fault zone of this report, appears on the tectonic map of the United States (King and others, 1944). Nevertheless, structurally less important faults that control the position of the gold ore bodies have been emphasized in discussions of the structural geology as well as the economic geology of parts of the region. New data now permit recognition of other major faults of the Foothills system and also allow a clearer distinction between the Foothills faults and structures that control the gold ore bodies and quartz veins of the Mother Lode belt.

Aside from early miners who believed there was a single, continuous Mother Lode, Knopf (1929) was the first to refer to a major throughgoing fault in the western Sierra Nevada. Speaking of the quartz veins of the Mother Lode belt, he said, "In places there is evidence that the veins occupy auxiliary fractures in a zone parallel to a great reverse fault" (Knopf, 1929, p. 46). This interpretation resulted from

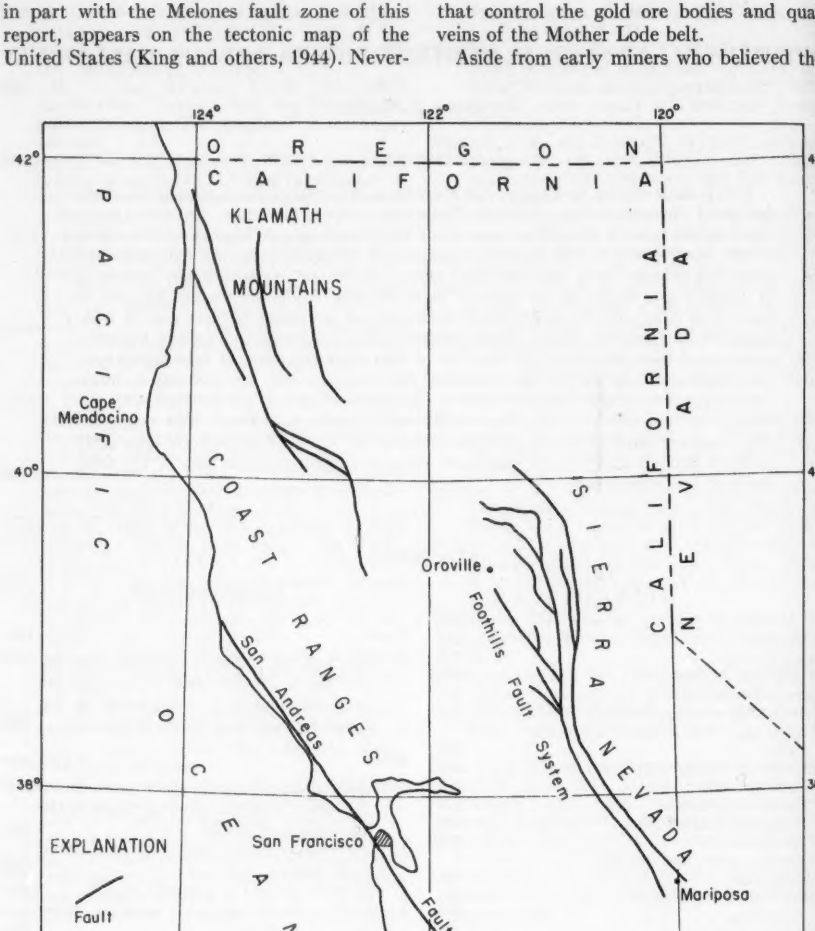

FIGURE 1.—INDEX MAP OF NORTHERN CALIFORNIA SHOWING LOCATION OF FOOTHILLS FAULT SYSTEM AND ITS AREAL RELATIONSHIP TO LARGE FAULTS IN THE COAST RANGES AND KLAMATH MOUNTAINS

(Klamath Mountains faults after Irwin, in press)

Knopf's recognition (1929, p. 46, Fig. 3) of a wide belt of greatly sheared rocks exposed about 1 mile east of the outcrops of gold-bearing quartz veins at Plymouth and Jackson (Pl. 1). Knopf's descriptions and illustrations of the quartz veins and their relationship to wall rocks provide the basis for the discussion of the relationships between the veins Knopf studied and a fault of the Foothills system given later in this paper. Ferguson and Gannett (1932, p. 20–21, 70) recognized in the Alleghany district a major fault that lies on the projection of the strike of the large fault in the Mother Lode belt mentioned by Knopf and speculated that these two segments might form parts of a single continuous structure. Ferguson and Gannett (1932, p. 22, 70) distinguished clearly between the major fault and faults of less structural importance that control the gold-quartz veins in the Alleghany district.

Knopf (1929) interpreted both the major fault and faults related to the Mother Lode fissure system as dip-slip reverse faults. Ferguson and Gannett (1932) described the major fault in the Alleghany district as a reverse fault but presented no conclusion regarding the direction of net slip. Taliaferro (1942, p. 90) speaks of a major fault as the Mother Lode thrust. D. K. Chandra (1953, unpub. Ph.D. thesis, Univ. of Calif.) has mapped as thrusts three faults near Colfax which coincide in part with elements of the Foothills fault system. Neither Taliaferro nor Chandra discuss the problem of determining the orientation of net slip. Cloos (1932b, p. 392–394; 1935, p. 234) discussed chiefly faults that controlled the quartz veins of the western Sierra Nevada and compared these faults to marginal thrusts related to batholiths. Cloos (1935, p. 238, 247) also, however, identified a long continuous fault as the "Mother Lode proper" and stated that "It seems possible that movement along this fault began long before intrusion of the larger batholithic masses."

In this paper, the term "Mother Lode" will be used to designate the quartz veins and gold ore bodies of the Mother Lode geographic belt rather than the major fault zone of the Foothills system that passes through the Mother Lode belt. This is consistent with early usage: Turner and Lindgren (1894) define the Mother Lode as "a belt of parallel though sometimes interrupted quartz-filled fissures," and Knopf used the term "Mother Lode system" to include the quartz veins and the structures that control them. It is not consistent with later usage that identifies a long continuous fault zone by the name "Mother Lode". The earlier usage is preferable because the temporal and genetic relationships between the Mother Lode fissures and the major fault zone are not yet adequately understood, and investigation of these relationships will be better served by a nomenclature that distinguishes between them than by one that tends to confuse them.

The material presented here was obtained during investigations by the U. S. Geological Survey in co-operation with the California Department of Natural Resources, Division of Mines. During early phases of this work, areal mapping near San Andreas and west of Angels Camp (Pl. 1) by Arvid A. Stromquist, Donald B. Tatlock, and the writer produced evidence of the existence of two distinct fault systems in that part of the Mother Lode region. During a later phase of the work the extent and pattern of the Foothills fault system were determined by reinterpretation of existing geologic maps on the basis of new structural and stratigraphic data gained by detailed mapping of geologic cross sections at intervals along the western Sierra Nevada. The cross sections were mapped in the canyons of the major streams of the region, which cross the geologic structure about at right angles and provide nearly continuous exposures. During about 16 months of field work, sections were mapped along all rivers from the Merced to the Middle Fork of the Yuba, inclusive. C. D. Rinehart, E. H. Pampeyan, N. K. Huber, J. A. Pitkin, and H. G. Stevens participated in this phase of the investigation. The author did reconnaissance of the fault zones in other parts of the area. Existing geologic maps have been used to project faults mapped in the cross sections through intervening areas.

The series of geologic folio maps prepared by Lindgren, Turner, and Ransome (Turner, 1894; 1897; 1898; Turner and Ransome, 1897; 1898; Lindgren, 1894; 1900; Turner and Lindgren, 1894; Lindgren and Turner, 1895; Ransome, 1900) covers nearly the entire area underlain by metamorphic rocks in the western Sierra Nevada and provided data on the greatest part of the area between traverse lines of the present investigation. These maps do not show faults, but rock types are differentiated sufficiently to allow rather certain recognition of the fault zones between areas studied in detail. More recent maps used to fill in the pattern of the fault system are those of Eric, Stromquist, and Swinney (1955, Pl. 1 and 2)

and Taliaferro and Solari (1949). The latter map, including the vicinity of Copperopolis, shows some of the component faults of one of the fault zones of the Foothills system.

Knopf (1929) has described some of the rocks of the Mother Lode belt as well as the ore deposits. Eric, Stromquist, and Swinney (1955) have described rocks of the part of the area lying between Sonora and Angels Camp, and Clark (1954) has described Paleozoic rocks exposed in a small area east of San Andreas. Diller (1908) and Durrell and Proctor (1948, p. 170–175) discuss the lithology and stratigraphy of metamorphic rocks in the extreme northeastern part of the region. Taliaferro (1942, p. 96) has presented a concise summary of geologic events in the western Sierra Nevada.

General Geology

The western Sierra Nevada is underlain largely by metamorphic rocks of Paleozoic and Mesozoic age. These rocks nearly everywhere dip steeply and are but sparsely fossiliferous. In the southern part of the region the most extensive Paleozoic rocks are black carbonaceous phyllite and schist with thinly interbedded metachert, but lenses of mafic volcanic rocks and limestone are widespread and locally attain thicknesses of several thousand feet. In the northern part of the region, mafic volcanic rocks, slate, and felsic tuff constitute about equal parts of the Paleozoic section; chert is abundant locally, but limestone is rare. Most of the Paleozoic rocks have been referred to the Calaveras formation, but those in the vicinity of the American River were divided into five formations (Lindgren, 1900). The Mesozoic section is characterized by alternating belts, each generally several miles wide, of mafic volcanic rocks and sedimentary rocks, chiefly slate and graywacke. All the Paleozoic and Mesozoic rocks have been metamorphosed, but the metamorphism is of low grade in most of the region, particularly west of the Melones fault zone (Pl. 1). Although cleavage is present in nearly all the rocks (Pl. 2, fig. 1), original structures such as graded bedding and delicate cross-lamination are well preserved in much of the region, particularly west of the Melones fault zone. Within the fault zones described herein, the amount of recrystallization and cataclastic deformation is notably greater than it is beyond the limits of the fault zones (Pl. 2, fig. 2).

The distribution of Mesozoic and Paleozoic metamorphic rocks can be stated only in general terms—the ages of rocks in some areas of considerable size in the northern part of the region are not well enough established to permit delineation on Plate 1. South of Placerville, rocks of Paleozoic age are confined to the area east of the Melones fault zone except for a narrow belt exposed between the Melones and Bear Mountains fault zones west of Jackson. North of Placerville, rocks of Paleozoic age likewise underlie most of the area east of this fault zone but also underlie large parts of the area west of the Melones fault zone at least as far westward as Auburn. In the southern half of the region, rocks of Mesozoic age are restricted to areas west of the Melones fault zone, but in the northern half of the region they are also present near the east side of the belt underlain by metamorphic rocks.

Ultramafic rocks form elongate bodies within and adjacent to major fault zones of the region; they intrude both Paleozoic and Mesozoic metamorphic rocks. By far the most abundant is serpentine, but some of the larger bodies contain some peridotite, pyroxenite, and dunite. Some of the serpentine has been altered to schists composed of talc, antigorite, and ankerite in various proportions. Most of the serpentine consists of faceted blocks with polished and commonly pronouncedly lineated faces, but some serpentine is schistose and some massive.

The metamorphic rocks and serpentine have been intruded by a number of isolated small granitic plutons and by the Sierra Nevada batholith. Most of the plutons west of the Melones fault zone range from gabbro to quartz diorite, whereas most of the Sierra Nevada batholith ranges from granodiorite to granite. The more mafic rocks west of the Melones fault zone apparently constitute a series of intrusions that is distinctly older than the Sierra Nevada batholith, which is about Middle Cretaceous.

Foothills Fault System

General Statement

The group of faults shown on Plate 1 is here named the Foothills fault system for its occurrence on the lower western slopes of the Sierra Nevada, a region widely known as the Sierra Foothills. The name Mother Lode is reserved to designate structures more directly related to gold deposits. Faults of the Foothills

system truncate major folds and regional trends of the metamorphic rocks. The faults dip steeply, as indicated by the attitudes of schistosity within the fault zones and by the straight traces of the zones across rugged topography. Schistosity and shearing within the fault zones in most places dip eastward more than 80° and are commonly vertical but in some places dip eastward as gently as about 70°.

South of the Cosumnes River, the Foothills fault system consists principally of two northwestward-trending fault zones. The easternmost zone, coinciding throughout part of its length with the Mother Lode belt, is here named the Melones fault zone after the mining town of Melones on the Stanislaus River. The westernmost is here named the Bear Mountains fault zone for a group of prominent northwestward-trending ridges about 9 miles west of Angels Camp (Pl. 1). North of the Cosumnes River, the Melones fault zone can be identified as far as pre-Cretaceous bedrock is exposed. West of this fault zone the Foothills fault system between the Cosumnes River and the Middle Fork of the Feather River consists of unnamed northward-trending and northwestward-trending components which form a braided pattern. Near the north end of the area of exposed bedrock, some of the fault zones turn sharply westward.

Exposures of the Foothills fault system are bounded on the north and west by overlapping younger rocks, and the system may be much more extensive than shown on Plate 1; it possibly extends through the western Klamath Mountains into southwestern Oregon (Fig. 1). At the northwest end of the region shown on Plate 1, faults of the Foothills system pass under nearly flat-lying deposits of Late Cretaceous and Tertiary age that overlap the metamorphic rocks. The strike of the Foothills faults here is toward a group of faults recognized by Irwin (in press) in the western Klamath Mountains (Fig. 1). Younger rocks conceal those cut by major faults for about 70 miles between the western Sierra Nevada and the Klamath Mountains. Little of the Klamath Mountains region has been mapped in detail, but what is known of the region indicates that its history of deposition, volcanism, deformation, and plutonic intrusion is similar to that of the western Sierra Nevada. Wells and Walker (1953) have mapped and described steep reverse faults very much like those of the western Sierra Nevada in the Galice area of southwestern Oregon. They did not determine the direction and amount of displacement on these faults.

The southward extent and width of the Foothills fault system likewise have not been determined. The Melones fault zone is cut south of Mariposa by a younger intrusive mass (Cloos, 1932a), presumably a lobe of the Sierra Nevada batholith, but may extend through the metamorphic rocks that underlie much of the western Sierra Nevada southeast of this pluton. These metamorphic rocks have been mapped in detail in only a few small areas. The southeastward extent of the Bear Mountains fault zone is unknown, but R. J. P. Lyon (1954, unpub. Ph.D. thesis, Univ. of Calif.) described a prominent shear zone near the place where the Bear Mountains fault zone intersects the south boundary of Plate 1 which indicates that it extends southeast beyond this point.

The great width of the Foothills fault system relative to the width of the exposed belt of metamorphic rocks suggests that other elements of the system may be concealed beneath the unconsolidated deposits of the Central Valley. On the east, too, the fault system may not be so sharply limited as suggested by Plate 1, for although only a single large fault is indicated east of the Melones fault zone, the absence of mapped faults may result from a scarcity of marker horizons, poor exposures, and general lack of detailed mapping in this part of the region.

Most of the "faults" shown on Plate 1 are a complex of smaller faults and shear zones and are more properly referred to as fault zones. Other faults have been indicated along boundaries of serpentine bodies where these have been found to mark the position of major stratigraphic discontinuities. The shear zones are distinguishable from bordering and less deformed rocks of the same original character by pronounced schistosity, cataclastic structure, and crumpling. Boundaries of the fault zones are marked by structural or stratigraphic discontinuity, a transition from sheared to unsheared rocks, or a combination of these. The sheared rocks of the fault zones are about as well exposed as the unsheared slates and phyllites of the bedrock sequences, and both the shear zones and the belts underlain by slate and phyllite are ordinarily marked by topographic depressions. The fault zones are generally well exposed in canyon bottoms and beds of larger tributary streams. Stream-polished exposures provide excellent opportu-

nities for study of detailed structure of the sheared rocks.

Widths of the fault zones range widely. Near the North Yuba River (Pl. 1), for example, rocks are greatly deformed between Downieville and the easternmost belt of serpentine in the Melones fault zone, a distance of about 3 miles, as well as between the two serpentine bodies west of Downieville. Along the North Fork of the Feather River, on the other hand, deformation of metamorphic rocks resulting from movement along the Melones fault zone is restricted to a belt about 1000 feet wide southwest of the serpentine body. Bedding is clearly distinguishable in metamorphic rocks within a few feet of the northeast side of the serpentine. In most places shear zones associated with Foothills faults are at least several hundred feet wide. Only rarely are they less than about 200 feet wide.

Relationship of Serpentine to Fault Zones

The Foothills fault system is well delineated by the serpentine bodies first mapped by Lindgren and Turner and shown on Plate 1. The pattern is accentuated by many smaller bodies found by more detailed mapping. Most previous authors (*for example*, Taliaferro, 1942, p. 94; Cater, 1948, p. 38–39) have held that the serpentine, or rock from which it was derived, was intruded as sills into beds that were subsequently folded. Ferguson and Gannett (1932, p. 21–22), on the other hand, suggested that the emplacement of serpentine in the Alleghany district was controlled by pre-existing faults. Data collected during this investigation support the thesis that emplacement of the serpentine was controlled by major faults. Bailey (1946, p. 211) has demonstrated a similar relationship of serpentine to faults in part of the Coast Ranges of California.

The serpentine and fault zones are geographically close (Pl. 1). Most of the serpentine is within major fault zones mapped on the basis of intensely deformed rocks and stratigraphic discontinuity. Some bodies, such as the large mass 9 miles southwest of Sonora and the smaller mass northwest of Mariposa, extend beyond the limits of fault zones into unsheared rocks and may be in part sills, but even such bodies are contiguous on one side with a fault zone. The structural setting of a few small serpentine bodies shown on Plate 1 is unknown, but serpentine has not been found in unsheared rocks at a distance from fault zones in areas that have been mapped in detail.

An alternate possibility is that ultramafic rocks, originally emplaced as sills, controlled the locus of subsequent faulting. Serpentine is an excellent substance for lubricating slip zones, and the presence of much schistose and slickensided serpentine attests to considerable shearing of the serpentine. Nevertheless, there is little to suggest that fault movements in the western Sierra Nevada have been effectively localized by serpentine. On the contrary, metamorphic rocks are greatly deformed for considerable distances beyond the limits of serpentine bodies both along and across the strike of serpentine masses and fault zones. The belts of sheared metamorphic rocks beside a serpentine body may be only 200 feet wide, but in most places they are much wider and may even be measurable in miles, as in the Melones fault zone near the North Yuba River. Serpentine certainly has not controlled the regular pattern of the fault zones, for in some it is not present in significant amounts for intervals of several miles.

Relationship of Fault Zones to Plutonic Rocks

Faults of the Foothills system are younger than two plutons but older than other plutons at localities that have been examined. A pluton emplaced prior to or during fault movement is exposed east of the Melones fault zone in the vicinity of the Cosumnes River. The western boundary of the pluton is nearly straight, indicating either that it has been truncated by fault movements or that the fault zone limited its westward spread during emplacement. Nevertheless, the pluton was certainly intruded before fault movement ceased, for the granitic rock has been transformed into a pronouncedly lineated schist composed of saussurite, quartz, and hornblende for a distance of more than 1 mile east of its western border. Farther east the granitic rock of this pluton is massive and unaltered.

Unlike the pluton near the Cosumnes River, the western part of a pluton near the Mokelumne River that shows a nearly straight western contact is only weakly and locally schistose, although it coincides with the Melones fault zone. Small exposures of schistose metavolcanic rocks and hornblende-rich gneiss on the banks of the Mokelumne River immediately west of the pluton suggest a shear zone at the contact. Eric, Stromquist, and Swinney (1955, p. 27) have noted a shear zone indicating postemplacement fault movement at the west

side of a gabbro pluton in the Melones fault zone about 5 miles southwest of Sonora.

Cloos (1932a, p. 301, 303) has shown that crystallization of the pluton that cuts the Melones fault zone southeast of Mariposa is younger than significant fault movements, although he holds that structures within the pluton indicate fault movements prior to solidification. Elsewhere the age relationships of plutonic rocks and fault zones are established by the contact aureoles developed in some of the fault zones. Aureoles showing isotropic textures resulting from contact metamorphism superimposed on earlier planar and linear structures developed during fault movements are well exposed in the banks of the American River near Folsom and in the South Fork of the Yuba River northwest of Nevada City. The granitic rocks show no evidence of shearing or recrystallization at either locality, and narrow granitic dikes in the contact zones show no evidence of deformation or recrystallization. On Plate 1, a fault zone has been indicated along the entire western side of the pluton that underlies Nevada City, on the assumption that the exposures in the South Yuba River are representative. The contact has not been studied farther north, and the pluton may have transgressed the fault zone in some places.

Internal Structures of Fault Zones

Gross structure.—Except for the ultramafic rocks, the rocks within the fault zones were derived from lithologic units exposed outside the fault zones. Those within the fault zones are generally more deformed, with attendant development of foliation, lineation, fragmental textures, and fluxion structures.

Fault zones are characterized by discontinuity of lithologic types resulting from the juxtaposition of blocks derived from different formations, as Heyl (1947) has pointed out. In places, large blocks are separated by relatively narrow component faults that form a braided pattern within a general belt referred to a single fault zone in this report. In the Alleghany district, Ferguson and Gannett (1932, Pl. 1) succeeded in mapping formations in blocks about 1 mile wide and more than 4 miles long situated between elongate belts of serpentine here interpreted to mark component faults of the Melones fault zone. A still larger isolated block, about 10 miles long and as much as 2 miles wide, extends from south of the Stanislaus River to a point northwest of Angels Camp in the Melones fault zone.

Smaller blocks, isolated in wide belts of strongly deformed rock, fall more readily into the category of horses. Eric and Stromquist (*in* Eric, Stromquist, and Swinney, 1955, Pl. 1) have mapped a thin, lenticular block of limestone about 1 mile long, probably derived from the Calaveras formation, near the west side of the Melones fault zone southwest of Angels Camp, and Stromquist (Written communication, 1953) has mapped a larger isolated body composed of limestone and other rocks characteristic of the Calaveras formation within the Melones fault zone about 2 miles south of San Andreas. Both localities are several miles distant from exposures of similar rocks outside the fault zone.

Eric, Stromquist, and Swinney (1955, p. 15) have described several areas of metavolcanic rocks with well-preserved original textures within the Melones fault zone. These areas are surrounded by schistose metavolcanic rocks and may be horses of different age than the surrounding schist or they may indicate the existence of some sort of pressure shadows in which original structures of the rocks were preserved.

Planar structures.—Structures resulting from recrystallization are more prominent than those resulting from cataclastic deformation in the metavolcanic rocks in the fault zones. Most of the metavolcanic rocks are schist, but some are massive. Most originally argillaceous rocks are altered to phyllite and schist, but some have developed fragmental structures (Pl. 3, fig. 2). Schistose metavolcanic rocks may be readily examined in roadside exposures in the western part of the Bear Mountains fault zone between the Stanislaus and Calaveras rivers, in the Melones fault zone along State Highway 49 between Angels Camp and Jackson, and in an unnamed fault zone south of Auburn at the State Highway 49 bridge across the American River. Volcanic breccia texture is preserved in some of this schist, but in a greater part original textures have been destroyed. Probably most of the schist that lacks relict original texture was tuff; tuff is more abundant than volcanic breccia in the less altered volcanic sequences outside the fault zones. Fragments in the schistose volcanic breccia are commonly massive but are flattened and elongate. Schistosity of the enclosing material is molded around the fragments. In most places, the schistosity within the fault zones is not deformed, but tightly crumpled chloritic schist probably derived from volcanic

rocks is exposed along the North Yuba River west of Downieville and in the eastern part of the Melones fault zone along the Bear River. Fluxion structure is a characteristic feature of shear-zone rocks of fragmental character. In both outcrops and thin sections, fluxion structure is much more commonly indicated by schistosity or cleavage and parallel arrangement of fragments than by trains of fragments, although trains have been found.

Fragmental structures.—Fragmental structures of cataclastic origin are abundant in the shear zones. These structures show a wide variety depending on the size distribution, size range, and packing of the fragments. Most fragments of megascopic size are flattish and rounded or lenticular in cross section; a few are nearly equidimensional, and some are angular. Microscopic fragments are commonly nearly equidimensional and angular (Pl. 3, fig. 1). These breccias reflect much more translation than the fault breccias in faults of moderate displacement, characterized by closely packed, angular fragments separated by voids or a mineral filling.

Very coarse fragmental rock forms a zone more than 200 feet wide in the western part of the Melones fault zone near the North Fork of the American River. The rock consists of flattish blocks of light-green, fine-grained, weakly schistose rock about 1 foot to 10 feet long and embedded in black, aphanitic phyllite with intermixed smaller fragments of the same kind of rock. The over-all aspect of the outcrop is much like that of the thin section (Pl. 3, fig. 1), although on a much larger scale. Blocks more than 1 foot long are generally separated from one another by seams of black phyllite a few inches to 3 feet thick, and the blocks compose less than half of the area of a cliff face normal to the schistosity. In thin section, the fragments are seen to be felsic porphyritic metavolcanic rocks with phenocrysts of quartz and plagioclase in a microcrystalline groundmass containing abundant fibrous amphibole. The black phyllite is composed of finely milled fragments of these rocks and their phenocrysts together with an unidentified black, opaque material.

Gross augen structure is also apparent east of the easternmost serpentine in road cuts along the North Yuba River. Here blocks of massive or weakly schistose rock are separated from one another by seams, commonly more than 1 foot wide, of phyllite or schist derived from rock similar to that forming the blocks (Pl. 2, fig. 2).

Near the Bear River, a belt about 1 mile wide at the western side of the Melones fault zone consists of blocks of chert and greenstone separated by septa of black carbonaceous phyllite and tectonic breccia. Many thin seams of schistose serpentine are also present. The greenstone and chert fragments range from microscopic to blocks several tens of feet long. Fragments of small and intermediate size are commonly streamlined or lens-shaped in cross section, but in this location no linear pattern was observed. Foliation of the phyllite and serpentine is molded around the fragments. Contorted bedding is preserved in some of the larger chert blocks, and some of the greenstone retains relict pyroclastic textures and amygdales, but original textures and structures have been destroyed in most of the fragments. Some blocks contain irregular seams or dikes of intrusive tectonic breccia derived from the material surrounding the blocks. The chert fragments consist of granoblastic microcrystalline quartz, cut by closely spaced slip surfaces marked by planes of mica. Thin partings of slaty material show that in some places the chert is intricately crumpled between slip surfaces. In thin sections it can be seen that in some places even phyllite composed almost solely of sericite has been broken into tiny fragments (Pl. 3, fig. 2).

The exposures described in the preceding

PLATE 2.—STRUCTURES OF ROCKS OUTSIDE OF AND WITHIN FAULT ZONES

FIGURE 1.—Bedding and cleavage at crest of anticline exposed along the Cosumnes River 5 miles east of west end of Cosumnes River section (Pl. 4). Bedding, prominent on fresh surfaces, is slightly arched. Cleavage, prominent in weathered parts of exposure, dips about 60° to the right (east). Photograph area is about 25 feet wide.

FIGURE 2.—Greatly sheared metavolcanic rocks in Melones fault zone showing gross augen structure. Both massive blocks and the schist separating them are derived from the same original material. Camera bag is 11 inches wide. Road cut on north side of North Yuba River 2 miles southwest of Downieville.

FIGURE 1

FIGURE 2

PHOTOGRAPHS SHOWING STRUCTURES OF ROCKS OUTSIDE OF AND WITHIN FAULT ZONES

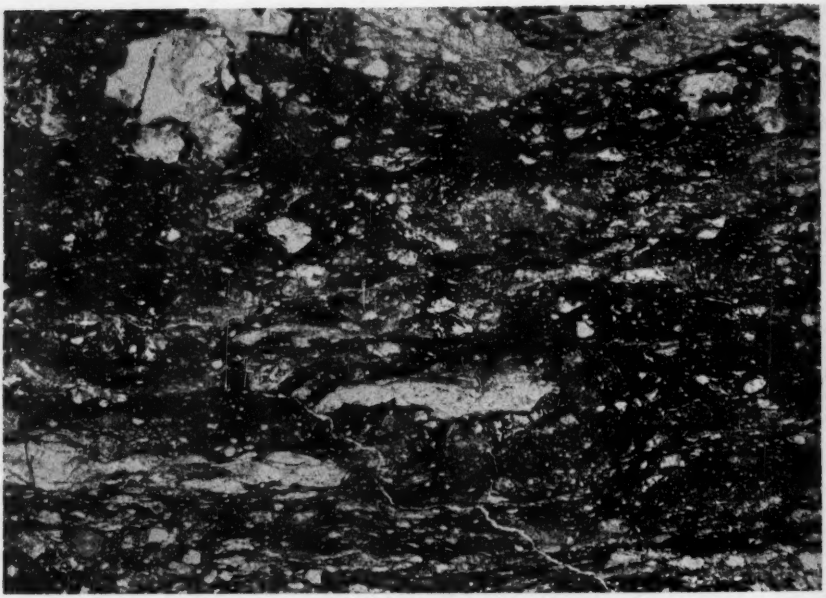

FIGURE 1 1mm

FIGURE 2 2mm

PHOTOMICROGRAPHS OF SHEARED ROCKS

paragraph constitute the Relief formation as mapped by Lindgren (1900) in the vicinity of the Bear River. This unit is shown on the Colfax folio (Lindgren, 1900) to underlie a notably straight belt about 1 mile wide and 10 miles long, extending about from the Bear River to the South Yuba River. The Bear River exposures suggest that the Relief formation as mapped by Lindgren is a fault zone containing deformed rocks derived from other formations, rather than a stratigraphic unit.

In parts of the Melones fault zone along the North Yuba River, the greenstone, composed largely of epidote and chlorite, is brecciated, but this rock differs from that in exposures previously described in that megascopic fragments constitute more than 95 per cent of any particular exposure. The rock consists of fragments of greenstone many feet to microscopic in size, separated by seams of black phyllite as much as 1 foot thick. The seams are composed of chlorite and sericite or talc with a small proportion of fine rock fragments. Fragments are angular to elliptical.

Not all the fragmental rocks in the fault zones are of cataclastic origin: some are conglomerates and sandstones of sedimentary origin, although at many localities cataclastic structures have been superimposed on the original structures of these rocks. Evidence suggests that most of the conglomerates in the region are polymictic (Pettijohn, 1949, p. 208)—they contain clasts of many different rocks, whereas the clasts in the tectonic breccias are derived from one or two rocks. Polymictic conglomerates included with the Cosumnes and Mariposa formations of Jurassic age are in contact with fault zones throughout much of the western Sierra Nevada, and those of Mariposa formation, at least, form blocks within the Melones fault zone. Similar conglomerate forms part of the Kanaka formation (Ferguson and Gannett, 1932, p. 7–12), of Carboniferous age, which lies between the two branches of the Melones fault zone in the Alleghany district, north of the Middle Yuba River. The degree of lithologic variety shown by the clasts does not necessarily, however, provide a reliable criterion for distinguishing between rocks of cataclastic and epiclastic origin. Small lenses of monolithologic intraformational breccia are present in the region, and possibly cataclastic breccias with a considerable variety of clasts might be formed in some circumstances. A problem of origin is also posed by some blocks of quartz-feldspar rock with well-developed cataclastic texture. When sufficiently milled, it is difficult or impossible to establish whether these were derived directly from granitic rock or from arkose, such as that forming minor parts of the Blue Canyon formation, of Carboniferous age.

Lineation.—Lineations within the fault zones lie in the plane of schistosity and rake nearly down-dip. In most places they plunge southeast, but in some places they plunge northeast. Lineation is formed most commonly by elongate fragments such as the clasts in volcanic breccia and in conglomerate. Most of these clasts are flat triaxial ellipsoids. Most show no evidence of having been rolled, but a fragment on a sawed face normal to lineation of one of the few conglomerates that was closely examined shows "snowball" structure. Lineation, parallel to the fragments, is also formed in the volcanic rocks by thin elongate pods of chlorite. Pronounced lineation in the sheared granitic rock exposed west of the Melones fault zone in the vicinity of the Cosumnes River is formed by stubby amphibole crystals. Steeply plunging pencil structure is formed by intersecting cleavages in a thin tongue of serpentine in the Bear Mountains fault zone exposed on the banks of the Stanislaus River.

Direction, Sense, and Amount of Movement

Direct evidence of the direction and sense of movement along the Foothills fault system and its individual elements has not yet been found.

PLATE 3.—PHOTOMICROGRAPHS OF SHEARED ROCKS

FIGURE 1.—Fine-grained tectonic breccia from Melones fault zone along the North Fork of the American River. Clear white grains are quartz; textured grayish grains are felsic metavolcanic rocks and feldspar. Dark matrix is composed of minute fragments of these rocks and minerals plus extremely fine-grained opaque material. Note broken quartz grain in upper-left corner. Plain light.

FIGURE 2.—Tectonic breccia derived from slate and chert. West side of Melones fault zone on Bear River. Scattered white fragments are metachert. Light- to dark-gray fragments are sericite slate. Black, opaque material on slip surfaces. Plain light.

Data suggest that the Foothills is a strike-slip fault system, but more study will be necessary to determine the orientation of net slip in anything approaching a satisfactory manner. Scarcity of evidence results in part from an inadequate knowledge of the stratigraphy of the region, the abundance of such lithologic types as slate and mafic volcanic rocks throughout the stratigraphic section, and near-parallelism of faults and bedding in much of the region. In part, too, it probably results from the fact that the amount of displacement, although unknown, is large enough so that corresponding points on opposite sides of a fault zone have not been revealed by areal mapping to date. Probably if displacement had amounted to only a few hundred or even a few thousand feet, at least its order of magnitude would already be known. The Bear Mountains and Melones fault zones in the southern part of the region have apparent reverse displacement as shown by the presence of the older rocks on the eastward or hanging-wall sides. In the northern part of the region, even the age relationships of the rocks on opposite sides of most of the component faults are unknown. Deep erosion since the latest significant movement of the Foothills faults has destroyed any physiographic evidence of the orientation and amount of net slip.

Although the Foothills faults are continuous for great distances and are straight throughout much of their length, they are more sinuous than previously described strike-slip faults. The areal pattern of the Foothills fault system somewhat resembles elements of a fracture system developed in a clay model under clockwise rotational (approximately right-lateral) deformation in an experiment performed by Cloos (1955, Pl. 2, fig. 3). The sinusoidal pattern developed by a prominent group of fractures in the clay model is a mirror image of the main elements of the Foothills fault system. Possibly part of the sinuosity may result from regional warping subsequent to fault movement, for although the Foothills fault system has been inactive since Late Jurassic time, it occurs within the circum-Pacific belt in which orogenic activity has been pronounced during Cretaceous and Tertiary time.

The steeply plunging lineations characteristic of the fault zones are probably parallel to the *b* tectonic axis. Observations of fold axes within the fault zones are too few to establish adequately the relationship of lineations to minor folds, but outside of fault zones, where more minor folds were found, lineations produced by parallel chlorite blebs and elongate conglomerate pebbles are consistently parallel to axes of steeply plunging minor folds. These steeply plunging lineations and minor folds are superimposed on structures related to the major folds of the region, which are characterized by nearly horizontal axes.

Cloos and Compton also have found evidence of strike-slip deformation in the minor structures of rocks near faults of the Foothills system at two widely separated localities. Cloos (1932b, p. 391–392), on the basis of his observations of feather joints, suggested right-lateral deformation in the western Sierra Nevada. Compton (1955, p. 14–16), in his study of the pluton crossed by the South Fork of the Feather River, interpreted here to lie between two major fault zones, describes a steeply dipping slip cleavage that has a large horizontal component. Lying within the plane of the slip cleavage is a lineation consisting of parallel actinolite crystals, mineral smears, and elongate fragments formed by the intersection of slip-cleavage surfaces or by curved slip-cleavage surfaces. Compton (1955, p. 15–16, 43) apparently regards these as *b* lineations. The minor folds in this area also plunge steeply (Compton, 1955, p. 14). Compton believes the slip cleavage and lineations are related to intrusion of the pluton, but because they are so similar to lineations that are widespread elsewhere in the region, even in localities distant from exposed plutonic bodies, it seems reasonable that those described by Compton are related to the fault system described here rather than to emplacement of the batholith.

In a detailed analysis of steeply plunging lineations (axes of microfolds) D. K. Chandra (1953, unpub. Ph.D. thesis, Univ. of Calif.) concluded that they were *b* lineations formed during strike-slip deformation of previously deformed rocks. The locality studied by Chandra is near the North Fork of the American River, 7 miles southeast of Colfax near the western branch of the Melones fault zone.

The horizontal component of movement of the Foothills faults cannot be estimated at this time, but a large apparent vertical component of movement is indicated by the distribution of strata in the part of the region that lies south of the Cosumnes River. The stratigraphy is much better known there than farther north. Within each of the three large blocks formed by the Melones and Bear Mountains fault zones, the oldest beds are exposed near the west side of the block and the youngest beds near the east

side of the block, as though the region lay on the west flank of a large synclinorium (Pl. 4, Cosumnes River section). This sequence is reversed by the major fault zones, for the youngest beds in the region are in the western block and the oldest are in the eastern block. The gross structure may be similar, although less evident, in the northern part of the region (Pl. 4, South Yuba River section).

Along the Melones fault zone, rocks of Jurassic age on the west are juxtaposed with rocks of Paleozoic age on the east from the Merced River to Placerville, a distance of 100 miles and perhaps more. Rocks of Jurassic age are not present between the Melones fault zone and the Sierra Nevada batholith within this interval. The apparent vertical component of displacement throughout this distance must be equal to or greater than the thickness of the Jurassic section west of the fault zone. Partial sections of these rocks, everywhere truncated by faults or erosion, range from 3000 feet to about 17,000 feet in thickness.

Few data are available for determining the apparent vertical component of displacement along the Bear Mountains fault zone except near the Cosumnes River. Here beds adjacent to the fault zone on the east belong to the Cosumnes formation which conformably underlies beds containing a fauna of Callovian (uppermost stage of the Middle Jurassic or lowermost stage of the Late Jurassic) age and is older than any beds exposed west of the fault zone. If this were a dip-slip reverse fault zone, the net slip near the Cosumnes River would be greater than the thickness of the section exposed on the east flank of the overturned anticline west of the fault zone. This section is about 15,000 feet thick. If, however, the faults are strike-slip, this cannot be regarded as even a minimum value for the net slip because the thicknesses of Mesozoic stratigraphic units vary widely, and stratigraphic sections on opposite sides of a fault zone at a given point cannot be compared for the purpose of determining displacement.

The possibility that movement along the Foothills fault system, if it is a strike-slip system, has totaled many tens of miles or more than 100 miles should be considered, for evidence of displacements of these magnitudes has been recognized in great strike-slip fault systems that have been studied in detail. Kennedy (1946) has demonstrated that displacement along the Great Glen fault of the Scottish Highlands is 65 miles; Wellman (1954) believes that movement along the Alpine fault of New Zealand amounts to about 300 miles since Jurassic time; and Hill and Dibblee (1953, p. 448) suggest that displacement along the San Andreas fault may be at least 350 miles since Jurassic time.

Mother Lode Fissure System

It is not yet clear whether the Mother Lode fissure system is related in origin to the Melones fault zone, or, indeed, whether it is related to a single tectonic episode or to more than one. The present writer has not studied the Mother Lode fissure system, and the descriptions given hereafter are based largely on published descriptions of the veins and the structures that control them. The resulting picture may be biased, for published descriptions are of the large mines where veins and ore zones have been explored for distances of several thousand feet along the dip or strike, or both. Veins and ore zones within the Melones fault zone that meet this qualification postdate significant movement along the major fault zone; otherwise the veins or their controlling structures would have been broken by fault-zone movements into trains of horses or boudins extremely difficult to trace in mining. If small remnants of ore bodies dating from an earlier stage do exist, they would receive slight consideration in any but the most exhaustive investigation of gold ore deposits of the Mother Lode belt.

From a point about halfway between the Merced and Tuolumne rivers northward to the Mokelumne River, most of the Mother Lode fissures are within the Melones fault zone, but near the southern end of the belt and from the Mokelumne River to the north end of the Mother Lode belt, northwest of Placerville, most of the fissures crop out 1 mile or more west of the Melones fault zone. Although the strike of some veins is moderately sinuous, the strike of most of the veins throughout the Mother Lode belt is about parallel to that of the Melones fault zone. Veins generally dip less steeply than cleavage and bedding west of the fault zone and schistosity within the fault zone. The veins dip eastward, mostly at angles between 50° and 70°, although one dips as gently as 20° for a considerable distance (Knopf, 1929, p. 24). Among the veins whose attitude is given by Knopf (1929) or Ransome (1900), no significant difference was noted between the dips of veins within the Melones fault zone and those west of the fault zone. Veins west of the fault zone cut and offset bedding in the country rock at acute angles. Some veins and zones of

replacement ore within the Melones fault zone bear similar relationships to schistosity and tabular bodies of rock drawn out parallel to the schistosity of the fault zone, but others are parallel to schistosity and contacts within the fault zone. Of the veins that crop out west of the fault zone, none are described as having been traced down-dip into the fault zone.

The movement picture of the Mother Lode fissure system evidently is not simple. Knopf (1929, p. 45) believed as a result of finding older rocks on the hanging-wall side of many veins that most of the veins occupied dip-slip reverse faults. He pointed out that flutings on post-mineral gouge indicate movement parallel to the dip in the Plymouth mine (Knopf, 1929, p. 52), but faulting that has produced the main fissure of the Central Eureka mine had horizontal displacement of 120 feet (p. 62); a strong lateral component of movement is suggested by structural relationships in the Argonaut mine (p. 67). The greatest measurable displacement found by Knopf was an apparent dip-slip displacement of 375 feet in the Gover shaft of the Fremont mine (Knopf, 1929, p. 25, 54). Cloos (1932b, p. 393–394) believed the fissures are related to emplacement of the Sierra Nevada batholith and are comparable to marginal thrusts.

The mine maps and sections prepared by Knopf provide evidence that some of the Mother Lode veins and gold ore bodies post-date most of the movement along the Melones fault zone. In several of the mines within the Melones fault zone, the principal ore bodies replace schist. Schistosity is much stronger in the Melones fault zone than in most of the bordering rocks and is apparently related to fault movements. Replacement of schistose rock by gold ore accordingly suggests that the ore is younger than fault movement. Ore bodies of this kind are found in the Eagle Shawmut and Clio mines which are in the Melones fault zone near the Tuolumne River. For these mines Knopf interprets the sequence of events as follows: (1) reverse faulting, (2) emplacement of peridotite or similar rock, (3) serpentinization of the peridote and renewed fault movement, and (4) deposition of ore. The first faulting was no doubt part of the Melones fault-zone movement—the later movement noted by Knopf may be related to the same tectonic episode or to a later episode.

In contrast with ore bodies at the Eagle Shawmut and Clio mines, some of those at Carson Hill, in the Melones fault zone about 1 mile north of the Stanislaus River, are associated with smaller faults that cross and offset structures characteristic of the chief movement along the major fault zone. Here, gold-quartz ore bodies were found at the intersection of gently dipping veins with a steeply dipping vein. Along at least one of the gently dipping veins, contacts of the wall rocks, including serpentine and schist, have been offset in a reverse direction (Knopf, 1929, p. 76–77, Fig. 23). Mapping by Eric and Stromquist (*in* Eric, Stromquist, and Swinney, 1955, Pl. 1) shows that in the vicinity of Carson Hill serpentine and schist form narrow bodies elongate parallel to schistosity in the Melones fault zone as they do elsewhere in the zone.

Age of Faulting

The Foothills fault system is of Late Jurassic and probably post-Oxfordian age as nearly as can be determined by current dating methods. The youngest rocks cut by the Melones fault zone (Mariposa formation) are of late Oxfordian or early Kimmeridgian (Late Jurassic) age, and the youngest rocks cut by the Bear Mountains fault zone conformably overlie beds of late Oxfordian or early Kimmeridgian age but are probably pre-Tithonian (Latest Jurassic). Irwin (in press) has shown that in the southern part of the Klamath Mountains and northwestern part of the Central Valley of California the major stratigraphic break is below the Knoxville formation, of Tithonian age, rather than between the Jurassic and Cretaceous rocks; available data in other parts of northern California are consistent with this. The upper age limit is placed by a dated pluton that truncates two faults of the Foothills system northeast of Folsom. Curtis, Evernden, and Lipson (1958, p. 6) have found that a granodiorite from this pluton has a radiometric age of 131 m.y. and a quartz diorite from the same pluton has an age of 143 m.y.

Geologists familiar with the Holmes (1947, Fig. 5) time scales will recognize a discrepancy between the paleontologic and potassium-argon dates. Curtis, Evernden, and Lipson (1958, p. 10–12) discuss this discrepancy, concluding that "the Mesozoic of the Holmes time scales is in need of modification" and that rock 143 million years old is of Late Jurassic age.

The Melones fault zone and other fault zones of the region have not been dated so closely but are presumably of about the same age. The Melones fault zone is probably not younger

than middle Cretaceous, for south of Mariposa it is cut by a pluton that is presumably a lobe of the Sierra Nevada batholith (Cloos, 1932a; 1935), p. 243–246). The Sierra Nevada batholith is Middle Cretaceous according to potassium-argon dates obtained by Evernden, Curtis, and Lipson (1958, p. 7–9).

Establishment of the age of the Foothills fault system has an interesting corollary: inasmuch as the faults truncate folds in the Jurassic rocks of the western Sierra Nevada, it would appear that most of the deformation of these rocks occurred prior to emplacement of the Sierra Nevada batholith. This deformation was therefore part of an earlier orogeny that preceded emplacement of diorite and quartz diorite plutons in the western Sierra Nevada and Klamath Mountains. Some faults of the Mother Lode fissure system may be related to emplacement of the Sierra Nevada batholith, as suggested by Cloos (1932b, p. 393–394).

References Cited

Bailey, E. H., 1946, Quicksilver deposits of the western Mayacmas district, Sonoma County, California: Calif. Jour. Mines and Geology, v. 42, p. 199–230

Cater, F. W., Jr., 1948, Chromite deposits of Calaveras and Amador counties, California: Calif. Div. Mines Bull. 134, pt. 3, ch. 2, p. 33–60

Clark, L. D., 1954, Geology and mineral deposits of the Calaveritas quadrangle, Calaveras County, California: Calif. Div. Mines Special Rept. 40, 22 p.

Cloos, Ernst, 1932a, Structural survey of the granodiorite south of Mariposa, California: Am. Jour. Sci., 5th ser., v. 23, p. 289–304

—— 1932b, "Feather joints" as indicators of the direction of movements on faults, thrusts, joints, and magmatic contacts: Natl. Acad. Sci. Proc., v. 18, p. 387–395

—— 1935, Mother Lode and Sierra Nevada batholith: Jour. Geology, v. 43, p. 225–249

—— 1955, Experimental analysis of fracture patterns: Geol. Soc. America Bull., v. 66, p. 241–256

Compton, R. R., 1955, Trondhjemite batholith near Bidwell Bar, California: Geol. Soc. America Bull., v. 66, p. 9–44

Curtis, G. H., Evernden, J. F., and Lipson, J., 1958, Age determination of some granitic rocks in California by the potassium-argon method: Calif. Div. Mines Special Rept. 54, 16 p.

Diller, J. S., 1908, Geology of the Taylorsville region, California: U. S. Geol. Survey Bull. 353, 128 p.

Durrell, Cordell, and Proctor, P. D., 1948, Iron-ore deposits near Lake Hawley and Spencer Lakes, Sierra County, California, p. 165–192 *in* Iron resources of California: Calif. Div. Mines Bull. 129, 304 p.

Eric, J. H., Stromquist, A. A., and Swinney, C. M., 1955, Geology of the Angels Camp and Sonora quadrangles, Calaveras and Tuolomne counties, California: Calif. Div. Mines Special Rept. 41, 55 p.

Evernden, J. F., Curtis, G. H., and Lipson, J., 1957, Potassium-argon dating of igneous rocks: Am. Assoc. Petroleum Geologists Bull., v. 41, p. 2120–2127

Ferguson, H. G., and Gannett, R. W., 1932, Gold quartz veins of the Alleghany district, California: U. S. Geol. Survey Prof. Paper 172, 139 p.

Heyl, G. R., 1947, Mother Lode fault zone between the Tuolumne and Stanislaus rivers, California (Abstract): Geol. Soc. America Bull., v. 58, p. 1192–1193

Hill, M. L., and Dibblee, T. W., 1953, San Andreas, Garlock, and Big Pine faults, California—a study of the character, history, and tectonic significance of their displacements: Geol. Soc. America Bull., v. 64, p. 443–458

Holmes, A., 1947, The construction of a geologic time scale: Geol. Soc. Glasgow Trans., v. 21, p. 118–152

Irwin, W. P., in press, Geological reconnaissance of the northern Coast Ranges and Klamath Mountains, California: Calif. Div. Mines

Jenkins, O. P., 1932, Geologic map of northern Sierra Nevada showing Tertiary river channels and Mother Lode belt: Calif. Div. Mines, 28th Ann. Rept. of the State Mineralogist, map accompanying part c

Kennedy, W. Q., 1946, The Great Glen fault: Geol. Soc. London Quart. Jour., v. 102, pt. 1, p. 41–72

King, P. B., and others, 1944, Tectonic map of the United States: Am. Assoc. Petroleum Geologists

Knopf, Adolph, 1929, The Mother Lode system of California: U. S. Geol. Survey Prof. Paper 157, 88 p.

Lindgren, Waldemar, 1894, Description of the gold belt; description of the Sacramento sheet, California: U. S. Geol. Survey Geol. Atlas, Sacramento folio (no. 5), 3 p., maps

—— 1900, Description of the Colfax quadrangle, California: U. S. Geol. Survey Geol. Atlas, Colfax folio (no. 66), 10 p., maps

Lindgren, Waldemar, and Turner, H. W., 1895, Description of the gold belt; description of the Smartsville sheet, California: U. S. Geol. Survey Geol. Atlas, Smartsville folio (no. 18), 6 p., maps

Pettijohn, F. J., 1949, Sedimentary rocks: N. Y., Harper and Brothers, 526 p.

Ransome, F. L., 1900, Description of the Mother Lode district, California: U. S. Geol. Survey Geol. Atlas, Mother Lode folio (no. 63), 11 p., maps

Taliaferro, N. L., 1942, Geologic history and correlation of the Jurassic of southwestern Oregon and California: Geol. Soc. America Bull., v. 53, p. 71–112

Taliaferro, N. L., and Solari, A. J., 1949, Geology of the Copperopolis quadrangle, California: Calif. Div. Mines Bull. 145 (map only)

Turner, H. W., 1894, Description of the gold belt; description of the Jackson sheet, California: U. S. Geol. Survey Geol. Atlas, Jackson folio (no. 11), 6 p., maps

—— 1897, Description of the gold belt; description of the Downieville quadrangle, California:

U. S. Geol. Survey Geol. Atlas, Downieville folio (no. 37), 8 p., maps

Turner H. W., 1898, Description of the gold belt; description of the Bidwell Bar quadrangle, California: U. S. Geol. Survey Geol. Atlas, Bidwell Bar folio (no. 43), 6 p., maps

Turner, H. W., and Lindgren, Waldemar, 1894, Description of the gold belt; description of the Placerville sheet, California: U. S. Geol Survey Geol. Atlas, Placerville folio (no. 3), 3 p., maps

Turner, H. W., and Ransome, F. L., 1897, Description of Sonora quadrangle, California: U. S. Geol. Atlas, Sonora folio (no. 41), 5 p., maps

—— 1898, Description of the gold belt; description of the Big Trees quadrangle, California: U. S. Geol. Survey Geol. Atlas, Big Trees folio (no. 51), 8 p., maps

Wellman, H. W., 1954, Active transcurrent faulting in New Zealand (Abstract): Geol. Soc. America Bull., v. 65, p. 1322

Wells, F. G., and Walker, G. W., 1953, Geology of the Galice quadrangle, Oregon: U. S. Geol. Survey Geol. Quadrangle Map Series (GQ-25)

U. S. Geological Survey, Menlo Park, California

Manuscript Received by the Secretary of the Society, December 23, 1958

Publication Authorized by the Director, U. S. Geological Survey

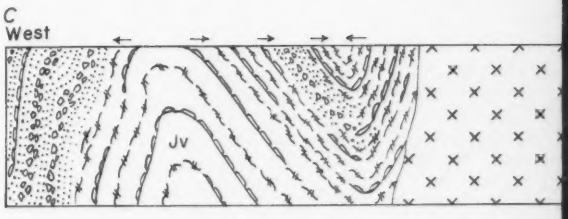

From west to east, letter symbols are; Jv, unnamed serpentine of Jurassic age; R_2^1d, Delhi formation

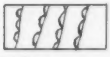
Pillow lava

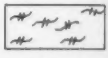
Lava

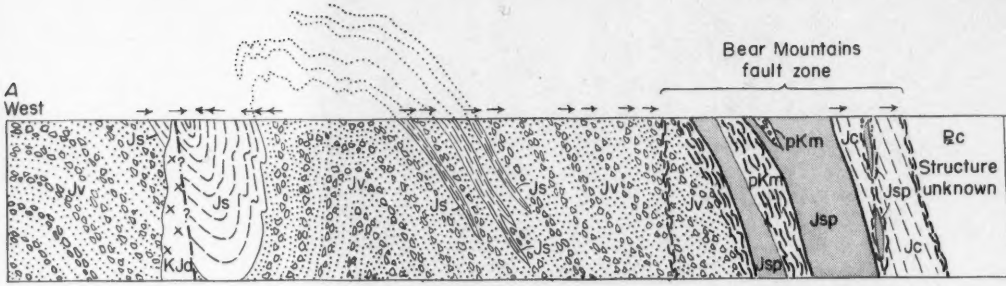

COSUMNES RIVER SECTION

From west to east, letter symbols are; Jv, unnamed volcanic rocks of Late Jurassic age; or Late Jurassic age ; Js, unnamed slate and minor graywacke of Late Jurassic age; Jurassic age; PKm, metavolcanic rocks of unknown pre-Cretaceous age; Jc, Cosumnes or early Late Jurassic age ; Pz c, Calaveras formation of Paleozoic age, Jl, Logtown Jurassic age; Jm, Mariposa formation of Late Jurassic age; KJg, metamorphosed granc Jurassic age. Structure is homoclinal between the Melones fault zone and the wes formation.

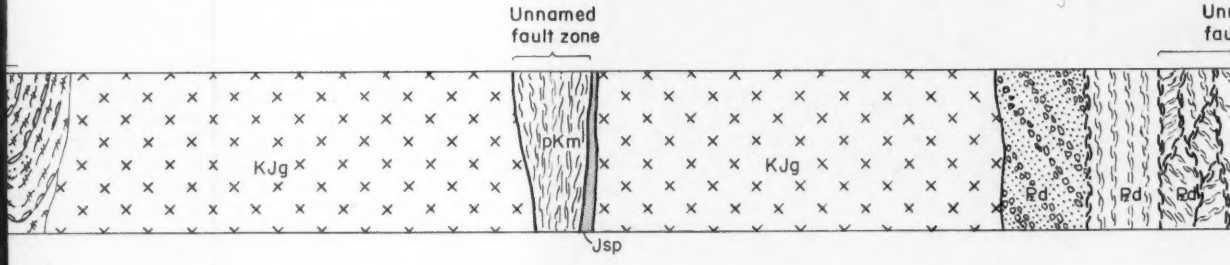

SOUTH YUBA RIVER SECTION

s are; Jv, unnamed volcanic rocks of probable Jurassic age; KJg, granitic rocks of Cretaceous or Jurass d, Delhi formation of Paleozoic age ; KJd, diorite of Cretaceous or Jurassic age; Pz ch, Cape Horn forn

Lava | Pyroclastic rocks | Sedimentary rocks | Schistose metasedimentary and metavolcanic rocks | Plutonic rocks

Arrows show direction of tops of beds indicated by graded

0 1 2 3 4 5 Miles

Horizontal and vertical scale

GEOLOGIC CROSS SECTIONS, WESTERN SIERRA NEVADA,

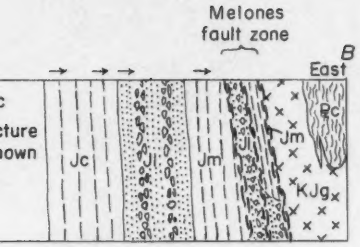

ge; KJd, diorite of Cretaceous
age; Jsp, serpentine of Late
nnes formation of late Middle
own formation of Middle or Late
granodiorite of Cretaceous or
western belt of Calaveras

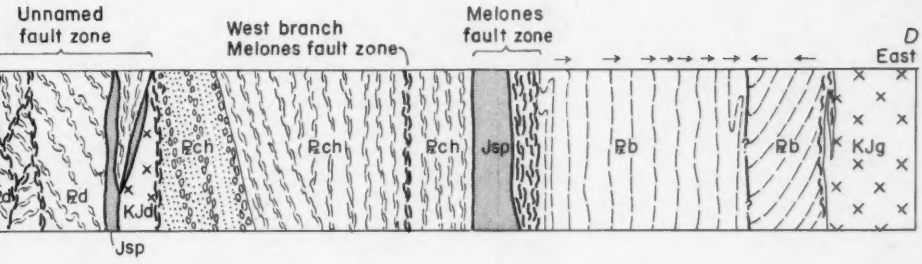

rassic age; pKm, schistose volcanic rocks of unknown pre-Cretaceous age; Jsp,
formation of Paleozoic age; P$_z$ b, Blue Canyon formation of Paleozoic age.

ocks Serpentine Fault Shear zone

ded bedding

DA, CALIFORNIA

Sala y
105°28′00″
east-northe
west of nc
Island, it b
visited, an
since its d
collected ro
note on the
is known to
also summ
and fauna
naval train
1935. Neit
been soun
sounders.
California–
Expedition
to explorin
Three geol
collect rock
F. Baird e
metric expl

Sala y G
axis of the
Rise (Fig.
Island as
Rise than
may exten
Island east
Ambrosio
most of its
be much les
East Pacifi
southeast f
Chile. How
great in the
this trend,
East Pacifi

Recent sc
"Highjump

Short Notes

BULLETIN OF THE GEOLOGICAL SOCIETY OF AMERICA
VOL. 71. PP. 497-502, 3 FIGS., 1 PL. APRIL 1960

BATHYMETRY AND GEOLOGY OF SALA Y GOMEZ, SOUTHEAST PACIFIC

BY ROBERT L. FISHER AND ROBERT M. NORRIS

Sala y Gomez, charted at 26°27′41″ S., 105°28′00″ W., is a low volcanic islet 415 km east-northeast of Easter Island and 3500 km west of northern Chile (Fig. 1). Like Easter Island, it belongs to Chile. Although it has been visited, and even landed upon, several times since its discovery in 1793, visitors had not collected rock samples systematically. Only one note on the petrology of the islet, from samples, is known to the writers. That note (Falke, 1941) also summarized observations of topography and fauna made during the visit of the Chilean naval training ship GENERAL BAQUEDAÑO in 1935. Neither had the area near Sala y Gomez been sounded with modern recording echo sounders. Accordingly, on the University of California—International Geophysical Year Expedition "Downwind," a day was devoted to exploring the islet and its bordering platform. Three geologists and two seamen landed to collect rocks while the research vessel SPENCER F. BAIRD engaged in a sight-controlled bathymetric exploration around the islet.

Sala y Gomez lies 750–1000 km east of the axis of the broad, north-trending East Pacific Rise (Fig. 1). This islet (and possibly Easter Island as well) is less closely related to the Rise than to an eastwest structural trend that may extend from 1200 km west of Easter Island eastward beyond San Felix and San Ambrosio nearly to the Chilean coast. Over most of its length this spur or zone appears to be much less active, seismically, than either the East Pacific Rise proper or the swell extending southeast from near Easter Island to southern Chile. However, shallow-focus seismicity is very great in the region west of Easter Island where this trend, projected, intersects the axis of the East Pacific Rise.

Recent soundings from U. S. Navy Operation "Highjump" and from "Downwind" Expedition indicate that the central segment of the structure is a narrow shoal ridge, more than 1200 km long. Several peaks extend to within 500 m of the sea surface. From sounding data now available, it is uncertain whether the main ridge extends westward to Sala y Gomez or whether it swings southwest, as contoured in Figure 1, with the islet an isolated peak off the north slope. It is likewise uncertain whether the ridge extends across the gap near 90° W Long. to join the seamounts and guyots west of San Felix Island. Soundings are practically nonexistent in the region bounded by Lat. 27° and 35° S. and Longs. 80° and 100° W. No shoal areas of comparable size are believed present there; the few soundings available indicate a general sea depth of 3500–4000 m. North of 25° S., between Peru and the East Pacific Rise, the sea floor is generally deeper than 4000–4500 m. It is suggested that this ridge, extending from near Sala y Gomez to at least 90° W. Long., be designated the Sala y Gomez Ridge.

There are similarities between the here-named Sala y Gomez Ridge and Clipperton Ridge in the northeastern Pacific, described by Menard and Fisher (1958). Both separate large areas with a depth difference of several hundred meters. Both are asymmetrical in cross section, steeper on the north, with one or more lines of seamounts capping the rise. In both cases a subordinate less well-defined northwest trend may be discerned. Of comparable widths, Clipperton Ridge has a greater relief, the Sala y Gomez Ridge a greater length. Both ridges appear as segments of large, east-west structural trends. Clipperton Ridge is part of the Clipperton Fracture Zone, more than 4000 km long. The adjacent well-defined Tehuantepec Ridge, off southern Mexico, is similar in trend, dimensions, and position to the Nasca Ridge off southern Peru. In each case, the east-west

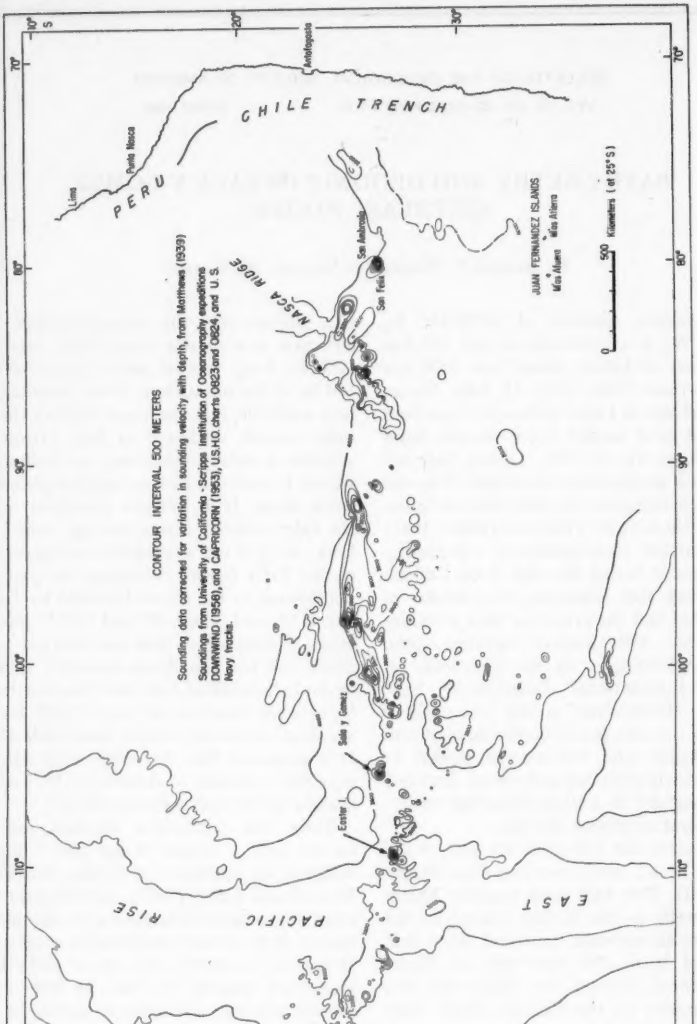

FIGURE 1.—TOPOGRAPHY OF THE SALA Y GOMEZ RIDGE AND ADJACENT AREA

trend is poorly developed east of the intersection of the northeast-southwest and east-west trends. It might be concluded that the structural trend extending from near the South American coast to Easter Island is another of the "fracture zones" like those described from the northeast Pacific (Menard, 1955). Both zones intersect the East Pacific Rise. Off Mexico, where it is called the "Albatross Plateau", the Rise bisects the Clipperton Fracture Zone. Off South America, it intersects the west portion of the "Sala y Gomez trend".

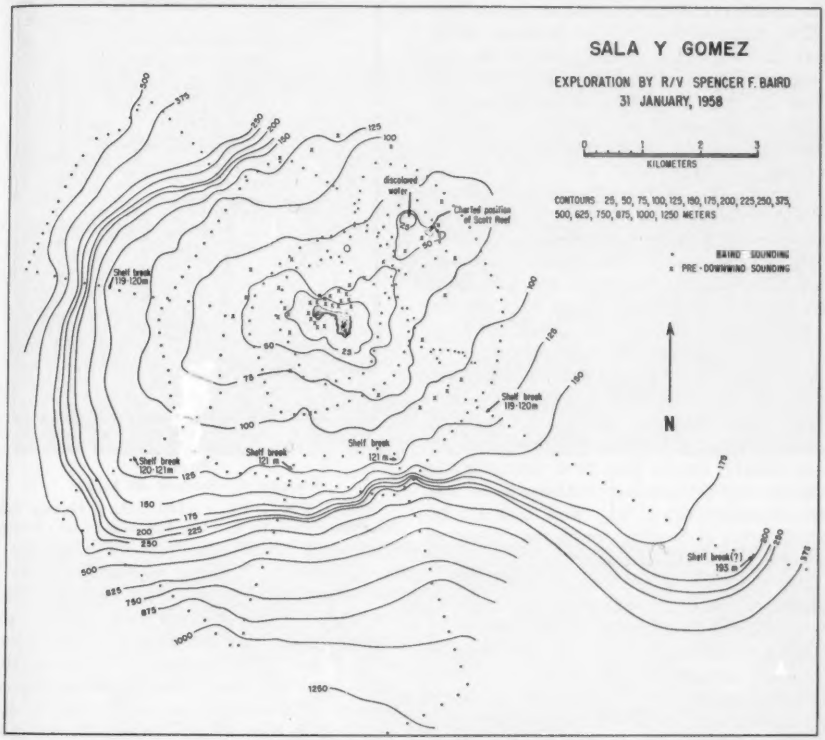
SALA Y GOMEZ
EXPLORATION BY R/V SPENCER F. BAIRD
31 JANUARY, 1958
0 1 2 3
KILOMETERS
CONTOURS 25, 50, 75, 100, 125, 150, 175, 200, 225, 250, 375, 500, 625, 750, 875, 1000, 1250 METERS
BAIRD SOUNDING
PRE-DOWNWIND SOUNDING
Discolored water
Charted position of Scott Reef
Shelf break 119-120m
Shelf break 121 m
Shelf break 120-121m
Shelf break 119-120m
Shelf break 121 m
Shelf break(?) 195 m
N

FIGURE 2.—PLOT OF NEAR-SHORE TOPOGRAPHY

Results of near-shore bathymetric exploration by R/V SPENCER F. BAIRD are shown in Figure 2. Soundings taken with a continuously recording echo sounder were recorded on a "precision depth recorder", so that soundings could be read to ± 1 m without difficulty. A sounding interval of 1 minute was used in constructing Figure 2. Slope corrections have not been made. Soundings recorded in fathoms, employing an assumed sounding velocity of 4800 feet/second, were corrected according to the tables of Matthews (1939) and converted to soundings in meters. Positions were taken at 1- or 2-minute intervals, depending upon the ship's speed and the rapidity with which bearings changed. Visual bearings on the highest pinnacle were taken simultaneously with radar ranges to the nearest readily identifiable point on the islet. The accuracy with which the shore line is represented on the available nautical charts is not known.

Sala y Gomez is the subaerial peak of a very large seamount. The extension of this seamount to the west, north, and northeast is not known, but it does extend more than 50 km southeast and 30 km southwest of the islet. Aprons and plains indicative of ponded sediments occur at the base of the slope, near 3500-m depth.

The shelf surrounding the islet is elongated in a northeast-southwest direction, with a mini-

mum width, south of the islet, of 2–2½ km. Its northeast limit was not determined. Five radial lines from "Downwind" show that this platform terminates in a well-defined break west, south, and east-southeast of the islet. The uniformity in this shelf-break depth, 119–121 m, suggests that little or no tilting of the peak has occurred since this platform was cut. East-southeast of the islet, there is a deep break in slope of about 193 m. Above this break the bottom shoals gradually to the platform break of 119–121 m. This gently sloping surface may represent an older tilted shelf or the top of a flow originating east of the present islet. No similar deep break in slope was observed on other radial sounding lines.

The shelf surface is rather smooth, with only broad irregularities, except off the east side of the island. There, narrow sharp pinnacles rise 7–10 m above the platform 30–50 m deep. Larger pinnacles lie north and northeast of the islet; one shoals to less than 50 m. A large patch of discolored water, probably indicating very shoal depths, lay 2 km northeast of the islet, on a bearing 032° from the highest point. An area probably shoaler than 50 m surrounds this pinnacle and extends east-southeast to include the charted position of Scott Reef. However, no discoloration or breaking waves were observed to occur at the latter position.

Sala y Gomez is saddle-bag shaped with a maximum length of 700 m in an east-west direction and a maximum width of 400 m in a north-south direction (Fig. 3). The greatest elevation, according to U.S.H.O. Publication 174 (1952, p. 210a), is 30 m (98 feet). Although no means were available for checking this during the "Downwind" survey, 15 or 16 m would appear to be a more reasonable estimate.

From the sea the islet presents a bleak appearance and seems composed solely of loose black rocks. Once ashore, however, one finds that the islet is made up of several lava flows, with exposed surfaces strewn with loose, apparently water-rounded boulders (Pl. 1, fig. 1) The surface irregularity is accentuated by crude jointing and weathered pillow structure and by the blocky aa type of lava that composes much of the uppermost flow.

The shore line is broken by numerous small inlets 3–30 m wide and up to 100 m long; these appear to have been excavated by waves working along joint planes or other zones of structural weakness. Numerous tide pools are present along the shore; some were observed as much as 3 m above the sea at the time of the visit. These higher pools are almost certainly maintained by spray from breaking waves because the maximum spring-tide range shown on the U. S. Navy H. O. Chart 1119 (1925) is only a little more than 1 m. The numerous rounded boulders on the surface of the islet also suggest that much of the islet is inundated during heavy seas.

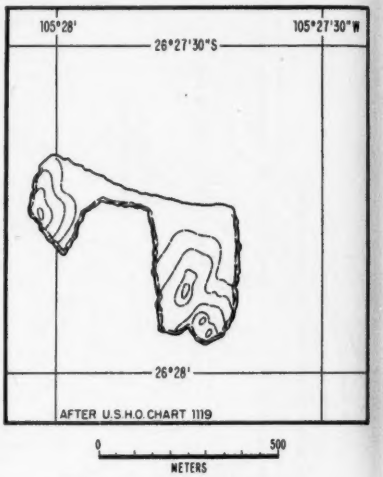

FIGURE 3.—SKETCH OF ISLET

After U.S.H.O. Chart 1119. Sala y Gomez was reported (1943) to lie 11½ km east of its charted position.

There are no landing places worthy of the name on the islet, although during calm weather a small boat easily can be brought close to the rocky shore. During the survey, in moderate weather, it was necessary to swim the last 50–60 m to shore in order to avoid dashing the boat against the rocks, a not entirely satisfactory procedure owing to the abundance of sharks.

PLATE 1.—ROCKS OF SALA Y GOMEZ ISLAND

FIGURE 1.—Looking southeast, showing highest portion of the island

FIGURE 2.—Altered zone between the two flows. Note the pillow structure in both flows and the steam pocket or evacuated pillow in the center right. Hammer in lower left gives scale.

FIGURE 1

FIGURE 2

ROCKS OF SALA Y GOMEZ ISLAND

No volcanic vents were found on Sala y Gomez, although a vent may have existed in the location now occupied by the embayment on the south side of the islet.

Three distinct rock units are exposed. The lowermost is a vesicular red to dark-gray andesitic olivine basalt. The middle unit, a discontinuous calcareous marine sedimentary deposit, is composed mostly of broken fragments of mollusk shells, Foraminifera, echinoid spines, and corals; this units rests disconformably on the eroded and altered upper surface of the lower basalt. The upper unit is also a vesicular to dense dark-gray andesitic olivine basalt. Both flows show pillow structure. A thin cover of calcareous shell debris is now accumulating on the lowest parts of the islet near the shore, particularly on the northeastern side.

The flows and the included sedimentary unit are probably Pleistocene or Recent. The minor amount of weathering on the surface of the last flow plus the near absence of soil make a greater age unlikely, although soil and other weathering products might be swept away by storm waves on such a low islet.

The lower unit is a reddish to dark-gray andesitic olivine basalt flow, locally scoriaceous and generally showing a well-developed trachytic texture. Vesicles are especially numerous near the upper surface of the flow and commonly show some flattening, which suggests that some movement of the lava occurred just prior to final cooling.

Transition from red to dark gray takes place downward in about a meter, suggesting that only the uppermost portion of the flow was exposed to atmospheric oxidation at the time of formation. Pillow structure and probable steam pockets are well developed in much of the exposed portion of the flow, indicating a submarine origin for the bulk of the unit (Pl. 1, fig. 2).

Feldspar laths, ranging from oligoclase to andesine (An_{30} to An_{40}) constitute 60–70 per cent of the rock. The laths are roughly parallel, giving the rock a trachytic texture. The feldspar crystals are generally unzoned and unaltered and average about 0.2 mm long.

Ferromagnesian minerals constitute the remaining 30–40 per cent of the rock and include very abundant small granules of iron ore, presumably mostly magnetite. Olivine is common, both as small grains averaging about 0.1 mm in diameter and as scattered large phenocrysts averaging about 1.0 mm in diameter. Associated with the olivine is iddingsite which has replaced nearly all the small olivine grains and which rims the larger phenocrysts. Augite, although present in small grains, is rare. The rarity of augite and other pyroxenes may be due to the relatively sodic character of the parent magma.

Parts of the upper surface of this lower unit are extensively altered. The resulting product is kaolinite, an unidentified zeolite, and a chloritic mineral. Both the groundmass and the included feldspar laths have been altered to the same material. Most of this altered material, which formerly probably covered much of the upper surface of the lower flow, has been removed by erosion before extrusion of the latest flow.

Intercalated between the upper and lower volcanic rocks is a discontinuous calcareous deposit containing subround to angular fragments of scoria, generally of pea size, presumably derived from the lower flow during the erosional period suggested above. The calcareous matrix is composed of Foraminifera tests, echinoid spines, fragments of reef-forming coral, and broken mollusk remains. Most of these organic remains are so badly leached that a reliable age determination is difficult. The freshness of the associated flows, however, suggests a Pleistocene or Recent age.

The deposit is nowhere more than 8 m above sea level and no more than 1 m thick. No great subsidence following formation of the first lava flow would be necessary to produce the requisite shallow-water environment.

The upper unit is a dense, fine-grained andesitic olivine basalt, locally sufficiently vesicular to be considered a scoria. The upper surface, where not destroyed by wave erosion or weathering, is mostly blocky and jagged, resembling a typical aa lava flow. Locally, the upper surface of the flow is smooth ropy pahoehoe. The base of this unit, where it rests on the lower flow or on the middle sedimentary bed, shows crude pillow structure suggesting that this flow too was extruded partly below the level of the sea. The upper flow rests directly on the lower unit in much of the eastern part of the islet and constitutes nearly all the exposed rock in the narrow isthmus.

Composition of the upper and lower units is similar. All specimens of the upper flow have a marked trachytic texture owing to the rough alignment of the abundant feldspar laths. Feldspars range from oligoclase to andesine (An_{28} to An_{37}) as in the lower flow. The crystals average about 0.2 mm long, are normally un-

zoned and unaltered, and constitute about 60–70 per cent of the rock.

Olivine occurs as large phenocrysts, averaging about 1.0 mm in diameter, and as abundant small grains (average diameter, 0.15 mm), together constituting nearly 20–25 per cent of the total rock. Only a few of the small grains are altered to red iddingsite, and alteration rims and cracks in the larger grains are much less prominent in the upper than in the lower unit. Olivine crystals in both rock units have a 2V near 90°.

Opaque, equant iron-ore granules, probably mainly magnetite, are exceedingly abundant in all samples from the upper flow. Although the grains are generally small, iron ore constitutes not less than 5 per cent of the total rock.

Augite, although not abundant in the upper flow, is not so rare there as in the lower unit. Most augite grains are small (average size about 0.05 mm) and occupy spaces between the feldspar laths. No augite phenocrysts were present. Most of the augite examined was colorless. A few grains are pale greenish and may be aegirine-augite.

The lava flows of Sala y Gomez are considered andesitic basalts on the basis of the abundance of olivine, the dark color of the rocks, and the sodic nature of the feldspars (Williams, Turner, and Gilbert, 1954, p. 43). The varietal name mugearite seems appropriate and conveys an accurate picture of the mineralogical nature of these rocks.

Acknowledgments

The writers are indebted to Gustaf Arrhenius, M. N. Bramlette, and Howel Williams for critical reading of the manuscript.

References Cited

Falke, H., 1941, Die Insel Sala y Gomez: Natur und Volk, Bank 71, Heft 3, p. 146–150

Matthews, D. J., 1939, Tables of the velocity of sound in pure water and sea water for use in echo-ranging and sound-ranging: British Admiralty Hydrog. Dept. H. D. no. 282, 52 p.

Menard, H. W., Jr., 1955, Deformation of the northeastern Pacific Basin and the west coast of North America: Geol. Soc. Am. Bull., v. 66, p. 1149–1198

Menard, H. W., Jr., and Fisher, Robert L., 1958 Clipperton fracture zone in the northeastern equatorial Pacific: Jour. Geology, v. 66, p. 239–253

U. S. Hydrographic Office chart 1119, 8th ed., 1925

U. S. Hydrographic Office Publication 174, 1952, Sailing directions for South America, volume 3 (west coast from Golfo Corcovado to Gulf of Panama, including off-lying islands), 392 p.

Williams, H., Turner, F. J., and Gilbert, C. M., 1954, Petrography: San Francisco, W. H. Freeman Co., 406 p.

Scripps Inst. of Oceanography, Univ. Calif., La Jolla, Calif.; Univ. Calif., Santa Barbara, College, Goleta, Calif.

Manuscript Received by the Secretary of the Society, November 16, 1959

BULLETIN OF THE GEOLOGICAL SOCIETY OF AMERICA
VOL. 71, PP. 503-504 APRIL 1960

OCCURRENCE OF NORMATIVE SODIUM METASILICATE IN WASHINGTON'S TABLES

BY FELIX CHAYES

From interpretation of experimental data, Tuttle and Bowen (1958, p. 84–87) have recently concluded that a molar excess of alkalis over available Al in the magmatic residue, a possibility not excluded by crystal fractionation of basaltic magma, would favor the occurrence of a gradual passage from granitic magma to hydrothermal solution, a matter of great and recurrent interest to petrology. They then pass (p. 88–89) to a citation of the incidence of normative acmite and sodium metasilicate (*ns*) in the analyses in Washington's (1917) Tables as direct evidence that "... granitic liquids contain alkalis in excess of that required to combine with all the alumina to form feldspars."

Since *ns* occurs only in the norms of alkaline* rocks, it is to be presumed that Washington's Tables overestimate its importance in the lithosphere in about the same way they overestimate the relative abundance of alkaline rocks as a whole—*i.e.*, by a very generous margin. This well-known sampling bias is given no consideration by Tuttle and Bowen. The ratio of *ns*-bearing to *ns*-free norms in the Tables is about 1:40, and on geological grounds it is entirely reasonable to suppose this is high by at least an order of magnitude.

Professional Paper 99 contains, according to my tally, 101 *ns*-bearing norms, of which about half are of volcanic rocks. The total is also about evenly divided between those with normative quartz and those with normative feldspathoids; nearly 75 per cent of the volcanic rocks fall in the former group, and more than 70 per cent of the plutonic and hypabyssal rocks in the latter. That *ns* and *ac* are about as common in the norms of subsilicic and femic rocks as in those of "granitic" ones is quite obviously a matter of critical importance. At first glance, in fact, its effect on the argument would appear to be almost lethal, although some reasonable escape from the dilemma may be available. The Tuttle-Bowen tally includes only "granitic" analyses, however, and their discussion makes no mention of this problem.

Although all the analyses must have survived the various rejection criteria set up by Washington, it is nevertheless possible that the presence of *ns* in many of these norms reflects nothing more than permissible—or, at any rate, expectable—analytical error. In nearly 60 per cent of the *ns*-bearing norms the amount of *ns* is less than 1 per cent, and in more than a third it is less than 0.5 per cent. Relatively small errors in the analytical partition of alkalis, of ferrous and ferric iron, of the R_2O_3 group, and even of silica and R_2O_3 could easily generate a few tenths of a per cent of normative *ns*. This is not to say that a norm showing only a few tenths of a per cent of *ns* is immediately suspect, but only that it contributes almost nothing to the argument unless the analysis from which it is calculated is known to have been made with special care. Some reasonable compromise could almost certainly have been found, but the need for it will not emerge from a discussion based on the incidence rather than the amount of *ns*.

As the Tuttle-Bowen tally shows, the characteristic occurrence of *ns* among volcanic rocks is in the norms of peralkaline trachytes and rhyolites. Of the 45 listed occurrences in norms of volcanic rocks, no fewer than 33 are of pantellerites, comendites, and paisanites, and 24 of these are from the Mediterranean and east African areas alone. Of some 575 tabled norms of rocks satisfying their definition of granite, however, they note that only four contain *ns*. To the extent that the composition of granite provides a reliable index of the composition of granite magma, it is clear that granite magmas must very rarely contain a molar excess of alkalis over available (Al + Fe***). This is not the conclusion reached by Tuttle and Bowen, so we must conclude that in their view the composition of granite magma is better indicated by rhyolite than by granite. This is certainly true if the rhyolite is a true glass, but is otherwise open to argument.

As Bowen (1928, p. 125) long ago pointed out, the only unimpeachable evidence of the composition of magma is that obtained from the composition of rock glasses. Now, although many of the volcanic rocks whose norms show

* Classes Ok, Sk, V, and W of the Shand system.

ns do contain glass, there is to date surprisingly little evidence that the glass of these rocks is deficient in (Al + Fe***). Indeed, evidence obtained in the only detailed study so far made (Washington, 1913) suggests rather strongly that normative *ns* representative of anything more than analytical error usually indicates the presence of cossyrite, a mineral whose norm shows more than 8 per cent *ns*. The lavas of Pantelleria are well known both for their cossyrite phenocrysts and for their normative *ns*. Washington records seven analyses of Pantellerian lavas which yield normative *ns*, but only one of these appears to be a true glass. The other six contain varying amounts of cossyrite, and Washington argues at some length that the presence of modal cossyrite "... goes hand in hand" with that of normative *ns*. He does not suggest, and in fact does not believe, that all the normative *ns* is contributed by modal cossyrite, but for two of the analyses in question the recorded amounts of *ns* and cossyrite make this seem very likely, for a third it is possible, and for a fourth no mode is given, although the rock is described as containing cossyrite, and there is very little *ns* in the norm. In sum, of the seven Pantellerian analyses exhibiting normative *ns*, one must be considered direct evidence of the strongest kind for the proposed magmatic deficiency of (Al + Fe***), two indirectly suggest such a deficiency, and four are at best noncommittal.

Although the name "cossyrite" is used only for small crystals in volcanic rocks, what appears to be the same substance occurs in large crystals in certain plutonic and pegmatitic rocks, where it is called aenigmatite. It will be recalled that aenigmatite occurs only in nepheline syenites. Normative *ns* may also be generated by arfvedsonite-type amphiboles, and this is in fact the original justification for use of the *ns* molecule in the CIPW norm (Cross *et al.*, 1903, p. 188). When we talk of an arfvedsonite rock we may or may not be talking about a granite, but we are certainly not talking about a common granite. And when we talk about an aenigmatite rock we are not talking about a granite at all. Yet it is precisely such rocks which provide the great majority of recorded occurrences of *ns* in the plutonic environment.

What Tuttle and Bowen propose is an end-stage alkali-silicate enrichment in the normal course of granite crystallization, and in support of this proposal they turn to Washington's Tables. What the *ns*- and *ac*-bearing norms of the Tables suggest, however, is an alkali enrichment, *with or without silica enrichment and often with marked silica impoverishment, occurring some time during the formation of of certain rare and usually titanium rich alkaline rocks*. In the absence of detailed geological and petrographic information this is little more than a tautology, for it is clear that rocks unduly rich in alkalis must at some time have become so.

For so long as attention is directed only to the question of whether or not *ns* is present in the norms of "granitic" analyses, the conclusion reached by Tuttle and Bowen seems not unreasonable. The relative scarcity of alkaline rocks, the relative profusion of analyses of such rocks, the characteristic occurrence of *ns* and *ac* in the norms of alkaline rocks of other than "granitic" composition, and the possible generation of small amounts of *ns* by analytical error are all nevertheless relevant to the inquiry. Consideration of these matters certainly suggests that evidence for the proposed end-stage alkali-silicate enrichment of granite magma must be sought elsewhere than in a table of rock analyses.

References Cited

Bowen, N. L., 1928, The evolution of the igneous rocks: Princeton, Princeton Univ. Press (reprinted 1956 by Dover Publications).

Cross, W., Iddings, J. P., Pirsson, L. V., and Washington, H. S., 1903, Quantitative classification of igneous rocks: Chicago, Univ. Chicago Press, 286 p.

Tuttle, O. F., and Bowen, N. L., 1958, Origin of granite in the light of experimental studies in the system $NaAlSi_3O_8$-$KAlSi_3O_8$-SiO_2-H_2O: Geol. Soc. America Mem. 74, 153 p.

Washington, H. S., 1913, The volcanoes and rocks of Pantelleria, Part II: Jour. Geology, v. 21, p. 683–713

—— 1917, Chemical analyses of igneous rocks: U. S. Geol. Survey Prof. Paper 99, 1201 p.

GEOPHYSICAL LABORATORY, CARNEGIE INST. OF WASHINGTON, WASHINGTON, D. C.

MANUSCRIPT RECEIVED BY THE SECRETARY OF THE SOCIETY, OCTOBER 22, 1959

BULLETIN OF THE GEOLOGICAL SOCIETY OF AMERICA
VOL. 71, PP. 505-506 APRIL 1960

OCCURRENCE OF NORMATIVE SODIUM METASILICATE IN WASHINGTON'S TABLES: A REPLY

BY O. F. TUTTLE

The preceding note by Chayes is a criticism of pages 88 and 89 of The Geological Society of America Memoir 74 (Tuttle and Bowen, 1958).

Bowen and Tuttle pointed out that phase-equilibrium considerations demonstrate that crystallization of hydrous granitic liquids containing an excess of alkalies over alumina[1] will produce residual liquids which exhibit a continuous gradation from hydrous silicate liquid to hydrothermal solution. Chayes (1960) has no objection to this basic premise, but he finds fault with the evidence cited to support our contention that many rocks contain a slight excess of alkalies. We suggested that the occurrence of normative metasilicate and acmite in the norms from Washington's Tables (1917) is evidence to support our observation. Chayes is concerned with this evidence, which is (Table 14, p. 88):

	"Granites"	"Rhyolites"
Alumina undersaturated	6.5%	21%
Alumina saturated	33.0%	30%
Alumina oversaturated	61.0%	49%

Chayes suggests that these alumina-undersaturated examples may represent nothing more than analytical errors. Perhaps he is right, but I venture to suggest it is a remarkable analytical error which is committed three times more often when analyzing extrusive rocks than when analyzing plutonic rocks. In the case of the granitic rocks (*sic*) the occurrence of alkali pyroxene and amphibole is *prima facie* evidence of alumina undersaturation; it is unnecessary to rely on the accuracy of chemical analyses to establish alumina undersaturation in these rocks. To be sure, hypersolvus granites, which apparently always carry an alkali amphibole (Bowen and Tuttle, 1958, p. 137), are not so common as the alumina-oversaturated mica granites, but their abundance is no measure of the importance in the present connection.

Chayes contends that the alumina-undersaturated rocks are rare alkaline rocks which presumably, therefore, can be thrown out of court. I would agree that nepheline syenites and nepheline-bearing rocks are rare, but to classify the hypersolvus granites which carry alkali pyroxenes and amphiboles with these alkaline rocks is not justified. A cursory glance at the phase diagrams for the systems Na_2O-Al_2O_3-SiO_2 and K_2O-Al_2O_3-SiO_2 (Schairer and Bowen, 1955; 1956) will convince the reader that the alkaline "nature" of the granites is a result of alumina undersaturation, whereas the alkaline nature of the true alkaline rocks is a result of silica undersaturation. A granite or a nepheline syenite can be alumina-undersaturated, and, in either case, the alumina undersaturation may, on crystallization, result in the development of hydrous liquids which will have a continuous solubility relation with water.

Chayes points out that sodium metasilicate and acmite are as common in the norms of subsilicic rocks as in granitic rocks, and, for some unexplained reason, he suggests this is of "critical importance" and "almost lethal" to some part of our argument. I see no connection between this fact and our argument, and it appears that Chayes has not considered carefully the phase relations discussed on pages 84–87.

[1] For the present discussion it will be convenient to refer to these rocks as "alumina-undersaturated". A rock with normative corundum will then be oversaturated with alumina, and a saturated rock will contain no corundum, sodium metasilicate, or acmite. In othe words, in an alumina-saturated rock, alumina and alkalies are present in the molecular ration 1:1 as in albite, orthoclase, nepheline, leucite, and kalsilite.

References Cited

Chayes, F., 1960, Occurrence of normative sodium metasilicate in Washington's Tables: Geol. Soc. America Bull. v. 71, p. 503–504

Schairer, J. F., and Bowen, N. L., 1955, The system K_2O-Al_2O_3-SiO_2: Am. Jour. Sci., v. 253, p. 681–746

——1956, The system Na_2O-Al_2O_3-SiO_2: Am. Jour. Sci., v. 254, p. 129–195

Tuttle, O. F., and Bowen, N. L., 1958, Origin of granite in the light of experimental studies in the system $NaAlSi_3O_8$-$KAlSi_3O_8$-SiO_2-H_2O: Geol. Soc. America, Mem. 74, 153 p.

Washington, H. S., 1917, Chemical analysis of igneous rocks: U. S. Geol. Survey Prof. Paper 99, 1201 p.

THE PENNSYLVANIA STATE UNIVERSITY, UNIVERSITY PARK, PA.

MANUSCRIPT RECEIVED BY THE SECRETARY OF THE SOCIETY, OCTOBER 30, 1959

BULLETIN OF THE GEOLOGICAL SOCIETY OF AMERICA
VOL. 71, PP. 507-510 APRIL 1960

SYMMICTITE: A NAME FOR NONSORTED TERRIGENOUS SEDIMENTARY ROCKS THAT CONTAIN A WIDE RANGE OF PARTICLE SIZES

By R. F. Flint, J. E. Sanders, and John Rodgers

Abstract

Existing terminology of till-like sedimentary deposits tends to emphasize genesis without considering all possible modes of origin and to suggest relationships to tillite that may be erroneous. Therefore new terms (*symmicton* for sediment; *symmictite*, for lithified equivalents) are proposed as general names for essentially nonsorted, noncalcareous, terrigenous deposits composed of sand and/or larger particles in a muddy matrix.

Nonsorted and poorly sorted terrigenous sediments that contain a wide range of particle sizes have attracted much attention recently because they have been discovered in many localities. In particular, essentially noncalcareous sediments containing pebbles and larger sizes dispersed through a fine-grained matrix have been discussed because of their similarity to till, of glacial origin. Many processes other than glacier ice, however, have been recognized as capable of forming till-like deposits: for example, landslides, earthflows, mudflows, solifluction, flowtill activity, subaqueous slumping and sliding, and subaqueous deposition and deformation by floating ice. Sand-size particles set in a muddy matrix (graywacke of some authors) constitute a related group of sediments which also originate in diverse ways. Because of the wide variety of origin of all these chaotic sediments, a general descriptive term is needed for them as a group, irrespective of mode of origin.

This paper reviews some recent attempts at naming coarse-grained sediments of this general kind. It proposes one name for the whole group of sediments (including the fine-grained varieties) and another, related name for their lithified equivalents.

D. J. Miller (1953, p. 26) faced the problem of nomenclature in describing what he termed *"conglomeratic" sandy mudstone* included in late Cenozoic glacial-marine deposits in Alaska. His review of the names applied to the sediments of Middleton Island indicated that all nongenetic terms suitable for either hand specimens or outcrops were "either inaccurate or inconveniently long." Examples of such terms include: boulder clay, sandy clay containing both angular and rounded boulders, massively bedded marine silty sandstones and shales containing large and moderate-size boulders, shale-matrix conglomerate, shale-matrix breccia-conglomerate, "conglomerate", cobble-bearing mudstone. Miller finally chose *"conglomeratic" sandy mudstone* as "the best descriptive name that can be devised for the tillite-like rock." He suggested informally, however, that the Alaskan glacial-marine deposits be called *yakatagite*, following the fashion of the term *spergenite*, proposed informally by Pettijohn (1949, p. 179, 301).

A classification of sediments based on texture, set up by R. L. Folk (1954), recognized 15 textural group names for various mixtures of grade sizes that include gravel (particle diameters larger than 2 mm), sand (particle diameters in range 2 to 0.0625 mm), and mud (refers to both silt and clay; particle diameters smaller than 0.0625 mm). Folk's classes are selected on the basis of gravel content of 80, 30, and 5 per cent and on the ratio of sand to mud. Three classes are based on sand:mud ratios of 9:1, 1:1, 1:9.

Folk's scheme employs the following names in the coarse-grained range:

Per cent gravel	*Rock name, based on matrix*
30–80	sandy conglomerate
	muddy conglomerate
5–30	conglomeratic sandstone
	conglomeratic mudstone
trace–5	slightly conglomeratic sandstone
	slightly conglomeratic mudstone

Pettijohn (1957, Chapter 6) proposed to subdivide conglomerate into *orthoconglomerate* ("gravels collected by ordinary water currents") and *paraconglomerate* ("those deposited by subaqueous turbidity flows and slides, and by glacial ice or other modes of mass transport"). The term *conglomeratic mudstone* was also used

for those deposits which "have a disrupted framework—one notable for the greater excess of matrix over gravel-sized fragments" (1957, p. 254). Pettijohn echoed D. J. Miller's opinion that existing terminology is inadequate, and therefore chose *paraconglomerate*: "As the term implies, something is amiss or aberrant. These rocks are not the products of normal aqueous flow" (1957, p. 261). The following synonyms for paraconglomerate were listed by Pettijohn:

conglomeratic mudstone
pebbly or cobbly mudstone
boulder clay (= till)
Geröllton (proposed by Ackermann, 1951, for nonglacial pebbly mudstone)
tilloid (nonglacial conglomeratic mudstones)

Pettijohn commented that the term *mudstone conglomerate*, used in a few instances for these rocks, indicates a conglomerate in which mudstone clasts are present.

Pettijohn recognized two varieties of paraconglomerate based on structure of the matrix: those in which the matrix is laminated and those in which the matrix is nonlaminated. He recognized also two other categories based on genesis: sediments of nonglacial origin, called *tilloid* (*Geröllton*); and those of glacial origin, called *tillite*. He noted that the latter is "in one sense a cataclastic deposit analogous to gouge" (Table 43, p. 255). In subsequent parts of the text (p. 261–265), where paraconglomerate is implied, the following additional terms also appear:

laminated pebbly mudstone
conglomeratic laminated lutite (rafted blocks)
laminated argillite with rafted blocks (= conglomeratic pellodites[1]).

Crowell (1957) recognized the possible diverse origins of sediment that may resemble till and advocated the use of *pebbly mudstone*, a term not unlike the "conglomeratic" sandy mudstone of Miller, "as a descriptive name for a rock composed of dispersed pebbles in a mudstone matrix without regard to manner of origin." He characterized these deposits by their poor sorting and by the presence of "too much matrix to qualify as a conglomerate" (p. 1003).

This diversity of opinion for the coarse-grained varieties has not appeared in the nomenclature of fine-grained sediments, for many geologists use the term graywacke for sandstones with muddy matrix. Others, however, define graywacke on the basis of composition of the sand-size particles and employ the presence of rock fragments, particularly of nonfeldspathic metamorphic rocks, as an essential parameter (Folk, 1954). The terms proposed herein offer the possibility of bringing the definition of graywacke into sharper focus by substituting a more general word for graywackes that have been recognized solely on a textural basis.

As emphasized by most of the authors cited, the nomenclature of nonsorted and poorly sorted terrigenous deposits is inadequate and tends to place too much emphasis on the similarity of coarse-grained varieties to till. Indeed, the lack of a simple group term for the whole spectrum of sediments similar in appearance to till may have led to overemphasis on till in describing sediments that contain large clasts within a lutite matrix, thereby making room for possible implication as to genesis. Folk's several classes based on quantitative estimates of the grain sizes present are a desirable refinement of nongenetic terminology; yet some of them have disadvantages. For example *conglomerate* implies a consolidated rock, with rounded fragments. Pebbly mudstone might perhaps better be called *gravelly mudstone*, so as to include a larger range of grain sizes than is suggested by *pebble* (2–64 mm in Udden-Wentworth scale); also it implies a rock rather than a sediment. Although *paraconglomerate* is useful in that it implies something peculiar, aberrant, or amiss about a rock, it too is a term for a rock rather than for a sediment. Further, the prefixes *ortho* and *para* have been used in rather different ways in rock nomenclature. Hence applying them to conglomerates with still different meanings seems to invite confusion. For example, an orthoconglomerate could be thought of as a coarse-grained equivalent of an orthoquartzite; a paraconglomerate might be supposed to have close connections with a paragneiss or paraconformity (Dunbar and Rodgers, 1957, p. 119).

Although we hesitate to add to geologic terminology, we believe that clear need exists for a comprehensive term to designate nonsorted essentially noncalcareous sediments consisting of sand and/or larger particles dispersed through a muddy matrix. The term should be applicable to till, to all other sediments that resemble till in respect to range of grain size and sorting, and to poorly sorted sands in a

[1] *Pelodite* was proposed by J. B. Woodworth (1912, p. 78) for lithified glacial rock flour. *Pelodite* was held to differ from *pelite* by its included glacial pebbles. The A.G.I. Glossary attributes *pellodite* to Schuchert (1924, p. 441), who evidently added a second *l* to Woodworth's term.

muddy matrix, without regard to mode of origin. A related but separate term is needed for the lithified equivalents of these sediments.

After consultation with Professor C. Bradford Welles, Department of Classics, Yale University, we propose for the sediment: *symmicton*, derived and anglicized from the Greek *symmeikton*, which refers to mixed substances of any nature. In this case it refers to the mixed size grades. For the lithified equivalents we propose *symmictite*.

A *symmicton*, therefore, is any nonsorted or poorly sorted terrigenous sediment that consists of sand and/or larger particles in a muddy matrix.[2] Size distribution is commonly bimodal or polymodal, with one or more modes in the coarse-grain range and one or more in the silt-clay sizes. A *symmictite* is a lithified *symmicton*. Both terms are noncommital as to genesis.

We believe there are two good reasons why these names are desirable:

(1) As far as we know, the existing nomenclature includes no general term embracing mixed terrigenous sediments of all kinds, regardless of origin. Such a term is needed for convenience. In facilitating description, the term should aid in avoiding commitment as to the origin of a sediment whose agency of deposition is uncertain. It seems likely that the existence of the specific terms *till* and *tillite*, in the absence of a general term, has encouraged glacial rather than other possible interpretation of mixed sediments and their rock equivalents. Use of the terms here proposed might, therefore, lead to reappraisal of the origin of some of the coarse-grained sediments and rocks originally interpreted as glacial. Some "tillites" may not survive such reappraisal (Crowell, 1957; Newell, 1957; Sanders and Cecioni, 1957; Van Houten, 1957).

(2) The proposed names discriminate fully and clearly between sediments and rocks.

[2] Certain limestones (shell fragments in a lime-mud matrix, for example) have the range of grain sizes indicated here and can even originate through some of the same processes suggested for the terrigenous deposits. However, because of their bioclastic origin we exclude them. But we do include sediments that contain abundant rock fragments of older limestone.

Acknowledgment

The authors are indebted to C. B. Welles for his suggestion of the terms proposed, and to C. M. Gilbert, F. J. Pettijohn, and F. B. Van Houten for reading the manuscript and making thoughtful comments.

References Cited

Ackermann, Ernst, 1951, Geröllton: Geol. Rundschau, v. 39, p. 237–239

Crowell, J. C., 1957, Origin of pebbly mudstones: Geol. Soc. America Bull., v. 68, p. 993–1010

Dunbar, C. O., and Rodgers, John, 1957, Principles of stratigraphy: New York, J. Wiley & Sons, 356 p.

Folk, R. L., 1954, The distinction between grain size and mineral composition in sedimentary-rock nomenclature: Jour. Geology, v. 62, p. 344–359

Miller, D. J., 1953, Late Cenozoic marine glacial sediments and marine terraces of Middleton Island, Alaska: Jour. Geology, v. 61, p. 17–40

Newell, N. D., 1957, Supposed Permian tillites in northern Mexico are submarine slide deposits: Geol. Soc. America Bull., v. 68, p. 1569–1576

Pettijohn, F. P., 1949, Sedimentary rocks, 1st ed.: New York, Harper and Bros., 526 p.

—— 1957, Sedimentary rocks, 2nd ed.: New York, Harper and Bros., 718 p.

Sanders, J. E., and Cecioni, G. O., 1957, Flysch and molasse (discussion): Am. Assoc. Petroleum Geologists Bull., v. 41, p. 2136–2139

Schuchert, Charles, 1924, A text-book of geology. Pt. 2, Historical geology. 2nd ed: New York, J. Wiley & Sons, 724 p.

Van Houten, F. B., 1957, Appraisal of Ridgway and Gunnison "tillites," southeastern Colorado: Geol. Soc. America Bull., v. 68, p. 383–388

Woodworth, J. B., 1912, Geological expedition to Brazil and Chile, 1908–1909: Mus. Comp. Zoology Bull., v. 56, no. 1, 137 p.

YALE UNIVERSITY, NEW HAVEN, CONN.

MANUSCRIPT RECEIVED BY THE SECRETARY OF THE SOCIETY, NOVEMBER 12, 1959

LEAC
IN

Goodin
presented
clay-enric
careous ti
and south
a paleosol
several wo
et al., 19
Kempton
1959) but
present su
in the ov
have beer
levels in t
good dra
underlain
therefore,
as remnan
basis for
has led t
Pleistocen
that the
the interp
classical
ing interv
not deny t

This pa
buried soil
presents C
zones in
two sites
believe sup

In addit
zones in
graphic lev
and southe
we observe
meeting o
what we b
developed
gravel ben
of London
Packer, 19
(1958, p.
clayey till
enriched z
by the gla

BULLETIN OF THE GEOLOGICAL SOCIETY OF AMERICA
VOL. 71, PP. 511-514 APRIL 1960

LEACHED, CLAY-ENRICHED ZONES IN POST-SANGAMON DRIFT IN SOUTHWESTERN OHIO AND SOUTHEASTERN INDIANA: NEW OBSERVATIONS AND DATA

BY ANSEL M. GOODING AND ERLING GAMBLE

Gooding, Thorp, and Gamble (1959) recently presented evidence showing that leached, clay-enriched zones in outwash beneath calcareous till, widespread in southwestern Ohio and southeastern Indiana, are not remnants of a paleosol of regional extent as interpreted by several workers (*see* references listed in Gooding *et al.*, 1959; Goldthwait and Burns, 1958; Kempton and Goldthwait, 1959; Goldthwait, 1959) but are downward extensions of the present surface soils through cracks and joints in the overlying calcareous till. These zones have been observed at various stratigraphic levels in the drift of the area wherever there is good drainage through jointed surface till underlain by sand and gravel. We implied, therefore, that the interpretation of these zones as remnants of a paleosol, and their use as a basis for stratigraphic correlations in Ohio, has led to erroneous conclusions about the Pleistocene history of this area. We believe that the evidence at hand does not support the interpretation of a post-Sangamon–pre-classical Wisconsin glaciation and soil-forming interval in this area, although we do not deny the possibility of such events.

This paper describes two similar pseudo buried soils outside the Ohio-Indiana area and presents C_{14} data on the leached, clay-enriched zones in outwash beneath calcareous till at two sites near Richmond, Indiana, which we believe support our earlier conclusions.

In addition to having observed these soil-like zones in many places and at several stratigraphic levels in the drift of southwestern Ohio and southeastern Indiana (Gooding *et al.*, 1959), we observed during the 1959 Eastern Section meeting of the Friends of the Pleistocene what we believe to be the same phenomenon developed in a thin layer of sand and fine gravel beneath a thin clayey till in the vicinity of London, Ontario, Canada (Dreimanis and Packer, 1959, Stop 12, unit 3, p. 23). Dreimanis (1958, p. 81) suggested a correlation of the clayey till that overlies the leached, clay-enriched zone with the till that was deposited by the glacial advance which reached beyond the Defiance moraine in eastern Ohio. White (1951, p. 976) suggested that this till is middle to late Cary in age.

Although clay-filled joints in the thin till overlying the leached, clay-enriched zone were not well displayed at Dreimanis and Packer's Stop 12, other evidences showed that the soil-like zone could not be a remnant of a paleosol. In places, the entire sand and gravel zone and a few inches of the top of the underlying till are leached and enriched with clay. In other places, however, the top of the leached, clay-enriched zone is irregular. It crosses the stratification of sands, leaving calcareous, clay-free "lenses" over the leached zone, and in some places the leaching and clay enrichment extend a few inches up into the base of the overlying clayey till. The last feature demonstrates beyond reasonable doubt that the leaching occurred after the upper clayey till was deposited. Dreimanis and Packer had asked the question: "Is this a paleosol or the result of underground water leaching?" (1959, p. 23). Dreimanis now agrees with us on its secondary origin (personal communication).

This apparent "buried soil" beneath probable middle to late Cary till in Ontario is clearly of the same origin as those occurring beneath tills of various earlier Wisconsin subages over wide areas of Ohio and Indiana.

Another new observation of particular significance has just been made by James Thorp in Africa. He reported recently on the occurrence of a similar weathered zone, with dark-brown clay skins, beneath the topmost volcanic ash deposit near Nanyuke, northwest of Mt. Kenya, Kenya. He has stated in a personal communication: "I thought at first it was a buried soil, but close examination showed that it connects, along cracks and joints in the ash, with the soil at the present surface. Furthermore, there is no A horizon."

The above two new observations suggest to us that an understanding of the origin of these false "buried soils", and the criteria by which they are recognized, may be of more far-reaching importance than just with respect to the

Ohio–Indiana Pleistocene problem. When workers find soil B horizonlike material on sand and gravel beneath calcareous till, or other material beyond drift regions, evidence for a connection with the present surface soils through cracks and joints should be sought. It is essential, also, to find at least a remnant of an A horizon in position before such zones are finally identified as paleosols and given stratigraphic status.

C_{14} dates have been obtained recently on leached, clay-enriched zones in outwash beneath calcareous till from two sections near Richmond, Indiana (the Middle Fork section is Fig. 1 in Gooding *et al.*, 1959, p. 922) which tend to support our previous conclusions on the secondary origin of these soil-like zones (discussed in detail in Gooding *et al.*, 1959) and show a valuable means of testing the validity of questionable "buried soils" in other areas.

Chemical analyses of the B horizon of the present surface Miami Family of soils in southwestern Ohio and southeastern Indiana show considerable colloidal organic material intimately mixed with the illuviated B horizon clay (Brown and Thorp, 1942, Table 8, p. 38). Samples of the leached, clay-enriched material in outwash beneath calcareous till from two sections were analyzed and found to contain colloidal organic matter in quantity similar to that present in the B horizons of the surface soils. We reasoned that, if the colloidal organic matter in these leached, clay-enriched zones beneath calcareous till could be extracted in large enough quantity, a C_{14} date on these zones would shed light on their true nature. If these zones are actually remnants of a true buried paleosol, C_{14} dates on their colloidal organic matter should be older than C_{14} dates on wood found in overlying till (providing the wood was not picked up from still older drift). On the other hand, if these zones are downward extensions of the present surface soil through cracks and joints in the overlying calcareous till, as we contend, C_{14} dates on their colloidal organic material should be more recent than dates on any wood found in the till which overlies them. Furthermore, if our interpretation of these zones is correct, the C_{14} dates on the colloidal organic matter from these zones would be expected to vary from one site to another, because the colloidal organic material might well be a mixture of different proportions of that which collected at various periods as soil formation advanced. The proportions of this mixture of older and younger colloidal organic matter in the illuviated zones on outwash beneath calcareous till would naturally vary from place to place.

A 25-pound can of leached, clay-enriched material developed in outwash beneath calcareous till was taken from each of two sites near Richmond, Indiana, and representative samples contained enough organic carbon for C_{14} dating. The organic carbon analyses were made by Mr. Roger Simkin, Earlham College Chemistry major, following the method outlined by Peech *et al.* (1947, p. 5–7). The samples were treated and dated at the Lamont Radiocarbon Laboratory, Columbia University, by Mr. Edwin Olson and Dr. Wallace S. Broecker.

Following are descriptions of the two sections near Richmond, Indiana:

Middle Fork Section: Exposed in 1958 along creek bank in NE 1/4 SW 1/4 Sec. 15, T. 14 N., R. 1 W., Wayne County, Indiana (this is the section shown in Fig. 1 of Gooding *et al.*, 1959, p. 922).

Unit	*Thickness* (Feet)	*Description*
8	1.9	Miami silt loam soil profile developed through 6 inches of loess and into till
7	3.2	Calcareous oxidized highly jointed till; leached brown clay concentrated along vertical joints. Sand inclusion bisected by a joint was leached and enriched with clay; some of till surrounding leached inclusion was also leached.
6	0.5	Leached, clay-enriched gravel with dolomite ghosts; greatest concentration of clay directly below joints. Gooding C_{14} sample No. 20 is from this unit.
5	0.5	Leached medium sand with some brown clay
4	0.5	Calcareous medium sand with irregular leached and clay-enriched lenses at bottom
3	0.5	Partially leached gravel with some brown clay
2	8.0	Calcareous sand and gravel
1	4.0	Calcareous, gray, unoxidized till Creek bed

Magaw Gravel Pit Section: Exposed in 1958 in SE 1/4, Sec. 30, T. 14 N., R. 1 W., Wayne County, Indiana.

Unit	*Thickness* (Feet)	*Description*
4	2.6	Miami silt loam soil profile developed through 12 inches of loess and into till
3	5.4	Calcareous oxidized highly jointed till; leached brown clay concentrated along vertical joints that extend through the till
2	1–2.0	Sand and pebble gravel, mostly

leached and containing much brown clay. Some dolomite ghosts remain in rotted gravel. Some fine sand zones and lenses at various levels still calcareous and contain little or no brown clay. Gooding C_{14} sample No. 21 is from this unit.

1 65.0 Calcareous sand and gravel
Bottom of exposure

The C_{14} dates from the above two sections are as follows:

L-474A, 13,300 ± 650, Middle Fork section, unit 6 (Gooding sample No. 20, collected July 1958).

L-474B, 4,800 ± 200, Magaw gravel pit section unit 2, (Gooding sample No. 21, collected July 1958).

Although no C_{14} dates are available in the immediate area on wood from the overlying till, in both cases the locations are south of Leverett and Taylor's (1915) "Bloomington" moraine where the surface till is "Champaign" (till sheet B in Gooding, 1957). A C_{14} date on wood from Bloomington back-water silts behind valley-train outwash in Illinois is 15,600 ± 600 (W-381) (Rubin and Alexander, 1958, p. 1478).

If interpretations in Ohio are correct, however, and the widely occuring leached, clay-enriched zones in outwash beneath calcareous till in this area are remnants of a post-Sangamon–pre-classical Wisconsin soil, C_{14} dates on the colloidal organic matter from these zones should be much older than we have interpreted for the age of the overlying till at the sections herein described. Ohio workers have correlated these soil-like zones in outwash beneath calcareous till with leached zones in till at the Sidney and Brush Creek, Ohio, exposures. Wood reportedly collected from the top of the Sidney, Ohio, buried soil gives a C_{14} date of 23,000 ± 800 (W-188) (Rubin and Suess, 1955, p. 483), and wood collected from the till which overlies the buried soil at Brush Creek, Ohio, gives a C_{14} date of 22,000 ± 1,000 (W-414) (Rubin and Alexander, 1958, p. 1477; La Rocque and Forsyth, 1957, p. 81, 88).

It is true that these dates (L-474A, 13,300 ± 650, and L-474B, 4,800 ± 200) on the leached, clay-enriched zones beneath calcareous till at the sections near Richmond do not prove that the "soil-like" zones are not remnants of a buried soil: they may merely demonstrate contamination of a true buried soil. The geological evidence (*see* Gooding *et al.*, 1959) from these and dozens of other sites, however, suggests that the colloidal organic matter in the dated zones is entirely of post-till age, and that the considerable difference between the dates is due to the expectable variation in the proportions of older and younger colloidal organic matter that has been illuviated during the time of surface soil formation. Additional C_{14} dates on these soil-like zones in Ohio and Indiana, especially those that are interpreted as true buried soils by Ohio workers, might help to clarify the present controversy over their origin and stratigraphic importance.

Acknowledgments

This paper developed out of Pleistocene geology and soil-genesis studies in the Whitewater basin of southeastern Indiana and surrounding areas supported by National Science Foundation Grants No. 997 and No. 3484, the Charles F. Kettering Foundation, and the Soil Conservation Service, U. S. Department of Agriculture.

Dr. James Thorp, Head, Department of Geology and Soil Science, Earlham College, and Dr. Morris M. Leighton, Chief Emeritus, Illinois Geological Survey, on separate occasions visited the Magaw gravel pit section with the writers. Both also read the manuscript critically and made helpful suggestions.

References Cited

Brown, Irvin C., and Thorp, James, 1942, Morphology and composition of some soils of the Miami Family and the Miami Catena: U. S Dept. Agriculture Tech. Bull. 834, 55 p.

Dreimanis, A., 1958, Wisconsin stratigraphy at Port Talbot on the north shore of Lake Erie, Ontario: Ohio Jour. Sci., v. 58, p. 65–84

Dreimanis, A., 1959, Proposed local stratigraphy of the Wisconsin glacial stage in the area south of London, southwestern Ontario: Friends of the Pleistocene, Eastern Section, 22nd Reunion, Guidebook, p. 24–30

Dreimanis, A., and Packer, R., 1959, Field Trip Guide: 22nd Reunion, Eastern Section, Friends of the Pleistocene Guidebook, p. 1–23

Goldthwait, R. P., 1959, Leached, clay-enriched zones in post-Sangamonian drift in southwestern Ohio and southeastern Indiana: a Reply: Geol. Soc. America Bull., v. 70, p. 927–928

Goldthwait, R. P., and Burns, G. W., 1958, Wisconsin age forests in western Ohio: Ohio Jour. Sci., v. 58, p. 209–230

Gooding, A. M., 1957, Pleistocene terraces in the upper Whitewater drainage basin, southeastern Indiana: Earlham Coll. Sci. Bull. no. 2, 65 p.

Gooding, A. M., Thorp, James, and Gamble, Erling, 1959, Leached, clay-enriched zones in post-Sangamonian drift in southwestern Ohio and southeastern Indiana: Geol. Soc. America Bull., v. 70, p. 921–925

Kempton, J. P., and Goldthwait, R. P., 1959,

Glacial outwash terraces in the Hocking and Sciota River valleys, Ohio: Ohio Jour. Sci., v. 59, p. 135–151

La Rocque, Aurèle, and Forsyth, Jane, 1957, Pleistocene molluscan faunules of the Sidney Cut, Shelby Co., Ohio: Ohio Jour. Sci., v. 57, no. 2, p. 81–89

Leverett, Frank, and Taylor, Frank, 1915, The Pleistocene of Indiana and Michigan and the history of the Great Lakes: U. S. Geol. Survey Mon. 53, 529 p.

Peech, Michael, Alexander, L. T., Dean, L. A. and Reed, J. F., 1947, Methods of soil analysis for soil-fertility investigations: U. S. Dept. Agriculture Circ. no. 757, 25 p.

Rubin, Meyer, and Alexander, Corrine, 1958, U. S. Geological Survey radiocarbon dates IV: Science, v. 127, p. 1476–1487

Rubin, Meyer, and Suess, H. E., 1955, U. S. Geological Survey radiocarbon dates II: Science, v. 121, p. 481–488

White, George W., 1951, Illinoian and Wisconsin drift of the southern part of the Grand River lobe in eastern Ohio: Geol. Soc. America Bull., v. 62, p. 967–978

Dept. Geology, Earlham College, Richmond, Ind.

Manuscript Received by the Secretary of the Society, July 20, 1959

BULLETIN OF THE GEOLOGICAL SOCIETY OF AMERICA
VOL. 71. PP. 515-520, 1 FIG. APRIL 1960

CLAY MINERALOGY OF THE SEDIMENTS OF THE GREAT SALT LAKE, UTAH

BY RALPH E. GRIM, GEORGES KULBICKI, AND ALBERT V. CAROZZI

Abstract

The modern lake sediments and those of post-Provo age immediately preceding the present Great Salt Lake have about the same clay-mineral composition. In these deposits, the montmorillonite shows a relatively poor organization which may be a consequence of the presence of considerable sodium. The montmorillonite may be either detrital or precipated or formed by alteration of volcanic ash.

The illite, probably detrital, is generally well organized showing only a very small amount of degrading. The presence of kaolinite in all the lake samples is noteworthy. It is almost certainly detrital. There is a general absence of substantial mixed-layer components as well as of any chlorite, and there is no suggestion of attapulgite-sepiolite clay minerals.

The Alpine and Provo sediments of the Lake Bonneville terraces have a clay-mineral composition somewhat different from that of the modern lake sediments; they show a highly degraded chlorite and a very well-ordered montmorillonite.

The green clays of Early Pleistocene age also have a distinctive clay-mineral composition corresponding to a high content of illite and a low content of montmorillonite associated with the presence of chlorite.

The clays occurring in the Great Salt Lake Desert west of Knolls contain at a depth of about a foot a thin bed of nearly pure, unconsolidated dolomite.

Introduction

Since the remarkable study of Eardley (1938) on the Great Salt Lake sediments, no systematic investigation of their clay-mineral composition has been reported.

Peculiar conditions of sedimentation such as those of the Great Salt Lake have often been considered as a possible favorable environment for the genesis of attapulgite-sepiolite clay minerals. Such a hypothesis led the writers to undertake in the summer of 1958 a systematic investigation of the entire shore-line development of the Great Salt Lake. To this basic scheme was added a scattered sampling of the sediments of the Great Salt Lake Desert and of the terraces of Lake Bonneville.

The writers analyzed 120 samples in the Clay Mineralogy Laboratory of the University of Illinois, and the results are considered here.

The clay-mineral determinations are based on X-ray diffraction using oriented aggregates (Johns, Grim, and Bradley, 1954). The samples were fractionated at 2 microns prior to analysis.

Acknowledgments

This project was made possible by a grant from the Penrose Bequest of The Geological Society of America which is gratefully acknowledged. The writers are also especially indebted to Professors Armand J. Eardley, Daniel J. Jones, and Ray E. Marsell, all of the University of Utah, Salt Lake City, for their invaluable and friendly co-operation at all stages of the investigation.

Analysis of Collected Materials

The samples have been classified into the following groups: green clays of Early Pleistocene age; Alpine and Provo sediments of Lake Bonneville terraces; post-Provo sediments immediately preceding the modern Great Salt Lake; and modern Great Salt Lake sediments.

Green clays of Early Pleistocene age

These green clays were sampled at an exposure along the Old Mill road, east of Salt Lake City and below the mouth of Big Cottonwood Canyon, just west of the Old Mill (Fig. 1, loc. 1). The exposure consists of well-indurated siltstones and claystones interbedded with beds of unconsolidated clays (Jones and Marsell, 1955).

The typical clay-mineral composition is illite 60%, chlorite 15%, kaolinite 15%, montmorillonite 10%. The illite is well crystallized, but the chlorite is thoroughly degraded, approaching a material with the characteristics of vermiculite.

Alpine and Provo sediments of Lake Bonneville terraces

Green and red to brownish Alpine silts were sampled in the railroad cut of the Jordan River Narrows (Fig. 1, loc. 2) and also south of Parleys Canyon (Fig. 1, loc. 3) where they alternate with gravels and sands. The Provo silts were sampled along Victory Road in Salt Lake City (Fig. 1, loc. 4) where they are interbedded with gravels and sands.

A typical sample of the Alpine silt has the following clay-mineral composition: illite 60%, a mixed-layer assemblage of chlorite and montmorillonite 30%, kaolinite 10%. The chlorite is thoroughly degraded, and the illite shows slight degrading.

The Provo silt samples have the following clay-mineral composition: montmorillonite 50%, illite 40%, kaolinite or chlorite 10%. The montmorillonite is distinctive material with diffraction characteristics similar to those of montmorillonite produced by the alteration of ash in bentonites. No positive identification can be made of the component listed as kaolinite or chlorite.

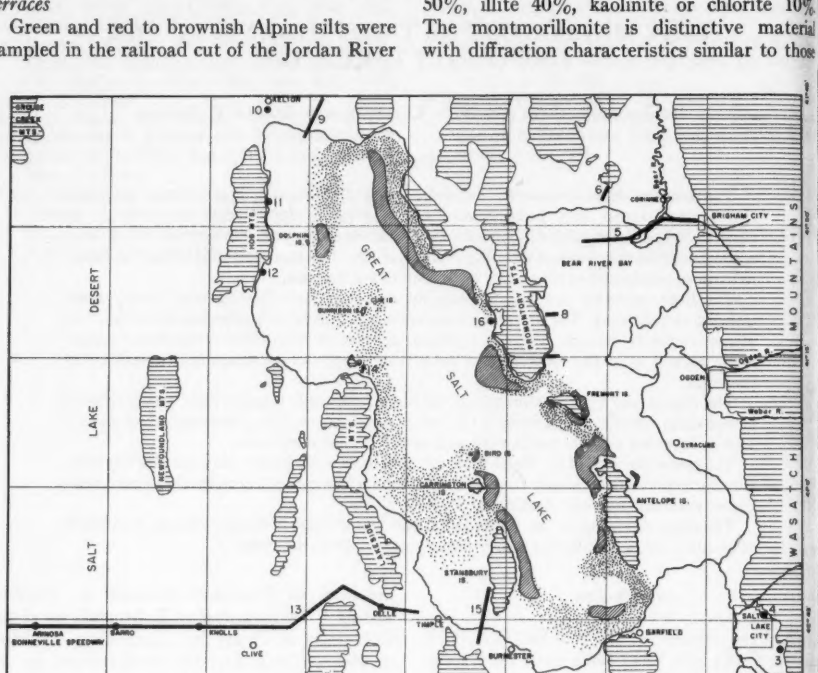

FIGURE 1.—MAP OF DISTRIBUTION OF SEDIMENTS IN THE GREAT SALT LAKE AREA
Showing location of localities investigated. Adapted from Eardley (1938).

Post-Provo sediments immediately preceding the modern Great Salt Lake

The post-Provo sediments are located below the Provo terrace and represent a number of shore lines corresponding to the progressive shrinking of the lake immediately preceding the present time boundaries. These sediments constitute the inland portion of several profiles

which were carried across the present lake shore line into the lake itself.

Profile 5 (Fig. 1, loc. 5) displays predominantly black clays under local salt crusts. It extends from Brigham City railroad station downstream along the Bear River to its mouth in the Bear River National Wildlife Refuge. The profile is 17 miles long, and a sample was collected each mile. The clay-mineral composition of all these samples is substantially the same, averaging, illite 50%, montmorillonite 40%, and kaolinite 10%.

Profile 6 (Fig. 1, loc. 6) consists of a sampling of post-Provo sediments, 8 miles west of Corinne, north and south of Utah Highway 83 in the vicinity of basaltic lava flows, in order to check their effect on the composition of the neighboring deposits. In these samples which appear as superficial gray silts becoming reddish toward the bottom of isolated and desiccated ponds, the clay-mineral composition is the same as in profile 5 except that the montmorillonite is slightly more abundant than the illite.

Profile 7 (Fig. 1, loc. 7) is located on the east coast of Promontory Mountains, 4 miles north of Promontory Point. It starts at the highway level and extends eastward into the salt flats for three quarters of a mile. The number of samples is 13. The beginning of the profile shows gray-blue to brown, humus-bearing clays underlying the vegetation. These clays grade lakeward into gray-blue to light-gray surface clays which become black and stinky immediately below the salt crust. Again the clay-mineral composition of all the samples is about the same, averaging kaolinite 15%; illite and montmorillonite make up the remainder in about equal proportions.

Profile 8 (Fig. 1, loc. 8) is located on the east coast of Promontory Mountains, 5 miles north of profile 7. It starts also at the highway level and extends eastward into the salt flats more than half a mile; 8 samples were collected. The clay-mineral composition is the same as in profile 7; here also the clays are predominantly gray blue at the surface and become varved, black, and stinky below the salt crust.

Profile 9 (Fig. 1, loc. 9) extends from south of High Butte along the highway from Snowville to Locomotive Springs National Wildlife Refuge, across the salt flats into the present lake. The length of the profile is 7 miles of which half a mile is in the lake itself; the number of samples is 20. The clay-mineral composition is the same as in the preceding profiles, except that two samples from close to a basalt flow have relatively more montmorillonite. As a whole, the clays of this profile are predominantly gray at the surface and become darker and stinky under the salt crust.

Additional samples of the post-Provo sediments were taken around Kelton (Fig. 1, loc. 10) as well as along the eastern foot of the Hogup Mountains, 15 and 25 miles south of Kelton (Fig. 1 loc. 11 and 12). Samples from these points do not differ in composition from those of the preceding profiles.

Profile 13 (fig. 1, loc. 13) was taken in the Great Salt Lake Desert and consists of irregularly distributed samples along an east-west-trending line extending parallel to U. S. Highway 40-50 from the entrance of the Bonneville Race Tracks eastward to 5 miles east of Delle. The profile is 65 miles long, and the number of samples is 15. All these samples contain about 10 per cent kaolinite; illite and montmorillonite in varying proportions make up the remainder of the clay mineral fraction. Generally, montmorillonite is appreciably more abundant than illite. Data are not at hand to determine the possible significance of this variation. In general, the samples of this profile appear as whitish to greenish dusty silts at the surface. They grade downward into plastic, laminated, and greenish clays interbedded with salt layers and containing at about a foot below the surface a thin bed of nearly pure, unconsolidated dolomite. This unusual carbonate sediment is presently undergoing further investigation by D. L. Graf of the Illinois Geological Survey.

Modern Great Salt Lake sediments

In addition to the lakeward portions of profiles 5, 7, 8, and 9, two profiles were sampled entirely in the Great Salt Lake itself.

Profile 14 (Fig. 1, loc. 14) was taken at Lakeside from the Union Pacific tracks northward into the mud flats and the lake sediments for half a mile. The number of samples is 9. Kaolinite makes up about 10 per cent of the clay fraction; montmorillonite and illite form the remainder. Montmorillonite is usually slightly more abundant than illite. The sediments of this profile are light-colored to whitish clays associated with layers of oölites and salt.

Profile 15 (Fig. 1, loc. 15) was taken across the mud flats which have joined Stansbury Island to the vicinity of U. S. Highway 40–50 forming a large peninsula. The length of the profile is 17 miles, and the number of samples is 9. The clay-mineral composition is the same as

in profile 14. Here the clays are black and associated with oölites near the island; they turn gray blue under the vegetation.

Additional samples were taken south of Indian Caves (Fig. 1, loc. 16), on the west coast of Promontory Mountains where the biohermal and oölitic belt is very narrow. The clay-mineral composition is the same as in profile 14.

General Conclusions

The clay-mineral composition of the modern Great Salt Lake sediments is about the same as that of sediments of post-Provo age immediately preceding the modern lake. In general, the montmorillonite shows relatively poor organization, which may be a consequence of the presence of considerable sodium with its high tendency to disperse the clay mineral. The degree of organization is particularly poor in samples containing considerable organic material and in those found at or immediately below the surface. Samples from the bottom of the lake, particularly those from below the lake bottom, show montmorillonite with better organization. The montmorillonite is relatively more abundant in samples collected close to basalt outcrops; this suggests that at least some of it is detrital in origin. There is no evidence to refute the belief that some of the montmorillonite formed by the alteration of ash which may have fallen into the lake or possibly was a direct precipitate from the lake waters.

The illite in the lake sediments is generally well organized showing only a very small amount of degrading; clearly it is detrital in origin.

The presence of kaolinite in all the lake samples is noteworthy. The mineral is almost certainly detrital, since the pH and the high alkalinity of salts in solution are foreign to the environment in which kaolinite would be expected to form. In all samples it is not possible to be certain that this mineral is in fact kaolinite and not chlorite; however, wherever a definite identification could be made the mineral was kaolinite.

The general absence of substantial mixed-layer components in the lake sediments is of particular interest. This can possibly be explained as follows: the illite carried into the lake was relatively little degraded and was not further degraded with the development of mixed layering after its deposition. The fact that the chlorite in older sediments surrounding the lake is highly degraded suggests that any chlorite carried to the lake would possibly be further degraded to completely expandable material, which would be classed in the lake sediments as montmorillonite. In other words, the illite and also the kaolinite in the highly sodium rich environment would be relatively unaffected, whereas the chlorite would be degraded beyond the mixed-layer stage so that it would be classed with montmorillonite.

The general absence of any chlorite in the lake sediments is also interesting. As indicated, any chlorite carried into the lake would probably have been lost by complete degrading to expandable material which would then be classed as montmorillonite.

The clay-mineral analyses of the lake sediments reveal no suggestion of attapulgite-sepiolite clay minerals. These components with a high content of magnesium have been reported in current evaporites in various parts of the world. It seems likely that these clay minerals would form only in a lake with relatively high magnesium and not in an environment with a high sodium content, such as Great Salt Lake.

The Alpine and Provo sediments of the Lake Bonneville terraces have somewhat different clay-mineral compositions from that of the lake sediments. The presence of highly degraded chlorite, of particular interest in these sediments, indicates, as noted, that this clay mineral is carried into the lake and is lost there. A further interesting point with regard to the Provo silt samples is the presence in them of very well-ordered montmorillonite. Some of the latter has certainly been carried into the present lake sediments; however, its absence is probably to be explained by the strong dispersing action of sodium.

The clay-mineral composition of the green clays of Early Pleistocene age distinguishes them from the present lake deposits and from the Alpine and Provo sediments of the lake Bonneville terraces. These green clays are characterized by high illite and low montmorillonite plus chlorite.

References Cited

Eardley, A. J., 1938, Sediments of Great Salt Lake, Utah: Am. Assoc. Petr. Geologists Bull., v. 32, p. 1305–1411.

Johns, W. D., Grim, R. E., and Bradley, W. F., 1954, Quantitative estimation of clay minerals by diffraction methods: Jour. Sed. Petrology, v. 24, p. 242–251.

Jones, D. J., and Marsell, R. E., 1955, Pleistocene sediments of Lower Jordan Valley, Utah: Utah Geol. Soc. Guidebook to the Geology of Utah, no. 10.

Department of Geology, University of Illinois, Urbana, Ill.

Manuscript Received by the Secretary of the Society, July 30, 1959

62. Cru
63. De
64. Mar
65. Floc
and
He
66. Stru
Eit
67. Bibl
Sta
Ne
$6.7
Pa

1. Stra
2. Pale
3. Evol
4. Geol
12. Revi
13. Penn
1 fi
14. Brac
15. Tung
16. Eoce
1 fi
18. Linea
(Lit
21. Origi
25. Evol
26. Bibl
27. Prop
28. Origi
34. Perm
37. Biblio
38. Lowe
39. Sedim
40. Revis
41. Amer
42. Maqu
43. 1940 E
45. Inter
47. Inter
48. Nort
51. Catal
52. Selec
53. Palec
54. Biost
55. Trilo
1 fi
56. North
figs.
57. Biblio
61. Strat
$3.00
64. Sunki
65. Handl
66. Cenoz
67. Treat
Vol
68. Beeki
69. Genu
70. *Fenest*
72. Coast
73. Meta
$4.50
74. Origin
Tutt
75. Selec
76. Type
Col
77. Relat
figs.,
78. Mollu
pls.
79. Rock

62. Crust of the Earth. Arie Poldervaart, *Editor*. 1955. 762 p. $6.50.
63. De Natura Fossilium, by Georgius Agricola. Translated by M. C. Bandy and J. A. Bandy. 1955. 240 p. $3.00.
64. Marysvale, Utah, Uranium Area. Paul F. Kerr *et al.* 1957. 212 p., 21 pls., 106 figs. $6.00.
65. Floors of the Oceans, I: North Atlantic. Part 1. Physiographic Diagram of the North Atlantic. By Bruce C. Heezen and Marie Tharp. 1958. In color; 54 by 27½ inches. $1.50. Part 2. Text to Accompany Physiographic Diagram. By Bruce Heezen *et al.* 1959. 122 p., 30 pls., 49 figs. $4.50.
66. Structural Conversions in Crystalline Systems and Their Importance for Geological Problems. Wilhelm Eitel. 1958. 178 p., 93 figs., 2 pls., $3.00.
67. Bibliography and Index of Literature on Uranium and Thorium and Radioactive Occurrences in the United States. Part 5. Connecticut, Delaware, Illinois, Indiana, Maine, Maryland, Massachusetts, Michigan, New Hampshire, New Jersey, New York, Ohio, Pennsylvania, Rhode Island, Vermont, and Wisconsin. Margaret Cooper. 1958. 472 p. $6.75. (Also available: Part 1. Ariz., Nev., N. Mex., 25 cents; Part 2. Calif., Idaho, Mont., Wash., Wyo., 25 cents; Part 3. Colo., Utah, 50 cents; Part 4. Mid-Continent, 50 cents)

MEMOIRS

1. Stratigraphy of Western Newfoundland. Charles Schuchert and C. O. Dunbar. 1934. 123 p., 11 pls., 8 figs. $2.40.
2. Paleozoic Plankton of North America. Rudolf Ruedemann. 1934. 141 p., 26 pls., 6 figs. $2.40.
3. Evolution of the Congo Basin. A. C. Veatch. 1935. 153 p., 10 pls., 8 figs. $2.10.
4. Geology in the Coastal Atlas of Western Algeria. R. Van V. Anderson. 1936. 450 p., 19 pls., 2 figs. $4.20.
12. Revision of the Upper Cambrian Fauna of New Jersey. B. F. Howell. 1945. 47 p., 8 pls., $1.00.
13. Pennsylvanian Geology of a Part of the Southern Appalachian Coal Field. H. R. Wanless. 1945. 162 p., 40 pls., 1 fig. $3.90.
14. Brachiopoda of the Independence Shale. M. A. Stainbrook. 1945. 76 p., 6 pls., 2 figs. $1.20.
15. Tungsten Mineralization in the United States. P. F. Kerr. 1946. 241 p., 23 pls., 34 figs. $3.50.
16. Eocene Faunas from the Department of Bolivar, Columbia. B. L. Clark and J. W. Durham. 1946. 126 p., 28 pls., 1 fig. $2.10.
18. Lineation: A Critical Review and Annotated Bibliography. Ernst Cloos. 1946. 122 p., 10 pls., 15 figs. Supplement (Literature for 1942–1952), 16 pages, 1953. Reprinted 1957 as one volume, $2.00.
21. Origin and Development of Craters. T. A. Jaggar. 1947. 508 p., 87 pls., 14 figs. $6.00.
25. Evolution of the Horse Brain. Tilly Edinger. 1948. 177 p., 4 pls., 24 figs. $2.00.
26. Bibliographic Index of Permian Invertebrates. C. C. Branson. 1948. 1049 p. $9.50.
27. Propagation of Sound in the Ocean. J. L. Worsel, Maurice Ewing, C. L. Pekeris. 1948. 205 p., 23 pls., 89 figs. $2.75.
28. Origin of Granite (Conference). James Gilluly, *Chairman*. 1948. 139 p., 13 pls., 5 figs. $1.80.
34. Permian Crinoid Calceolispongia. Curt Teichert. 1949. 132 p., 26 pls., 24 figs. $2.50.
37. Bibliography of Fossil Vertebrates, 1939–1943. C. L. Camp, S. P. Welles, and Morton Green. 1949. 371 p., $4.50.
38. Lower Cretaceous Stratigraphy in Southeastern Arizona. Alexander Stoyanow. 1949. 169 p., 27 pls., 2 figs. $2.50.
39. Sedimentary Facies in Geologic History. C. R. Longwell, *Chairman*. 1949. 171 p. $1.75.
40. Revision of the Families and Genera of the Devonian Tetracorals. E. C. Stumm. 1949. 92 p., 25 pls. $2.00.
41. American Permian Nautiloids. A. K. Miller and Walter Youngquist. 1949. 218 p., 59 pls., 39 figs. $3.60.
42. Maquoketa Brachiopoda of Iowa. Y. Wang. 1950. 55 p., 12 pls. $1.40.
43. 1940 E. W. Scripps Cruise to Gulf of California. C. A. Anderson *et al.* 1950. 362 p., 65 pls., 28 figs. $6.50.
45. Interpretation of Ore Textures. E. S. Bastin. 1950. 101 p., 28 figs. $1.75.
47. Interpretation of Aeromagnetic Maps. V. Vacquier *et al.* 1951. 151 p., 14 pls., 83 figs. $2.25.
48. North American Geosynclines. Marshall Kay. 1951. 143 p., 16 pls., 20 figs. $2.00.
51. Catalogue of the Cenozoic Plants of North America through 1950. Robert S. LaMotte. 1952. 381 p., 5 figs. $5.50.
52. Selected Petrogenic Relationships of Plagioclase. R. C. Emmons, *Editor*. 1953. 142 p., 38 figs., 16 pls. $2.00.
53. Paleozoic and Mesozoic Arachnida of Europe, Alexander Petrunkevitch. 1953. 128 p., 58 pls. $3.00.
54. Biostratigraphy of the Maqfi Section, Egypt. L. W. LeRoy. 1953. 73 p., 4 figs., 14 pls. $1.75.
55. Trilobites from the Lower Champlainian Formations of the Appalachian Valley. Byron N. Cooper. 1953. 68 p., 1 fig., 19 pls. $1.75.
56. North American and European Stropheodontids: Morphology and Systematics. Alwyn Williams. 1953. 67 p., 5 figs., 13 pls. $1.50.
57. Bibliography of Fossil Vertebrates. 1944–1948. C. L. Camp, *et al.* 1953. 465 p. $5.50.
61. Stratigraphy and History of the Moenkopi Formation of Triassic Age. E. D. McKee. 1954. 133 p., 19 figs., 12 pls. $3.00.
64. Sunken Islands of the Mid-Pacific Mountains. E. L. Hamilton. 1956. 97 p , 12 figs., 13 pls. $2.50.
65. Handbook of South American Geology. W. F. Jenks, *Editor*. 1956. 378 p., 13 figs., 11 pls. $5.50.
66. Cenozoic Foraminifera from Micronesia. Shoshiro Hanzawa. 1957. 163 p., 12 figs., 41 pls. $4.50.
67. Treatise on Marine Ecology and Paleoecology. Volume 1. Ecology. Joel W. Hedgpeth, *Editor*. 1957. 1296 p. $12.50. Volume 2. Paleoecology. Harry S. Ladd, *Editor*. 1957. 1078 p. $10.00.
68. Beekmantown Group (Lower Ordovician) of Maryland. William J. Sando. 1957. 162 p., 20 figs., 15 pls. $5.00.
69. Genus *Pentremites* and its Species. J. J. Galloway and H. V. Kaska. 1957. 104 p., 5 figs , 13 pls. $2.50.
70. *Fenestella* from the Permian of West Texas. M. K. Elias and G. E. Condra. 1957. 158 p., 17 figs., 23 pls. $3.50.
72. Coastal Sand Dunes of Oregon and Washington. William S. Cooper. 1958. 170 p., 12 figs., 22 pls. $3.50.
73. Metamorphic Reactions and Metamorphic Facies. W. S. Fyfe, F. J. Turner, and J. Verhoogen. 1958. 260 p., 108 figs. $4.50.
74. Origin of Granite in the Light of Experimental Studies in the System $NaAlSi_3O_8$—$KAlSi_2O_6$—SiO_2—H_2O. O. F. Tuttle and N. L. Bowen. 1958. 154 p., 67 figs., 6 pls. $3.75.
75. Selected Bibliographies of Hydrothermal and Magmatic Mineral Deposits. John Drew Ridge. 1958. 200 p. $3.75.
76. Type Specimens of Marine Mollusca Described by P. P. Carpenter from the West Coast (San Diego to British Columbia). K. V. W. Palmer. 1958. 376 p., 35 pls. $7.50.
77. Relation of Ore Deposition to Doming in the North American Cordillera. Edward Wisser. 1960. 118 p., 34 figs., 2 pls. $4.00.
78. Molluscan Faunas of the Flagstaff Formation of Central Utah. Aurèle La Rocque. 1960. 100 p., 2 figs., 4 pls. $4.50.
79. Rock Deformation. David Griggs and John Handin, *Editors*. 1960. 382 p., 40 pls., many line illustrations. $12.00.

Publications of The Geological Society of America

Publications currently in stock may be purchased at prices indicated below, on order accompanied by remittance addressed to The Geological Society of America, 419 West 117 Street, New York 27, N. Y. Consult lists on current Bulletins to be assured that items of interest are in stock.

BULLETIN

Monthly. Advance subscription, $15 per year; separate number $1.50; back yearly volumes, as available: prior to 1935, $12.00 per volume; 1935–, $15.00 per volume. Ten-year indexes covering vols. 31–40, 41–50, $1.50 per copy; covering vols. 51–60, $1.00 per copy.

GUIDEBOOKS FOR ANNUAL MEETING FIELD TRIPS

Guides to Southeastern Geology. (New Orleans). Richard J. Russell, *Editor*. November 1955. $3.00.
Guidebook for Field Trips. (Minneapolis). G. M. Schwartz, *Editor*. November 1956. $4.00.
Guidebook for Field Trips. (Atlantic City). Erling Dorf, *Editor*. November 1957. $2.75.
Guidebook for Field Trips. (Pittsburgh). Field Trip Committee. November 1959. $2.00.

VOLUMES IN ENGINEERING GEOLOGY

Application of Geology to Engineering Practice, Sidney Paige, *Chairman* (Berkey Volume). By 18 Authors (13 papers) 1951, 327 p. $2.75.
Engineering Geology Case Histories, P. D. Trask, *Editor*. No. 1, 66 p., 1957. $1.00; No. 2, 48 p., 1958, $1.00; No. 3, 76 p., 1959, $1.00.
Teaching Aids and Allied Materials, G. A. Kiersch, *Chairman* 36 p., 1957. 75 cents.

PENROSE VOLUME

Life and Letters of R. A. F. Penrose, Jr., H. R. Fairbanks and C. P. Berkey. 1952. 765 p. $4.00.

BIBLIOGRAPHY OF GEOLOGY EXCLUSIVE OF NORTH AMERICA

Annually, 1933–1940; biennially, 1941–1946; annually, 1947–. By Marie Siegrist, Marcia Lakeman, and Mary Grier. Vols. 1–, inclusive, $2.50 per volume; Volumes 8–12 out of stock; Volume 13, $3.25; Volume 14, $3.00; Volume 15, $3.00; Volume 16, $4.50; Volume 17, $5.75; Volume 18, $5.50; Volume 19, $7.50; Volume 20, $8.00; Volume 21, $10.00; Volume 22, $10.00.

SPECIAL COLORED MAPS

Glacial Map of North America. (Special Paper 60). By Committee on Glacial Map. R. F. Flint, *Chairman*. 1945. $2.00.
Glacial Map of the United States East of the Rocky Mountains. By Committee of National Research Council. R. F. Flint, *Chairman*. 1959. $6.00.
Tectonic Map of Canada. By Geological Association of Canada. 1950. $1.50.
Pleistocene Eolian Deposits of the United States, Alaska, and Parts of Canada. James Thorp and H. T. U. Smith, *Cochairmen*. 1952. $3.00.

ROCK-COLOR CHARTS

Prepared by Committee of National Research Council. $7.00 per set.

TREATISE ON INVERTEBRATE PALEONTOLOGY

Raymond C. Moore, *Editor*

Part D. Protista 3. Chiefly Radiolarians and Tintinnines). By A. S. Campbell and R. C. Moore. 1955. 195 p., 92 figs. $3.00.
Part E. Archaeocyatha and Porifera. By V. J. Okulitch and M. W. de Laubenfels. 1955. 122 p., 88 figs. $3.00.
Part F. Coelenterata. By F. M. Bayer *et al.* 1956. 498 p., 358 figs. $7.00.
Part G. Bryozoa. By Ray S. Bassler. 1954. 253 p., 175 figs. $3.00.
Part L. Mollusca 4 (Cephalopoda; Ammonoidea). By W. J. Arkell *et al.* 1957. 490 p., 588 figs. $8.50.
Part O. Arthropoda 1 (Trilobitomorphs). By 18 authors. 1959. 560 p., 415 figs. $10.50.
Part P. Arthropoda 2 (Chelicerata, Pycnogonida, Palaeoisopus). By L. Störmer, A. Petrunkevitch, J. W. Hedgpeth. 1956. 181 p., 123 figs. $3.50.
Part V. Graptolithina. By O. M. B. Bulman. 1955. 101 p., 72 figs. $3.00.

SPECIAL PAPERS

1. Bibliography and Index of Paleozoic Ostracoda. R. S. Bassler and Betty Kellet. 1934, 500 p., 24 figs. $3.00.
2. Fossil Crustacea of the Atlantic and Gulf Coastal Plain. M. J. Rathbun. 1935. 160 p., 26 pls., 2 figs. $1.50.
3. Fossil Non-Marine Mollusca of North America. Junius Henderson. 1935. 313 p. $2.10.
5. Geology of Saint John, New Brunswick. A. O. Hayes and B. F. Howell. 1937. 146 p., 9 pls., 4 figs. $1.50.
7. Atlantic Submarine Valleys of the United States and the Congo Submarine Valley. A. C. Veatch and Paul A. Smith. 1939. 101 p., 5 charts, 10 pls., 28 figs. $4.80.
11. Geology and Paleontology of the Mingan Islands, Quebec. W. H. Twenhofel. 1938. 132 p., 24 pls., 1 fig., $1.50.
12. Tertiary Flora from the Rio Pichileufu, Argentina. E. W. Berry. 1938. 149 p., 56 pls., 11 figs. $2.10.
21. Paleontology and Stratigraphy of the Silurian Rocks of the Port Daniel Black Cape Region, Gaspe. S. A. Northrop. 1939. 302 p., 28 pls., 1 fig. $3.00.
28. Review of the Pelycosauria. A. S. Romer and L. I. Price. 1949. 538 p., 46 pls., 71 figs. $4.20.
29. Phacopid Trilobites of North America. D. M. Delo. 1940. 135 p., 13 pls., $1.20.
33. Numerical Structure Factor Tables. M. J. Buerger. Reprinted 1953. 119 p., 4 figs. (Cloth bound) $1.50.
37. Ozarkian and Canadian Cephalopods, Part I, Nautilicones. E. O. Ulrich, Aug. F. Foerste, A. K. Miller and W. M. Furnish. 1942. 157 p., 57 pls., 23 figs. $2.40.
40. Hadrosaurian Dinosaurs of North America. R. S. Lull and N. E. Wright. 1942. 242 p., 31 pls., 90 figs. $2.70.
49. Ozarkian and Canadian Cephalopods. Part II: Brevicones. E. O. Ulrich, A. F. Foerste, and A. K. Miller. 1943. 240 p., 70 pls., 15 figs. $3.00.
60. Glacial Map of North America. By Committee on Glacial Map. R. F. Flint, *Chairman*. 1945. $2.00.

(Continued on inside back cover)